THE DETERMINATION OF THORIUM AND URANIUM BY REVERSED-PHASE LIQUID CHROMATOGRAPHY

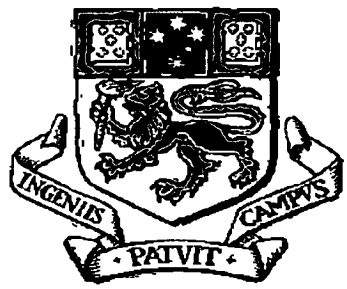

by

Fuping Hao, B. Sc. (Hons.), MRACI

Submitted in fulfilment of the requirements

for the degree of

Doctor of Philosophy

Department of Chemistry

University of Tasmania

Hobart, Australia

October, 1995

DECLARATION

I hereby declare that this submission is my own work and that, to the best of my knowledge and belief, it contains no material previously published or written by any other person, nor material which to any substantial extent has been accepted for the award of any other degree or diploma at a university or other institute of higher learning, except where due acknowledgment is made in the text. This thesis may be made available for load copying of any part of this thesis is prohibited for two years from the date this statement was signed; after that time limited copying is permitted in accordance with the *Copyright Act* 1968.

Hao Jupiing

Date 20/10/95

ACKNOWLEDGMENTS

During the three years that it has taken to complete this thesis, many people in the University of Tasmania have contributed their time and support towards this project. I would like to express my sincere gratitude and appreciation to all those who have helped me along the way, and in particular the following people:

- Professor Paul R. Haddad, my supervisor, for guidance and friendship over the years. He brought me to Tasmania and provided a scholarship, without which I could not have enrolled or finished this study.

- Dr. Peter E. Jackson at Millipore Australia, Waters Chromatography Division, for his assistance and cooperation on this project.

- Dr. Brett Paull for his help with the correction of this thesis and Dr. Wolfgang Buchberger, Department of Analytical Chemistry, Johannes-Kepler University, Linz, Austria, and Professor Richard M. Cassidy, Department of Chemistry, University of Saskatchewan, Saskatoon, Canada, for their many suggestions regarding my work.

- The staff members of the Department of Chemistry, University of Tasmania, especially Anne Kelly for her help all the time, Peter Dove and John Davis for their assistance whenever there were instrumental problems.

- My fellow Chromatography group research students in the Department over the past years: Peter, Soehendra, Tony, Simon, Sarah, Christine, Ana, Mirek, Vasina, Phillip, John, Ignatius and Per for their warm friendship and help.

- My Chinese student friends in the Department over the last three years: Yan-ping Sun, Cai-ping Li and Duo Li, for their friendship and company.

- Finally, I would like to thank my family: my wife, Li Li, for her love, patience and genial assistance throughout the years of our stay in Tasmania; my

daughter, Meng, for her help whenever I had difficulty in spelling, and my mother for her love and continuous encouragement for many years. At the time of submission of my thesis I miss my late father very much. I came to Australia with his great expectations, but he is not here to share my success. It is to him that I dedicate this thesis.

ABSTRACT

This thesis presents the results of a systematic study of the reversed-phase high performance liquid chromatographic determination of thorium(IV) and uranyl as their α-hydroxymonocarboxylic acid complexes. Various parameters which affect complexation and retention have been investigated. The aims of this study were to elucidate the retention mechanism of these complexes and use this knowledge for the development of methodology for the determination of low concentrations of thorium and uranium, especially in complex sample matrices. Throughout this study, a conventional reversed-phase chromatographic system was used, which employed a C_{18} reversed-phase column with aqueous methanolic mobile phases containing a complexing agent. Thorium(IV) and uranyl were detected at 658 nm after post-column derivatisation with Arsenazo III.

The retention behaviour of thorium(IV) and uranyl α-hydroxyisobutyric acid (HIBA) complexes was firstly investigated. When the percentage of methanol in the mobile phase was varied, both thorium(IV) and uranyl complexes exhibited typical reversed-phase behaviour. Decreased retention was observed when the concentration of HIBA in the eluent increased due to competition by the neutral, protonated HIBA in the eluent for the adsorption sites on the stationary phase. Elevation of the mobile phase pH caused the retention of both thorium(IV) and uranyl to increase as a result of the decreased concentration of the neutral ligand acid in the mobile phase. A retention mechanism based on hydrophobic adsorption was therefore suggested.

The hydrophobic adsorption mechanism was further confirmed when glycolate or mandelate were used as ligands in the mobile phase. Varying the percentage of methanol, the ligand concentration in the mobile phase, or the pH, showed that both glycolate and mandelate complexes gave similar retention behaviour to that of HIBA. However, the degree of retention observed for glycolate complexes was weak due to

the short carbon chain in the ligand, whereas the mandelate complexes were retained much longer because of the increased hydrophobicity arising from the aromatic moeity in the ligand. The elution characteristics of thorium(IV) and uranyl complexes were therefore shown to be dependent chiefly on the ligand hydrophobicity.

A reversed-phase chromatographic method was developed for the determination of thorium(IV) and uranyl in mineral sands, using 400 mM HIBA as the eluent. A range of sample dissolution and clean-up procedures was evaluated, with the optimal sample preparation procedure involving a tetraborate fusion and nitric acid leach, followed by either cation-exchange pretreatment, or simple dilution in concentrated HIBA. The results obtained using the chromatographic method showed good agreement with X-ray fluorescence results and gave detection limits about 1.0 μg/ml for the two analytes.

Trace levels of thorium(IV) and uranyl were determined using an on-line preconcentration method which employed a short C_{18} column as the concentrator. Different ligands were added to the sample solution to enhance retention of the analytes on the concentrator, with 42 mM mandelate being optimal. The sample loading speed was found to have no effect on recoveries if maintained below 5.0 ml/min. A linear relationship between the peak area and the loaded sample volume existed up to 50 ml of sample. The interferences of most common mineral acids and cations were investigated. The on-line preconcentration method, which gave detection limits of 5 ppb , was applied to the determination of trace levels of thorium(IV) and uranyl spiked in sea water.

An on-line matrix elimination procedure was then developed as a means of eliminating interference effects and was applied to the determination of thorium(IV) and uranyl in a digested phosphate rock solution. Theoretical calculations predicted that it was impossible to separate thorium(IV) and uranyl from the matrix in one step. Phosphate and other anions were firstly removed from the sample on a cation-

exchange precolumn with a dilute nitric acid eluent. Then thorium(IV) and uranyl were separated from lanthanides on a short C_{18} precolumn using a mandelate eluent. Finally thorium(IV) and uranyl were transferred onto the C_{18} analytical column for separation and quantification. The matrix elimination procedure was performed automatically by a programmable HPLC pump.

List of Publications from This Thesis

1. Studies on the Retention Behaviour of α-Hydroxyisobutyric Acid Complexes of Thorium(IV) and Uranyl Ion in Reversed-Phase High Performance Liquid Chromatography.
   • Fuping Hao, Paul R. Haddad, Peter E. Jackson and Joe Carnevale.
   • *Journal of Chromatography*, 640 (1993) 187.
   (Work from Chapter Four of this thesis)

2. Determination of Thorium and Uranium in Mineral Sands by Ion-Chromatography.
   • Peter E. Jackson, Joe Carnevale, Fuping Hao and Paul R. Haddad.
   • *Journal of Chromatography,* 671 (1994) 181.
   (Work from Chapter Six of this thesis)

3. The Retention Behaviour of Thorium(IV) and Uranyl on a Reversed-Phase Column Using Glycolate and Mandelate Eluents.
   • Fuping Hao, Brett Paull and Paul R. Haddad.
   • *Journal of Chromatography,* submitted for publication.
   (Work from Chapter Five of this thesis)

4. The Determination of Trace Levels of Thorium(IV) and Uranyl by Reversed-Phase Chromatography with On-Line Preconcentration.
   • Fuping Hao, Brett Paull and Paul R. Haddad.
   • paper in preparation.
   (Work from Chapter Five and Seven of this thesis)

5. Chromatographic Determination of Trace Levels of Thorium(IV) and Uranyl in Phosphate Rocks by On-Line Matrix Elimination.
   • Paul R. Haddad and Fuping Hao.
   • paper in preparation. (Work from Chapter Eight of this thesis)

List of Presentations from This Thesis

1. Mechanism of Retention of Uranium and Thorium in Ion-Chromatography Using Hydroxycarboxylic Acids as Eluents.
   • Fuping Hao and Paul R. Haddad.
   • A paper presented at *The 12th Australian Symposium on Analytical Chemistry*, September, 1993, Perth, Australia. Paper No. 97.
   (Work from Chapter Five of this thesis)

2. Determination of Trace Levels of Thorium and Uranium with an On-line Preconcentration Technique.
   • Paul R. Haddad and Fuping Hao.
   • A poster presented at *Chromatography '94*, July, 1994, Sydney, Australia. Poster No. PO4.
   (Work from Chapter Seven of this thesis)

3. Determination of Thorium and Uranium in Nitrophosphate Solution by On-line Matrix Elimination Reversed-phase Chromatography.
   • Fuping Hao and Paul R. Haddad.
   • A paper presented at *The 13th Australian Symposium on Analytical Chemistry*, July, 1993, Darwin, Australia. Paper No. AK4.
   (Work from Chapter Eight of this thesis)

4. Micro Determination of Thorium(IV) and Uranyl by Reversed-Phase Chromatography with On-Line Preconcentration and Ligand-Exchange Analysis.
   • Paul R. Haddad and Fuping Hao.
   • To be presented at *The International Ion Chromatography Symposium*, October, 1995, Dallas, USA.
   (Work from Chapters Five and Seven of this thesis)

Table of Contents

Chapter 1
Introduction 1

Chapter 2
Literature Review 4

2.1 INTRODUCTION 4
2.2 CHEMISTRY OF THORIUM AND URANIUM 5
2.2.1 Chemistry of Thorium 5
2.2.2 Chemistry of Uranium 7
2.3 NON-CHROMATOGRAPHIC METHODS FOR THORIUM AND URANIUM DETERMINATION 7
2.3.1 Introduction 7
2.3.2 Neutron Activation Analysis 7
2.3.3 Atomic Absorption Spectroscopy 10
2.3.4 Inductively Coupled Plasma-Atomic Emission Spectroscopy 11
2.3.5 X-Ray Fluorescence Spectroscopy 12
2.4 CHROMATOGRAPHIC METHODS FOR THORIUM AND URANIUM DETERMINATION 12
2.4.1 Introduction 12
2.4.2 Chromatographic Separation Methods 13
2.4.2.1 Cation-Exchange Chromatography 13
2.4.2.2 Ion-Interaction Chromatography 18
2.4.2.3 Reversed-Phase Chromatography 20
2.4.3 Chromatographic Detection Methods 22
2.4.3.1 Conductivity Detection 22
2.4.3.2 Spectrophotometric Detection 23
2.4.3.3 Post-Column Reaction Detection 24
2.5 PRECONCENTRATION TECHNIQUES FOR TRACE ELEMENTS 28
2.5.1 Principles of Preconcentration 28
2.5.2 Precolumn Preconcentration 31
2.5.2.1 Single-Valve On-Line Preconcentration System 31
2.5.2.2 Two-Valve Preconcentration System 33
2.5.3 Factors Affecting On-Line Preconcentration 35
2.5.3.1 The Characteristics of the Concentrator Column 36

2.5.3.2 The Eluent 36
2.5.3.3 Sample Loading Parameters 38
2.5.4 Evaluation of Preconcentration Performance 38
2.6 AIMS OF THIS STUDY 39
2.7 REFERENCES 40

Chapter 3
Experimental 47

3.1 INTRODUCTION 47
3.2 CHROMATOGRAPHIC SYSTEMS AND GENERAL EXPERIMENTAL PROCEDURES 48
3.2.1 Instrumentation 48
3.2.1.1 The Direct Injection System
3.2.1.2 The Preconcentration System 48
3.3 REAGENTS 51
3.3.1 Solvents and Reagents 51
3.3.2 Standard Solutions 51
3.3.3 Mobile Phases 54
3.3.4 Post-Column Reaction Reagents 54
3.4 GENERAL 56
3.5 REFERENCES 56

Chapter 4
The Retention Behaviour of α-Hydroxyisobutyric Acid Complexes of Thorium(IV) and Uranyl in Reversed-Phase Liquid Chromatography 57

4.1 INTRODUCTION 57
4.2 THORIUM(IV) AND URANYL HIBA COMPLEXES 58
4.2.1 General Properties of HIBA as a Ligand 59
4.2.2 Thorium(IV) and Uranyl HIBA Complexes 60
4.2.3 Distribution of Thorium(IV) and Uranyl HIBA Complexes 65
4.2.3.1 Effect of HIBA Concentration on Complex Formation 65
4.2.3.2 Effect of pH on Complex Formation 67
4.2.3.3 Combined Effects of Ligand Concentration and pH on Complex Formation 70
4.3 EXPERIMENTAL 75
4.3.1 Instrumentation 75

4.3.2 Reagents 75
4.4 RESULTS AND DISCUSSION 76
4.4.1 Preliminary Investigations 76
4.4.1.1 Spectra of Thorium(IV) and Uranyl Complexes 76
4.4.1.2 Reversed-Phase Chromatography of HIBA Complexes 83
4.4.2 Factors Affecting Retention 86
4.4.2.1 Organic Modifier in the Mobile Phase 86
4.4.2.2 Column Temperature 86
4.4.2.3 HIBA Concentration in the Mobile Phase 90
4.4.2.4 The Eluent pH 90
4.4.2.5 Ion-Interaction Reagents in the Mobile Phase 96
4.4.3 Mechanism of Retention 96
4.5 CONCLUSIONS 100
4.6 REFERENCES 101

Chapter 5
The Retention Behaviour of Thorium(IV) and Uranyl on a Reversed-Phase Column Using Glycolate and Mandelate Eluents 103

5.1 INTRODUCTION 103
5.2 CHEMISTRY OF THORIUM(IV) AND URANYL COMPLEXES WITH GLYCOLATE AND MANDELATE 105
5.2.1 General Properties of Glycolic and Mandelic Acids as Complexing Ligands 105
5.2.2 Character of Glycolate and Mandelate Complexes 106
5.2.2.1 Effect of Ligand Concentration on Complex Formation 108
5.2.2.2 Effect of pH on Complex Formation 111
5.3 EXPERIMENTAL 114
5.3.1 Instrumentation 114
5.3.2 Reagents 114
5.4 RESULTS AND DISCUSSION 115
5.4.1 Preliminary Investigations 115
5.4.1.1 Spectra of Glycolate, Mandelate and Their Complexes 115
5.4.1.2 Preliminary Chromatographic Studies 115
5.4.2 Factors Affecting Retention of Glycolate and Mandelate Complexes 121
5.4.2.1 Organic Modifier in the Mobile Phase 121
5.4.2.2 Column Temperature 124

5.4.2.3 Ligand Concentration in the Mobile Phase 125
5.4.2.4 The Eluent pH 129
5.4.3 Mechanism of Retention 133
5.5 CONCLUSIONS 137
5.6 REFERENCES 138

Chapter 6
Determination of Thorium(IV) and Uranium in Mineral Sands by Reversed-Phase Liquid Chromatography 139

6.1 INTRODUCTION 139
6.1.1 Thorium and Uranium in Mineral Sands 140
6.2 EXPERIMENTAL 141
6.2.1 Instrumentation 141
6.2.2 Reagents 141
6.2.3 Sample Dissolution Procedures 143
6.2.4 Cation-Exchange Pretreatment Procedure 145
6.3 RESULTS AND DISCUSSION 145
6.3.1 Preliminary Experiments 145
6.3.2 Sample Pretreatment with Various Cation-Exchanger Cartridges 151
6.3.3 Comparison of Fusion/Digestion Methods 157
6.3.4 Direct Injection 163
6.4 CONCLUSIONS 165
6.5 REFERENCES 167

Chapter 7
Determination of Trace Levels of Thorium(IV) and Uranyl by an On-Line Preconcentration Technique 169

7.1 INTRODUCTION 169
7.2 EXPERIMENTAL 171
7.2.1 Instrumentation 171
7.2.2 Reagents 172
7.2.3 Preconcentration System and Procedures 172
7.3 RESULTS AND DISCUSSION 174
7.3.1 Preliminary Investigation 174
7.3.2 Concentrator Column 176
7.3.2.1 Assessment of Different Types of Concentrator 176

7.3.2.2 Breakthrough Volume 179
7.3 3 Effect of Ligand in the Sample Solution 180
7.3.3.1 Comparison of HIBA, Glycolate and Mandelate in Sample 180
7.3.3.2 Effect of Mandelate Concentration in Sample 184
7.3.4 Effect of Sample Loading Parameters 186
7.3.4.1 Effect of Sample Loading Speed 186
7.3.4.2 Calibration Using Loading Volume 186
7.3.4.3 Calibration Using Sample Concentration 188
7.3.5 Interference Effects 188
7.3.5.1 Anions in the Sample Solution 188
7.3.5.2 Cations in the Sample Solution 181
7.3.6 Precision Of Preconcentration. 192
7.4 DETERMINATION OF TRACE LEVELS THORIUM(IV) AND URANYL SPIKED INTO SEA WATER 192
7.4.1 Initial Experiments 192
7.4.2 Modification of the Eluent Composition 198
7.4.3 Selection of A Suitable Concentrator Column 198
7.4.4 Calibration Plots 204
7.4.5 Single Column Preconcentration and Analysis 204
7.5 CONCLUSIONS 207
7.6 REFERENCES 209

Chapter 8
Chromatographic Determination of Thorium and Uranium in Digested Phosphate Rock Solution Combined with On-Line Matrix Elimination 210

8.1 INTRODUCTION 210
8.2 EXPERIMENTAL 212
8.2.1 Instrumentation 212
8.2.2 Reagents 214
8.2.3 Procedure for On-Line Matrix Elimination 214
8.3 RESULTS AND DISCUSSION 217
8.3.1 Preliminary Investigation 217
8.3.2 Lanthanide Separation 220
8.3.3 Phosphate Interference 225
8.3.4 On-Line Matrix Elimination 231
8.4 CONCLUSIONS 235

8.5 REFERENCES 239

Chapter 9
Conclusions 240

Chapter 1

Introduction

Thorium and uranium are traditionally determined using techniques such as neutron activation analysis, atomic absorption spectroscopy, inductively coupled plasma-atomic emission spectroscopy and X-ray fluorescence. However, these techniques are often not suitable for routine analysis because of their high running costs or time consuming nature.

Ion-chromatography has been widely applied to inorganic ion analysis since 1975 due to its simplicity, reliability and low cost. Many methods in separation and detection methodology have been developed since then. Chromatographic techniques used for the determination of thorium and uranium in the past include cation-exchange and ion-interaction methods. A suitable ligand, such as α-hydroxyisobutyric acid (HIBA), is added to the mobile phase to reduce the effective charge on the injected metal ions in order to elute the analytes within a reasonable time. The advantage of ion-interaction chromatography is the ease with which the column ion-exchange capacity and selectivity can be altered.

In previous studies it has been found that thorium(IV) and uranyl showed different retention behaviour to that of the lanthanides, suggesting that a different retention mechanism could be applied. Whilst some of the factors influencing the retention of thorium(IV) and uranyl HIBA complexes have been reported, the mechanism of their retention on the reversed-phase column remains unclear.

This thesis presents the results of a systematic study of the retention behaviour of thorium(IV) and uranyl on a reversed-phase column using a mobile phase containing a hydrophobic acid ligand. Different ligands and various factors which affect retention and complexation have been examined in detail.

Prior to the presentation of the experimental procedures, literature concerning thorium and uranium analysis is reviewed in Chapter Two. Both traditional and current analytical methods are discussed with the emphasis on chromatographic separation and detection techniques. In addition, on-line chromatographic preconcentration techniques are also considered.

Chapter Three outlines the experimental details of the chromatographic systems used in this study, together with the reagents used. Further experimental conditions and operating procedures are given in experimental sections in each of the subsequent chapters.

The results obtained for thorium(IV) and uranyl HIBA complexes are presented in Chapter Four. The characteristics of these complexes are initially examined by theoretical calculation. The effects of various experimental parameters are then investigated, such as the organic modifier in the eluent, the mobile phase pH, HIBA concentration, and the column temperature.

Chapter Five concerns the retention mechanism using glycolic acid or mandelic acid as complexing ligands. These acids have similar characteristics when they form complexes with thorium(IV) and uranyl, but differ in hydrophobicity. The same experimental parameters are investigated as those for HIBA in Chapter Four.

In Chapter Six the reversed-phase chromatographic method is applied to the determination of trace levels of thorium and uranium in mineral sands. A number of digestion/fusion methods are tried, such as peroxide, borate, and hydroxide fusion. The digested sample is then pretreated with various types of cation-exchange cartridges, or simply diluted in HIBA solution prior to chromatographic injection.

Chapter Seven describes an on-line preconcentration study of thorium(IV) and uranyl using a short C_{18} cartridge as the concentrator and preparing the sample in mandelate solution. Various factors which affect the preconcentration efficiency are

examined, such as the ligand concentration, sample loading speed, and the type of matrix ions in the sample. The on-line preconcentration technique is applied to the determination of ppb levels of thorium(IV) and uranyl spiked into sea water.

Chapter Eight describes the analysis of phosphate rock using the reversed-phase method combined with a two-precolumn on-line matrix elimination system. Phosphate and other anions are first removed from the sample on a cation-exchange cartridge using a HNO_3 eluent, then the lanthanides and transition metals are separated on a short C_{18} precolumn using a mandelate eluent. Finally the thorium(IV) and uranyl are transferred onto the C_{18} analytical column where they are separated and quantified.

Chapter Nine summarises this study.

Chapter 2

Literature Review

2.1 INTRODUCTION

Thorium and uranium were discovered 200 years ago. However, their chemistry was not fully investigated until the discovery of nuclear fission in the 1940's. When uranium is hit by slow neutrons, its isotope $_{92}U^{235}$ undergoes a nuclear fission with liberation of enormous amounts of energy:

$$_{92}U^{235} + n \longrightarrow {}_{56}Ba^{140} + {}_{36}Kr^{96} + 3n + \sim 200 \text{ mev} \qquad (2.1)$$

If this reaction is complete, one pound of U^{235} can produce up to 10^7 kilowatt hours of "heat energy equivalent" [1]. This reaction has been used to generate power and for military purposes in the past 50 years. Most of the trans-uranium elements have been synthesised by nuclear reactions since then. Unfortunately, nuclear applications also create environment problems due to the release of radioactivity. Research on nuclear power needs sensitive and fast methods to quantitatively analyse thorium and uranium.

Many analytical methods have been developed for the determination of thorium and uranium, such as neutron activation analysis, atomic absorption spectroscopy, X-ray fluorescence spectroscopy and inductively coupled plasma atomic emission spectroscopy. These instrumental methods offer high sensitivity for thorium and uranium detection and some provide special advantages, such as non destruction of the sample, but these methods are either time consuming or have high running costs, and may not be suitable for routine analysis.

Since Small *et al.*[2] published the first paper on ion-chromatography (IC) in 1975, this technique has been used widely for the analysis of inorganic ions and has

proven to be a simple, reliable and inexpensive tool. The application of IC for thorium and uranium analysis could be traced back to the 1970's [3, 4]. Most of the early IC analyses were performed with a cation-exchange column using a strong acid solution as the mobile phase [5]. The dynamic ion-exchange separation method was soon introduced [6, 7], in which a conventional reversed-phase column was coated with an ion-interaction reagent (IIR), such as octanesulfonate, to convert it into a dynamic cation-exchange column, and an organic-aqueous solution used as the eluent. This method proved suitable for the separation of transition metals and the lanthanides.

In these dynamic cation-exchange chromatography studies it was noted that the thorium(IV) and uranyl showed different retention behaviour to that of the lanthanides. Thorium(IV) and uranyl could be either eluted amongst the lanthanides or after them by varying the octanesulfonic acid concentration in the mobile phase. They could be retained on the reversed-phase column without the presence of the IIR, providing there was a complexing ligand present in the mobile phase, which suggested that a different retention mechanism could be operating [8, 9]. In this thesis the retention mechanism and the factors affecting the retention of thorium(IV) and uranyl complexes on a reversed-phase column were investigated, these results have been used to select suitable chromatographic conditions for thorium and uranium analysis.

As the commencement of the study, this chapter reviews both traditional and ion-chromatographic methods which are used for thorium and uranium analysis, as well as preconcentration techniques used for trace level analysis. General concepts of thorium and uranium chemistry are also presented in this chapter.

2.2 CHEMISTRY OF THORIUM AND URANIUM

2.2.1 CHEMISTRY OF THORIUM [10]

Thorium is distributed widely in nature and there are large deposits of the principal minerals, such as monazite (a complex phosphate). The average thorium

content of the outermost layer of the earth's crust is about 12 parts per million (ppm). It is about as abundant as lead (16 ppm) and about three times as abundant as uranium. Thorium is one of the heaviest elements in the periodic table. The most probable electronic structure of thorium valence shells is $6d^2 7s^2$. The four valence electrons are easily lost forming Th(IV) when thorium takes part in a chemical reaction. The redox potentials of Th^{4+} in acid and basic solution are given in Eqn. 2.2 and Eqn. 2.3, respectively.

$$Th \leftrightharpoons Th^{4+} + 4e^- \qquad E_A^o = 1.90\ v \qquad (2.2)$$

$$Th + 4OH^- \leftrightharpoons Th(OH)_4 + 4e^- \qquad E_B^o = 2.48\ v \qquad (2.3)$$

Compared to zirconium or cerium, thorium appears to be more electropositive, about as electropositive as magnesium. Thorium reacts with many strong mineral acids forming Th(IV) salts, amongst the most common being $Th(NO_3)_4 \cdot nH_2O$. Here, the number of the water molecules depends on whether the salt is produced in dilute, concentrated or fuming nitric acid. In aqueous solution thorium has only one stable oxidation state, +4. Compared with other +4 cations the Th^{4+} cation is more resistant to hydrolysis [11], but it undergoes extensive hydrolysis when the solution pH exceeds 3, and produces some very complicated species of composition dependent on the conditions of pH, the nature of anions and concentration, etc. For example, in perchlorate solutions Th^{4+} forms various hydrolysed ions, such as $Th(OH)^{3+}$, $Th(OH)_2^{2+}$, $Th_2(OH)_2^{6+}$ and $Th_4(OH)_8^{8+}$, while the final product is the hexamer $Th_6(OH)_{15}^{9+}$, and all of these ions carry additional water molecules. The multi-vacated orbitals present in Th^{4+} permit it to accept donated electrons, so thorium(IV) often exhibits very high coordination numbers when it forms complexes [12]. Thorium(IV) reacts with most of the common anions except perchlorate, forming multistep complexes.

2.2.2 CHEMISTRY OF URANIUM [13]

Although uranium was discovered 200 years ago (1789), it had little commercial importance until its use for nuclear fission was developed in 1939. Prior to this time uranium was only used for making coloured glass and ceramics. The most probable electronic structure of the uranium valence shell is $5f^36d^17s^2$. The uranium metal can be oxidised in different stages, based on the strength of the oxidation reagent. The redox potentials of uranium ions in 1 M perchloric acid solution (2.4) and in alkaline solution (2.5) are listed below:

$$U \xrightarrow{+1.800V} U^{3+} \xrightarrow{+0.631V} U^{4+} \xrightarrow{-0.580V} UO_2^{+} \xrightarrow{-0.063V} UO_2^{2+} \qquad (2.4)$$

($-0.320V$ for $U^{4+} \rightarrow UO_2^{+}$)

$$U \xrightarrow{+2.17V} U(OH)_3 \xrightarrow{+2.14V} U(OH)_4 \xrightarrow{+0.62V} UO_2(OH)_2 \qquad (2.5)$$

Here, the uranium +6 and +5 states are present as dioxide forms even in solution. The uranium ion gives various species in solution, because not only does it have four oxidation states, but all of these form complexes with most common anions (except perchlorate) and the species formed undergo hydrolysis. In an aqueous solution, the U^{3+} is an unstable ion unless prepared in a strongly acidified solution, and reacts rapidly with water forming U^{4+}. The U^{4+} undergoes extensive hydrolysis. The penta-positive state of uranium, UO_2^{+}, is the least stable of all the uranium oxidation states. Only the +6 oxidation state, uranyl, is the familiar stable oxidation state of uranium. It has been proved that the uranyl exists in water as UO_2^{2+}. X-ray studies have found that the structure of UO_2^{2+} in crystal compounds, such as UO_2F_2 and $NaUO_2(CH_3COO)_3$, is in a linear group O-U-O. The most common uranyl salt is nitrate, $UO_2(NO_3)_3 \cdot nH_2O$, in which the number of water molecules depends on the nitric acid concentration which uranium reacts with. An unusual and significant property of uranyl nitrate is its solubility in numerous ethers, alcohols, ketones and esters, and it distributes itself between the organic and aqueous phases.

2.3 NON-CHROMATOGRAPHIC METHODS FOR THORIUM AND URANIUM DETERMINATION

2.3.1 INTRODUCTION

Non-chromatographic instrumental methods used for thorium and uranium analysis can be classified as shown in Fig. 2.1. These methods have long been used for thorium and uranium analysis. It has been reported that neutron activation analysis [14] and inductively coupled plasma-mass spectroscopy [15] can also be used as detection methods for chromatographic analysis. Some further traditional analytical methods, such as titration and UV absorption are not included in this chapter on the basis that they are either insensitive or time consuming.

2.3.2 NEUTRON ACTIVATION ANALYSIS

Neutron activation analysis (NAA) is an important method for the determination of radioactive elements [16, 17, 18]. It is based on the measurement of the radioactivity induced in a sample when it is irradiated by thermal neutrons produced from a reactor [19]. Here, the radiation is beta or gamma emission, both of which can be monitored. NAA methods can be further classified as sample destructive or non destructive, with the former being the most commonly used. With the destructive method the irradiated sample is prepared in a solution and the analyte separated from the matrix by chemical or physical means, and then counted for its gamma or beta activity. A standard containing a known mass W_S of the analyte is measured simultaneously in the same neutron flux as the sample. The activity is proportional to mass, if no other components of the sample produce detectable radioactivity. The weight of the element in the sample, W_X, can be simply calculated as below:

$$W_X = \frac{A_X}{A_S} W_S \qquad (2.6)$$

where A_X and A_S represent the activities of the sample and standard, respectively.

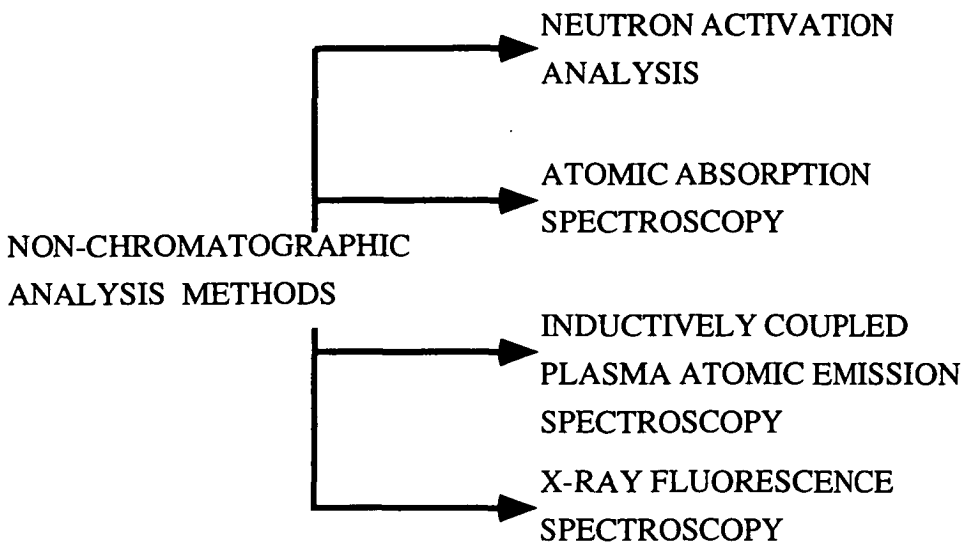

Fig. 2.1 Classification of non-chromatographic methods used for thorium and uranium analysis.

Combined with some sample pretreatment techniques, such as ion-exchange [20], trace amounts of radioactive elements can be determined without interference by the matrix. The NAA method has been used for thorium and uranium analysis in various types of sample, such as geological materials [21], plants [22], or medical substances [23]. The great advantage of this method is its high sensitivity. However, the accuracy of the method is very poor as many factors can influence the analysis, such as self-shielding, unequal neutron flux at sample and standard, counting uncertainties and counting errors. The total error can be 10% R.S.D.

2.3.3 ATOMIC ABSORPTION SPECTROSCOPY

Thorium is commonly measured with atomic absorption spectroscopy (AAS) [24]. The AAS instrument usually employs a metal hollow cathode lamp (in this case made of thorium) as the line light source, a flame burner (or a graphite furnace), a monochromator for isolating the absorption line and a photoelectric detector [25]. Thorium standards and the sample are prepared in a nitric acid solution ($pH < 2$) and aspirated into the flame, where the thorium is atomised at a high temperature (about 2800 °C). When the light beam passes through the flame, it will be absorbed by the atomised thorium. The degree of absorption depends on the amount of the atomised thorium which is further governed by the thorium concentration in the sample. In a certain range there is a linear relationship between the atomic absorption and the analyte concentration, therefore the thorium in a sample can be quantified. With a nitrous oxide-acetylene flame and using the 324.58 nm line, the sensitivity of AAS for thorium determination is 850 ppm/1% absorption [26]. Many samples can be directly analysed after digestion using strong acids without further pretreatment. Uranium can also be detected by the AAS method at 351 nm with a nitrous oxide-acetylene flame, with which the sensitivity is about 250 ppm/1% absorption [12, 27].

The characteristic of AAS is its high selectivity because a metal hollow cathode lamp is used. The lamp emits a sharp line light which is only absorbed by the metal

that is to be determined. Sometimes the molecules present in the flame may also absorb the light, which produces background absorption. This background absorption can be eliminated by using an extra deuterium lamp or double-beam light source. The disadvantage of AAS is that its detection limits are variable, for instance the uranium detection limit is about 30 ppm, because only a small portion of the sample solution is atomised in the flame.

2.3.4 INDUCTIVELY COUPLED PLASMA-ATOMIC EMISSION SPECTROSCOPY

Inductively coupled plasma-atomic emission spectroscopy (ICP-AES) is another widely used method for thorium and uranium determination [24]. This method relies on the measurement of the atomic emission of the analytes at high temperature. The heart of the ICP-AES instrument is a quartz tube, or torch, to which a flow of ionised argon gas is passed. The torch is surrounded by a water-cooled coil through which a radiofrequency electric field is applied. A gaseous plasma is created and sustained by the continuing ionisation of argon which is inductively coupled with the frequency field. A sample aerosol is generated with a nebuliser and carried into the plasma through the injector tube which is located within the torch. Almost all the molecules in the sample are completely dissociated at the high temperature used (in excess of 6000 °C), and each of the elements produces its characteristic atomic emission. By measuring the emission strength, all the elements in the sample can be quantified simultaneously. The great advantage of the ICP-AES method is that it gives a linear range of four to six orders of magnitude for many elements. Many publications have reported using the ICP-AES method to determine thorium and uranium in various types of sample, such as glass [28], minerals [29], alloy [15] or as the impurity in a metal [30]. Despite the wide linear range and low detection limit, the ICP-AES method is restricted by the high cost of the instrumentation.

2.3.5 X-RAY FLUORESCENCE SPECTROSCOPY

X-ray spectroscopy is used for chemical analysis in much same way as common UV and visible spectroscopy. The X-ray source is usually obtained by bombarding a metal target with accelerated electrons produced under a high DC voltage. For example bombarding a tungsten metal target under 35 kv can produce a continuous X-ray spectrum. Under the same conditions with a molybdenum target, a line spectrum can be produced.

When a X-ray beam with a designated wavelength impinges on a sample, it can be absorbed by the analyte atoms to produce excited ions with a vacated K shell. After a brief period, these excited ions are back to their ground state and release their energy in X-ray emission form. Usually the emission wavelength is longer than that of the exciting X-ray, so the process is called X-ray fluorescence (XRF). In a defined range of concentration, there is a linear relationship between the analyte concentration in the sample and the X-ray fluorescence emission. This method has long been used for thorium [31] and uranium [32, 33] analysis. The advantage of the XRF method is that many samples can be directly analysed without destruction of the sample. This is especially important for paintings, archaeological specimens, jewellery and other precious objects. The chief drawback of this method is the high cost of the instrumentation.

2.4 CHROMATOGRAPHIC METHODS FOR THORIUM AND URANIUM DETERMINATION

2.4.1 INTRODUCTION

Ion-exchange has long been used as a method for the determination of inorganic ions [34, 35]. When a mixture of ions is passed through an ion-exchange column, the components are separated on the column by virtue of their different distribution coefficients between the mobile and stationary phases. Collecting the

column effluent fractions permits each component in the sample to be quantified with a suitable analytical method, such as titration [36], potentiometry [37], spectroscopy [38] fluorimetry [39] and so on. However, such discontinuous procedures are time consuming and generally offer poor analytical sensitivity.

In 1975 Small *et al.* [2] published the first paper on suppressed ion-chromatography (IC), which combined ion-exchange separation with conductivity detection for anion analysis. Since then numerous alternative IC separation methods have been developed, such as ion-interaction and ion-exclusion. Whilst the early IC analyses used a conductivity detector, many other detection methods have since been introduced as the technique of IC has developed. Some of the commonly used chromatographic separation and detection methods for the determination of thorium and uranium are listed in Fig. 2.2.

2.4.2 CHROMATOGRAPHIC SEPARATION METHODS

2.4.2.1 Cation-Exchange Chromatography

Usually, the separation of thorium(IV) and uranyl are performed with a cation-exchange column using a strong acid solution as the eluent, such as HCl [40] or H_2SO_4 [41, 42]. The column can be either a silica-based[43] or a resin-based [44, 45] cation-exchanger. The silica-based cation-exchange column is made by chemically binding sulfonic acid groups onto micro-particulate silica. Many different types of functionalised silica ion-exchangers have been developed since non-suppressed ion-chromatography was introduced in 1979 [46]. The chief advantage of silica-based ion-exchange columns is their high chromatographic efficiency [47]. In addition, silica is available in small size particles which produce a uniform and stable chromatographic bed that is not subject to stringent pressure or flow-rate limitations [48]. However, the chief drawback of the silica-based materials is the restriction of the eluent working pH to the range of 2-7. Continual use at lower pH will decrease the ion-exchange capacity due to cleavage of the functionalised groups, whilst alkaline

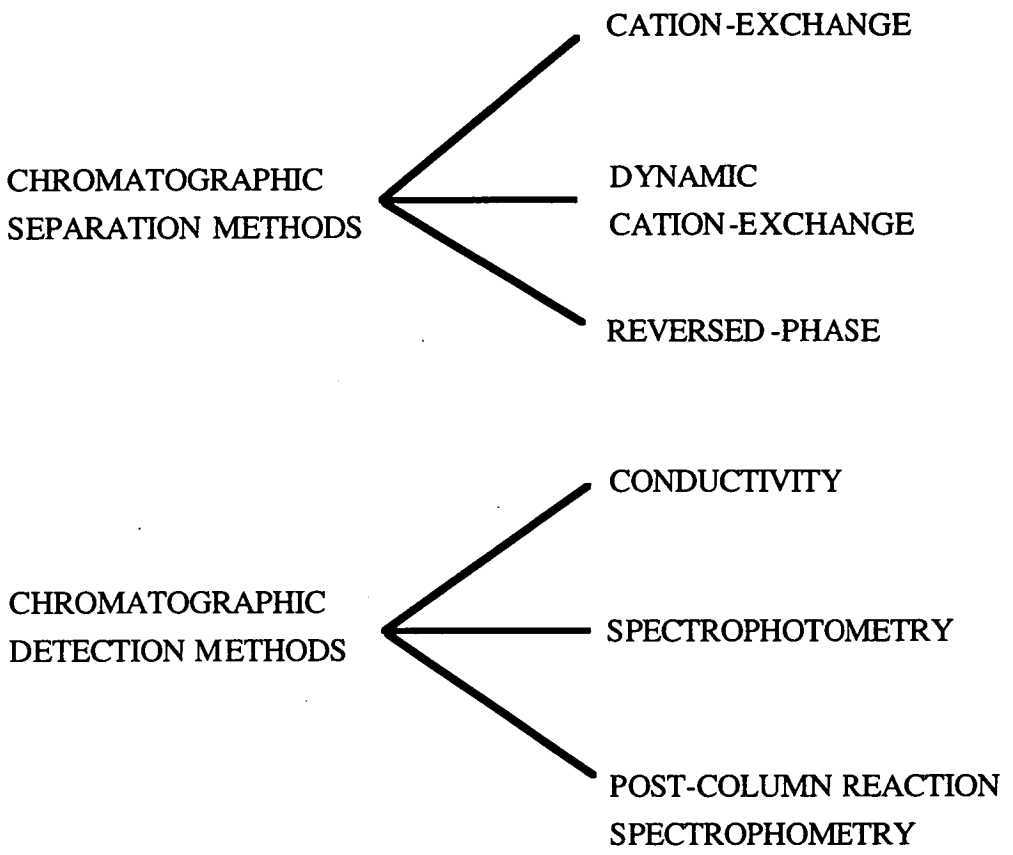

Fig. 2.2 Classification of chromatographic separation and detection methods used for thorium and uranium analysis.

samples or eluents can dissolve the silica matrix [49]. Additionally, the silica-based exchangers are usually prepared in a low ion-exchange capacity form, so the sample size is limited.

Resin-based cation-exchangers are usually produced by surface sulfonating polystyrene-divinylbenzene (PS-DVB) copolymers. The main advantage of this type of packing is its pH tolerance which allows the eluent and sample pH to vary from 0 to 14. This is benefit in cation separations, for a strong inorganic acid is often used as the eluent, and some metal cations are only stable in acidic solution. Most thorium and uranium cation-exchange analyses are performed with resin-based columns [50, 51]. The chief drawback of resin-based columns is that their length and eluent flow-rate are limited because the polymeric resin is a relatively soft material.

The separation of thorium(IV) and uranyl by cation-exchange chromatography is based on the differences in distribution coefficients of the two analytes on the column. As described in the previous section, in an aqueous solution uranium is usually present as a divalent cation, UO_2^{2+}, whilst thorium exists as the tetravalent Th^{4+}. Considerable differences are therefore observed in their relative affinity for a cation-exchanger. Tables 2.1 to 2.3 list the distribution coefficients of thorium(IV) and uranyl (and Fe^{3+} as a reference) in different acids and various concentrations on a cation-exchange resin. Using a hydrochloric acid or nitric acid eluent, a relatively low acid concentration can be used to elute uranyl from the cation-exchange column, but elution of thorium(IV) requires a higher acid concentration. In order to overcome this problem, thorium(IV) cation-exchange chromatography is usually performed by gradient elution, for example, with a gradient of hydrochloric acid from 1 to 4 M [52]. However, this can often cause difficulties in detection.

Compared to hydrochloric acid and nitric acid, the thorium(IV) distribution coefficients in sulfuric acid solution are relatively low at the same concentrations. Perhaps the complexation of thorium(IV) with sulfate [53] reduces its affinity for the

cation-exchange resin. Harrold *et al.* [54] has used a sulfate eluent to separate thorium(IV) on a cation-exchange column (Dionex CS2), using a gradient of sodium sulfate from 0.6 M HCl to 0.6 M HCl-0.5 M Na_2SO_4 within 15 minutes. More recently, Al-Shawi and Dahl [55] have reported the determination of thorium(IV) and uranyl with an ammonium sulfate gradient from 0.4 M HCl-0.1 M $(NH_4)_2SO_4$ to 0.4 M HCl-1.0 M $(NH_4)_2SO_4$ within 5.0 minutes, or from 0.25 M HNO_3-0.1 M $(NH_4)_2SO_4$ to 0.25 M HNO_3-1.0 M $(NH_4)_2SO_4$ in 5 minutes, using a Dionex IonPac CS10 cation-exchange column.

Alternatively, it has been reported that the cation-exchange chromatographic eluent could be prepared by mixing an inorganic acid with a suitable complexing ligand, such as hydrochloric acid-ammonium citrate [56] and hydrochloric acid-sodium tartrate [57]. The purpose of adding the ligand to the eluent is to reduce the effective charge on the solutes, therefore decreasing their affinity for the cation-exchanger.

Table 2.1 WEIGHT DISTRIBUTION COEFFICIENTS FOR METAL CATIONS IN HYDROCHLORIC ACID AND A CATION-EXCHANGE RESIN [58]

Cation	HCl (M)			
	0.1	0.2	0.5	1.0
UO_2^{2+}	5420	860	102	19.2
Th^{4+}	$>1x10^5$	$>1x10^5$	$>1x10^5$	2049
Fe^{3+}	9000	3400	225	35.45

Table 2.2 WEIGHT DISTRIBUTION COEFFICIENTS FOR METAL CATIONS IN NITRIC ACID AND A CATION-EXCHANGE RESIN [59]

Cation	HNO_3 (M)			
	0.1	0.2	0.5	1.0
UO_2^{2+}	659	262	69.0	24.4
Th^{4+}	$>1x10^4$	$>1x10^4$	$>1x10^4$	1180
Fe^{3+}	$>1x10^4$	4100	362	74

Table 2.3 WEIGHT DISTRIBUTION COEFFICIENTS FOR METAL CATIONS IN SULFURIC ACID AND A CATION-EXCHANGE RESIN [60]

Cation	H_2SO_4 (M)			
	0.1	0.25	0.5	1.0
UO_2^{2+}	118	29.2	9.6	3.2
Th^{4+}	3900	264	52.0	9.0
Fe^{3+}	2050	255	58.0	13.5

2.4.2.2 Ion-Interaction Chromatography

Of all the chromatographic methods employed for thorium and uranium analysis, ion-interaction chromatography is perhaps the best developed. This method is also referred to as ion-pair chromatography [61], dynamic ion-exchange chromatography [62], mobile phase chromatography [63] and so on. In this method a conventional reversed-phase column is generally used with a mobile phase containing a hydrophobic ion-interaction reagent (IIR), such as n-octanesulfonate acid (OSA), which assists the retention of the ionic solutes on the reversed-phase column. A complexing ligand is usually added into the eluent in order to reduce the effective charge on the cation analytes. Most of the ion-interaction eluents are prepared in an aqueous solution containing a certain percentage of organic modifier, so the solutes can be eluted within a reasonable time [64]. The chief advantage of ion-interaction chromatography is its flexibility which allows manipulation of the ion-exchange capacity and selectivity of the stationary phase.

A large volume of literature focused on the study of ion-interaction mechanisms has been published. Three models have been suggested based on the establishment of different equilibria. The first is the so called ion-pair model, which presumes that the solute ion and the hydrophobic IIR form a neutral ion-pair in the eluent, then adsorbed on the hydrophobic stationary phase in the same manner as the retention of any neutral molecule on a conventional reversed-phase column. Therefore the retention of the solute depends on the hydrophobicity of the ion-pair, which is further determined by the hydrophobicity of the IIR. An increased percentage of organic modifier in the mobile phase will decrease the affinity of the ion-pair for the stationary phase, which results in reduced retention. Solutes with the same charge as the IIR will not form ion-pairs, so they are eluted at the solvent front unless they have sufficient hydrophobicity to show retention.

The dynamic ion-exchange model suggests that the hydrophobic IIR is

dynamically adsorbed on the stationary phase, which converts the column to a dynamic ion-exchanger because the IIR carries a negative or positive charge. The ion-exchange capacity of the column is dependent on the amount of IIR adsorbed on the column, which is further determined by the hydrophobicity of the IIR, its concentration in the eluent and also the organic modifier concentration. When solutes having the opposite charge to the IIR pass through the dynamic ion-exchange column, they are retained on it in the same manner as in a conventional ion-exchange column. Solutes with the same charge as the IIR will be eluted at the solvent front due to repulsion from the charged stationary phase, whilst the retention of neutral solutes is unaffected by the presence of the IIR.

The ion-interaction model contains elements of the two previous models, which suggests that an electric double-layer is formed on the stationary phase. The hydrophobic IIR is dynamically adsorbed on the stationary phase and forms the primary charged layer, which attracts oppositely charged ions (usually the counter ion of the IIR) to form the secondary charged layer. The amount of charge in both layers is dependent on the amount of IIR adsorbed, which further depends on the hydrophobicity of the IIR, its concentration and also the amount of the organic modifier in the mobile phase. When a solute with opposite charge to the IIR is passed through this column, it penetrates to the primary layer. In order to keep the charge balance, an IIR ion is also adsorbed to the primary layer. The result is that a pair of ions, namely a solute anion and the IIR ion, are retained on the column, but not necessarily in an ion-pair form.

Although a wide range of stationary phases is available, thorium(IV) and uranyl ion-interaction chromatography is usually performed with a conventional C_{18} silica-based reversed-phase column [65, 66]. The advantage of the silica-based column is that it gives high chromatographic efficiency and allows operation at high pressures, due to the possibility of column being packed with very small particles of silica, such as 3 μm and 5 μm [8]. In addition, the pH limitation of the silica-based

column has little effect on ion-interaction chromatographic analysis, because most of the eluents are buffered in a weak acid (the complexing agent) solution, such as α-hydroxyisobutyric acid [8] and lactate [62]. This technique has also been reported using a neutral PS-DVB column [67] for the analysis of thorium and uranium. The choice between stationary phases is generally based on the considerations of chromatographic efficiency, pH stability and particle size, rather than on chromatographic selectivity.

The IIR is the most important component in the ion-interaction chromatography eluent. The capacity of a dynamically-coated ion-interaction column is primarily determined by the amount of the IIR adsorbed on the stationary phase, which is directly related to IIR hydrophobicity and concentration, as well as the nature and percentage of the organic modifier in the eluent. Cation separations are usually performed using alkylsulfonic acids as the IIR, such as pentanesulfonic acids [68] and butanesulfonic [69]. Most previous reports used sodium n-octanesulfonate (OSA) as the IIR for the separation of thorium(IV) and uranyl [70, 71].

α-hydroxyisobutyric acid (HIBA) is the commonly used complexing ligand for thorium(IV) and uranyl ion-interaction chromatographic analysis [8, 72], for it forms stable complexes with these metals. Usually, HIBA is prepared in the mobile phase, so its complexes are formed *in-situ*. It has also been reported [61] that thorium(IV) and uranyl were complexed prior to loading onto the dynamically coated ion-exchange column.

2.4.2.3 Reversed-phase Chromatography

In previous ion-interaction chromatographic studies, it has been noted that thorium(IV) and uranyl could be retained on reversed-phase columns without the presence of any anionic IIR (such as OSA), providing a complexing ligand was prepared in the mobile phase [73, 74]. In this method, a reversed-phase column [75, 76] is used with an aqueous solution containing an organic modifier as the mobile

phase. The metal cations are complexed with a hydrophobic ligand either prior to injection or *in-situ*. Many papers have been published on the determination of metal cations using reversed-phase chromatographic techniques. Hutchins *et al.* [77] used diethyldithiocarbamate to derivatise a range of cations, such as cadmium, lead, cobalt, selenium, and separated these complexes on a C_{18} silica column using a mobile phase comprising 40% methanol, 35% acetonitrile and 25% water. The above technique has also been reported using a neutral polymer resin-based cartridge as the analytical column [78]. Main and Fritz [79] used a PS-DVB reversed-phase column to separate titanium, iron, vanadium, thorium and uranium after precolumn derivatisation with 2,6-diacetylpyridine-bis(aroylhydrazone). It has been reported that an auxiliary complexing reagent, such as EDTA [81], was added in the mobile phase to serve as a masking agent. Strongly hydrophobic reagents, such as cetyltrimethylammonium bromide (CTAB) [80, 81], and tetrabutylammonium (TBA) hydroxide [82], have also been added to eluents, with the resulting metal complexes being strongly retained on the reversed-phase column.

Most of the cation reversed-phase chromatographic analyses was performed by complexing the cations prior to injection, this is the so called precolumn derivatisation. A suitable complexing ligand is selected which forms strong and mostly neutral complexes with the analyte cations. In order to increase the stability of these complexes the complexes were usually kept for a short period after derivatisation, or stabilised with heat treatment [83]. For example, Jen and Yang [84] kept the complex reaction for 20 min when derivatising the VO^{2+} and VO_2^+ with EDTA. Iki *et al.* [85] heated 2-pyridylaldehydebenzoylhydrazone chelates at 60 °C for 15 min for the derivatisation of transition metal cations. The resulting solutions often need dilution before the chromatographic injection due to the derivatisation usually being performed in concentrated solution.

Some complexing derivatisation reactions occur very fast at room temperature and do not need precolumn derivatisation. In this case the complexing reagent can be

simply prepared in the chromatographic eluent, so the derivatisation takes place *in-situ*. Cassidy and Chauvel [86] were prepared HIBA as the complexing ligand in mobile phase to separate the lanthanides on a C_{18} column. The advantage of *in-situ* derivatisation is its simplicity and that the working conditions can be easily altered by adjusting certain parameters, such as the complexing ligand concentration. In addition, most examples of precolumn derivatisation still require the addition of the complexing ligand to the mobile phase to prevent the complex dissociating during the chromatographic procedure [87].

The precolumn derivatisation reagents (PDR) for metal analysis are generally multidentate ligands which form stable chelates with certain metal cations. The function of the PDR here is to increase the hydrophobicity of the metal cation, so it can be retained on a reversed-phase column. Early examples of this technique included dithiocarbamate [88] and its derivatives which were widely used as the PDR, for example bis(2-hydroxyethyl) dithiocarbamate [89] and diethyldithiocarbamate [90]. Many papers reported using colour forming reagents as the PDR, such as 2-pyridylaldehydebenzoylhydrazone (PAB) [84], 1-(2-pyridylazo)-2-naphthol (PAN) [82], 4,4'-bis-(dimethylamino)-thiobenzophenone (TMK) [86], and 4-(2-pyridylazo)-resorcinol (PAR) [91]. The advantage of precolumn derivatisation with a colour forming reagent is that the chromatography can be directly monitored with a spectrophotometer without any further treatment, such as post-column reaction. Fluorescence reagents have also been employed for precolumn derivatisation [92] with a fluorescence spectrophotometer for detection.

2.4.3 CHROMATOGRAPHIC DETECTION METHODS

2.4.3.1 Conductivity Detection

Conductivity detection is one of the earliest detection methods used in ion-chromatography. It offers simplicity and serves as a universal method for the detection of ionic species. In aqueous eluents the ionic species are dissociated. A

signal is observed when the ions pass through the conductivity cell. The signal results from the difference in the conductivity (ΔG) between the solute ions and the eluent ions. Take anion-exchange as an example:

$$\Delta G = \frac{(\lambda_{S^-} - \lambda_{E^-})C_S}{10^{-3}K} \qquad (2.7)$$

where λ_{S^-} and λ_{E^-} are the limiting equivalent ionic conductances of the solute and the eluent anions, respectively, C_S is the concentration of the solute, and K is the cell constant. Eqn. 2.7 indicates that the bigger the difference between the limiting equivalent ionic conductance of the solute and the eluent, the higher the signal observed in the conductivity detector. If the conductance of the eluent is lower than that of the solute, a positive peak results. This is termed direct conductivity detection. For direct conductivity detection potassium hydrogen phthalate or sodium benzoate is often used in the eluent for anion analysis, because of their low conductance. If the eluent has a high conductance, the solute ion gives a negative peak. This is termed indirect conductivity detection, which can be observed when a hydroxide eluent is used for anion analysis, or a mineral acid eluent is used for cation analysis.

Conductivity detection is usually combined with ion-exchange separation techniques. Smith and Pietrzyk [93] has used conductivity to detect the lanthanides using ion-chromatography with 0.8 mM lithium tartrate at pH 4.5 as the eluent, obtaining a detection limit of about 1 ppm. Tong *et al.* [94] also reported that all the lanthanides could be monitored with conductivity detector after the separation using cation-exchange chromatography.

2.4.3.2 Spectrophotometric Detection

Spectrophotometry is another widely used method for ion-chromatographic detection. The photometric signal (ΔA) results from the difference in absorption between the solute and eluent ions as a solute passes through the detector cell. Taking an anion-exchange system with a fully dissociated solute as an example, ΔA can be

calculated based on the Beer's law:

$$\Delta A = (\varepsilon_{S^-} - \varepsilon_{E^-})\, C_S\, m \qquad (2.8)$$

where C_S is the solute concentration, m is the path-length of the detector cell, ε_{S^-} and ε_{E^-} are the molar absorptivities of the solute and the eluent anions, respectively. If the molar absorptivity of the solute anion exceeds that of the eluent anion, ΔA is a positive value. This is termed direct spectrophotometric detection. If the molar absorptivity of the solute anion is less than that of the eluent anion, ΔA is negative, resulting in indirect spectrophotometric detection. The direct detection is one of the most straightforward detection methods used in ion-chromatographic analysis, for many inorganic anions, metal cations and their complexes exhibit UV absorption [95, 96, 97]. With indirect detection the signal results from the "vacancy" absorption as the solute passes through the detector, so its detection limit can be improved by increasing the eluent absorption, for example by selecting a maximum absorption wavelength for the eluent ion. However, this improvement is limited because it also increases the baseline noise.

2.4.3.3 Post-Column Reaction Detection

Thorium(IV) and uranyl exhibit a weak UV absorption when they are detected directly by spectrophotometry. Most of previous IC analyses monitored thorium(IV) and uranyl after post-column reaction (PCR). With the PCR technique a chemical reagent is introduced into the column effluent to react with the solutes prior to their entering the detector. The chief aim of this approach is to increase the sensitivity and specificity of the detection method, so it can monitor the analytes at low concentrations or in the presence of high concentrations of interfering ions. There are several techniques to introduce the PCR reagent. Usually, it is prepared in a solution then pumped into the column effluent, as shown in Fig. 2.3.

Previous studies have shown that the baseline noise observed using PCR

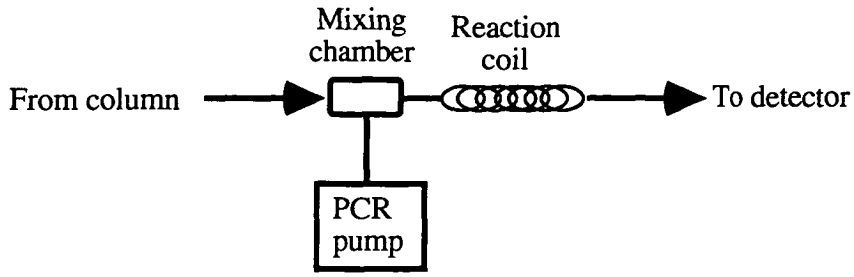

Fig. 2.3 Schematic diagram of post-column reaction system.

detection mainly resulted from pump pulsations. Therefore syringe pumps are often preferred for PCR reagent solution delivery. Alternatively, a simple over-head pressured pneumatic delivery system is often used. Both of these pumps are commercially available. For the latter mode, the necessary hardware is usually made from non-metallic materials, so it is specially suitable for cation analysis.

The PCR solution and the column effluent are mixed together in a mixing chamber. The mixing efficiency directly affects the analyte peak. Several types of mixing apparatus have been suggested, including tee-pieces, Y type devices, and membrane reactors [98, 99, 100]. Generally, a 90° tee-piece is used because of its simplicity and ease of construction, with two inlet tubes for the column effluent and the PCR reagent and an outlet tube for the mixed solution to the reaction coil or directly to the detector. Usually, the post-column reaction between inorganic ions and the PCR reagent are carried out swiftly, so the reaction coil is not necessary as it may result in peak broadening.

PCR detection is used mostly in cation analysis, especially for transition metals, the lanthanides and the actinides. In fact, this method has been developed as the optimal detection mode for these metals. It is of primary importance to select a suitable PCR reagent for this type of detection. The PCR reagent should give a strong

signal after reaction with the analytes, be stable in the eluent, and not produce undesirable products such as precipitates or gases when mixed with the effluent. 4-(2-pyridylazo)-resorcinol (PAR), 2-(4,5-dihydroxy-2,7-disulfo-3-naphthylazo)-phenylarsonic acid (Arsenazo I) and 2,7-bis(2-arsonophenylazo)-1,8-dihydroxynaphthalene-3,6-disulfonic acid (Arsenazo III) are typical PCR reagents. The structures of PAR, Arsenazo I and Arsenazo III are shown in Fig. 2.4. These reagents all form coloured chelates with certain metal cations which result in strong absorption. Previous reports have shown that PAR is especially suitable for the transition metals [4, 101, 102], and Arsenazo III is the optimal reagent for the lanthanides [103, 104].

PAR [105] in free acid form is an orange-red amorphous powder, which is slightly soluble in water, its solubility increasing in acidic or alkaline solutions. The PCR solution is usually prepared in an alkaline buffer, such as 3 M ammonia-1 M acetate. As a non-selective ligand PAR reacts with a variety of metal cations forming stable chelates, in which PAR behaves as a bidentate or tridentate ligand. Most of these PAR chelates are red or red-violet in colour, and can be detected using a spectrophotometer in the range 500-540 nm. The detection limit for the PAR chelate is dependent on the conditions used, especially the PAR concentration for it contributes to the baseline noise. It is recommended that the concentration of PAR in PCR solution should be as low as possible.

Arsenazo I [106] is available commercially as a disodium salt, which is a dark red crystalline powder. It is easy to dissolve in an aqueous solution and exhibits an orange-red colour. In acidic solution (pH 1-8) it reacts with a variety of metal cations to form coloured chelates. For example, its thorium(IV) complex is blue violet, whilst its uranyl and rare earth complexes are orange-red in colour. The metal:ligand ratio of the Arsenazo I complex is usually 1:1. Previous work [107] has shown that the absorption spectra of these Arsenazo I complexes in aqueous solution are pH dependent. Increasing the solution pH will result in a shift of λ_{max} toward the higher

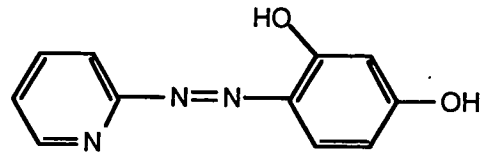

(a)

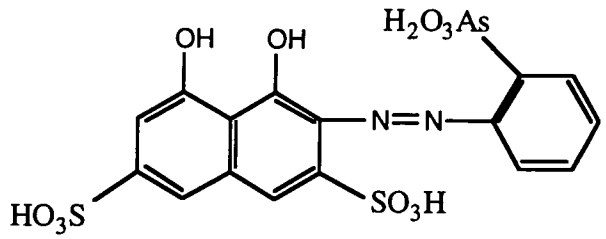

(b)

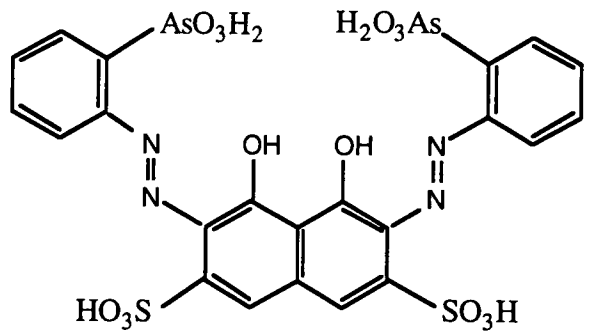

(c)

Fig. 2.4 Structures of PAR (a), Arsenazo I (b) and Arsenazo III (c).

wavelengths. Now, a more sensitive reagent, Arsenazo III, is available which has replaced Arsenazo I in the use of metal spectrophotometric analysis.

Arsenazo III [108] is a highly sensitive photometric reagent, especially for thorium(IV), uranyl and other hydrolysable multivalent metal ions. It is slightly soluble in water, and the solubility increases with raising the solution pH. Arsenazo III reacts with a range of metal cations in solution at pH values from acidic to alkaline. It has been shown that Arsenazo III has high sensitivity and selectivity when used as a PCR reagent for the detection of the lanthanides. The molar absorptivities of these coloured complexes are in the order of 10^5. The metal:ligand ratio for the Arsenazo III chelates varies from 1:1 to 1:3, or 2:2, depending on the nature of the metal cation, mixing ratio and the solution conditions. Fig. 2.5 shows some structures of Arsenazo I and Arsenazo III chelates. The PCR method with Arsenazo III as the PCR reagent has been widely used for the analysis of transition metals and the lanthanides combined with ion-exchange or ion-interaction chromatography.

2.5 PRECONCENTRATION TECHNIQUES FOR TRACE ELEMENTS

2.5.1 PRINCIPLES OF PRECONCENTRATION

The sensitivity of an IC method is strongly dependent on the type of detector used. Previous publications have reported that the practical detection limits of conductivity and indirect spectrophotometry average around 100 ppb for a 100 µl injection. Considering matrix interferences, routine IC analysis requires that the solute concentration should be about 1 ppm or higher in order to obtain a reliable result. Below this concentration a larger volume of sample solution can be injected, or preconcentration techniques can be applied prior to the chromatographic analysis.

Solvent extraction is one of the simplest and most straightforward methods used for the concentration of trace levels analytes. With this method the sample is initially prepared in an aqueous solution, then mixed with an organic solvent. The

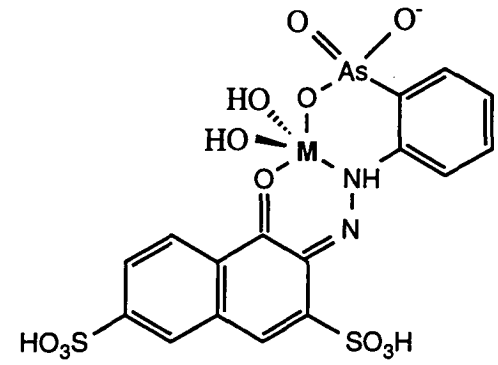

(a)

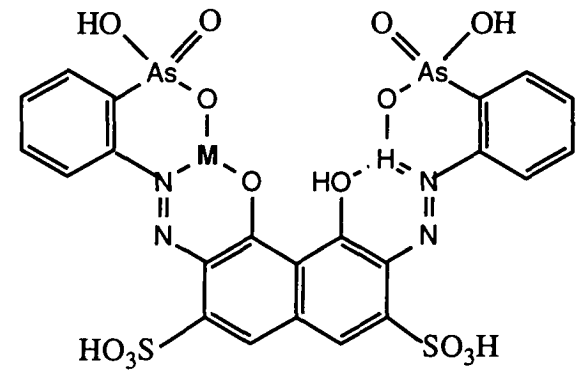

(b)

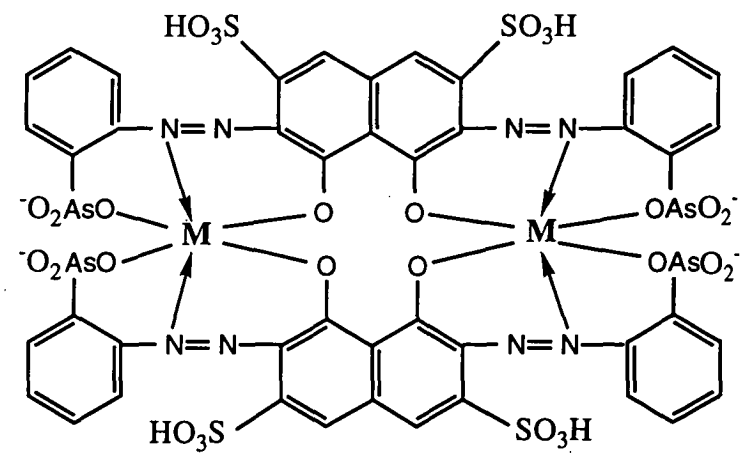

(c)

Fig. 2.5 Structures of (a) metal-Arsenazo I, (b) and (c) metal-Arsenazo III complexes.

analytes are distributed between the two immiscible phases. At a given temperature there is an equilibration for the distribution:

$$A_a \leftrightharpoons A_o \tag{2.9}$$

where A is the analyte, and the subscripts a and o refer to the aqueous and organic phases, respectively. The proportion of the analyte transferred from the aqueous phase to the organic phase is given by the distribution coefficient, D_A, which is defined as:

$$D_A = \frac{[A_o]}{[A_a]} \tag{2.10}$$

The extraction efficiency, E, is related to the distribution coefficient by the following equation:

$$E = \left(\frac{[A_o]V_o}{[A_a]V_a + [A_o]V_o} \right) \times 100\% \tag{2.11}$$

where the V_a and V_o are the volumes of the aqueous and organic phase, respectively. Introducing the distribution coefficient D_A (Eqn. 2.10) into Eqn. 2.11:

$$E = \left(\frac{1}{\frac{1}{D_A} \times \frac{V_a}{V_o} + 1} \right) \times 100\% \tag{2.12}$$

It can be seen that the extraction efficiency depends on the value of the distribution coefficient, D_A, and the ratio of the two phase volumes, V_a/V_o. For simplicity, the activity coefficient of the solute is taken as unity, and it is assumed that the solute exists in only one form in each phase.

Solvent extraction has the advantage of simple and low cost equipment, but the operation is time consuming and often unsuitable for routine analysis. However, the general concept of concentration is applied to other extraction techniques. The

chromatographic preconcentration technique involves using solid stationary phase which replaces the organic solvent, so it is referred to as solid extraction. With this method, the stationary phase is preconditioned with a suitable solution, then equilibrated with the sample. The components of the sample are distributed between the sample solution and the stationary phase in a similar manner to that of solvent extraction. Back-extraction of the trapped solutes occurs from the stationary phase into a small volume of solution, resulting in concentration of the analytes prior to analysis.

2.5.2 PRECOLUMN PRECONCENTRATION

Chromatographic preconcentration is usually performed using a precolumn. That is, a solid stationary phase packed into a column is used as the concentrator, through which a measured volume of sample solution is passed for enrichment. This column preconcentration technique can be performed either off-line or on-line. In the off-line mode, the preconcentration procedure and chromatographic analysis are operated separately. Sample solution is loaded on the concentrator manually or using a pump, then stripped with a suitable eluent for chromatographic injection. Clearly, separate operation in the off-line preconcentration is time consuming. This disadvantage can be overcome by coupling the preconcentration and chromatographic system together using a high-pressure valve, and all the procedures of sample loading, back-extraction and chromatographic analysis can be performed automatically by a computer program. This is termed on-line preconcentration. In this study both off-line and on-line preconcentration techniques have been used for the determination of trace level thorium and uranium.

2.5.2.1 Single-Valve On-Line Preconcentration System

The first on-line preconcentration system could be traced back to the late 1970's [109]. Since then this technique has been extensively developed, with the single-valve preconcentration system being most commonly used. A typical single-

valve preconcentration system consists of a concentrator column, a sample loading pump and a high-pressure valve. The concentrator is switched in and out of the chromatographic eluent flow-path by rotating the valve, as shown in Fig. 2.6. Usually, the rotary valve is a six-port high-pressure valve which can be operated either manually or automatically.

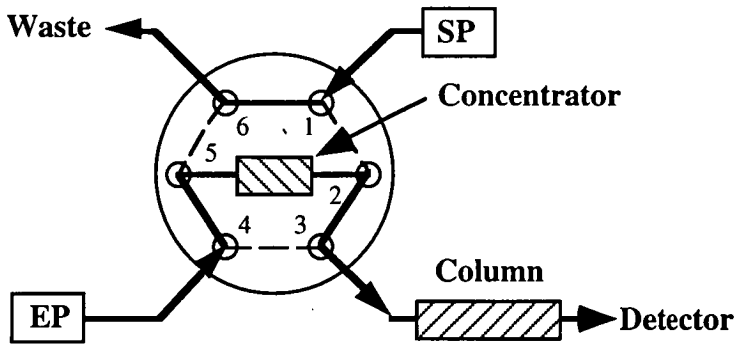

Fig. 2.6 Schematic diagram of a single-valve preconcentration system, which comprises a concentrator column, a sample loading pump (SP) and a single high-pressure valve. The preconcentration system is combined together with the chromatographic system through the switching valve.

The single-valve preconcentration system is usually performed in a sequence of four steps [110]:

(a) Column equilibration. Firstly, the chromatographic eluent is pumped through both the concentrator and analytical columns to remove any residues from the previous sample and to equilibrate them. This is an important step to achieve reproducible results. Meanwhile, the sample pump delivers the sample solution through the valve being directly to waste for flushing the tubs.

(b) Loading sample. In this step the valve is rotated to switch the concentrator column into the sample flow-path with the effluent being directed to waste, whilst the

chromatographic eluent flows continually through the analytical column. The volume of sample loaded can be measured by monitoring the flow-rate during the loading period. The concentrator column is so selected that all the interested analytes in the sample are selectively bound onto it during this stage.

(c) Sample stripping. After loading a measured amount sample the valve is rotated back to allow the chromatographic eluent to pass through the concentrator to elute the enriched analytes onto the analytical column.

(d) Chromatographic analysis. Finally, the valve is rotated to remove the concentrator from the chromatographic eluent flow-path. The analytes are separated and quantified on the analytical column as in normal chromatographic analysis.

Technically, the sample loading direction is opposite to that used in the sample stripping step, so this is called a "back-flush". It is expected that the analytes can be bound to the area of sorbent near to the end of the concentrator column where the sample is introduced. This helps to reduce the stripping volume required, therefore minimising band broadening effects.

The chief advantage of the single-valve preconcentration system is its simplicity and ease of operation. However, one major drawback of this system is that the same eluent is used to equilibrate the concentrator column, to strip the enriched components, and to separate the analytes on the analytical column. This may have an effect on quantitative analysis.

2.5.2.2 Two-Valve Preconcentration System

Most of the disadvantages of the single-valve preconcentration system can be overcome by using a two-valve preconcentration system. Fig. 2.7 shows the schematic diagram of a two-valve preconcentration system, which consists of a concentrator, two high-pressure valves, a low-pressure solvent selection valve, and a sample loading pump, in addition to the chromatographic analysis system.

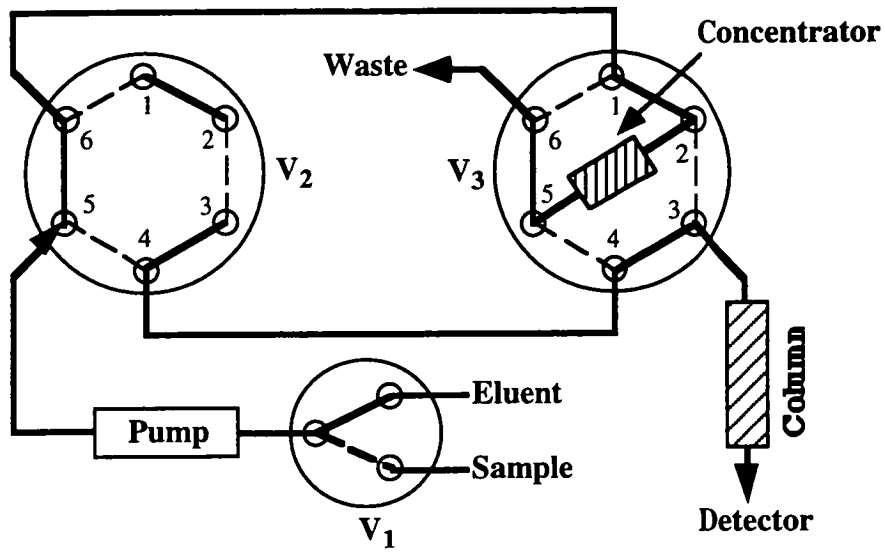

Fig. 2.7 Schematic diagram of a two-valve preconcentration system, which is comprised of a concentrator, two high-pressure valves (V_2, V_3), a low-pressure solvent selection valve (V_1) and a sample loading pump. The preconcentration system is combined together with the chromatographic system through the valves.

The two-valve preconcentration system is usually operated in a sequence of seven steps:

(a) Column equilibration. Firstly, the chromatographic eluent is pumped through both the concentrator and the analytical columns for equilibration.

(b) Sample flushing. In this step, both the concentrator and the analytical columns are removed from the flow-path, and the solvent selection valve is switched to sample. The sample solution is then flushed through all the tubing.

(c) Loading sample. The concentrator column is inserted into the flow-path and a measured volume of sample is loaded.

(d) Eluent flushing. The low-pressure valve is switched back to the eluent. The eluent is then flushed through all the tubing.

(e) Concentrator washing. The concentrator column is inserted into the flow-path. A small volume of eluent is pumped through it in the same direction as that used for sample loading with the effluent being directed to waste. The purpose of this step is to remove any unwanted sample components which were retained on the concentrator.

(f) Sample stripping. The concentrator column is then inserted into the chromatographic eluent flow-path to transfer the enriched analytes from the concentrator onto the analytical column.

(g) Chromatographic analysis. Finally, the concentrator column is removed from the flow-path and the chromatographic eluent is pumped directly to the analytical column where the analytes are separated and quantified. The analytes are eluted in the opposite direction to that of the loading steps.

It should be noted that there is a flushing step whenever the eluent or sample solutions are switched. This is a necessary step, especially prior to loading the sample. The pump and tubes contain solution left from the previous run, which if not removed will reduce the accuracy of the sample volume. This flushing can be performed at a high flow-rate since no column is present in the flow-path.

If required, one more low-pressure valve can be added in order to equilibrate the concentrator with a solution which differs to the chromatographic eluent [111]. The two-valve preconcentration system appears complicated, but it is simple to operate, particularly if the procedure is performed automatically by means of a programmable pump or a computer.

2.5.3 FACTORS AFFECTING ON-LINE PRECONCENTRATION

The efficiency of the preconcentration process is primarily dependent upon two factors: the analytes should be quantitatively bound on the concentrator during the loading step and quantitatively transferred onto the analytical column in the following

step. There are several parameters affecting the binding and transferral efficiencies, such as the capacity of the concentrator, the composition of the equilibration eluent, and the sample loading manner. Using anion preconcentration as an example, the major parameters which affect the preconcentration efficiency are discussed below.

2.5.3.1 The Character of the Concentrator Column

The concentrator column is the heart part of the preconcentration system, which provides the residence sites for the analytes during the sample loading step. Previous studies have shown that the nature of the packed materials in the concentrator column generally affect the preconcentration efficiency [112]. The requirements of the concentrator are twofold. Firstly, the concentrator capacity should be as high as possible in order to quantitatively bind the solutes during the sample loading step. This can be achieved by using a strong anion-exchange column. Secondly, eluting the bound components requires that the stripping eluent volume should be as small as possible in order to minimise band broadening effects, this however suggests the use of a concentrator with a small capacity factor. It has been suggested that the optimal total capacity factor of the concentrator should be around 40% of that of the analytical column [112].

The dimension requirement is that the concentrator column should be as small as possible. Using a small size concentrator enables the analytes to be concentrated within a small region and to be easily stripped with a small volume of eluent. Another advantage of a small size concentrator column is that the sample solution can be loaded at a higher flow-rate, as it produces a lower back-pressure when inserted into the chromatographic eluent flow-path. Guard columns are commonly used as concentrators because they are easy to operate and maintain [113].

2.5.3.2 The Eluent

In most cases, a single eluent is employed for the on-line preconcentration

analysis. The eluent provides three functions during the preconcentration operation. Prior to the sample loading step, the eluent is used to condition the concentrator, permitting the analytes to be quantitatively bound during the following loading step. In the stripping step the eluent transfers the bound components from the concentrator onto the analytical column. This requires the eluent to be strong enough to quantitatively remove the analytes. Finally, it is used as the chromatographic eluent in the analysis step, so it must provide an appropriate resolution for the solutes on the analytical column.

Of the above three functions, perhaps the requirement for an acceptable chromatographic separation is the most important consideration when selecting the eluent [114]. It has been suggested that the analytes should be eluted within a range of capacity factor of 4-30 [115]. The lower limit of 4 is chosen here because a relatively large solvent peak is usually produced in the chromatogram when an on-line preconcentration method is applied and this can overlap early-eluting solutes if their capacity factor is too small. The upper limit of 30 is chosen to prevent excessive retention which is not practical for routine analysis. To strip the trapped components from the concentrator requires the eluent should be as strong as possible. In practice, if the eluent is able to separate the analytes on the analytical column, it must be strong enough to remove these components from the short concentrator column.

However, the requirement to equilibrate the concentrator is in contradiction with the two criteria above, since an equilibration generally requires the use of a weak eluent. This problem can be solved by using two different eluents: one to condition the concentrator, with the other being used as the stripping and chromatographic eluent. For example [116], an anion-exchange concentrator column can be equilibrated with a weak eluent, such as OH^-, and the bound components stripped with a strong eluent, such as HCO_3^-, or CO_3^{2-}. This is usually performed with a two-valve preconcentration system.

2.5.3.3 The Sample Loading Parameters

After choosing a suitable concentrator and eluent, there are some loading parameters to consider which can affect preconcentration efficiency, such as the sample volume and loading speed. Preconcentration methods are usually applied to samples in which the solutes are present at trace level concentrations. One of the primary aims of preconcentration is to increase the sensitivity. It is therefore advantageous to load as large a volume of sample as possible, preferably loaded at a high flow-rate to reduce analysis time. The total volume of sample loaded on the concentrator without loss of analyte is dependent upon the concentrator capacity, which can be determined by measuring the breakthrough volume as described later. With a fixed-site anion-exchange concentrator the maximum flow-rate is dependent on the nature of the eluent used to equilibrate the concentrator column prior to sample loading [117].

2.5.4 EVALUATION OF PRECONCENTRATION PERFORMANCE

Having assembled a preconcentration system, the efficiency of the system can be evaluated with two useful parameters: recovery and breakthrough volume. The recovery of an analyte is determined by comparing the preconcentration result with that obtained by direct injection of an equivalent amount of the analyte. For example, if 10 ml of 20 ppb of an analyte solution is loaded for preconcentration, a 20 μl of 10 ppm of the analyte should be direct injected for comparison. Clearly, the recovery indicates the overall efficiency of the preconcentration performance.

Another useful parameter to assess a preconcentration system is the breakthrough volume [118], which measures the total volume of sample that can be loaded on the concentrator without loss of the analyte. This measurement is accomplished by continually pumping the sample solution through the concentrator column with the effluent being monitored at the outlet, until the analyte starts to appear. The breakthrough volume therefore indicates the amount of analyte which the

concentrator is able to quantitatively bind. Fig. 2.8 shows a typical breakthrough curve which plots the recovery of an analyte by comparing the signals measured at the outlet and inlet of the concentrator against the loading volume.

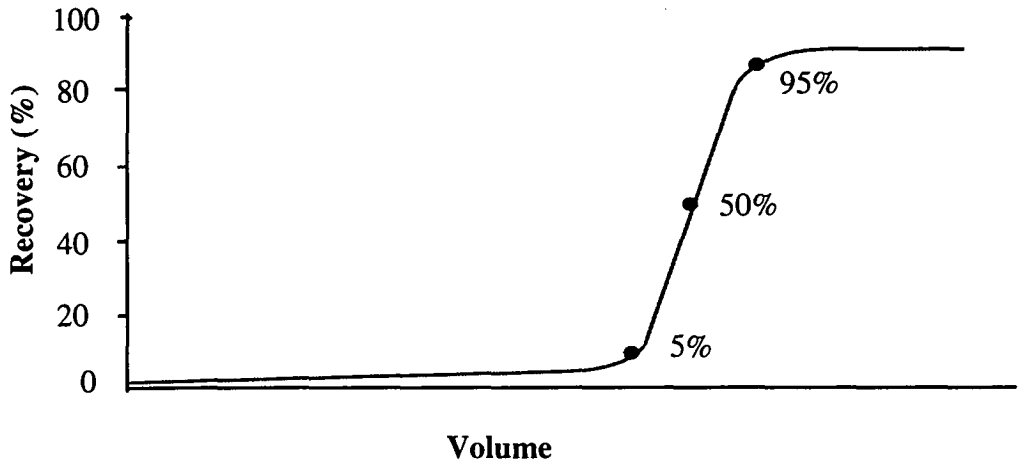

Fig. 2.8 Typical breakthrough curve for a concentrator column.

2.6 AIMS OF THIS STUDY

This project aims to investigate the retention mechanism of thorium(IV) and uranyl on a conventional reversed-phase column using an eluent containing a complexing ligand. This will be achieved by using different ligands and examination of various experimental parameters. The optimal chromatographic conditions will be selected based on this study and applied to the determination of trace levels of thorium and uranium.

2.7 REFERENCES

1 J. J. Katz and G. T. Seaborg, *The Chemistry of the Actinide Elements*, Methuen & Co. Ltd., London, 1957, p. 94.

2 H. Small, T. S. Stevens and W. C. Bauman, *Anal. Chem.*, 47 (1975) 1801.

3 J. S. Fritz and E. M. Moyers, *Talanta*, 23 (1976) 590.

4 G. Schwedt, *Chromatographia*, 12 (1979) 613.

5 J. S. Fritz and J. N. Story, *Anal. Chem.*, 46 (1974) 825.

6 R. M. Cassidy and S. Elchuk, *Anal. Chem.*, 54 (1982) 1558.

7 R. M. Cassidy and M. Fraser, *Chromatographia*, 18 (1984) 369.

8 D. J. Barkley, M. Blanchette, R. M. Cassidy and S. Elchuk, *Anal. Chem.*, 58 (1986) 2222.

9 S. Elchuk, K. I. Burns, R. M. Cassidy and C. A. Lucy, *J. Chromatogr.*, 558 (1991) 197.

10 J. J. Katz and G. T. Seaborg, *The Chemistry of the Actinide Elements*, Methuen & Co. Ltd., London, 1957, p. 16.

11 S. Hietanen and L. G. Sillen, *Acta. Chem. Scand.*, 22 (1968) 265.

12 F. A. Cotton and G. Wilkinson, *Advanced Inorganic Chemistry*, Wiley Interscience, New yeark, 2nd ed., 1967, p. 1090.

13 J. J. Katz and G. T. Seaborg, *The Chemistry of the Actinide Elements*, Methuen & Co. Ltd., London, 1957, p. 94.

14 Y. Okada, S. Hirai, Y. Suzuki and T. Mitsugashira, Science Reports to the Research Institutes Tohoku University Series A-Physics Chemistry and Metallurgy, 40 (1994) 25.

15 Y. Nakamura, Y. Kobayashi and Y. Kakurai, *Bunseki Kagaku*, 42 (1993) 525.

16 M. Franek and V. Krivan, *Analytica Chimica Acta*, 274 (1993) 317.

17 Y. Okada, S. Hirai and T. Mitsugashira, *Bunseki Kagaku*, 42 (1993) 779.

18 Y. Okada, S. Hirai, Y. Suzuki and T. Mitsugashira, Science Reports of The Research Institutes, Tohoku University Series A-Physics Chemistry and Metallurgy, 40 (1994) 25.

19 D. A. Skoog and D. M. West, *Principles of Instrumental Analysis*, Sauders College, Philadelphia, 2nd ed., 1980, p. 467.

20 Y. Okada and S. Hirai, *Bunseki Kagaku*, 42 (1993) 249.

21 M. Rahman, N. I. Molla, A. K. M. Sharif, S. Basunia, S. Islam, R. U. Miah, S. M. Hossain, M. I. Chowdhury, A. D. Bhuiyan and P. Stegnar, *J. Radioanaly. & Nucl. Chemistry-Articles*, 173 (1993) 17.

22 G. D. Kanias, E. Tsitsa, A. Loukis and V. Kilikoglou, *J. Radioanaly. & Nucl. Chemistry-Articles*, 169 (1993) 483.

23 J. C. G. Caburo, M. E. Wrenn, N. P. Singhand and K. Crawford, *J. Radioanaly. & Nucl. Chemistry-Articles*, 182 (1994) 53.

24 L. S. Clesceri, A. E. Greenberg and P. R. Trussell (Editors), *Standard Methods for the Determination of Water and Wastewater*, American Public Health Association, Washington, DC, 17th ed., 1989.

25 J. E. Cantle, *Atomic Absorption Spectrometry*, Elsevier Scientific Publishing Company, Amsterdam, 1982.

26 G. F. Kirkeright and M. Sargent, *Atomic Absolution and Fluorescence Spectroscopy*, London, 1974.

27 Bernhard Welz, *Atomic Absorption Spectroscopy*, Verlag Chemie, 1976.

28 U. Rohr, L. Meckel and H. M. Ortner, *Fresenius J. Anal. Chem.*, 348 (1994) 356.

29 O. Fujino, S. Umetani and M. Matsui, *Analytica Chimica Acta*, 296 (1994) 63.

30 T. Obata, Y. Kobayashi and Y. Kakurai, *Bunseki Kagaku*, 42 (1993) 763.

31 P. Arikan, *J. Radioanal. Chem.* 76 (1983) 267.

32 V. V. Berdikov and B. S. Iokhin, *Radiokim.* 24 (1982) 525.

33 V. L. R. Salvador, Thesis, Inst. de Pesquisas Energeticas e Nucleares, Sao Paulo, Brazil, 1982 p. 91.

34 J. Inczedy, *Analytical Application of Ion-Exchangers*, Pergamon, London, 1966.

35 W. E. Rieman and H. F. Walton, *Ion-Exchange in Analytical Chemistry*, Pergamon, London, 1970.

36 S. Barret, A. G. Croft and A. W. Hartley, *J. Sci. Food Agric.*, 22 (1971) 173.

37 M. S. Front and J. W. Ross, *Anal. Chem.*, 40 (1968) 1169.

38 P. R. Buck, S. Singhadeja and L. B. Rogers, *Anal. Chem.*, 26 (1954) 2603.

39 J. R. Thayer and R. C. Huffaker, *Anal. Chem.*, 26 (1980) 110.

40 J. S. Fritz and J. N. Story, *Anal. Chem.*, 46 (1974) 825.

41 J. J. Byerley, J. M. Scharer and G. F. Atkinson, *Analyst*, 112 (1987) 41.

42 Dionex Application Note, 48, 1983.

43 P. R. Haddad, P. W. Alexander and M. Trojanowicz, *J. Chromatogr.*, 324 (1985) 319.

44 J. E. Girard, *Anal. Chem.*, 51 (1979) 836.

45 J. J. Byerley, J. M. Scharer and G. F. Atkinson, *Analyst*, 112 (1987) 41.

46 D. T. Gjerde, J. S. Fritz and G. Schmuckler, *J. Chromatogr.*, 186 (1979) 509.

47 P. R. Haddad, P. E. Jackson and A. L. Heckenberg, *J. Chromatogr.*, 346 (1985) 139.

48 J. E. Girard and J. A. Glatz, *Amer. Lab.*, 13 (1981) 26.

49 P. R. HAddad and A. L. Hechenberg, *J. Chromatogr.*, 300 (1984) 357.

50 R. M. Cassidy and S. Elchuk, *J. Liquid Chromatogr.*, 4 (1981) 379.

51 Dionex Application Note 48, 1983.

52 J. S. Fritz and J. N. Story, *Anal. Chem.*, 46 (1974) 825.

53 A. E. Martell and R. M. Smith, *Critical Stability Constants*, Vol. 4, Plenum Press, New Yeark.

54 M. Harrold, A. Siriraks and J. Riviello, *J. Chromatogr.*, 602 (1990) 119.

55 A. W. Al-Shawi and R. Dahl, *International Ion Chromatography Symposium '94*, Turin, Italy, 1994, paper No. 10.

56 J. S. Fritz and J. N. Story, *Anal. Chem.*, 46 (1974) 825.

57 J. E. Girard, *Anal. Chem.*, 51 (1979) 836.

58 F. W. E. Strelow, *Anal. Chem.*, 32 (1960) 1185.

59 F. W. E. Strelow, R. Rethemeyer and C. J. C. Bothma, *Anal. Chem.*, 37 (1965) 106.

60 F. W. E. Strelow, R. Rethemeyer and C. J. C. Bothma, *Anal. Chem.*, 37 (1965) 106.

61 X.-X. Zhang, M.-S. Wang and J.-K. Cheng, *Anal. Chim. Acta*, 237 (1990) 311.

62 R. Kuroda, M. Adachi, K. Oguma and Y. Sato, *Chromatographia*, 30 (1990) 263.

63 C. Horvath, W. Melander, I. Molnar and P. Molnar, *Anal. Chem.*, 49 (1977) 2295.

64 R. M. Cassidy, F. C. Miller, C. H. Knight, J. C. Roddick and R. W. Sullivan *Anal. Chem.*, 58 (1986) 1389.

65 R. M. Cassidy and M. Fraser, *Chromatographia*, 18 (1984) 369.

66 R. M. Cassidy, S. Elchuk, N. L. Elliot, L. W. Green, C. H. Knight, B. M. Recoskie, *Anal. Chem.*, 58 (1986) 1181.

67 M. V. Main and J. S. Fritz, *Anal. Chem.*, 61 (1989) 1272.

68 B. A. Bidlingmeyer, S. N. Deming, W. P. Price, Jr., B. Sachok and M. Petrusek, *J. Chromatogr. Sci.*, 186 (1979) 419.

69 A. D. Kirk and A. K. Hewavitharana, *Anal. Chem.*, 60 (1988) 797.

70 R. M. Cassidy and M. Fraser, *Chromatographia*, 18 (1984) 369.

71 R. M. Cassidy, S. Elchuk, N. L. Elliot, L. W. Green, C. H. Knight and B. M. Recoskie, *Anal. Chem.*, 58 (1986) 1181.

72 R. M. Cassidy and M. Fraser, *Chromatographia*, 18 (1984) 369.

73 A. Kerr, W. Kupferschmidt and M. Attas, *Anal. Chem.*, 60 (1988) 2729.

74 R. M. Cassidy, S. Elchuk, L. W. Green, C. H. Knight, F. C. Miller and B. M. Recoskie, *J. Radio. Nucl. Chem.*, 139 (1990) 55.

75 K. Inoue and M. Zenki, *Bunseki Kagaku*, 42 (1993) 805.

76 A. Ramesh, *Talanta*, 41 (1994) 355.

77 S. R. Hutchins, P. R. Haddad and S. Dilli, *J. Chromatogr.*, 252 (1982) 185.

78 M. V. Main and J. S. Fritz, *Anal. Chim. Acta*, 229 (1990) 101.

79 M. V. Main and J. S. Fritz, *Anal. Chem.*, 61 (1989) 1272.

80 H. Irth, G. J. De Jong, U. A. T. Brinkman and R. W. Frei, *Anal. Chem.*, 59 (1987) 98.

81 E. M. Basova, T. A. Bol'shova, I. P. Alimarin and E. N. Shapovalova, *Zavod. Lab.*, 56 (1990) 11.

82 H. Hoshino, K. Nakano and T. Yotsuyanagi, *Analyst,* 115 (1990) 133.

83 H. Inoue and K. Ito, *Microchemical Journal*, 49 (1994) 249.

84 J. F. Jen and S. M. Yang, *Analytica Chimica Acta*, 20 (1994) 97.

85 N. Iki, H. Hoshino and T. Yotsuyanagi, *Mikrochimica Acta*, 113 (1994) 137.

86 R. M. Cassidy and C. Chauvel, *Chem. Geol.*, 74 (1989) 189.

87 X. S. Zhang, C. S. Lin, L. Z. Liu and G. J. Qiao, *J. Chromatogr.*, 684 (1994) 354.

88 G. Schwedt and P. Schneider, *Fres. Z. Anal. Chem.*, 325 (1986) 116.

89 J. N. King and J. S. Fritz, *Anal. Chem.*, 59 (1987) 703.

90 R. M. Smith and L. E. Yankey, *Analyst*, 107 (1982) 744.

91 E. M. Basova, T. A. Bol'shova, I. P. Alimarin and E. N. Shapovalova, *Zavod. Lab.*, 56 (1990) 11.

92 K. Inoue and M. Zenki, *Bunseki Kagaku*, 42 (1993) 805.

93 R. L. Smith and D. J. Pietrzyk, *Anal. Chem.*, 56 (1984) 610.

94 C. Tong, Z. L. Shan, and P. L. Zhu, *Chromatographia*, 27 (1989) 316.

95 R. P. Buck, S. Singhadeja and L. B. Rogers, *Anal. Chem.*, 26 (1954) 1240.

96 L. Goodkin, M. D. Seymour and J. S. Fritz, *Talanta*, 22 (1975) 245.

97 R. J. Willams, *Anal. Chem.*, 55 (1983) 851.

98 R. M. Cassidy, S. Elchuk and P. K. Dasgupta, *Anal. Chem.*, 59 (1987) 85.

99 S. Elchuk and R. M. Cassidy, *Anal. Chem.*, 51 (1979) 1434.

100 G. J. Schmidt and R. P. W. Scott, *Analyst* (London), 109 (1984) 997.

101 J. S. Fritz and J. N. Story, *Anal. Chem.*, 46 (1974) 825.

102 J. J. Byerley, J. M. SCharer and G. F. Åtkinson, *Analyst*, 112 (1987) 41.

103 R. M. Cassidy and S. Elchuk, *Inter. J. Environ. Anal. Chem.*, 10 (1981) 287.

104 R. M. Cassidy, Elchuk S., N. L. Elliot, L. W. Green, C. H. Knight, B. M. Recoskie, *Anal. Chem.*, 58 (1986) 1181.

105 K. Ueno, T. Imamura and K. L. Cheng, *Handbook of Organic Analytical Reagents*, 2nd ed., CRC press, Tokyo, 1992, p. 219.

106 K. Ueno, T. Imamura and K. L. Cheng, *Handbook of Organic Analytical Reagents*, 2nd ed., CRC press, Tokyo,1992, p. 179.

107 B. Budesinsky, *Talanta*, 16 (1969) 1277.

108 K. Ueno, T. Imamura and K. L. Cheng, *Handbook of Organic Analytical Reagents*, 2nd ed., CRC press, Tokyo, 1992, p. 185.

109 J. Lankelma and H. Poppe, *J. Chromatogr.*, 149 (1978) 587.

110 P. R. Haddad and P. E. Jackson, *Ion-Chromatography: Principle and Application*, Elsevier, Amsterdam, 1990, p. 444.

111 Waters Manul of Model 590 prgrammable pump, 1989.

112 P. E. Jackson and P. R. Haddad, *J. Chromatogr.*, 389 (1987) 65.

113 P. R. Haddad and P. E. Jackson, *J. Chromatogr.*, 367 (1986) 301.

114 P. E. Jackson, and P. R. Haddad, *J. Chromatogr.*, 87 (1986) 355.

115 Z. B. Alfassi and C. M. Wai, *Preconcentration Techniques for Trace Elements*, CRC Press, London, 1992, p. 253.

116 H. Takehara, *Bunseki Kagaku*, 36 (1987) 457.

117 P. R. Haddad and P. E. Jackson, *J. Chromatogr.*, 367 (1986) 301.

118 Z. B. Alfassi and C. M. Wai, *Preconcentration Techniques for Trace Elements*, CRC Press, London, 1992, p. 245.

Chapter 3

Experimental

3.1 INTRODUCTION

In this study the retention behaviour of thorium(IV) and uranyl complexes on a reversed-phase column has been investigated, using a mobile phase containing a complexing ligand, such as α-hydroxyisobutyric acid (HIBA), glycolate or mandelate. Thorium(IV) and uranyl standard solutions prepared at ppm level concentration were injected directly into the chromatographic system and detected with a UV/Vis spectrophotometer after post-column reaction with Arsenazo III. This is referred to as *direct injection*. Various parameters which affect the complexation and retention have examined under this mode.

For the determination of low concentration samples, a *preconcentration* technique was employed. In this mode a large volume of ppb level of thorium(IV) and uranyl solution was loaded onto a short C_{18} cartridge, then the enriched solutes were transferred onto the analytical column where they were separated and quantified in the same manner as that performed in the direct injection mode. The preconcentration procedures were automatically operated by a programmable pump. The efficiency of the preconcentration performance was evaluated by comparing the results with those obtained using the direct injection mode. Different concentrators and loading parameters were investigated.

This Chapter outlines the instrumentation and the configurations used in both direct injection and preconcentration studies, together with the reagents and the general experimental procedures. Further operational details for each of the two modes and the specific application are given in the experimental sections in subsequent chapters.

3.2 CHROMATOGRAPHIC SYSTEMS AND GENERAL EXPERIMENTAL PROCEDURES

3.2.1 INSTRUMENTATION

3.2.1.1 The Direct Injection System

The liquid chromatographic system used for the direct injection studies consisted of a Millipore-Waters (Milford, MA, USA) Model 510 pump, a Model U6K injector and a Model 481 UV/Vis spectrophotometric detector coupled to a Maxima 820 Chromatography Data Station. A Waters μ-Bondapak C_{18} reversed-phase column (300 x 3.9 mm I.D.) was used as the analytical column, which was fitted with a C_{18} guard column housed in a Waters Guard-Pak precolumn module. The post-column reaction (PCR) reagent solution was delivered with a Waters pneumatic reagent delivery module (RDM), and mixed with the column effluent in a standard tee piece. The chromatogram was recorded and integrated with the Chromatography Data Station. The instrumental arrangement for the direct injection mode is shown in Fig. 3.1.

3.2.1.2 The Preconcentration System

For the on-line preconcentration studies, a concentrator column was added between the injector and the analytical column in the direct injection system described above. An Automated Switching Valve (Waters) was employed to insert the concentrator column into the analytical eluent flow-path, or to withdraw it, and the required volume of sample was loaded by a Model 590 pump (Waters). In most cases a C_{18} Guard-Pak was used as the concentrator column. Fig. 3.2 shows the schematic diagram of the preconcentration chromatographic system used in this work. The preconcentration procedures were automatically operated by a program edited into the Model 590 programmable pump. The detection procedures were the same as those used in the direct injection mode.

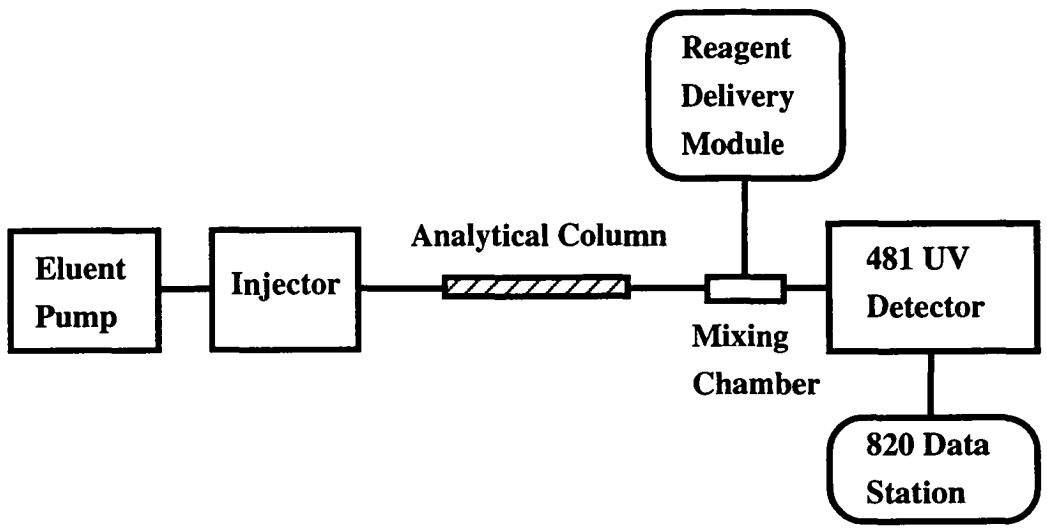

Fig. 3.1 Schematic diagram of the chromatographic system used for direct injection studies.

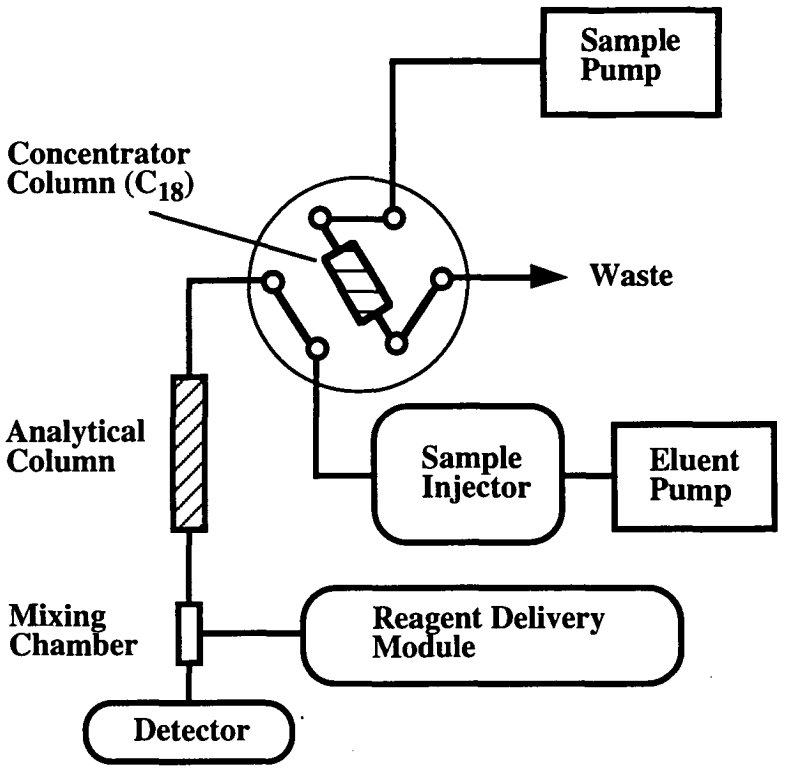

Fig. 3.2 Schematic diagram of the chromatographic system used for preconcentration studies.

3.3 REAGENTS

3.3.1 Solvents and Reagents

Throughout this study all the water was doubly distilled and purified with a Millipore Milli-Q type purification system, and further filtered through a 0.45 μm membrane filter (Millipore, Type HA). HPLC grade methanol or acetonitrile was used as the organic modifier in the analytical mobile phase and was obtained from Millipore-Waters.

All other chemicals used in this study were of analytical reagent grade, as shown in Table 3.1 which also included the supplier details. These chemicals were all used directly without further purification.

3.3.2 Standard Solutions

Thorium and uranium standards were prepared from thorium(IV) nitrate ($Th(NO_3)_4 \cdot 6H_2O$) (GR grade, May & Baker, Dagenham, UK) and uranyl nitrate ($UO_2(NO_3)_2 \cdot 6H_2O$) (GR grade, Ajax Chemicals, Sydney, Australia), respectively. Stock solutions of 1000 mg/l were prepared initially, and then freshly diluted with the mobile phase as required prior to chromatographic injection. The stock solution also contained about 1% nitric acid to prevent precipitation.

The reference neutral substance, Phenol (Ajax Chemicals, Sydney, N.S.W.), stock solution (1000 mg/l) was obtained by dissolving it in Milli-Q water, then diluted each day prior to use. The lanthanides and transition metal stock solutions were prepared from their nitrate salts or oxides (Table 3.2) without further purification, for these metals were used for the interference effect studies. In the case of metal oxides, a weighed sample was first dissolved in concentrated nitric acid (heated if necessary), then diluted in a volumetric flask with Milli-Q water. These stock solutions were further diluted as required.

Table 3.1 MISCELLANEOUS APPARATUS USED IN THIS STUDY

Apparatus	Model	Supplier
Milli-Q water system	N/A	Millipore, Bedford, MA, USA
pH meter	101	Activon, Sydney, Australia
pH electrode	BJ-312	Activon, Sydney, Australia.
Ultrasonic bath	FX-12	Unisonics, Sydney, Australia.
Analytical balance	ER-180A	A&D Company, Tokyo, Japan
Semi-analytical balance	FA-2000	A&D Company, Tokyo, Japan
Vacuum filtration system	N/A	Millipore, Bedford, MA, USA
Filter membrane	Type HV	Millipore, Bedford, MA, USA
Glass syringes	25 µl, 100 µl, 500 µl	Scientific Glass Engineering, Vic., Australia.
UV-Vis-Nir Spectrophotometer	Cary 5E	Varian Techtron Pty. Ltd., Australia.
Muffle furnace	GLM 11/3	Carbolite, Bamford, Sheffield, England.
Hot plate	502 Series	Imbros Pty. Ltd., Hobart, Australia.
Centrifuge	Capsull HF-120	Tomy Seko Co. Ltd., Tokyo, Japan.

N/A: not applicable.

Table 3.2 CHEMICALS FOR STANDARD SOLUTIONS

Chemical	Formula	Grade	Supplier
Rare earth metals			
Lanthanum oxide	La_2O_3	AR	Light Co. Ltd., Colnbrook, England.
Praseodymium Nitrate	$Pr(NO_3)_3$	AR	Light Co. Ltd., Colnbrook, England.
Neodymium Oxide	Nd_2O_3	AR	Light Co. Ltd., Colnbrook, England.
Samarium Oxide	Sm_2O_3	AR	Light Co. Ltd., Colnbrook, England.
Europium Oxide	Eu_2O_3	AR	Light Co. Ltd., Colnbrook, England.
Gadolinium Oxide	Gd_2O_3	AR	Light Co. Ltd., Colnbrook, England.
Dysprosium Oxide	Dy_2O_3	AR	Light Co. Ltd., Colnbrook, England.
Holmium Oxide	Ho_2O_3	AR	Light Co. Ltd., Colnbrook, England.
Erbium Oxide	Er_2O_3	AR	Light Co. Ltd., Colnbrook, England.
Ytterbium Oxide	Yb_2O_3	AR	Light Co. Ltd., Colnbrook, England.
Transition metals			
Copper Oxide	CuO	AR	Ajax Chem. Sydney, Australia.
Zinc Oxide	ZnO	AR	Ajax Chem. Sydney, Australia.
Cadmium Carbonate	$CdCO_3$	AR	Ajax Chem. Sydney, Australia.
Lead Nitrate	$Pd(NO_3)_2$	AR	Ajax Chem. Sydney, Australia.
Chromium Oxide	Cr_2O_3	AR	Ajax Chem. Sydney, Australia.
Vanadyl Sulphate	$VOSO_4$	AR	Ajax Chem. Sydney, Australia.
Manganese Nitrate	$Mn(NO_3)_2$	AR	Ajax Chem. Sydney, Australia.
Ferric nitrate	$Fe(NO_3)_3$	AR	Ajax Chem. Sydney, Australia.
Cobalt Acetate	$Co(CH_3COO)_2$	AR	Ajax Chem. Sydney, Australia.
Nickel Acetate	$Ni(CH_3COO)_2$	AR	BDH Chem. Ltd, Poole, England

3.3.3 Mobile Phases

Most of the mobile phases used for the mechanistic studies comprised 400 mM α-hydroxyisobutyric acid (HIBA) (Sigma, St. Louis, MO, USA) [1, 2] and 10% methanol, adjusted to pH 4.0 with sodium hydroxide. In some cases, various concentrations of ion-interaction reagents (IIR), such as tetrabutylammonium (TBA) or octanesulfate (OSA) (see Table 3.3), were also prepared in this mobile phase, in order to observe their effects on the retention of thorium(IV) and uranyl complexes.

Alternatively, glycolic acid (Sigma Chemical Co. St. Louis, MO, USA) and mandelic acid (Light Co. Ltd., Colnbrook, England) were also used to prepare the eluent. These acids form similar complexes with thorium(IV) and uranyl to those of HIBA, but have different structures. The pH values of these two eluents were the same as that of HIBA but the ligand concentration and methanol percentage were adjusted in order to elute thorium(IV) and uranyl at a proper time.

3.3.4 Post-Column Reaction Reagents

After being eluted from the analytical column thorium(IV) and uranyl were derivatised with a post-column reaction (PCR) reagent prior to entering the detector. Most of the PCR solutions were composed of 0.13 mM 2,7-bis(2-arsonophenylazo)-1,8-dihydroxy-3,6-naphthalene disulfonic acid (Arsenazo III) [3, 4] (BDH Laboratory Chemical Division, UK), buffered in 10 mM urea and 62 mM acetic acid. In some cases, 2-(4, 5-dihydroxy-2, 7-disulfo-3-naphthylazo)phenylarsonic acid (Arsenazo I) [5, 6] and 4-(2-pyridylazo)-resorcinol (PAR) [7, 8] were also used as the PCR reagents. The Arsenazo I PCR solution was prepared at the same concentration and same buffer as that of Arsenazo III described above. When PAR used as the PCR reagent, it was prepared at 0.2 mM concentration in an acetic acid-ammonia buffer (1:3 molar ratio). Both the mobile phases and PCR solutions were filtered through a 0.45 μm filter membrane (Waters) and degassed in an ultrasonic bath prior to use.

Table 3.3 MISCELLANEOUS CHEMICALS USED IN THIS STUDY

Chemical	Grade	Supplier
Mobile phases		
Acetonitrile	Spectrograde	Ajax, Sydney, Australia.
1-Octanesulfonic acid (OSA)	AR	Sigma, St. Louis, USA.
Tetrabutylammonium Hydroxide (TBA)	AR	Aldrich, Milwaukee, WIS., USA.
Chemicals for sample fusion		
Sodium peroxide	AR	Ajax, Sydney, Australia.
Sodium carbonate	AR	Ajax, Sydney, Australia.
Sodium tetraborate	AR	Ajax, Sydney, Australia.
Potassium pyrosulphate	N/A	Ajax, Sydney, Australia.
Perchloric acid	AR	Ajax, Sydney, Australia.
General Chemicals		
Urea	AR	May and Baker, Australia.
Nitric Acid	AR	May and Baker, Australia.
Sulphuric acid	AR	Ajax, Sydney, Australia.
Acetic acid	AR	BDH. Victoria, Australia.
Sodium hydroxide	AR	Ajax, Sydney, Australia.
Potassium chloride	AR	May and Baker, Australia.
Nitrogen Gas	Industrial	Ajax, Sydney, Australia.

N/A: not applicable.

3.4 GENERAL

All data points shown in this thesis are the mean of at least two experiments. The sizes of the points in each plot have been selected so that they encompass the range of the results obtained. For this reason, error bars are not shown.

3.5 REFERENCES

---

1 D. J. Barkley, M. Blanchette, R. M. Cassidy and S. Elchuk, *Anal. Chem.*, 58 (1986) 2222.

2 R. M. Cassidy, S. Elchuk, N. L. Elliot, L. W. Green, C. H. Knight, B. M. Recoskie, *Anal. Chem.*, 58 (1986) 1181.

3 R. Kuroda, M. Adachi, K. Oguma and Y. Sato, *Chromatographia*, 30 (1990) 263.

4 C. H. Knight, R. M. Cassidy, B. M. Recoskie and L. W. Green, *Anal. Chem.*, 56 (1984) 474.

5 G. J. Sevenich and J. S. Fritz, *React. Polym.*, 4 (1986) 195.

6 N. E. Fortier and J. S. Fritz, *Talanta*, 34 (1987) 415.

7 G. Schwedt, *Chromatographia*, 12 (1979) 613.

8 J. J. Byerley, J. M. Scharer and G. F. Atkinson, *Analyst*, 112 (1987) 41.

Chapter 4

The Retention Behaviour of α-Hydroxyisobutyric Acid Complexes of Thorium(IV) and Uranyl in Reversed-phase Liquid Chromatography

4.1 INTRODUCTION

Ion-interaction chromatography using dynamically coated columns has been applied widely to the separation of the lanthanides [1, 2, 3]. With this method, a C_{18} column is generally used, which is coated with sodium n-octanesulfonate (OSA) as the ion-interaction reagent (IIR) to convert it into a dynamically coated cation-exchange column. A suitable ligand, usually α-hydroxyisobutyric acid (HIBA), is added to the mobile phase and serves the purpose of reducing the effective charge on the injected metal ions, so enabling them to be eluted within a reasonable time. Detection has generally been performed by spectrophotometry after post-column reaction (PCR) with a suitable dye, usually 2,7-bis(2-arsonophenylazo)-1,8-dihydroxynaphthalene-3,6-disulfonic acid (Arsenazo III) or 4-(2-pyridylazo)-resorcinol (PAR). The advantage of ion-interaction chromatography is the ease with which the column ion-exchange capacity and selectivity can be altered. Several studies have confirmed that the lanthanide ions are separated predominantly by a cation-exchange mechanism with retention being moderated by the complexing effects of the eluent ligand. Gradient elution may be effected in these systems by progressively increasing the concentration of HIBA in the mobile phase [1].

In previous studies it has been noted that thorium(IV) and uranium(VI) (as uranyl ion) which were eluted in the early part of the chromatogram showed similar retention times to some of the lanthanides. However, when eluent parameters were

varied, the behaviour of thorium(IV) and uranyl showed some differences to that of the lanthanides, suggesting that a different retention mechanism could be operating. Thorium(IV) and uranyl could either be eluted amongst the lanthanides or after them by varying the OSA concentration in the mobile phase. Retention of thorium(IV) and uranyl as HIBA complexes on a C_{18} column was then demonstrated without the presence of an anionic IIR (such as OSA) in the mobile phase and this effect was used subsequently as a means to preconcentrate these species [4, 5]. When the eluent ligand was changed to mandelic acid, thorium(IV) and uranyl showed greater retention than the lanthanides and again could be retained without the use of an anionic IIR in the mobile phase [6].

Whilst some of the factors influencing retention of HIBA complexes of thorium(IV) and uranyl have been reported, the mechanism of their retention on a reversed-phase column remains unclear. In this chapter the characteristics of thorium(IV) and uranyl HIBA complexes are first examined theoretically and then the factors which affect the retention of these complexes are investigated in detail. The trends observed are then related to the nature of the HIBA complexes that exist under the chromatographic conditions used. A coherent retention mechanism is then described.

4.2 THORIUM(IV) AND URANYL HIBA COMPLEXES

Polyvalent cations, such as Th^{4+} and UO_2^{2+}, are not suited to direct cation-exchange methods because the magnitude of the electrostatic interactions of these species with the functional groups on the ion-exchanger is such that these cations are strongly retained. They are best separated chromatographically as complexes with a suitable ligand and these complexes can be formed either prior to the separation step or *in-situ* by adding the ligand into the mobile phase. Generally, the latter is the more convenient and was pursued in this work.

Thorium(IV) and uranyl are known to form complexes with a wide range of

ligands, the most stable complexes being with hydroxycarboxylic acids, such as glycolic, mandelic, lactic and hydroxyisobutyric acids [7]. In many previous reports HIBA is added to the mobile phase to separate lanthanides by ion-interaction chromatography [8, 9, 10].

4.2.1 GENERAL PROPERTIES OF HIBA AS A LIGAND

Early reports show that HIBA forms more stable complexes with thorium(IV) and uranyl than with any other metals [11]. The structure of HIBA is shown below:

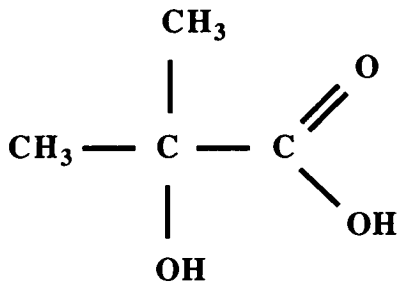

HIBA is a weak acid, it is partially dissociated in an aqueous solution:

$$HL \leftrightharpoons H^+ + L^- \qquad (4.1)$$

where HL and L^- represent HIBA [$(CH_3)_2C(OH)COOH$] and the anion of dissociated HIBA [$(CH_3)_2C(OH)COO^-$], respectively. The equilibrium constant for this dissociation is:

$$K_a = \frac{[H^+]\ [L^-]}{[HL]} \qquad (4.2)$$

At 25 °C (in 1M $NaClO_4$ solution) [11]:

$$\log K_a = -3.77$$

The fraction of the total HIBA existing in the dissociated form is given by α_{L^-}, which can be expressed as:

$$\alpha_{L^-} = \frac{[L^-]}{C_{HL}} = \frac{[L^-]}{[L^-]+[HL]} = \frac{K_a}{K_a+[H^+]} \qquad (4.3)$$

where C_{HL} represents the total concentration of HIBA in both acid and dissociated anion forms. Here it should be noticed that the α_{L^-} value emphasises an important point: the fraction of dissociated HIBA merely depends on the solution pH, not on the total HIBA concentration.

Calculated using Eqn. 4.3 the distribution of the dissociated HIBA anion at various pH values is plotted in Fig. 4.1. Clearly, the higher the pH of the solution, the more L^- will be formed. Below pH 2 most HIBA (>98%) exists as the acid form. The fraction of dissociated anion is increased as the solution pH increases. When the pH exceeds 6, more than 99% of the total HIBA exists in the ionic form. This is favourable for the complex formation, but many metal cations will be precipitated at this pH. In this experiment most of the HIBA eluents were adjusted to pH 4, which is near the HIBA pK_a, to enable it to also act as a buffer acid in the mobile phase. The pH effects were examined within the range pH 2-6.

4.2.2 THORIUM(IV) AND URANYL HIBA COMPLEXES

As discussed in section 2.2, there are some vacant orbitals (6d and 7s) in Th(IV) and UO_2^{2+}, which can accept electrons from electron-donating groups to form multi-step complexes. Magon *et al.* [7, 12] have found that HIBA formed four step complexes with thorium(IV), and three step complexes with uranyl. The formation procedure for these complexes, taking Th(IV)-HIBA as an example, is given below:

$$Th^{4+} + L^- \leftrightharpoons (ThL)^{3+} \qquad (4.4)$$

$$(ThL)^{3+} + L^- \leftrightharpoons (ThL_2)^{2+} \qquad (4.5)$$

$$(ThL_2)^{2+} + L^- \leftrightharpoons (ThL_3)^{+} \qquad (4.6)$$

$$(ThL_3)^{+} + L^- \leftrightharpoons ThL_4 \qquad (4.7)$$

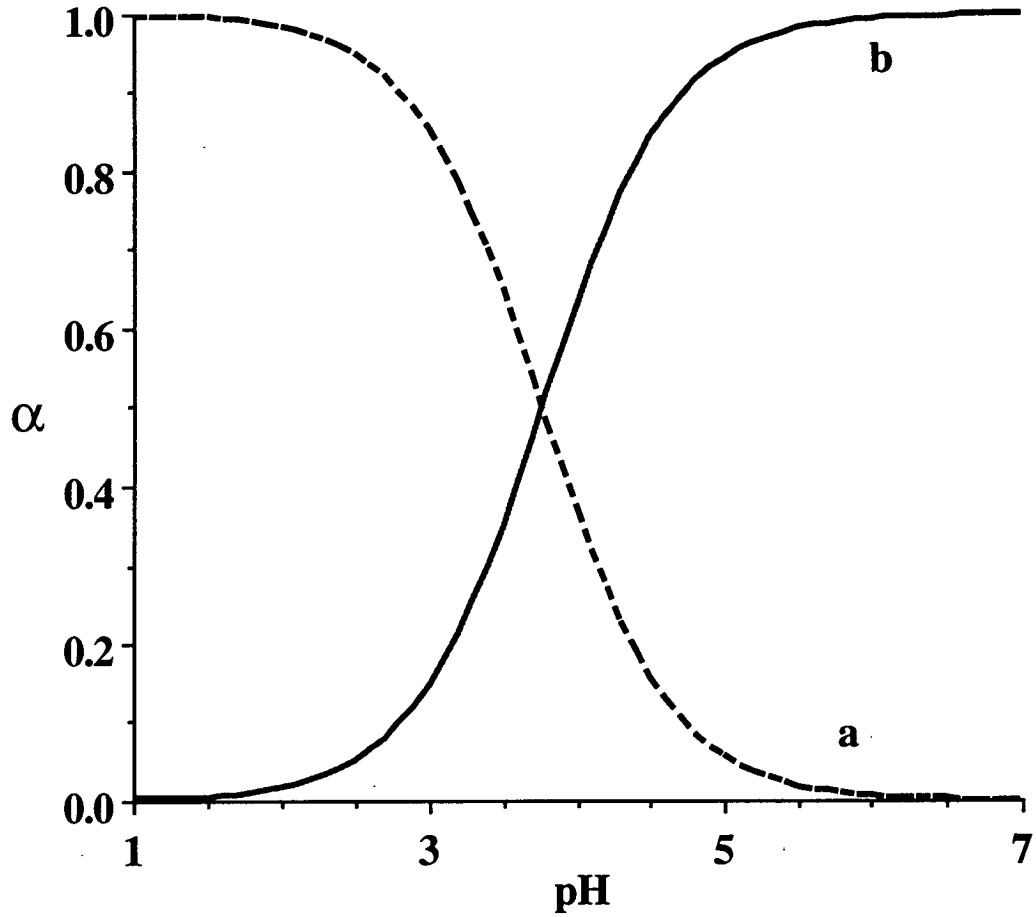

Fig. 4.1 Distribution of HIBA at various pH values. (a) acid (HL), (b) anion (L^-).

where L^- represents the dissociated HIBA anion.

There is a stepwise formation constant for each above equilibrium step which is designed by K_n, where, in this example, the subscript n takes an integral value to indicate the addition of the nth HIBA ligand to a thorium(IV) complex species which contains (n - 1) HIBA molecules. An example is the first stepwise formation constant, K_1, given by:

$$K_1 = \frac{[(ThL)^{3+}]}{[Th^{4+}]\,[L^-]} \tag{4.8}$$

and the fourth stepwise formation constant, K_4, (from Eqn. 4.7):

$$K_4 = \frac{[ThL_4]}{[(ThL_3)^{+}]\,[L^-]} \tag{4.9}$$

These complex reactions of thorium(IV) and HIBA can be rewritten as below:

$$Th^{4+} + L^- \leftrightharpoons (ThL)^{3+} \tag{4.10}$$

$$Th^{4+} + 2\,L^- \leftrightharpoons (ThL_2)^{2+} \tag{4.11}$$

$$Th^{4+} + 3\,L^- \leftrightharpoons (ThL_3)^{+} \tag{4.12}$$

$$Th^{4+} + 4\,L^- \leftrightharpoons ThL_4 \tag{4.13}$$

For each of the above reactions, the equilibrium constants are called overall formation constants, which are designated by β_n, where the subscript n gives the total number of HIBA ligands bound to the original thorium(IV) cation. For example, the third overall formation constant, β_3, refers to the addition of three HIBA ligands to thorium(IV) cation to form ThL_3^+, and the pertinent equilibrium expression is:

$$\beta_3 = \frac{[(ThL_3)^{+}]}{[Th^{4+}]\,[L^-]^3} \tag{4.14}$$

Obviously, there is a simple relationship between the stepwise formation

constants and the overall formation constants for any particular system. This may be illustrated if we multiply the numerator and denominator of the equation defining β_3 by the quantity $[ThL^{3+}]\,[ThL_2^{2+}]$:

$$\beta_3 = \frac{[(ThL_3)^+]}{[Th^{4+}]\,[L^-]^3} \times \frac{[(ThL)^{3+}]\,[(ThL_2)^{2+}]}{[(ThL)^{3+}]\,[(ThL_2)^{2+}]} \tag{4.15}$$

This expression can be rearranged as follows:

$$\beta_3 = \frac{[(ThL)^{3+}]}{[Th^{4+}]\,[L^-]} \times \frac{[(ThL_2)^{2+}]}{[(ThL)^{3+}]\,[L^-]} \times \frac{[(ThL_3)^+]}{[(ThL_2)^{2+}]\,[L^-]} \tag{4.16}$$

The three terms on the right side of this equation correspond, from left to right, to the stepwise constants K_1, K_2 and K_3, respectively:

$$\beta_3 = K_1 K_2 K_3 \tag{4.17}$$

In similar fashion it is possible to derive the relation between each of the overall formation constants and the stepwise formation constants as below:

$$\beta_1 = K_1$$

$$\beta_2 = K_1\, K_2$$

$$\beta_3 = K_1\, K_2\, K_3$$

$$\beta_4 = K_1\, K_2\, K_3\, K_4 \tag{4.18}$$

Uranyl forms three step complexes with HIBA [12]. The expressions for each of the stepwise formation constants and overall formation constants are similar to the above Th(IV)-HIBA complexes, except without K_4 and β_4. The overall formation constants of thorium(IV) and uranyl HIBA complexes are listed in Table 4.1.

The distinct characteristics of thorium(IV) and uranyl HIBA complexes are their high stability compared to other hydroxymonocarbonate ligands, such as β-hydroxy, or γ-hydroxy carboxylates. Magon *et al.* [7, 12] have suggested that the

Table 4.1 THE OVERALL FORMATION CONSTANTS OF HIBA COMPLEXES Measured in 1M $NaClO_4$ at 20 °C [11].

	$\log \beta_1$	$\log \beta_2$	$\log \beta_3$	$\log \beta_4$
Th^{4+}	4.43	8.15	11.06	13.60
UO_2^{2+}	3.18	5.13	6.67	--
La^{3+}	2.62	4.42	5.53	--
Ce^{3+}	2.80	4.74	5.95	--
Pr^{3+}	2.84	4.91	6.21	--
Nd^{3+}	2.88	5.02	6.30	--
Sm^{3+}	2.99	5.39	6.77	--
Eu^{3+}	3.09	5.54	7.32	--
Gd^{3+}	3.08	5.51	7.19	--
Tb^{3+}	3.11	5.63	7.43	--
Dy^{3+}	3.27	5.90	7.87	--
Ho^{3+}	3.31	5.98	7.96	--
Er^{3+}	3.35	6.04	8.13	--
Tm^{3+}	3.52	6.22	8.39	--
Yb^{3+}	3.64	6.42	8.69	--
Lu^{3+}	3.67	6.47	8.82	--
Mn^{2+}	0.90	1.48	1.70	--
Co^{2+}	1.45	2.43	2.70	--
Ni^{2+}	1.67	2.80	3.20	--
Cu^{2+}	2.74	4.34	5.70	--
Zn^{2+}	1.70	2.99	3.40	--
Cd^{2+}	1.24	2.16	2.50	--
Pb^{2+}	2.03	3.20	3.40	--

α-hydroxy group on HIBA also took part in the first complex formation, i.e. formed one chelate ring between HIBA and the central atom. Studies on uranyl-glycolate complexes with infrared spectrophotometry have confirmed that the first complex was a pure chelate, and the second and third also formed chelates but *via* a water molecule [13]. In this chapter, HIBA is selected for the studies of retention mechanisms of thorium(IV) and uranyl complexes on a reversed-phase column, because it forms the most stable complexes with these metals.

4.2.3 DISTRIBUTION OF THORIUM(IV) AND URANYL HIBA COMPLEXES

4.2.3.1 Effect of HIBA Concentration on Complex Formation

When thorium(IV) and HIBA are mixed, several complex species could coexist in the same solution for a certain HIBA concentration. Each of these Th(IV)-HIBA complexes varies with the concentration of free (uncomplexed) HIBA anion, which is further determined by the total ligand concentration and the solution pH, as described in Section 4.2.1. Whenever a pH value is selected, the distribution of each of the complexes can be calculated at various HIBA concentrations.

In the Th(IV)-HIBA complex solution the total thorium(IV) concentration, C_{Th}, equals the sum of the concentrations of free (uncomplexed) metal ion and all the thorium(IV) containing complexes:

$$C_{Th} = [Th^{4+}] + [(ThL)^{3+}] + [(ThL_2)^{2+}] + [(ThL_3)^{+}] + [ThL_4] \qquad (4.19)$$

Introducing the overall formation constants (Eqn. 4.18) into Eqn. 4.19 gives:

$$C_{Th} = [Th^{4+}] + \beta_1[Th^{4+}][L^-] + \beta_2[Th^{4+}][L^-]^2 + \beta_3[Th^{4+}][L^-]^3 + \beta_4[Th^{4+}][L^-]^4$$

$$= [Th^{4+}] \{1 + \beta_1[L^-] + \beta_2[L^-]^2 + \beta_3[L^-]^3 + \beta_4[L^-]^4 \}$$

$$= [Th^{4+}] C_T \qquad (4.20)$$

Here C_T is a term computed as below:

$$C_T = 1 + \beta_1[L^-] + \beta_2[L^-]^2 + \beta_3[L^-]^3 + \beta_4[L^-]^4$$

Assuming that each Th(IV)-HIBA complex takes a fraction, α_n (where the subscript, n, indicates the number of HIBA ligands coordinated to the central thorium atom), and α_o represents the fraction of the uncomplexed thorium(IV) in the solution, we can derive:

$$\alpha_0 = \frac{[Th^{4+}]}{C_{Th}} = \frac{1}{C_T}$$

$$\alpha_1 = \frac{\beta_1[Th^{4+}]\,[L^-]}{C_{Th}} = \frac{\beta_1[L^-]}{C_T}$$

$$\alpha_2 = \frac{\beta_2[Th^{4+}]\,[L^-]^2}{C_{Th}} = \frac{\beta_2[L^-]^2}{C_T}$$

$$\alpha_3 = \frac{\beta_3[Th^{4+}]\,[L^-]^3}{C_{Th}} = \frac{\beta_3[L^-]^3}{C_T} \qquad (4.21)$$

$$\alpha_4 = \frac{\beta_4[Th^{4+}]\,[L^-]^4}{C_{Th}} = \frac{\beta_4[L^-]^4}{C_T}$$

The sum of all the fractions equals unity:

$$1 = \alpha_o + \alpha_1 + \alpha_2 + \alpha_3 + \alpha_4 \qquad (4.22)$$

It should be noted here that the fraction of each of the Th(IV)-HIBA complexes is dependent only upon the equilibrium concentration of free HIBA anion, but not on the total thorium(IV) concentration, C_{Th}. Similar formulae can be derived for the uranyl-HIBA complexes.

Calculation using Eqn. 4.21 at pH 4.0, the distribution of each species of Th(IV)-HIBA and uranyl-HIBA complexes (replacing the overall stability constants of

Th(IV)-HIBA complexes with those of uranyl-HIBA) at various HIBA concentrations in the range of 1-200 mM are plotted in Fig. 4.2a and Fig 4.2b, respectively. These figures may be used to select experimental conditions under which only one type of complex with each metal ion is present in solution, so that the resultant chromatography can be simplified. Fig. 4.2a shows that the thorium(IV) *tetra*(HIBA) complex dominates at most HIBA concentrations. However, this species does not become the sole complex present until the HIBA concentration reaches at least 400 mM (not shown in Fig. 4.2). On the other hand, Fig. 4.2b shows that the distribution of uranyl-HIBA complexes varies markedly with HIBA concentration. Even at 400 mM HIBA the uranyl ion is distributed chiefly as the *tris*(HIBA) complex (89.4%) and *bis*(HIBA) complex (10.1%). If thorium(IV) and uranyl were injected into a 400 mM HIBA solution buffered at pH 4.0, it would therefore be expected that the thorium would be present solely as the *tetra*(HIBA) complex, whilst the uranyl would be present predominantly as the *tris*(HIBA) complex. Since HIBA can be expected to be present in the deprotonated form in metal complexes, the thorium complex should be neutral, whilst the uranyl complex should be anionic. At lower HIBA concentrations there is a maximum distribution of the thorium(IV) and uranyl complexes containing low numbers of ligands.

4.2.3.2 Effect of pH on Complex Formation

In Eqn. 4.2.1 the term $[L^-]$ represents the equilibrium concentration of *uncomplexed* HIBA anion. Usually the ligand concentration is far higher than that of the metal, therefore the ligand consumed by complexation can be neglected. That is, the total ligand concentration will not be affected by the complexation. For example, suppose 100 µl of 100 ppm thorium(IV) was injected into the 400 mM mobile phase, only 1.72×10^{-7} mole HIBA would take part in the complexation.

As discussed in section 4.2.1, HIBA is partially dissociated in aqueous solution, the dissociated HIBA anion concentration being determined by the total

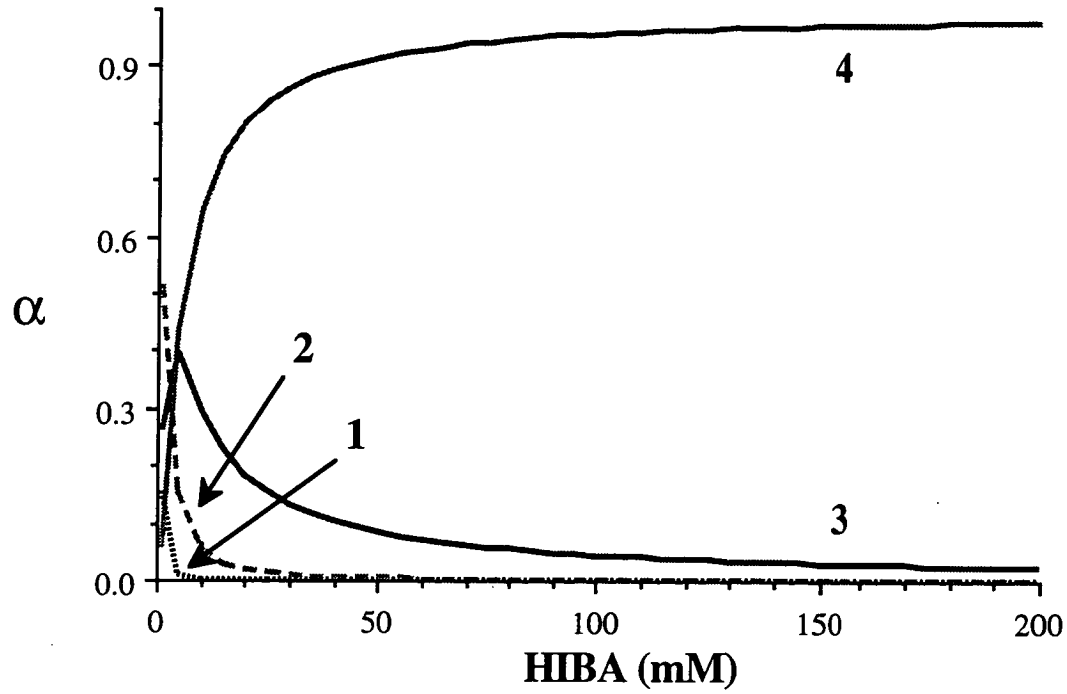

(a)

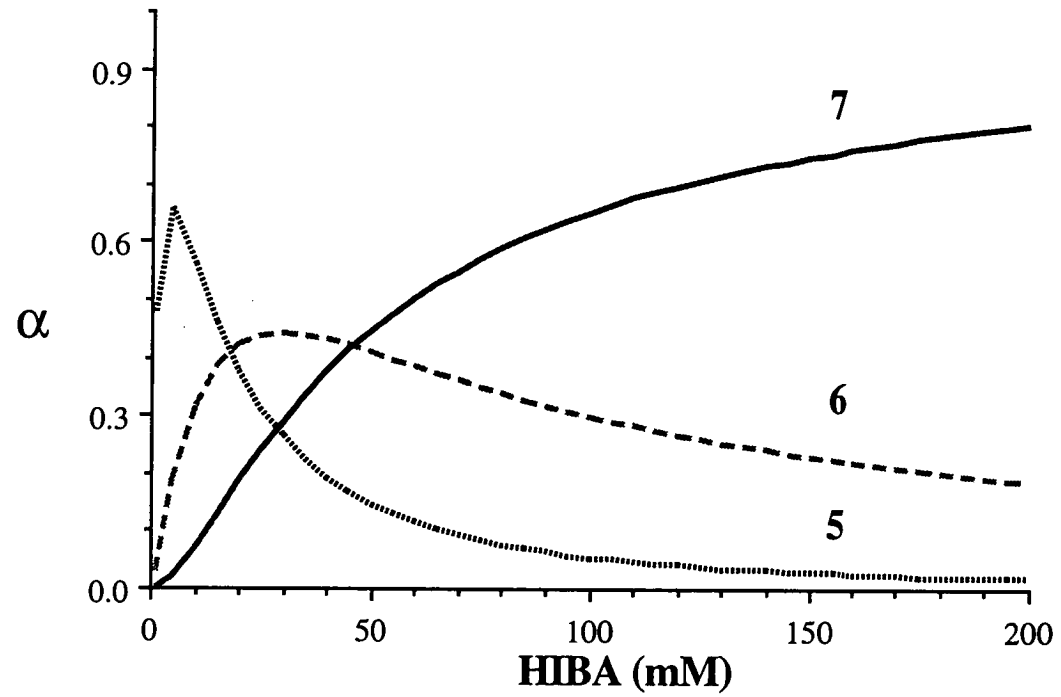

(b)

Fig. 4.2 Fraction (α) of each species of (a) thorium(IV) and (b) uranyl HIBA complexes presents at various ligand concentrations. (1) ThL^{3+}, (2) ThL_2^{2+}, (3) ThL_3^{+}, (4) ThL_4, (5) UO_2L^{+}, (6) UO_2L_2, (7) $UO_2L_3^{-}$. Calculated at pH 4.0 using the overall formation constants given in Table 4.1.

HIBA concentration and the solution pH:

$$[L^-] = \alpha_{L^-} C_{HL} \tag{4.23}$$

where C_{HL} is the total HIBA concentration of both acid and anion forms, which takes a constant value in a given solution. Substitution of Eqn. 4.23 into Eqn. 4.8 gives:

$$K_1 = \frac{[(ThL)^{3+}]}{[Th^{4+}]\,[L^-]} = \frac{[(ThL)^{3+}]}{[Th^{4+}]\;\alpha_{L^-} C_{HL}} \tag{4.24}$$

When the pH of the solution is fixed, α_{L^-} is constant and can be included on the left hand side of the equation:

$$K_1' = K_1\,\alpha_{L^-} = \frac{[(ThL)^{3+}]}{[Th^{4+}]\;C_{HL}} \tag{4.25}$$

This is termed the conditional formation constant, which includes only the effect of ligand, HL but not any other ligands (eg. OH^-) which may present. Similarly, the overall conditional formation constants can be derived as below:

$$\beta_1' = \beta_1 \alpha_{L^-}$$

$$\beta_2' = \beta_2 (\alpha_{L^-})^2$$

$$\beta_3' = \beta_3 (\alpha_{L^-})^3$$

$$\beta_4' = \beta_4 (\alpha_{L^-})^4 \tag{4.26}$$

The overall conditional formation constant is a measure of the effective stability of the Th(IV)-HIBA complex for a particular condition. That is, β_1' (as well as β_2', β_3' and β_4') has a specific value for a given pH. Replacing the overall formation constant, β_n, in Eqn. 4.2.1 with the conditional formation constant, β_n', the fraction of each Th(IV)-HIBA (as well as uranyl-HIBA) complex can be computed at a given pH value. The overall conditional formation constants change as the solution pH

varies, therefore the distribution of each of these complexes is a function of the pH. Fig. 4.3a and Fig. 4.3b show the distribution of thorium(IV) and uranyl HIBA complexes at various pH values in the presence of 400 mM HIBA. These figures may be used to design the chromatographic experiments. Fig. 4.3a shows that the thorium(IV) *tetra*(HIBA) complex is the dominant species when the solution pH is greater than 2. However, this species does not become the sole complex present (α >0.95) until the pH is higher than 3. On the other hand, Fig. 4.3b shows that the distribution of uranyl-HIBA complexes varies markedly in the low pH range. At pH 3.0 there is about 6% of the total uranyl present as the *mono*(HIBA) complex and 31.2% as the *bis*(HIBA) complex. When the solution pH is raised to 4.0, the uranyl *tris*(HIBA) complex rapidly becomes the predominant species. However, only a small change in the uranyl complex distribution is observed as the solution pH is continually increased over 4. That is, the pH sensitive range for these complexes is located between pH 2 and 4. Later in this chapter, the effect of pH on the chromatographic behaviour of the HIBA complexes was investigated in this range. In order to simplify the chromatography, the HIBA mobile phase is adjusted to pH 4.0. At this pH in 400 mM HIBA eluent, it can be expected that thorium(IV) will be present solely as the *tetra*(HIBA) complex, whilst the uranyl would be mainly present as the *tris*(HIBA) complex. Under these conditions the thorium complex should be neutral, whilst the uranyl complex should be anionic.

4.2.3.3 Combined Effects of Ligand Concentration and pH on Complex Formation

Combination of the two effect factors discussed above, the distribution of each of the HIBA complexes is a function of the ligand concentration and the solution pH. For a given ligand concentration and solution pH, the fraction of each complex can be calculated using a Microsoft Excel program. Fig. 4.4 shows the distribution of some species of thorium(IV) and uranyl HIBA complexes at various ligand concentrations and pH values, plotted as three dimensional graphs.

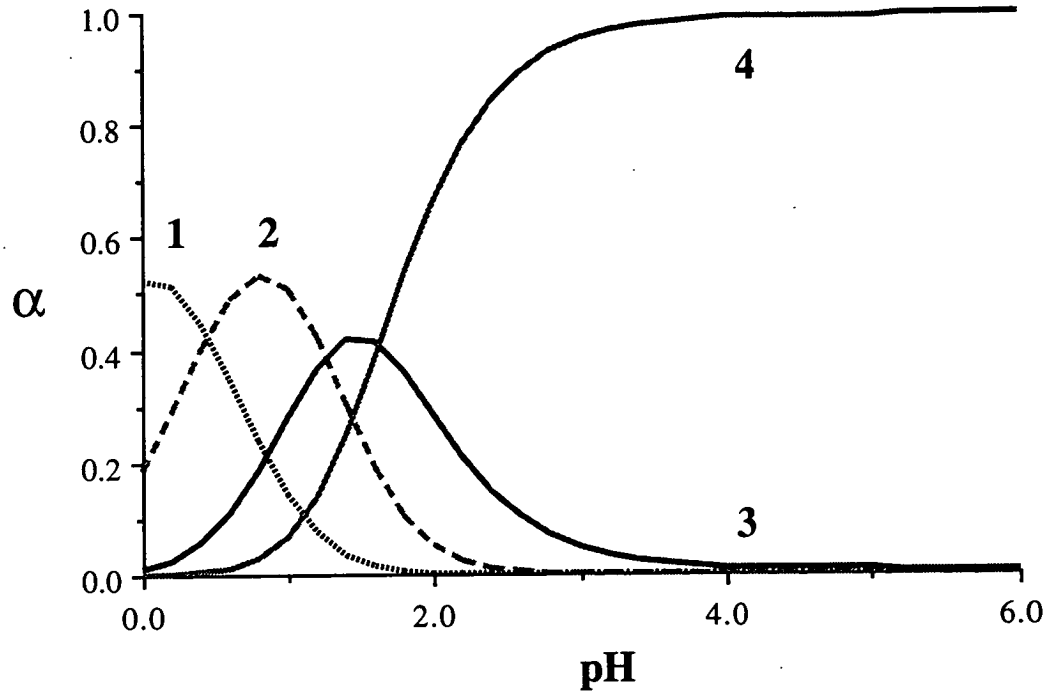

(a)

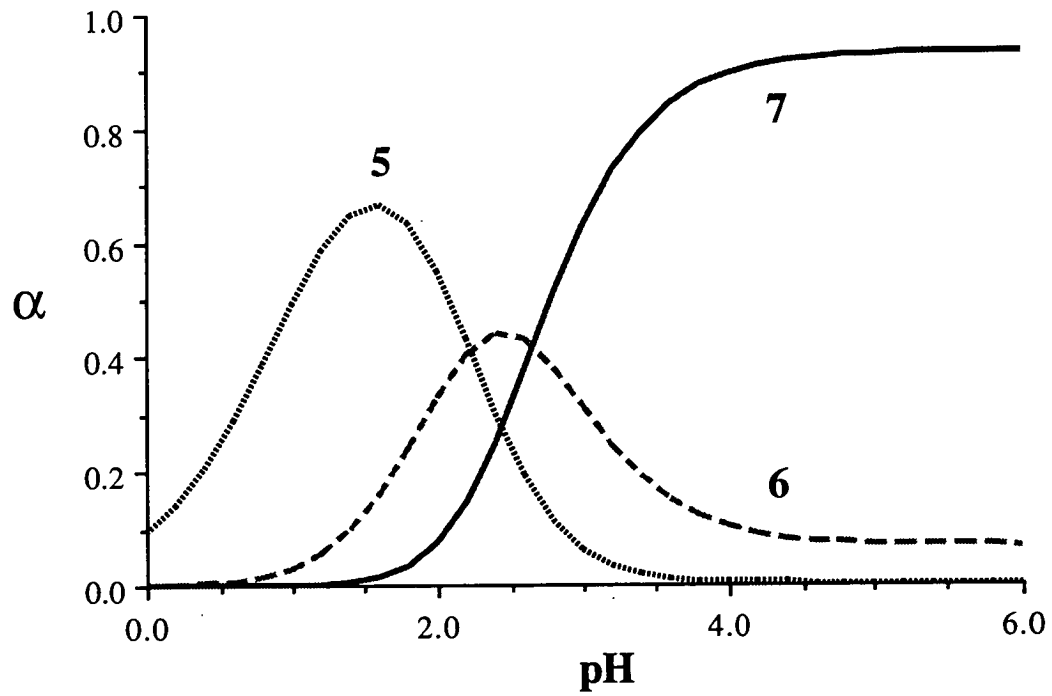

(b)

Fig. 4.3 Fraction (α) of each species of (a) thorium(IV) and (b) uranyl HIBA complexes presents at various pH values. (1) ThL^{3+}, (2) ThL_2^{2+}, (3) ThL_3^{+}, (4) ThL_4, (5) UO_2L^{+}, (6) UO_2L_2, (7) $UO_2L_3^{-}$. Calculated at 400 mM HIBA concentration using the overall formation constants given in Table 4.1.

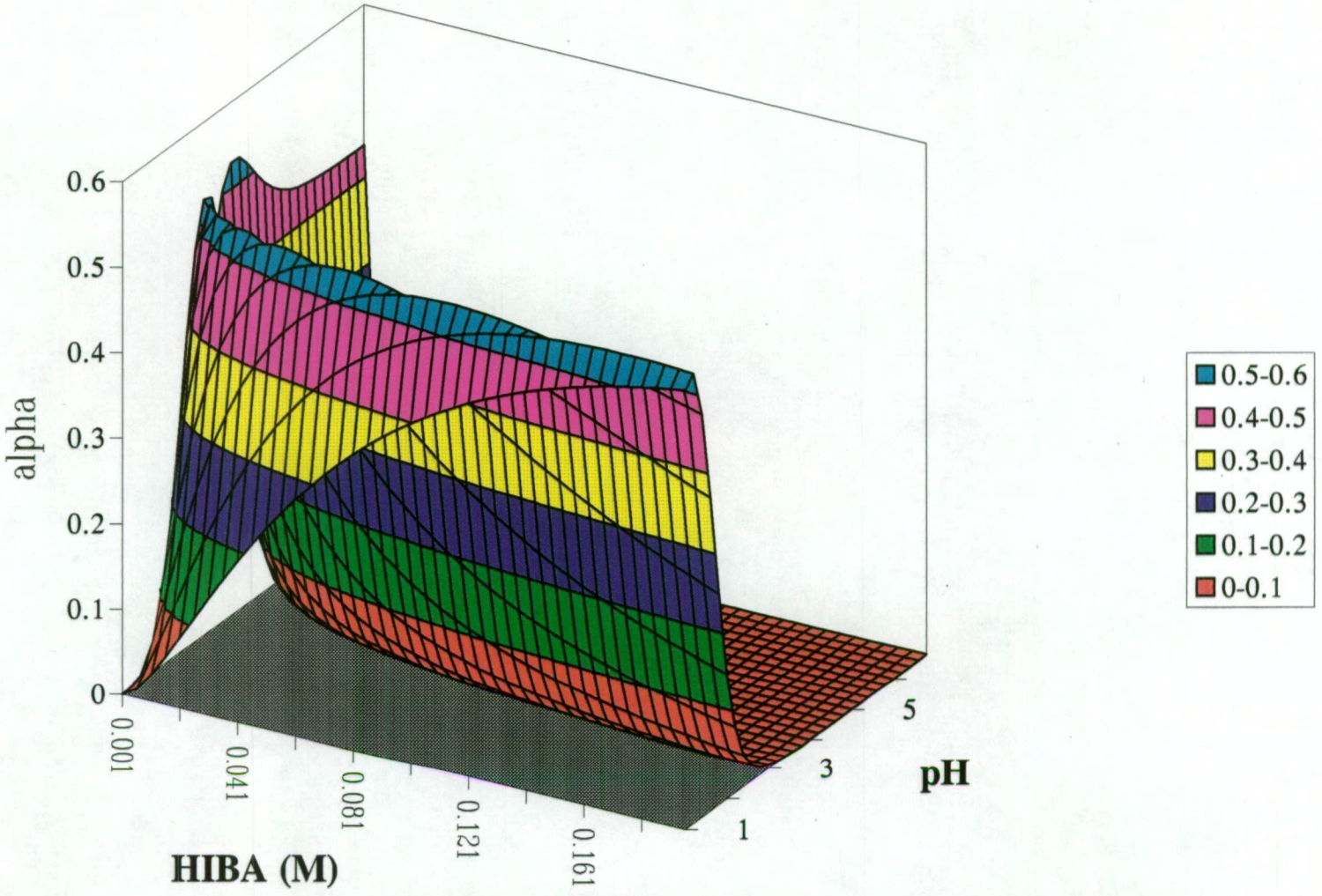

Fig. 4.4a The distribution of thorium(IV) *bis*(HIBA) complex at various HIBA concentrations and pH values.

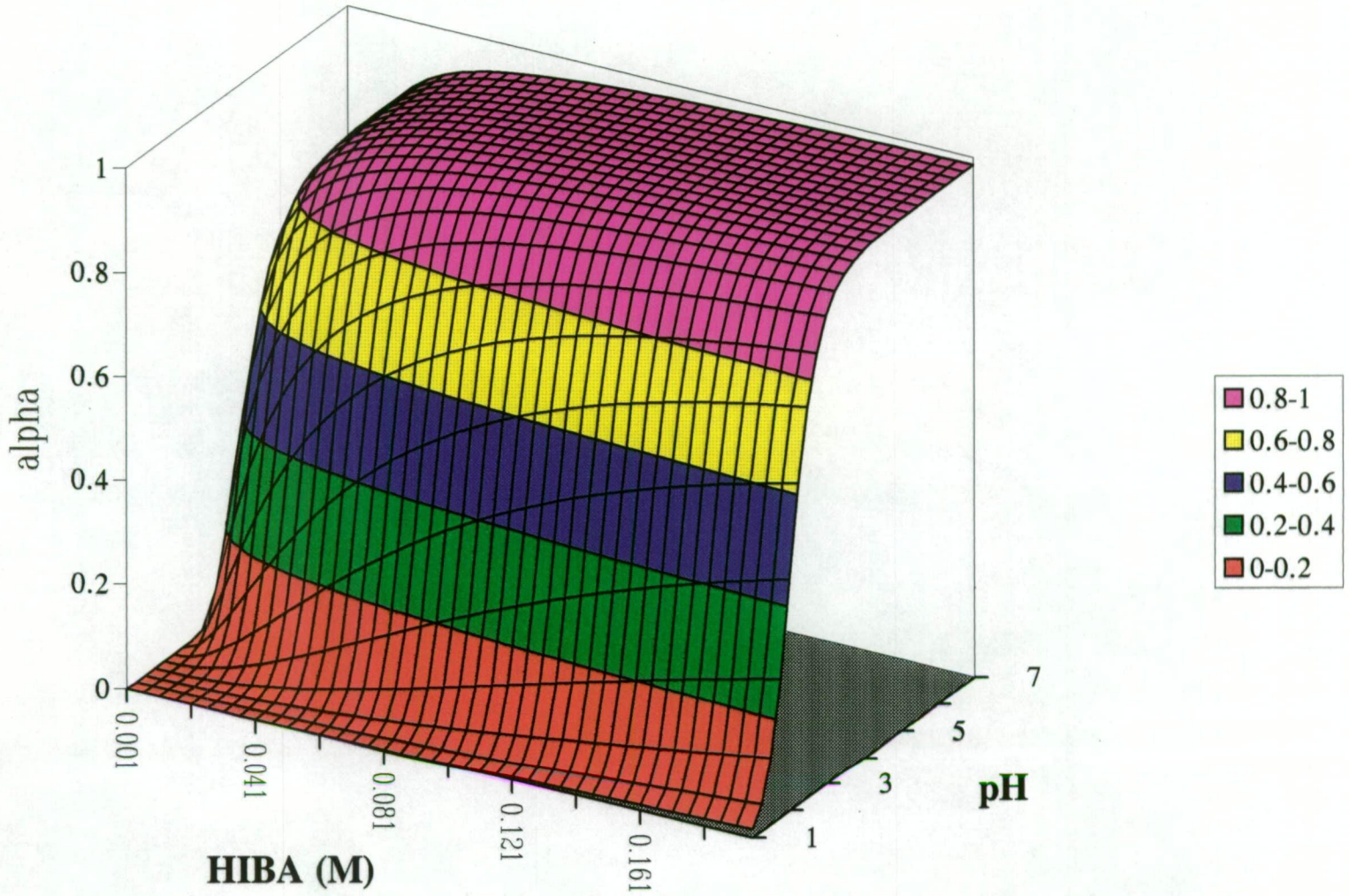

Fig. 4.4b The distribution of thorium(IV) *tetra*(HIBA) complex at various HIBA concentrations and pH values.

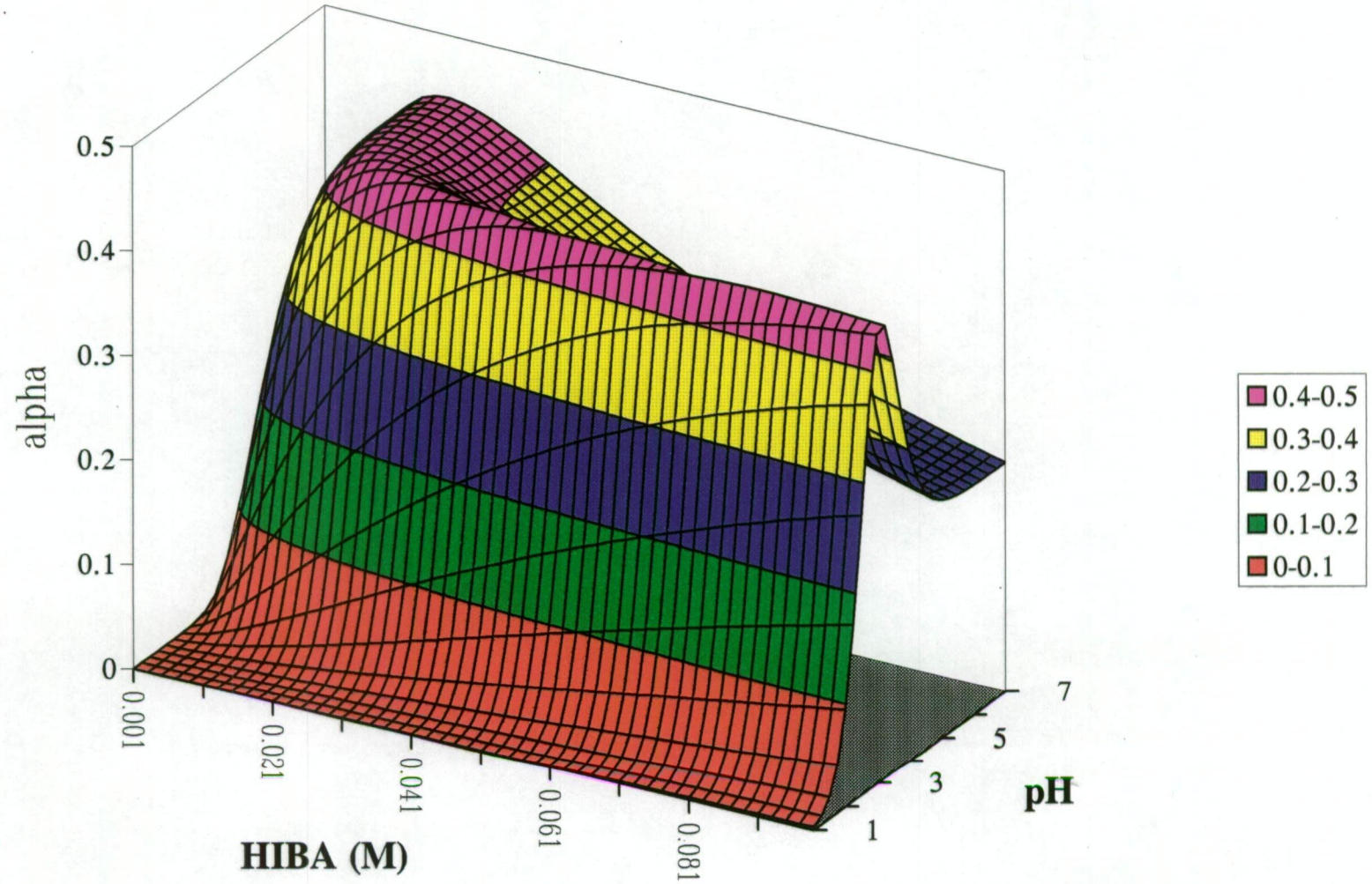

Fig. 4.4c The distribution of uranyl *bis*(HIBA) complex at various HIBA concentrations and pH values.

4.3 EXPERIMENTAL

4.3.1 INSTRUMENTATION

In this chapter the direct injection liquid chromatographic system, as outlined in Chapter 3, was used. A Cary 5E UV-Vis-Nir Spectrophotometer (Varian Techtron Pty. Ltd, Australia) was used in the investigation of absorption spectra using Milli-Q water as the reference. Samples were measured over the range of 200-800 nm in quartz cells (1.0 x 1.0 cm).

4.3.2 REAGENTS

The eluent most frequently used in this chapter comprised 400 mM HIBA and 10% methanol, adjusted to pH 4.0. In addition, some other mobile phases were also prepared as listed below:

(1) 80 mM HIBA;

(2) 80 mM HIBA and 5 mM tetrabutylammonium (TBA);

(3) 400 mM HIBA and 5 mM TBA;

(4) 80 mM HIBA and 5 mM n-octanesulfate (OSA);

(5) 400 mM HIBA and 5 mM OSA.

All these eluents were prepared in 10% methanol and adjusted to pH 4.0 with sodium hydroxide.

10 ppm thorium(IV) and uranyl standards were diluted daily from their concentrated stock solutions with the analytical mobile phase.

The column and the chromatographic system were equilibrated with the mobile phase for at least 20 min prior to starting injections. The entire experiment was carried

out at room temperature, except for the study of temperature effects. Each data point throughout this research was obtained at least in duplicate.

4.4 RESULTS AND DISCUSSION

4.4.1 PRELIMINARY INVESTIGATIONS

4.4.1.1 Spectra of Thorium(IV) and Uranyl Complexes

In ion-chromatography metal cations are usually monitored by a UV detector after post-column derivatisation with a photometric reagent, such as PAR, Arsenazo I or Arsenazo III. PAR is a non selective ligand which can be reacted with various metal cations to form coloured complexes. Typically, it is used for the detection of transition metals [14]. Arsenazo I is suitable for the detection of Al, Be, In, Th, Zr and lanthanides, which form coloured complexes in an acidic or neutral aqueous solution (pH 1-8) [15]. Compared with PAR and Arsenazo I, Arsenazo III is found to give the highest sensitivity for thorium(IV) and uranyl, as well as other hydrolysable multivalent metal ions [15]. The chief characteristic of this reagent is that it forms highly coloured ($\varepsilon \cong 10^5$) soluble chelates even in a strong mineral acidic solution.

All of the three PCR reagents have been reported for the detection of thorium(IV) and uranyl in ion-chromatography [16, 17, 18]. However, in previous work the PCR detection was designed for monitoring thorium(IV) and uranyl together with other metal cations, such as the lanthanides and transition metals. Prior to the retention mechanism study, the spectra of PAR, Arsenazo I and Arsenazo III complexes with thorium(IV) and uranyl, as well as the lanthanides and some transition metals, were examined in order to choose a suitable post-column reaction detection system for thorium(IV) and uranyl.

The Arsenazo III PCR solution, which consisted of 0.13 mM Arsenazo III, 10 mM urea and 62 mM acetic acid (at pH 3) was diluted four times for the spectra investigation in order to keep the absorption to be less than one unit. The Arsenazo I

PCR solution was prepared under the same conditions as Arsenazo III, whilst 0.2 mM PAR dissolved in 3 M NH_4OH and 1 M acetic acid (pH 9) as the PCR solution, then diluted four times. Thorium(IV) and uranyl HIBA complex solutions were prepared based on their metal:ligand stoichiometric ratio, 1:4 (0.06 M:0.24 M) and 1:3 (0.08 M:0.24 M), respectively.

All solutions were measured from 200 to 800 nm with Milli-Q water as the reference. The Arsenazo III spectrum showed a maximum absorption at 540.6 nm, with the absorption peak ended (5% maximum absorption) at about 630 nm (Fig. 4.5). On the other hand, the maximum absorption for Th(IV)-Arsenazo III and uranyl-Arsenazo III complexes appeared at somewhat longer wavelengths, 618 nm and 651 nm, respectively. The lanthanide-Arsenazo III complexes showed strong absorption at around 660 nm, as listed in Table 4.2. It has been reported [2] that thorium(IV) was eluted before uranyl in a reversed-phase chromatography system when HIBA alone was used as the mobile phase. If the detector is set at 660 nm, it can be expected that this will increase the uranyl sensitivity with only a small sacrifice in thorium(IV) sensitivity.

Under the same conditions, the Arsenazo I spectrum is very similar to those of the thorium(IV) and uranyl complexes (see Fig. 4.6a). It should be noted here that a 50 µl of 500 ppm metal cation was mixed with 3.5 ml of the photometric reagent solution, which was far more than the sample size injected into the chromatographic system. Similarly, the spectra of PAR and its thorium(IV) and uranyl complexes showed little difference (Fig. 4.6b). Compared to Arsenazo III, PAR has no selectivity for thorium(IV) and uranyl detection. It can be concluded that Arsenazo III is the most suitable reagent for thorium(IV) and uranyl post-column derivatisation using a UV detector at wavelength around 660 nm. At this wavelength there is no interference from HIBA and its thorium(IV) and uranyl complexes, as shown in Fig. 4.6c.

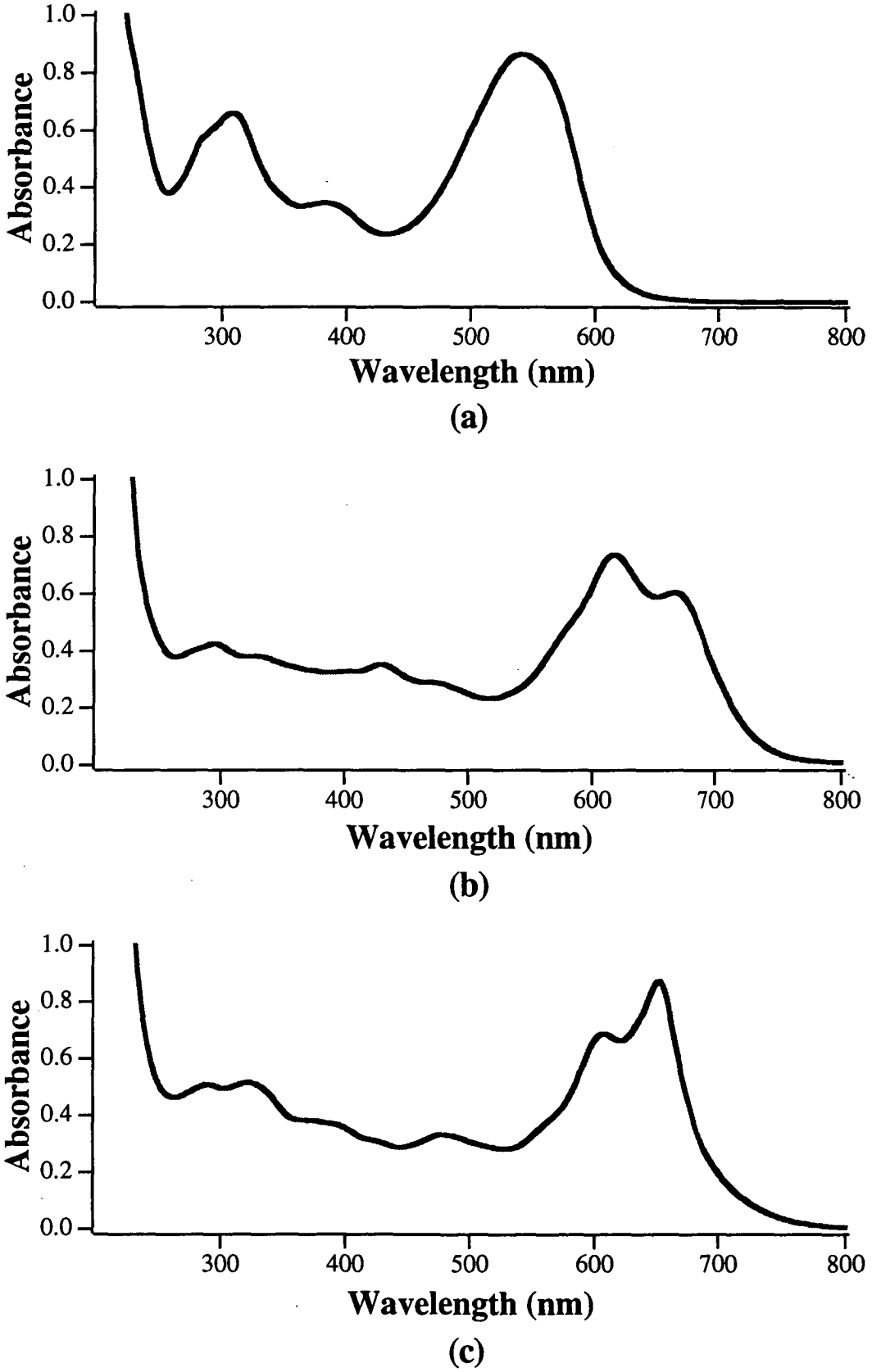

Fig. 4.5 Spectra of (a) Arsenazo III and its (b) thorium(IV) and (c) uranyl complexes. 0.13 mM Arsenazo III was prepared in an acetic acid-urea buffer.

Table 4.2 THE WAVELENGTH OF MAXIMUM ABSORPTION OF ARSENAZO III COMPLEXES

The UV spectrophotometer was scanned from 200 nm to 800 nm. 50 µl of 500 ppm metal solution was mixed with 3.5 ml 0.03 mM Arsenazo III and measured in 1.0 cm quartz cells. Milli-Q water was used as the reference.

Complexes	$\lambda_{max.}$ (nm)	Complexes	$\lambda_{max.}$ (nm)
Arsenazo III	540.6	Er(III)-Arsenazo III	652.8
Th(IV)-Arsenazo III	617.8	Yb(III)-Arsenazo III	663.3
Uranyl-Arsenazo III	651.1	Pb(II)-Arsenazo III	597.2
La(III)-Arsenazo III	651.1	Cd(II)-Arsenazo III	540.0
Pr(III)-Arsenazo III	658.9	Zn(II)-Arsenazo III	540.0
Nd(III)-Arsenazo III	661.1	Cu(II)-Arsenazo III	556.7
Sm(III)-Arsenazo III	661.1	Ni(II)-Arsenazo III	540.0
Eu(III)-Arsenazo III	662.2	Co(II)-Arsenazo III	540.6
Gd(III)-Arsenazo III	662.8	Fe(III)-Arsenazo III	552.2
Dy(III)-Arsenazo III	663.3	Mn(II)-Arsenazo III	540.6
Ho(III)-Arsenazo III	663.3		

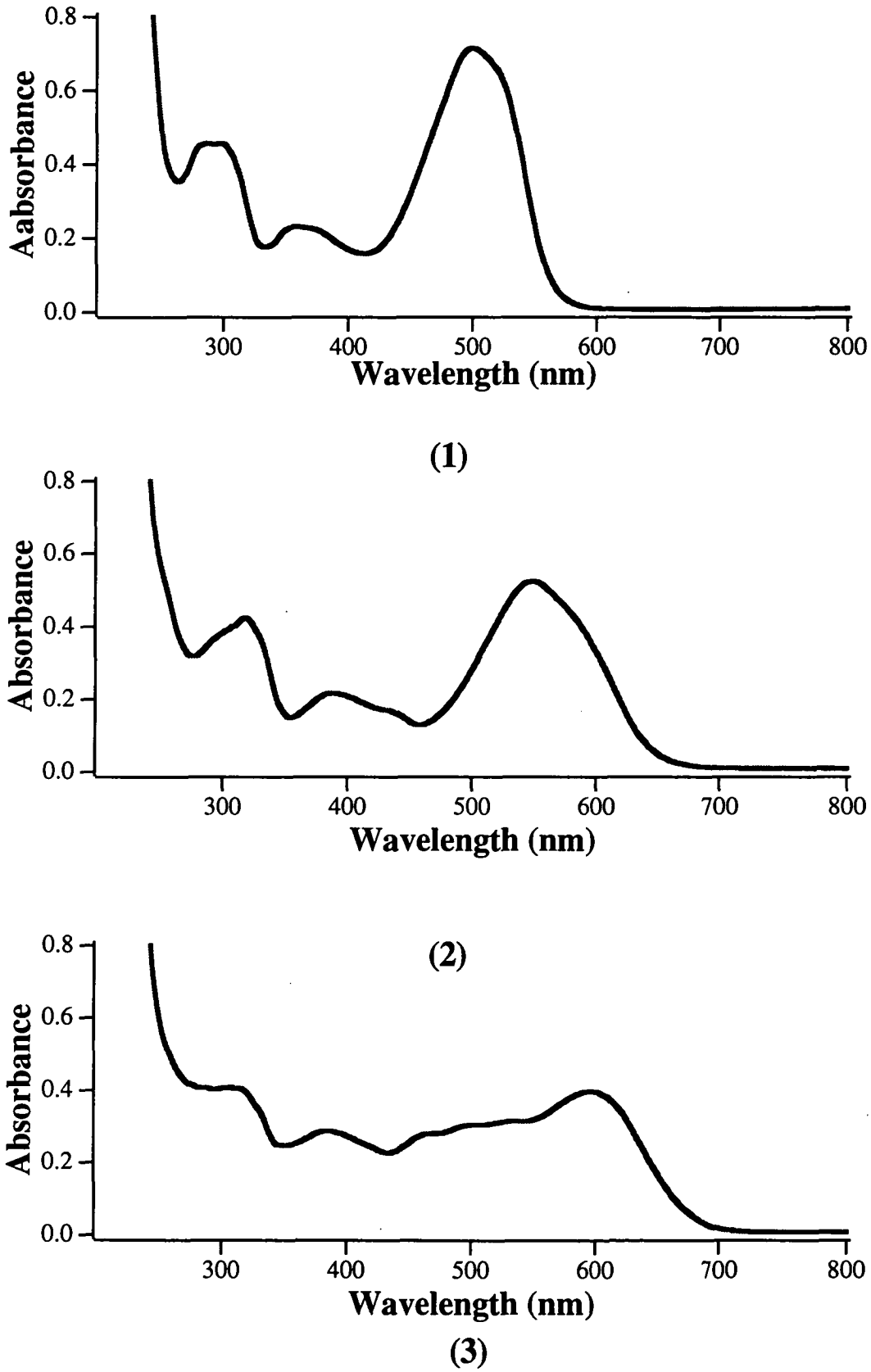

Fig. 4.6a Spectra of (1) Arsenazo I and its (2) thorium(IV) and (3) uranyl complexes. 0.13 mM Arsenazo I was prepared in an acetic acid-urea buffer.

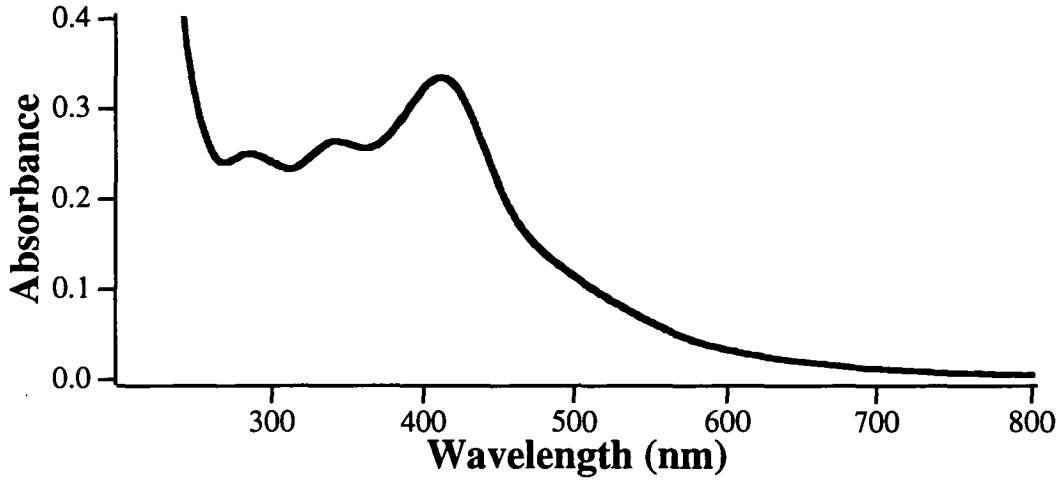

(4)

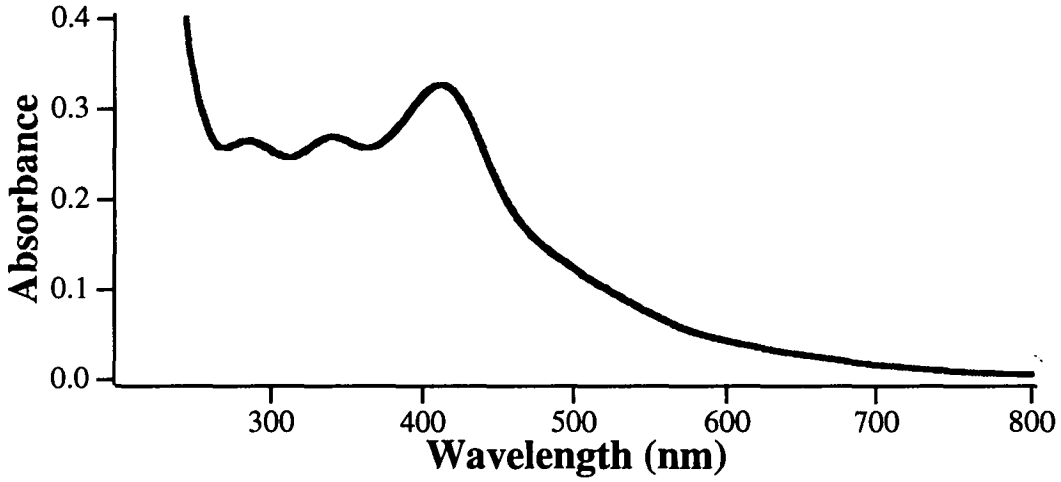

(5)

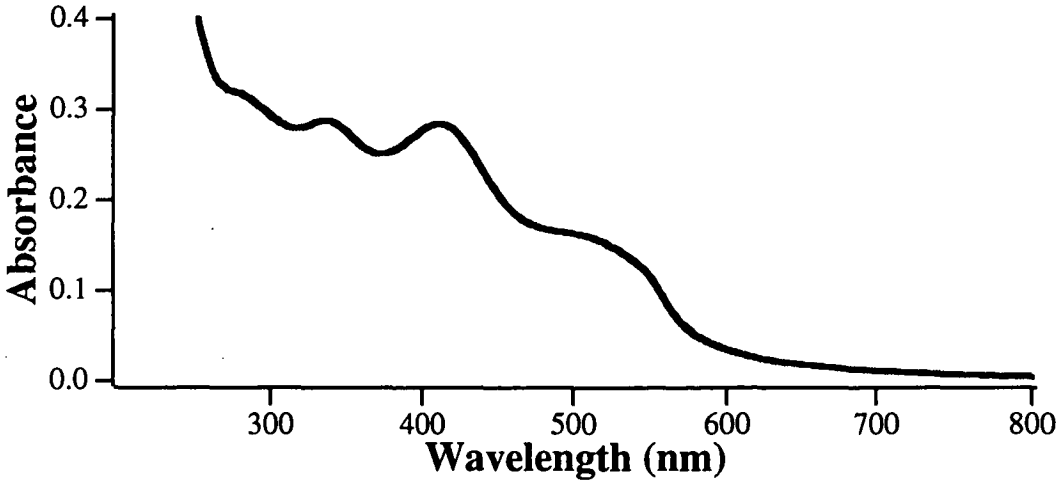

(6)

Fig. 4.6b Spectra of (4) PAR and its (5) thorium(IV) and (6) uranyl complexes. 0.05 mM PAR was prepared in an acetic acid-ammonium buffer.

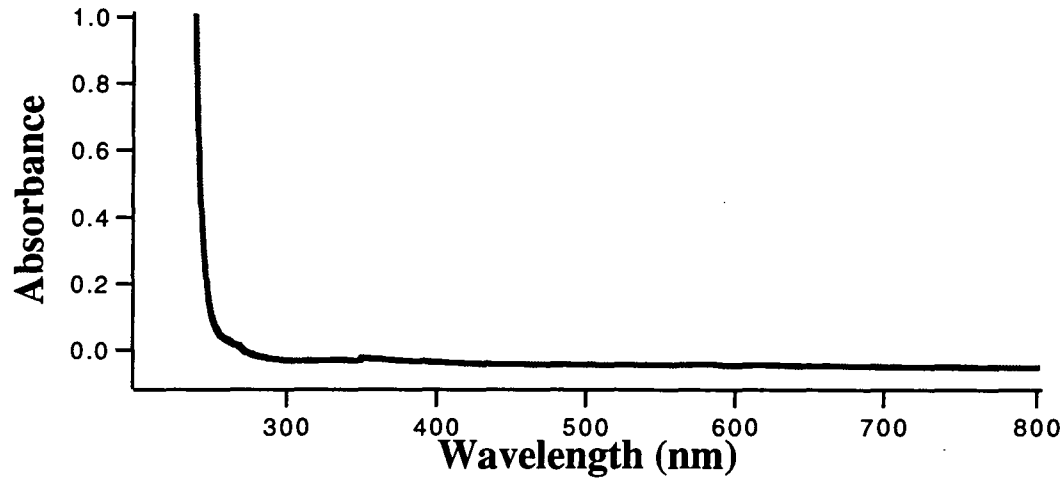

(7)

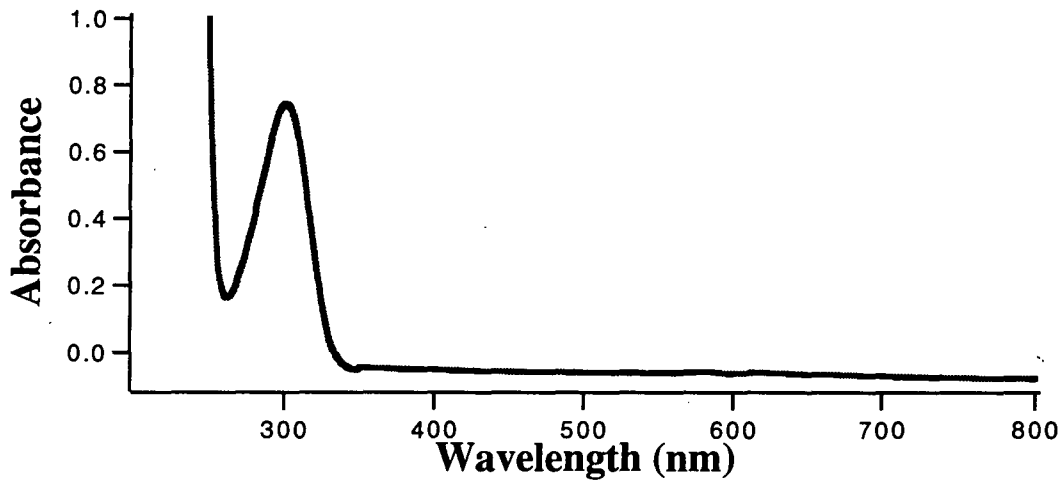

(8)

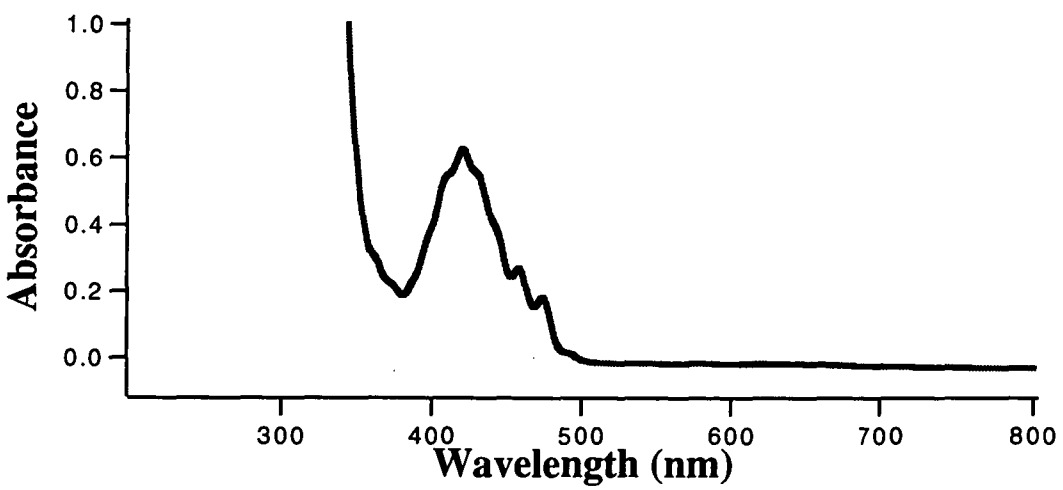

(9)

Fig. 4.6c Spectra of HIBA and its complexes. (1) 0.24 M HIBA, (2) 0.030 M Th(IV)-HIBA and (3) 0.040 M uranyl-HIBA.

4.4.1.2 Reversed-phase Chromatography of HIBA Complexes

Previous ion-interaction chromatography studies have reported that thorium and uranyl could be eluted either between or after the lanthanides dependent on the concentration of the ion-interaction reagent. Lanthanides and some transition metals also form complexes with HIBA, but the overall formation constants are different to those of thorium(IV) and uranyl. It can be expected that the retention of these metals should differ in a reversed-phase chromatography system.

A preliminary investigation with reversed-phase chromatography was carried out using an eluent consisting of 100 mM HIBA and 10% methanol (pH 4.0) without adding any IIR. Thorium(IV), uranyl, lanthanides and some transition metal standards were injected into the chromatographic system individually. The results showed that thorium(IV) and uranyl could be retained on the reversed-phase column, whilst lanthanides and transition metals were eluted at the solvent front or showed very weak retention, as listed in the third column of Table 4.3. Decreasing the organic modifier from 10% to 1% increased the retention of thorium(IV) and uranyl by a factor of approximately 2, but only minor changes were observed for the lanthanides and transition metals, as listed in the second column of Table 4.3. This indicated that the retention of thorium(IV) and uranyl probably occurred through a reversed-phase mechanism. Reducing the mobile phase pH from 4.0 to 2.5 resulted in a decreased retention for all the solutes, whilst the uranyl capacity factor dropped rapidly from 3.87 to 0.72. With a HIBA eluent at pH 2.5 thorium(IV) and uranyl could not be separated. Changing the organic modifier from 10% to 5% and increasing the HIBA concentration from 100 mM to 300 mM gave no significant change of retention for all the solutes. Since a decrease in organic modifier should lead to an increase in thorium(IV) and uranyl retention, it can be concluded that increasing the concentration of HIBA has the function of decreasing solute retention. Fig. 4.7 shows a chromatogram of thorium(IV) and uranyl obtained using a C_{18} column (300 x 3.9 mm I.D.) with 0.4 M HIBA in 10% methanol at pH 4.0 as the mobile phase.

Table 4.3 RETENTION OF METAL-HIBA COMPLEXES ON A REVERSED-PHASE CHROMATOGRAPHIC SYSTEM

A μ-Bondapak C_{18} column (300 x 3.9 mm I.D.) was used with 100 mM HIBA and the indicated percentage of methanol as the mobile phase, delivered at 1.0 ml/min. Detection by an absorbance at 658 nm after PCR with Arsenazo III.

Metals	100 mM HIBA 1% methanol pH 4.0 tr (min)	100 mM HIBA 10% methanol pH 4.0 tr (min)	100 mM HIBA 10% methanol pH 2.5 tr (min)	300 mM HIBA 5% methanol pH 4.0 tr (min)
Th^{4+}	13.30	6.85	5.14	5.95
UO_2^{2+}	38.36	14.93	5.15	15.52
La^{3+}	3.87	3.50	3.05	3.73
Ce^{3+}	3.94	3.58	3.08	3.77
Pr^{3+}	4.01	3.62	3.11	3.82
Nd^{3+}	4.10	3.67	3.11	3.88
Sm^{3+}	4.53	3.91	3.19	4.18
Eu^{3+}	4.70	4.00	3.30	4.24
Ga^{3+}	4.75	4.03	3.34	4.26
Dy^{3+}	4.85	4.08	3.43	4.29
Ho^{3+}	4.85	4.09	3.46	4.29
Er^{3+}	4.85	4.09	3.50	4.30
Yb^{3+}	4.86	4.10	3.65	4.30
Cu^{2+}	5.20	4.10	--	--
Zn^{2+}	3.58	3.39	--	--
Cd^{2+}	3.37	3.30	--	--
Co^{2+}	3.42	3.32	--	--
Ni^{2+}	3.52	3.37	--	--

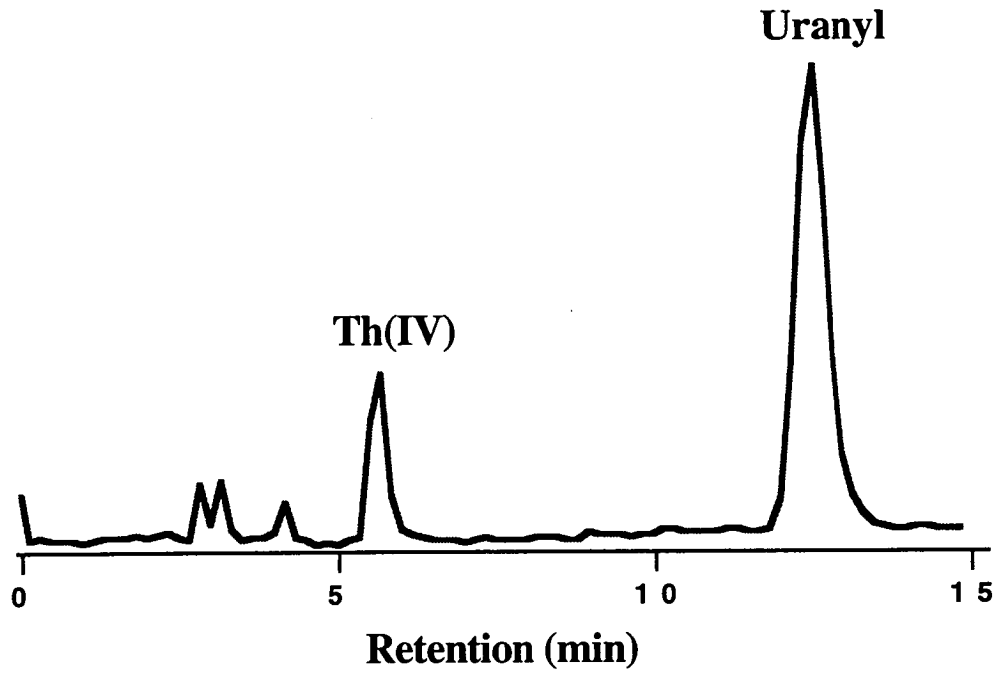

Fig. 4.7 Chromatogram of thorium(IV) (1 ppm) and uranyl (4 ppm) HIBA complexes. A μ-Bondapak C_{18} column (300 x 3.9 mm I.D.) was used with 400 mM HIBA in 10% methanol at pH 4.0 as the eluent, delivered at 1.0 ml/min. Detection at 658 nm after post-column reaction with Arsenazo III.

4.4.2 FACTORS AFFECTING RETENTION

4.4.2.1 Organic Modifier in the Mobile Phase

One of the characteristics of reversed-phase chromatography is that the retention is greatly affected by the organic modifier. Increasing the percentage of methanol (or acetonitrile) in the mobile phase will decrease the interaction between the solute and the hydrophobic stationary phase, thereby reducing the solute retention. In this study the effects of both methanol and acetonitrile on the retention of thorium(IV) and uranyl HIBA complexes have been examined. The influence of the percentage of organic modifier in the mobile phase is shown in Fig. 4.8. Retention changes were measured over the range 0-20% methanol at 400 mM HIBA for both thorium(IV) and uranyl (Fig. 4.8a), and at 20 mM HIBA for thorium(IV) (Fig. 4.8b). For comparison, the retention of a neutral reference compound, phenol, was also measured and is included in Fig. 4.8b. In all cases, a linear relationship for log k' *versus* the percentage of methanol was obtained, indicating that these solutes were being retained by a reversed-phase mechanism. It should be noted that this conclusion applies for the thorium(IV) complex even when the HIBA concentration is as low as 20 mM (Fig. 4.8 b). Similar results to those shown for methanol were also obtained using acetonitrile as the organic modifier over the range 0-10% (Fig. 4.8 c).

4.4.2.2 Column Temperature

The effect of the column temperature on capacity factor was studied over the range 15-50 °C, as shown in Fig. 4.9. The progressive decrease in capacity factor for uranyl with increasing temperature is in accordance with typical reversed-phase behaviour [19]. It is similar to the result obtained for the neutral reference, phenol. However, anomalous effects were observed for thorium(IV), which showed an increase in capacity factor with temperature. Similar effects for thorium(IV) and uranyl have been reported for eluents containing mandelic acid [6].

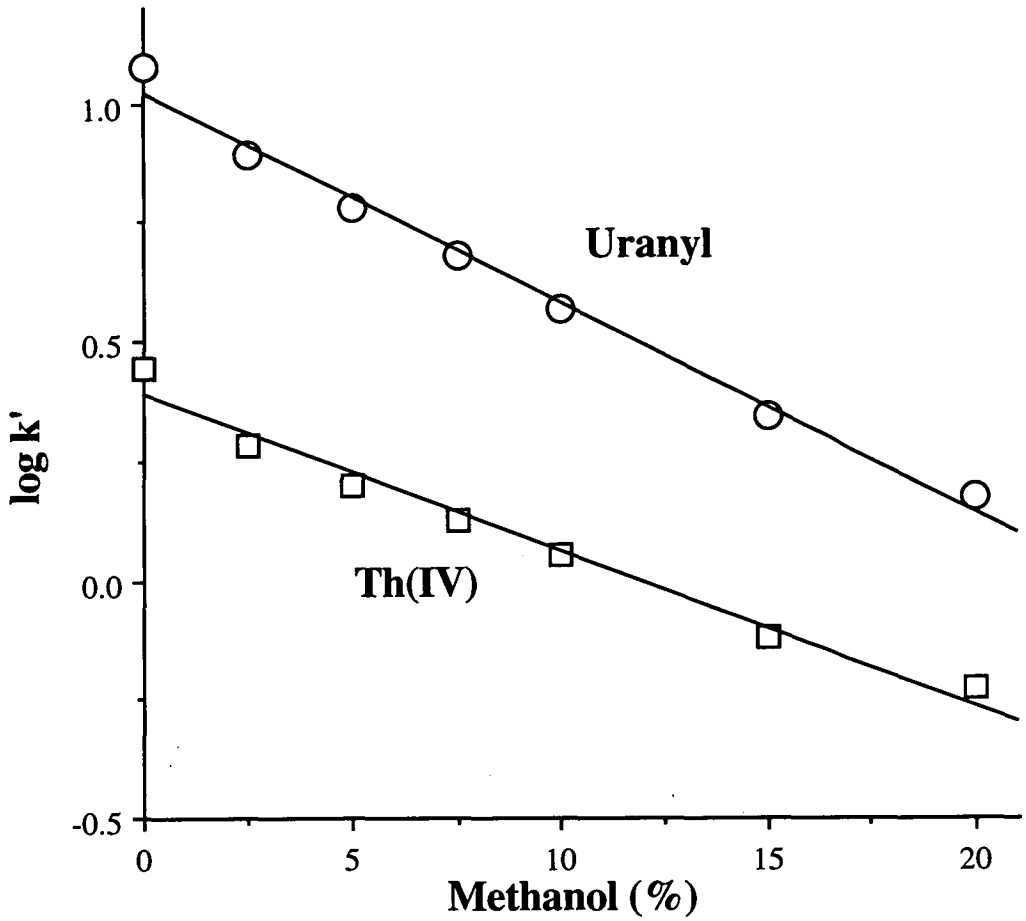

(a)

Fig. 4.8 Effect of organic modifier on thorium(IV) and uranyl HIBA complexes retention. The eluent comprised 400 mM HIBA and indicated percentage of methanol (pH 4.0). Other conditions were the same as in Fig. 4.7.

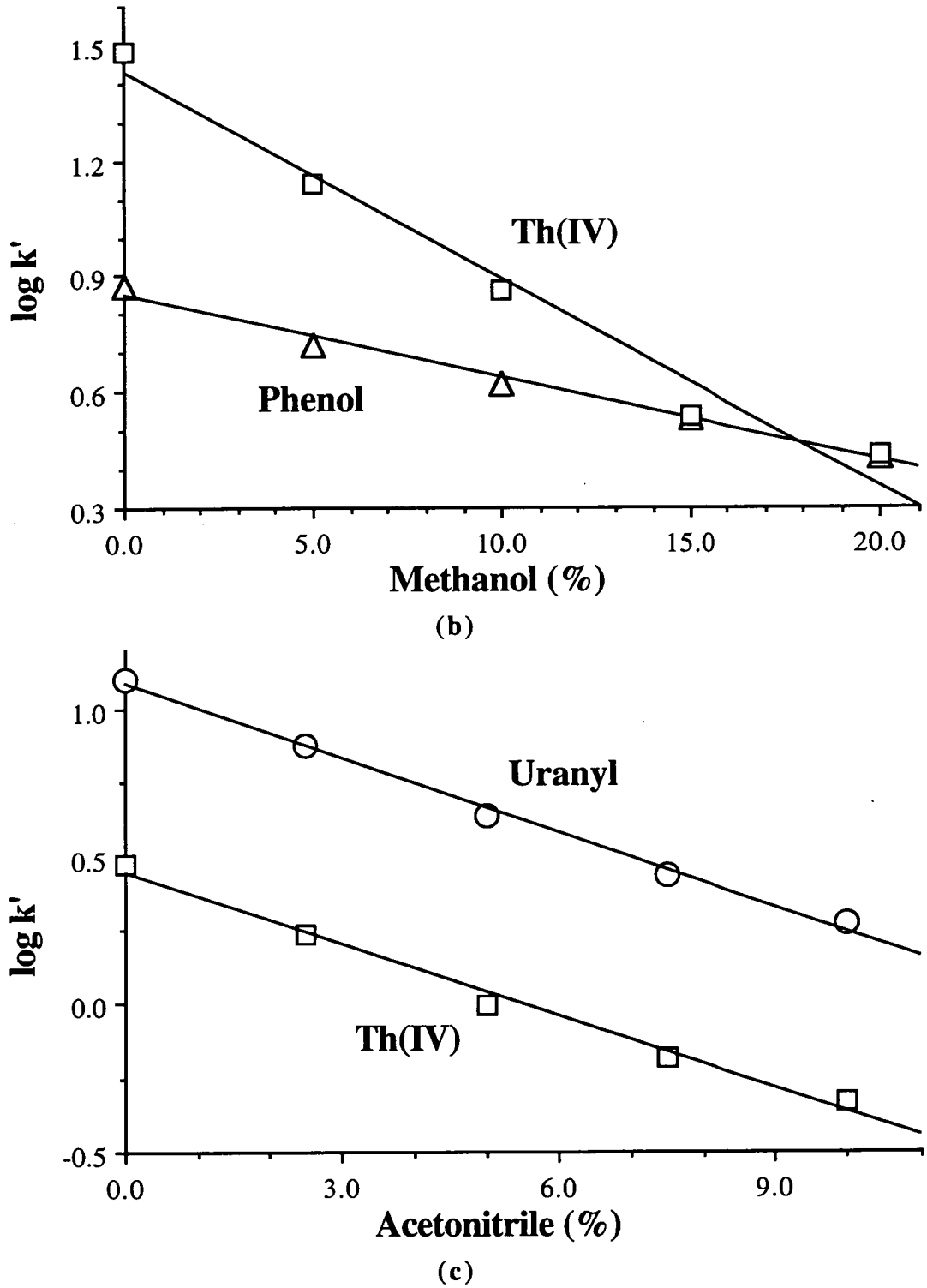

Fig. 4.8 (continued) Effect of organic modifier on thorium(IV) and uranyl HIBA complexes retention. The eluent comprised (b) 20 mM HIBA and the indicated percentage of methanol (pH 4.0), (c) 400 mM HIBA and the indicated percentage of acetonitrile (pH 4.0).

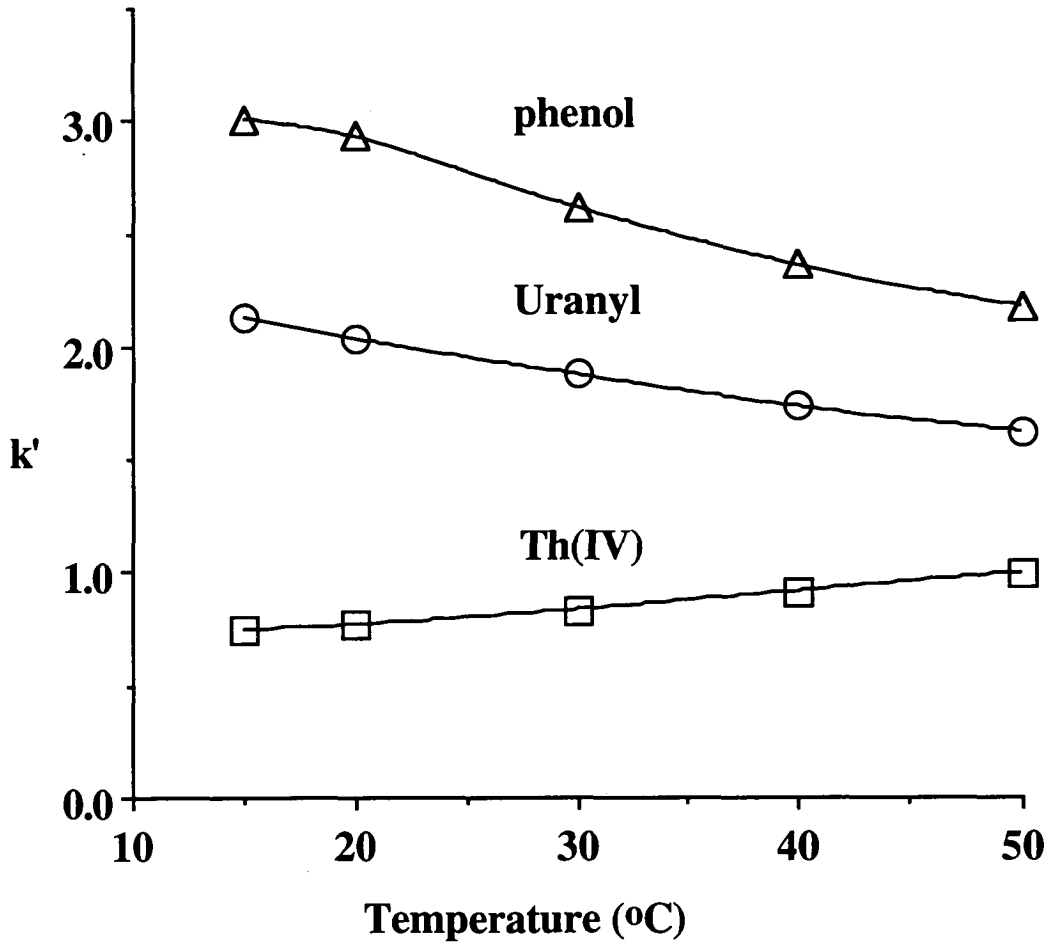

Fig. 4.9 Effect of column temperature on the retention of thorium(IV), uranyl and phenol. Chromatographic conditions were the same as in Fig. 4.7 with the exception of temperature. Phenol was directly detected at 254 nm.

4.4.2.3 HIBA Concentration in the Mobile Phase

As discussed in 4.3.2.1, the distribution of thorium(IV) and uranyl HIBA complexes at a given pH was dependent on the ligand concentration. It can be expected that the retention of these complexes will also vary with changes in the ligand concentration. The effect of HIBA concentration on thorium(IV) and uranyl retention is shown in Fig. 4.10, which indicates that the capacity factors for both thorium(IV) and uranyl decreased with increasing HIBA concentration, with the most rapid changes being observed for thorium(IV) at HIBA concentrations of less than 50 mM. It should be possible to compare these observations with the predicted forms of the metal complexes shown in Fig. 4.2, however, contradictions emerge. In the range 0-50 mM HIBA, Fig. 4.2a suggests that there is an increasing proportion of the neutral thorium(IV) *tetra*(HIBA) complex present, so that one would expect retention to increase progressively as the HIBA concentration is raised. The opposite trend occurs in Fig. 4.10. Similarly, the proportion of the uranyl *tris*(HIBA) complex rises progressively over the range 100-200 mM HIBA, but retention decreases.

4.4.2.4 The Eluent pH

The pH of the HIBA mobile phase was varied over the range 2.5-4.5 and the retention of both thorium(IV) and uranyl was found to increase, as shown in Fig. 4.11. There are two possible explanations for the eluent pH effect. Firstly, increasing the eluent pH assists the complexation, as discussed in the theory section above (refer to Fig. 4.3). At high pH there are larger proportions of complexes with high ligand number, which increases the hydrophobicity of the complex, so a longer retention was observed on the reversed-phase column. Another possibility is that increased pH results in a decrease in the concentration of neutral HIBA in the mobile phase (refer to Fig. 4.1), reducing competition of this species with the complexes for adsorption sites on the column. However, the eluent pH can be seen to exert almost no effect on the retention of phenol (the neutral reference substance) over the range of pH 2.5-4.5

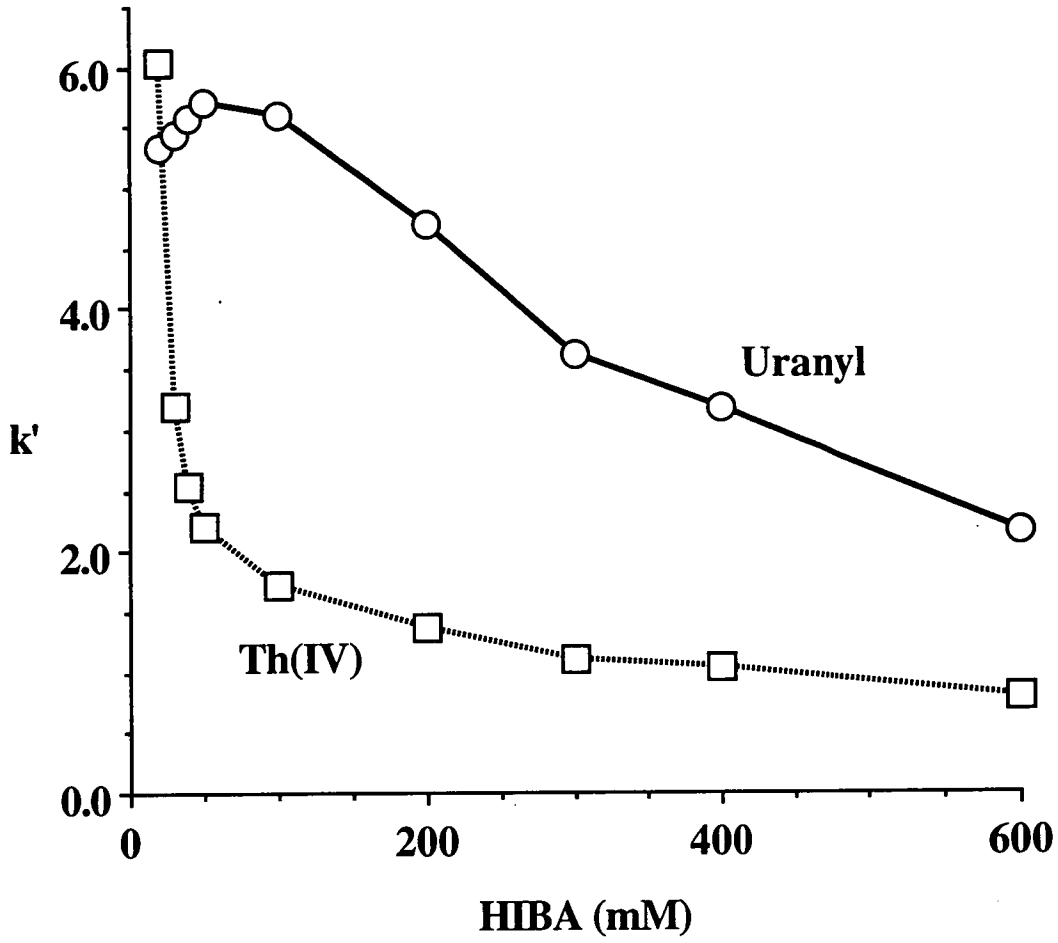

Fig. 4.10 Effect of ligand concentration on thorium(IV) and uranyl retention. Various concentrations of HIBA prepared in 10% methanol adjusted to pH 4.0 were used as the mobile phase. Other conditions were the same as in Fig. 4.7.

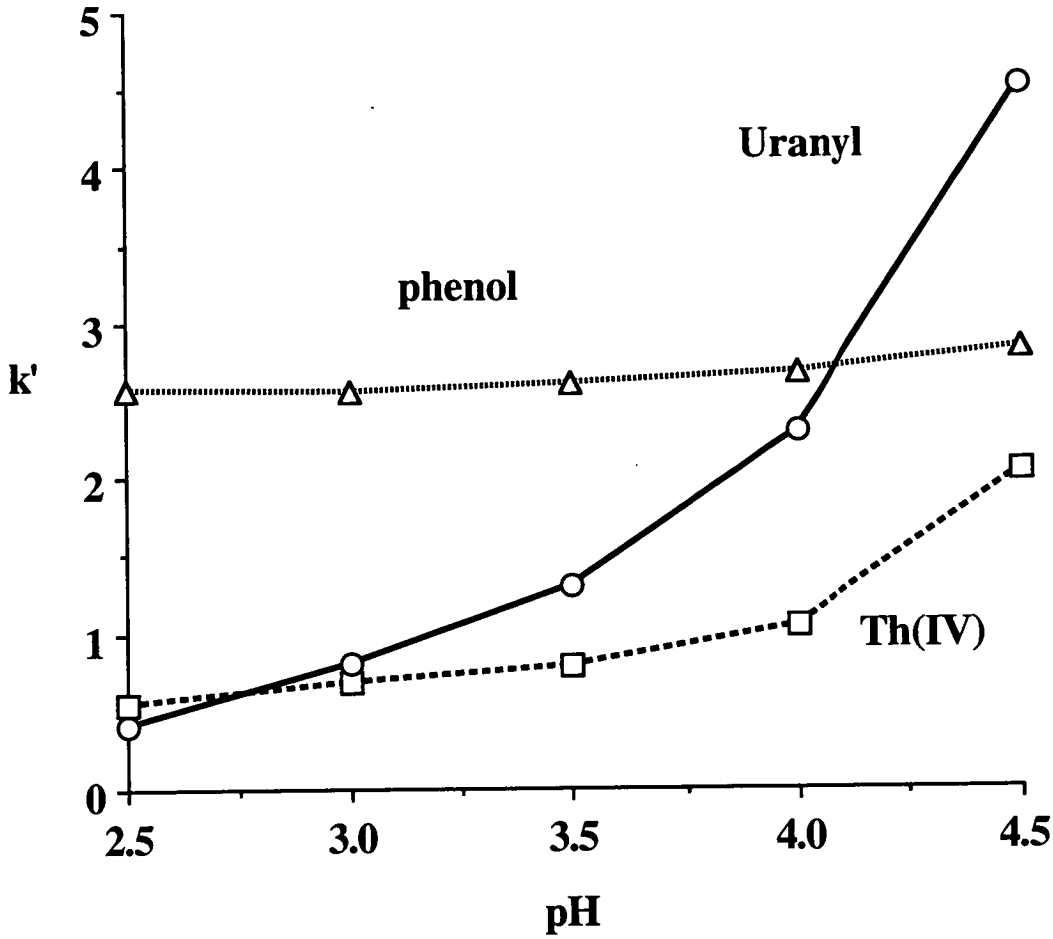

Fig. 4.11a Effect of eluent pH on thorium(IV) and uranyl retention. The eluent comprised 50 mM HIBA and 20% methanol, adjusted to the indicated pH value. Phenol was directly detected at 254 nm. Other conditions as in Fig. 4.7.

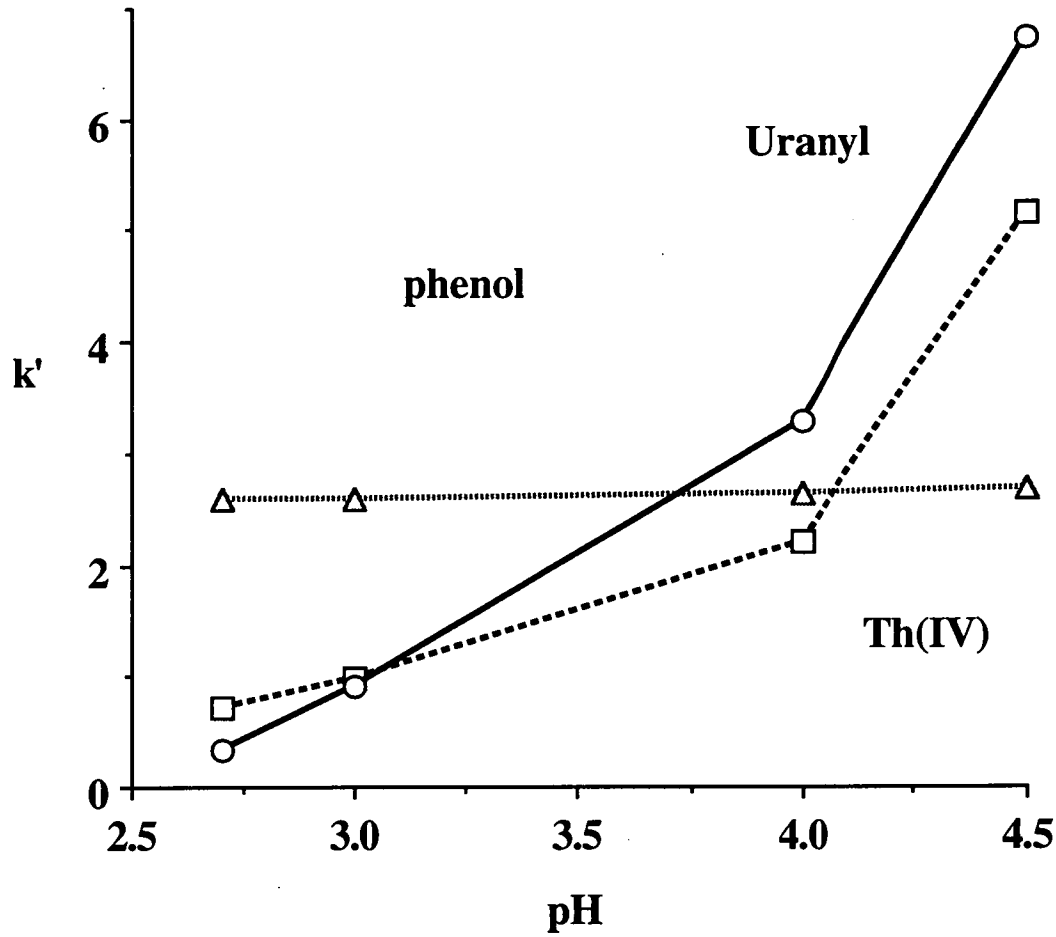

Fig. 4.11b Effect of eluent pH on thorium(IV) and uranyl retention. The eluent comprised 28 mM HIBA and 20% methanol, adjusted to the indicated pH value. Other chromatographic conditions as in Fig. 4.11a.

which indicated that the increased retention of thorium(IV) and uranyl resulted mainly from an increased level of complexation.

However, the changes in retention with pH for thorium(IV) and uranyl are different, so their separation is affected by the eluent pH. For example, at pH 2.5 thorium(IV) was eluted prior to uranyl, but the elution order reversed when the pH value was over 3.0. The two complexes could be separated completely when the pH was higher than 4.0.

In this experiment 50 mM HIBA was used because the effective charge on the uranyl-HIBA complex was changed from positive to negative when the solution pH varied from 2.5 to 4.5 at this concentration. It was expected that maximum retention would be observed when a minimum effective charge was present on the complex. The effective charge, δ, on these complexes was calculated using the formula below:

$$\delta_{Th(IV)} = 3 \times \alpha_1 + 2 \times \alpha_2 + 1 \times \alpha_3 + 0 \times \alpha_4$$

$$\delta_{Uranyl} = 1 \times \alpha_1 + 0 \times \alpha_2 + (-1) \times \alpha_3$$

where α_n represents the fraction of each species of these complex, and the subscript indicates the number of ligands coordinated to the central metal atom. The effective charge on uranyl-HIBA complexes is listed in Table 4.4 (calculated at 50 mM ligand concentration). However, the experimental results show that there was no simple relationship between the retention and the effective charge for the uranyl-HIBA complex.

The pH effect was also examined at a lower ligand concentration, 28 mM HIBA. Similar results were obtained, as shown in Fig. 4.11b.

Table 4.4 DISTRIBUTION OF URANYL-HIBA COMPLEXES AT VARIOUS pH VALUES

Calculated using the overall formation constants at 0.050 M HIBA.

pH	α_o UO_2^{2+}	α_1 UO_2L^+	α_2 UO_2L_2	α_3 $UO_2L_3^-$	effective charge
2.00	0.424	0.535	0.040	0.001	0.534
2.50	0.172	0.664	0.151	0.013	0.650
3.00	0.048	0.526	0.340	0.086	0.440
3.50	0.011	0.283	0.440	0.267	0.016
4.00	0.003	0.145	0.407	0.444	-0.299
4.50	0.002	0.097	0.366	0.535	-0.438
5.00	0.0012	0.083	0.347	0.569	-0.486
5.50	0.001	0.078	0.341	0.580	-0.502
6.00	0.001	0.076	0.339	0.584	-0.507

Note: L^- represents the HIBA anion.

4.4.2.5 Ion-interaction Reagents in the Mobile Phase

Studies were undertaken in which both cationic and anionic ion-interaction reagents (IIRs) were added to the mobile phase as a means of determining whether the eluted metal ions were present as anionic, neutral or cationic species. In each case, the column was equilibrated with the desired mobile phase, thorium(IV), uranyl and phenol (as a neutral marker compound) were injected and the relative retention time (comparative to that of phenol) of each metal was calculated. The results are given in Table 4.5, which shows that at higher HIBA concentrations, the only significant change observed was a reduction in the relative retention time for uranyl in the presence of octanesulfonate as the IIR. This suggests that the uranyl complex may be anionic under these conditions, but the observed increase in relative retention time in the presence of tetrabutylammonium as the IIR was only slight. The conclusions reached from these studies were twofold. First, any charge present on the complexes is sufficiently diffuse that it does not exert a great effect on retention. Second, there is a consistent trend for all solutes, including the neutral marker, for retention time to decrease as the concentration of HIBA is increased. This suggests that HIBA itself is adsorbed onto the stationary phase, and at the high concentrations used, probably precludes any appreciable adsorption of the IIR (which is present at much lower concentrations than HIBA), thereby preventing the IIR from significantly influencing retention. Decreases in relative retention times for thorium(IV) in the presence of octanesulfonate also suggest an anionic complex, but corresponding increases in retention when tetrabutylammonium was added to the mobile phase were not observed.

4.4.3 MECHANISM OF RETENTION

Evaluation of the above factors affecting retention of the HIBA complexes of thorium(IV) and uranyl on a reversed-phase column was undertaken in order to suggest a retention mechanism that explains all the observed trends. The behaviour of

Table 4.5 EFFECTS OF ANIONIC AND CATIONIC ION-INTERACTION REAGENTS ON RETENTION

A μ-Bondapak C_{18} column (300 x 3.9 mm I.D.) was used with the indicated mobile phase. Thorium(IV) and uranyl were detected at 658 nm after post-column reaction with Arsenazo III. Phenol was detected directly at 254 nm.

Mobile phase	Retention time (min)			Relative retention [a]	
	Phenol	Th(IV)	UO_2^{2+}	Th(IV)	UO_2^{2+}
80 mM HIBA, 5 mM TBA	11.0	4.6	8.2	0.42	0.74
400 mM HIBA, 5 mM TBA	9.7	3.7	7.4	0.38	0.76
80 mM HIBA	11.0	5.3	8.1	0.48	0.74
400 mM HIBA	9.3	4.3	6.1	0.46	0.66
80 mM HIBA, 5 mM OSA	11.0	4.2	5.1	0.38	0.46
400 mM HIBA, 5 mM OSA	9.5	3.5	4.0	0.37	0.42

TBA = tetrabutylammonium

OSA = octanesulfonate

[a] Compared to phenol under the same conditions.

the uranyl complex is perhaps the more straightforward. The effects of increasing the percentage of organic modifier (Fig. 4.8) and the temperature effect (Fig. 4.9) are consistent with reversed-phase adsorption. Despite the fact that complete complexation leads to the formation of the anionic *tris*(HIBA) complex, the resultant charge distribution must be sufficiently diffuse for the complex to exhibit a degree of hydrophobicity that permits reversed-phase adsorption. The decreased retention noted when the concentration of HIBA in the mobile phase was increased above 80 mM can be considered to result from increasing competition for the stationary phase adsorption sites by the considerable amount of non-ionised HIBA in the mobile phase. This effect has been suggested previously to explain a similar retention trend for mandelic acid complexes of uranyl on a reversed-phase column [6]. Evidence in support of this hypothesis can be seen from the retention behaviour of phenol at the two different HIBA concentrations given in Table 4.5. Here, a decrease in the retention time of phenol was noted with increasing HIBA concentration. This factor contributes to the behaviour shown in Fig. 4.8. In addition, increased formation of the anionic *tris*(HIBA) complex of uranyl would be expected to favour decreased retention. The retention maximum observed for uranyl at about 50 mM HIBA in Fig. 10 corresponds closely to the point where maximum formation of the neutral *bis*(HIBA) uranyl complex occurs (Fig. 4.2b). Finally, the increased retention observed with increasing pH (Fig. 4.11) can be attributed to increased complexation of uranyl and a concomitant decrease in the concentration of neutral HIBA in the mobile phase.

The retention behaviour of the thorium(IV) complex is somewhat anomalous in that under most of the conditions examined, it is eluted prior to the uranyl complex, despite the fact that it is expected to be a neutral complex with four ligand molecules, compared to a maximum of three for uranyl. Fig. 4.8 confirms that reversed-phase retention applies even at low concentrations of HIBA, but the temperature effect shown in Fig. 4.9 is the opposite to that normally encountered in reversed-phase chromatography. Further anomalies are evident in Fig. 4.10, where the retention of

the thorium(IV) complex is seen to decrease rapidly as the HIBA concentration is increased from 15-50 mM and then to show a modest decrease with higher concentrations of HIBA. Fig. 4.2a would suggest the opposite trends of a rapid increase in retention followed by a plateau region as formation of the neutral *tetra*(HIBA) complex dominates. Allowing for competition for the stationary phase adsorption sites by unreacted HIBA in the mobile phase could suggest decreased retention at high HIBA concentrations, so that a maximum might be expected in the plot for thorium(IV) in Fig. 4.10. The effect of pH on retention of thorium(IV) is similar to that observed for uranyl and can again be attributed to increased complex formation and reduced levels of neutral HIBA in the mobile phase.

One possible explanation for these results lies by considering the known propensity for thorium(IV) to hydrolyse in aqueous solution, even at acidic pH values [20], in juxtaposition with the fact that thorium(IV) often exhibits very high coordination numbers when complexed [21]. It is therefore likely that one or more hydroxyl ligands are incorporated into the coordination sphere of the thorium(IV), thereby reducing the overall charge on the complex. This would lead to the *bis*(HIBA) or *tris*(HIBA) complexes being neutral, whilst the *tetra*(HIBA) complex would be anionic. Comparison of the retention times of the thorium(IV) and uranyl complexes in a mobile phase containing 400 mM HIBA and considering the higher stoichiometry of the former complex, suggests that the negative charge on the thorium(IV) complex should be greater than for the uranyl complex. This indicates the presence of at least two hydroxyls in the thorium(IV) complex. Some evidence for this is the rapid decline in retention observed for thorium(IV) in Fig. 4.10 over the HIBA concentration range in which there is conversion of the *bis*(HIBA) complex (presumably neutral if two hydroxyls are present) into the *tris*(HIBA) complex (presumably anionic). Decreasing stability of the mixed ligand species at higher temperatures may account for the anomalous increase in retention observed with increasing temperature.

4.5 CONCLUSIONS

The elution characteristics of HIBA complexes of thorium(IV) and uranyl are dependent on the particular complexes existing in solution under the chromatographic conditions used. In the case of uranyl, the anionic *tris*(HIBA) complex dominates at 400 mM HIBA (pH 4.0) and is retained on a reversed-phase column by hydrophobic adsorption, despite its anionic nature. On the other hand, thorium(IV) forms a neutral *tetra*(HIBA) complex, which hydrolyses readily to produce an anionic complex probably containing at least two coordinated hydroxyl ions. This complex is also retained by hydrophobic adsorption, but to a lesser extent than the uranyl complex. The behaviour of thorium(IV) and uranyl in mobile phases containing HIBA is quite different to that exhibited by lanthanide ions, which are retained by a cation-exchange mechanism. This difference can be explained by the smaller formation constants and lower ligand:metal ratios of these species in comparison to thorium(IV) and uranyl.

4.6 REFERENCES

1 C. H. Knight, R. M. Cassidy, B. M. Recoskie and L. W. Green, *Anal. Chem.*, 56 (1984) 474.

2 D. J. Barkley, M. Blanchette, R. M. Cassidy and S. Elchuk, *Anal. Chem.*, 58 (1986) 2222.

3 R. M. Cassidy, S. Elchuk, N. L. Elliot, L. W. Green, C. H. Knight and B. M. Recoskie, *Anal. Chem.*, 58 (1986) 1181.

4 A. Kerr, W. Kupferschmidt and M. Attas, *Anal. Chem.*, 60 (1988) 2729.

5 R. M. Cassidy, S. Elchuk, L. W. Green, C. H. Knight, F. C. Miller and B. M. Recoskie, *J. Radioan. Nucl. Chem.*, 139 (1990) 55.

6 S. Elchuk, K. I. Burns, R. M. Cassidy and C. A. Lucy, *J. Chromatogr.*, 558 (1991) 197.

7 L. Magon, A. Bismondo, L. Maresca, G. Tomat and R. Portanova. *J. Inorg. Nucl. Chem.*, 35 (1973) 4237.

8 S. Elchuk and R. M. Cassidy, *Anal. Chem.*, 51 (1979) 1434.

9 J. D. Baker, R. J. Gehrke, R. C. Greenwood and D. H. Meikrantz, *J. Radioanal. Chem.*, 74 (1982) 117.

10 B. D. Karcher and I. S. Krull, *J. Chromatogr. Sci.*, 25 (1987) 472.

11 A. E. Martell, R. M. Smith, *Critical Stablility Constants*, Plenum Press, New York (1985) Vol. 3, p. 36.

12 L. Magon, G. Tomat, A. Bismondo, R. Potanova and U. Croatto., *Gazzetta Chimica Italiana*, 104 (1974) 967.

13 R. Larsson, *Acta Chemica Scandinavica*, 19 (1965) 783.

14 N. T. Basta and M. A. Tabatabai, *Soil Sci. Soc. Am. J.*, 54 (1990) 1289.

15 K. Ueno, T. Imamura and K. L. Cheng, *Handbook of Organic Analytical Reagents*, 2nd ed., CRC Press, Boca Taton, 1992, p.179.

16 J. J. Byerley, J. M. Scharer and G. F. Atkinson, *Analyst*, 112 (1987) 41.

17 G. J. Sevenich and J. S. Fritz, *J. Chromatogr.*, 371 (1986) 361.

18 R. Kuroda, M. Adachi, K. Oguma and Y. Sato, *Chromatographia*, 30 (1990) 263.

19 P. J. Schoenmakers, *Optimization of Chromatographic Selectivity*, Elsevier, Amsterdam, 1986, p.67.

20 S. Hietanen and L. G. Sillen, *Acta Chem. Scand.*, 22 (1968) 265.

21 F. A. Cotton and G. W. Wilkinson, *Advanced Inorganic Chemistry*, 2nd ed., Wiley Interescience, New York, 1967, p.1090.

Chapter 5

The Retention Behaviour of Thorium(IV) and Uranyl on a Reversed-Phase Column Using Glycolate and Mandelate Eluents

5.1 INTRODUCTION

In Chapter 4 the retention behaviour of thorium(IV) and uranyl on a C_{18} reversed-phase column was examined, using a α-hydroxyisobutyric acid (HIBA) mobile phase without the presence of any ion-interaction reagent (IIR). Thorium(IV) and uranyl were injected directly into the chromatographic system, and formed complexes with HIBA *in-situ*. It was found that these complexes were retained on the reversed-phase column based on a hydrophobic absorption mechanism. This is different from that of lanthanides which are retained through a cation-exchange mechanism [1, 2, 3]. Lanthanides and transition metals, such as Cu(II), Zn(II), Cd(II), Pb(II), Mn(II), Co(II), Ni(II), Fe(III) showed little or no retention on the reversed-phase column under these conditions.

Some unusual retention behaviour for thorium(IV) was also noted in Chapter 4. In 400 mM HIBA at pH 4.0, calculations based on the overall formation constants predicted that thorium(IV) should be present as the neutral *tetra*(HIBA) complex, whilst uranyl should exist as anionic *tris*(HIBA) complex. However, the reversed-phase chromatogram showed that thorium(IV) was eluted prior to uranyl. Another anomaly was that the retention of the thorium(IV) complex decreased rapidly when the HIBA concentration increased from 20 to 50 mM at pH 4.0, and then showed a modest decrease as the HIBA concentration continually increased. This behaviour is just the opposite to the theoretical prediction, which suggested that the formation of the neutral thorium(IV)*tetra*(HIBA) species first increased rapidly, and then was followed

by a plateau region. A further anomaly is that the retention of the thorium(IV) HIBA complex increased as the column temperature raised. This observation is contrasted to that usually encountered in reversed-phase chromatography. It was assumed that two or more hydroxyls were also incorporated into the thorium(IV) coordination sphere, thereby giving the thorium(IV) *tetra*(HIBA) complex a double or more negative charge, causing it to show weak retention. The mixed ligand thorium(IV) complex is less stable at high temperature, so it showed somewhat unusual behaviour when varying the column temperature.

Recently, Elchuk *et al.* [4] used mandelic acid to prepare the eluent for the separation of the lanthanides and transition metals with an ion-interaction method. In this work a C_{18} column was used and coated with sodium n-octanesulfonate (OSA) to covert it into a dynamic cation-exchange column. Lanthanides and other metals were separated on this column as mandelate complexes. The purpose of adding mandelic acid into the mobile phase was to reduce the effective charge on these metals. Elchuk *et al.* also noted that thorium(IV) and uranyl as well as the lanthanides could be retained on the reversed-phase column when OSA was not present in the eluent.

In order to extend the investigation presented in Chapter 4, in this chapter the retention behaviour of thorium(IV) and uranyl on the reversed-phase column was examined using a glycolic or mandelic acid eluent. These acids also form complexes with thorium(IV) and uranyl [5, 6] which are similar to those of HIBA, but they are different in hydrophobicity. If the hydrophobic adsorption mechanism is also applied to these complexes, it can be expected that the glycolate complexes should be retained for a shorter period because this ligand has less hydrophobicity. On the other hand, there is a strong hydrophobic group on mandelic acid, so its complexes should be retained much longer on the reversed-phase column.

In this chapter the experiments were carried out under the same conditions as in Chapter 4. All the factors which affect thorium(IV) and uranyl complexation and

retention, such as organic modifier, ligand concentration, eluent pH and column temperature, were examined in detail with both glycolate and mandelate eluents. These chromatographic results were then compared with those obtained using the HIBA eluent. A reference neutral substance, phenol, was also injected for comparison with thorium(IV) and uranyl complexes. Prior to the chromatographic study, the UV absorption of thorium(IV) and uranyl complexes with glycolate and mandelate were investigated, in order to make sure that they not interfere with the PCR detection.

5.2 CHEMISTRY OF THORIUM(IV) AND URANYL COMPLEXES WITH GLYCOLATE AND MANDELATE

It has been reported that thorium(IV) and uranyl form very stable complexes with α-hydroxymonocarboxylic acids, such as glycolic, lactic, mandelic and α-hydroxyisobutyric acids [5, 6]. An infrared spectrophotometry study showed that the α-hydroxy group of glycolate was also coordinated to the central uranium atom forming a five member ring [7]. These ligands all form four step complexes with thorium(IV) and three step complexes with uranyl. Other acetate type acids are also reported to form complexes with thorium(IV) and uranyl, but they are either of a different type or less stable. For example, thorium(IV) forms three step complexes with β-hydroxybutyrate, two step complexes with γ-hydroxybutyrate [5] and five step complexes with acetate [8]. The characteristics of the thorium(IV) and uranyl glycolate and mandelate complexes were initially examined by theoretical calculation and compared to those of HIBA complexes.

5.2.1 GENERAL PROPERTIES OF GLYCOLIC AND MANDELIC ACIDS AS LIGANDS

The structures of glycolic (hydroxyacetic) and mandelic (phenylhydroxyacetic) acids are shown in Fig. 5.1. There is a α-hydroxy group on both acids, but their carbon chains are different. Compared with HIBA, glycolic acid has a shorter carbon chain that makes it less hydrophobic. For the mandelic acid a phenyl group replaces

one of the methyl groups present on HIBA, which greatly increases the acid hydrophobicity. Glycolic and mandelic acids are weak acids, they are partially dissociated in aqueous solution. The acid dissociation constants (at 25 °C in 1M $NaClO_4$) are 2.40 x 10^{-4} for glycolic acid, and 6.76 x 10^{-4} for mandelic acid, respectively [8].

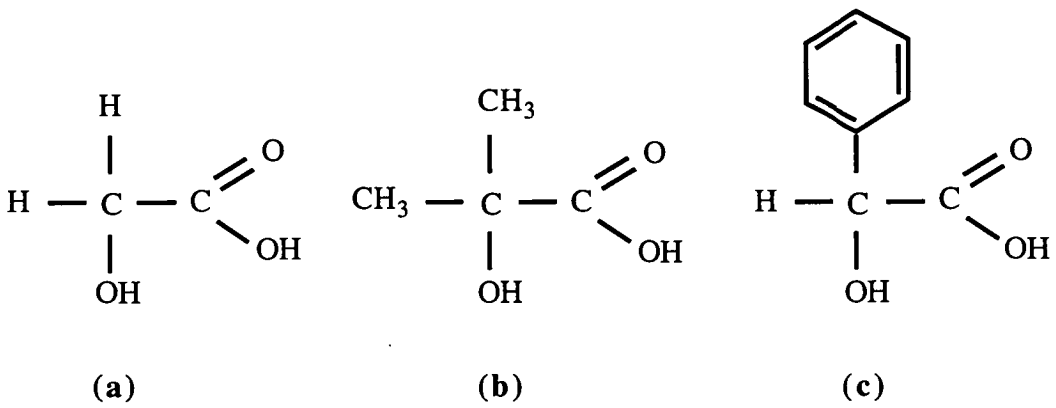

Fig. 5.1 Chemical structures of (a) glycolic acid, (b) HIBA and (c) mandelic acid.

As an acid, glycolic acid is weaker than mandelic acid, but they are both stronger than HIBA. Using these dissociation constants the distribution of glycolic and mandelic acids can be calculated at various pH values and plotted in Fig. 5.2. Compared to HIBA, glycolic and mandelic acids start to dissociate at a somewhat lower pH value, and their dissociation degrees are higher at the same conditions in the range of pH 1-6. For instance, at pH 3.6 about 73% of mandelic acid and 49% glycolic acid are ionised, whilst the figure is only 40% for HIBA. High dissociation favours the complex formation when the acid is coordinated to a metal cation.

5.2.2 CHARACTER OF GLYCOLATE AND MANDELATE COMPLEXES

Glycolic and mandelic acids have a similar complexation character to that of

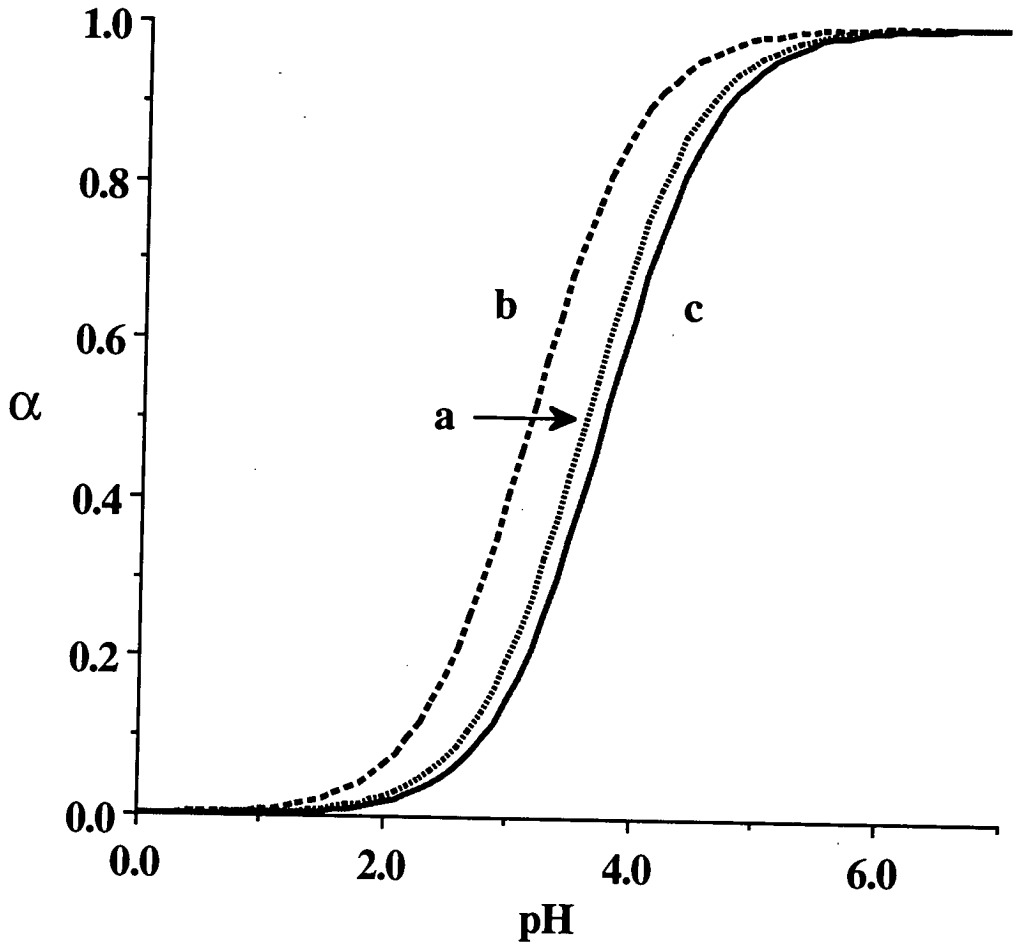

Fig. 5.2 Deprotonation of (a) glycolic acid, (b) mandelic acid and (c) HIBA at various pH values.

HIBA. They all form four step complexes with thorium(IV) and three step complexes with uranyl. However, the overall formation constants of glycolate and mandelate complexes are somewhat smaller than those of the HIBA complex (see Table 5.1).

Table 5.1 OVERALL FORMATION CONSTANTS OF THORIUM(IV) AND URANYL COMPLEXES WITH HIBA, GLYCOLATE AND MANDELATE Measured in 1M $NaClO_4$ at 20 °C [5, 6].

Metals	Acid	log β_1	log β_2	log β_3	log β_4
	Glycolic	3.98	7.36	9.95	11.95
Th(IV)	Mandelic	3.88	6.89	9.69	11.98
	HIBA	4.43	8.15	11.06	13.60
	Glycolic	2.38	3.95	5.18	--
Uranyl	Mandelic	2.57	4.10	5.32	--
	HIBA	3.18	5.13	6.67	--

5.2.2.1 Effect of Ligand Concentration on Complex Formation

Using the Eqn. 4.21 and the overall formation constants given in Table 5.1, the distribution of thorium(IV) and uranyl complexes with glycolate and mandelate are calculated at various ligand concentrations at pH 4.0, and plotted in Fig. 5.3 and Fig. 5.4, respectively. These figures show that the distribution trend of each of these complexes is very similar to that of the HIBA species. However, the fraction of the

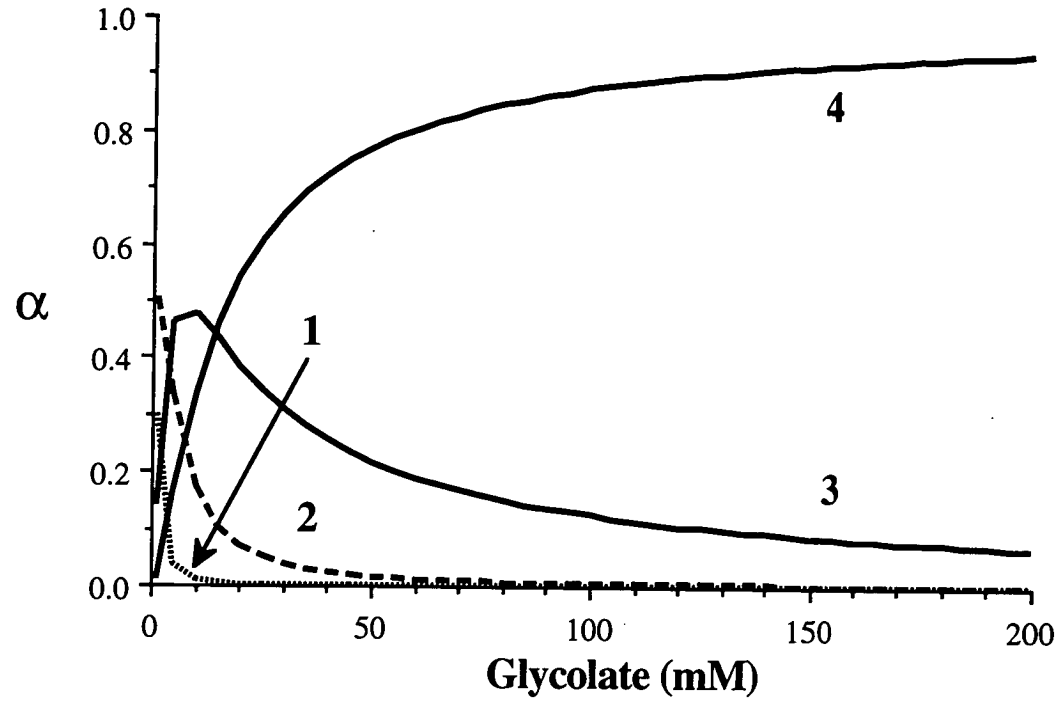

(a)

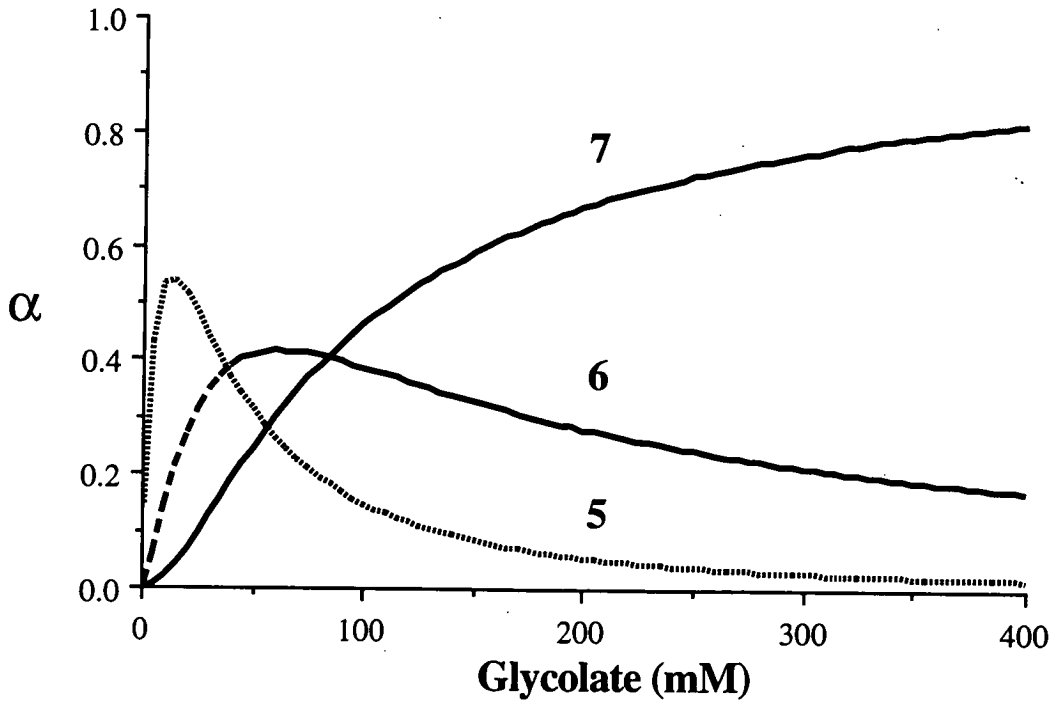

(b)

Fig. 5.3 Fraction (α) of each species of (a) thorium(IV) and (b) uranyl glycolate complexes presents at various ligand concentrations. (1) ThL^{3+}, (2) ThL_2^{2+}, (3) ThL_3^{+}, (4) ThL_4, (5) UO_2L^{+}, (6) UO_2L_2, (7) $UO_2L_3^{-}$. Calculated at pH 4.0 using the overall formation constants given in Table 5.1.

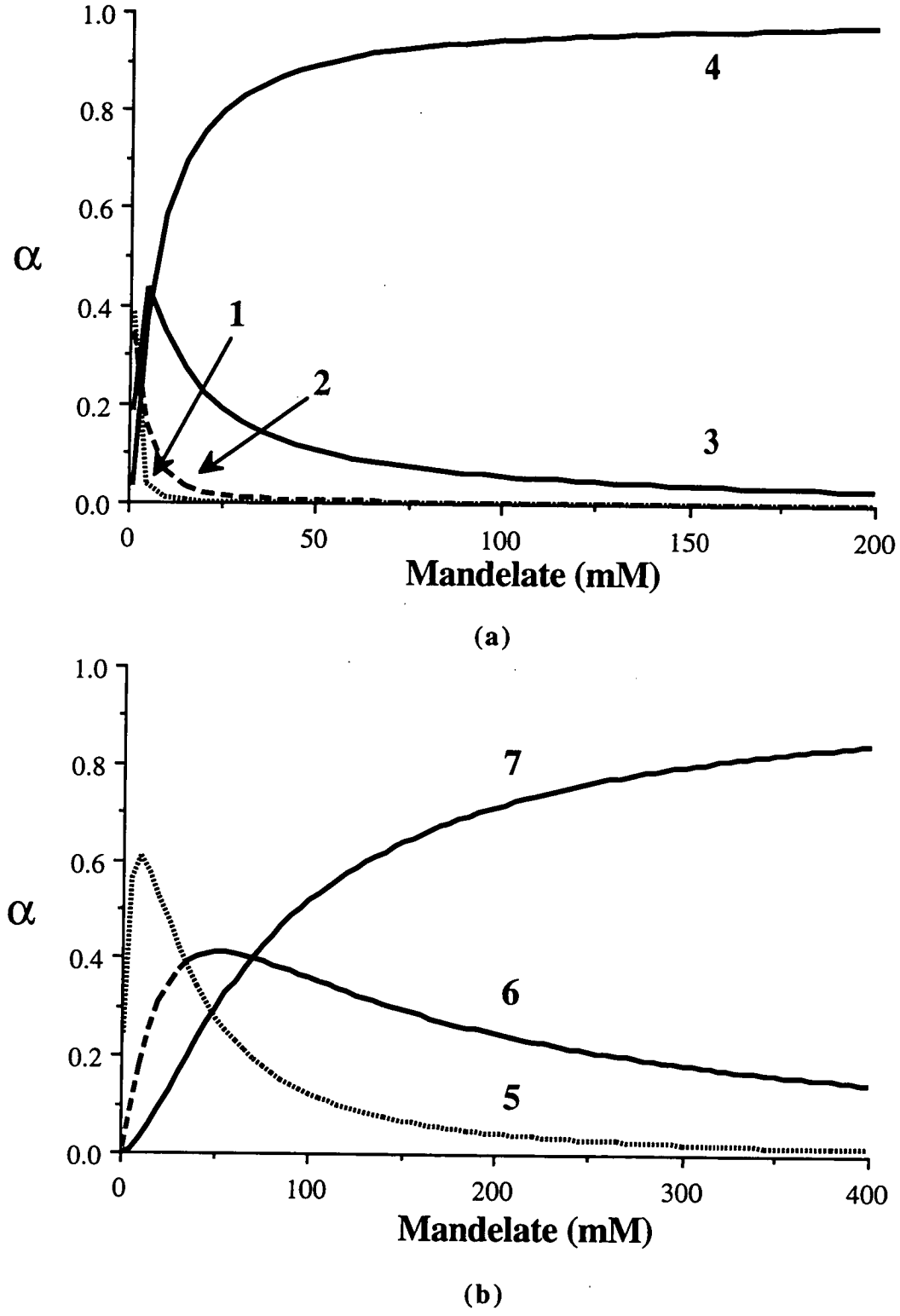

Fig. 5.4 Fraction (α) of each species of (a) thorium(IV) and (b) uranyl mandelate complexes presents at various ligand concentrations. (1) ThL^{3+}, (2) ThL_2^{2+}, (3) ThL_3^{+}, (4) ThL_4, (5) UO_2L^{+}, (6) UO_2L_2, (7) $UO_2L_3^{-}$. Calculated at pH 4.0 using the overall formation constants given in Table 5.1.

complexes with a higher ligand number, such as thorium(IV) *tetra*(ligand) and uranyl *tris*(ligand), is smaller than that of HIBA complexes under the same ligand concentration. For example, in 10 mM ligand solution (at pH 4.0) the fraction of thorium(IV) *tetra*(glycolate) is about 34%, *tetra*(mandelate) 59%, whilst the *tetra*(HIBA) is 65%; when the ligand is prepared at 60 mM concentration (pH 4.0), only 30% uranyl exists as *tris*(glycolate) species, and 39% as *tris*(mandelate), in contrast to 50% *tris*(HIBA). If we simply consider the effect of complexation on retention, the thorium(IV) complex should be retained longest when using a HIBA eluent, and shortest with a glycolate eluent under the same ligand concentration, whilst the uranyl complex should be opposide.

5.2.2.2 Effect of pH on Complex Formation

Fig. 5.5 and Fig. 5.6 show the distribution of thorium(IV) and uranyl complexes at various pH values, calculated at 0.400 M ligand concentration. The proportion of thorium(IV) t*etra*(ligand) and uranyl *tris*(ligand) complexes increases rapidly when the pH is raised in an acidic solution, followed by a plateau when the solution pH exceeds 4.0. At high pH there is no difference among the three ligands for the proportion of thorium(IV) *tetra*(ligand) complexes. However, the distributions of uranyl *tris*(glycolate) and *tris*(mandelate) species are lower than that of uranyl *tris*(HIBA); the maximum fraction of uranyl *tris*(glycolate) is only 86.4% when the solution pH exceeds 6.0. The lower distribution of anionic species should be of benefit for the uranyl glycolate complexes retained on the reversed-phase column.

On the other hand, the distribution of the neutral species of uranyl *bis*(glycolate) is much higher than that of *bis*(HIBA) and *bis*(mandelate) when the solution pH exceeds 3.0. At even higher pH the fraction of the *bis*(glycolate) remains constant at 12.7% and the *bis*(mandelate) 13.0% ,whilst the *bis*(HIBA) only 6.7%. If we simply consider the effect of solution pH on the uranyl retention, it can be expected that a longer retention should be observed with glycolate and mandelate eluents.

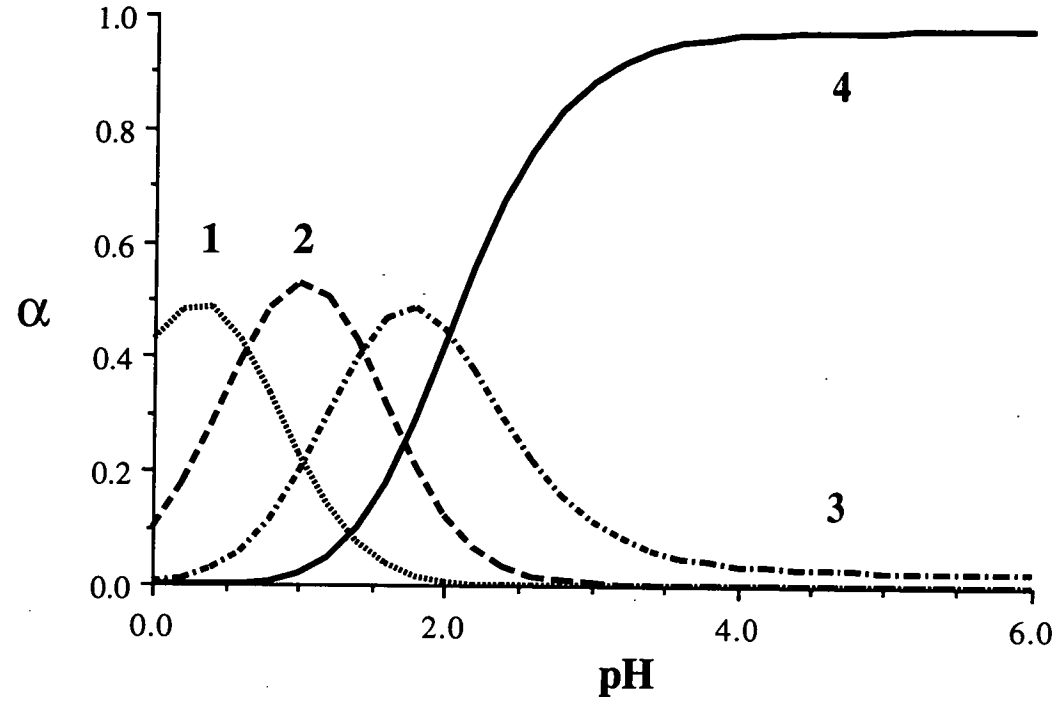

(a)

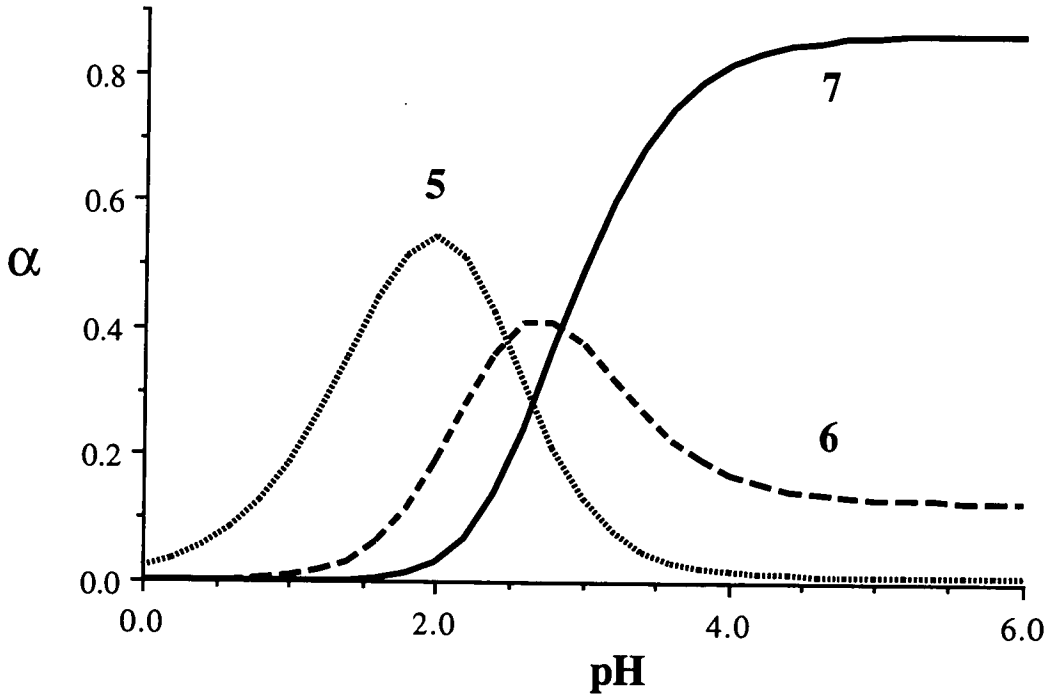

(b)

Fig. 5.5 Fraction (α) of each species of (a) thorium(IV) and (b) uranyl glycolate complexes presents at various pH values. (1) ThL^{3+}, (2) ThL_2^{2+}, (3) ThL_3^{+}, (4) ThL_4, (5) UO_2L^{+}, (6) UO_2L_2, (7) $UO_2L_3^{-}$. Calculated at 400 mM glycolate concentration using the overall formation constants given in Table 5.1.

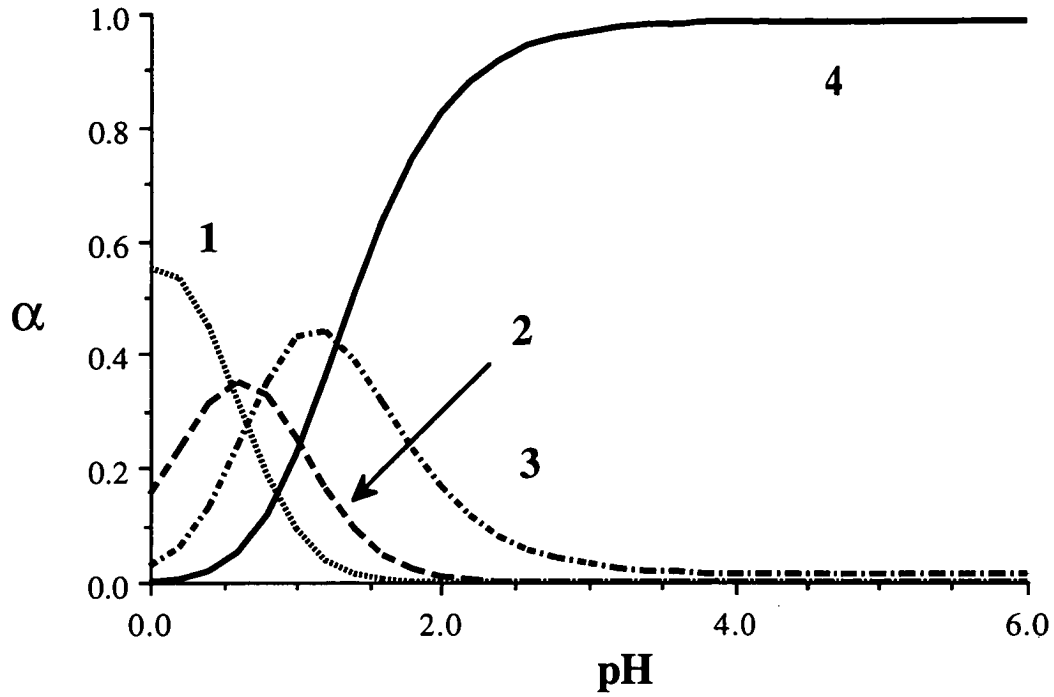

(a)

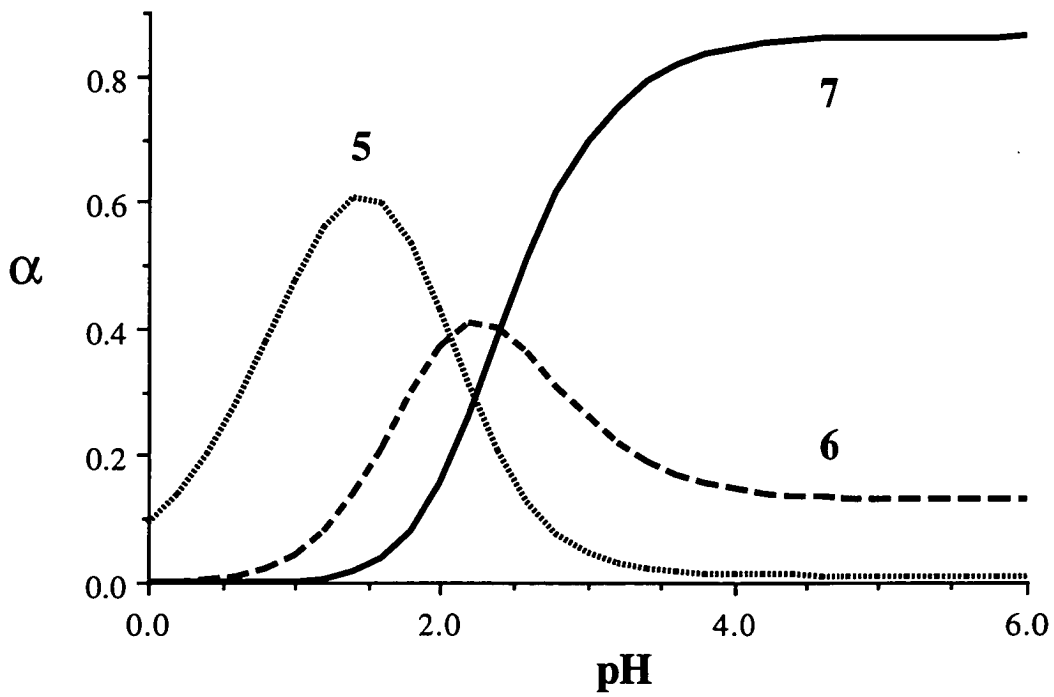

(b)

Fig. 5.6 Fraction (α) of each species of (a) thorium(IV) and (b) uranyl mandelate complexes presents at various pH values. (1) ThL^{3+}, (2) ThL_2^{2+}, (3) ThL_3^{+}, (4) ThL_4, (5) UO_2L^{+}, (6) UO_2L_2, (7) $UO_2L_3^{-}$. Calculated at 400 mM mandelate concentration using the overall formation constants given in Table 5.1.

5.3 EXPERIMENTAL

5.3.1 INSTRUMENTATION

Following the previous experiment in Chapter 4, the same direct injection chromatographic system was also used in the present studies. The instrument configuration was shown in Fig. 3.1.

5.3.2 Reagents

Analytical grade glycolic (Sigma Chemical Company) and mandelic acids (Koch-light Laboratories Ltd, Colnbrook, Bucks, England) were used to prepare the mobile phase without further treatment. In order to compare the results with those obtained using HIBA as the eluent, most mobile phases used in this study were buffered at pH 4.0, except those used in the determination of eluent pH effect. The post-column reaction (PCR) reagent, Arsenazo III (B.D.H. Laboratory Chemical Division, England) solution was prepared as before. Both the mobile phase and the PCR solution were prepared freshly each day, and filtered through a Millipore 0.45 μm membrane, then degassed in an ultrasonic bath prior to use. The mandelate mobile phase was stored in the dark to prevent decomposition.

10 ppm standard solutions of thorium(IV), uranyl, phenol, the lanthanides and transition metals solutions were prepared daily by dilution the concentrated stock solutions using the chromatographic mobile phase.

The elution of phenol was monitored at 270 nm without the post-column reaction when the mandelate mobile phase was used, as there is a strong absorption for the mandelate eluent itself at lower wavelengths.

A Cary 5E UV-Vis-Nir Spectrophotometer (Varian Techtron Pty. Ltd, Australia) was used in the preliminary investigation, and operated with automatic background correction. Absorbance was measured in quartz cells (1.0 x 1.0 cm).

5.4 RESULTS AND DISCUSSION

5.4.1 PRELIMINARY INVESTIGATIONS

5.4.1.1 Spectra of Glycolate, Mandelate and Their Complexes

Prior to the chromatographic experiments, the absorption spectra of glycolic and mandelic acids, as well as their thorium(IV) and uranyl complexes were initially examined. The purpose was to ensure that these acids and their complexes do not interfere with the chromatographic detection after PCR reaction with Arsenazo III. The acid solutions were obtained by directly dissolving glycolic and mandelic acid in Milli-Q water. The complex solutions were prepared based on their metal:ligand stoichiometric ratio, 1:4 (0.06 M:0.24 M) and 1:3 (0.08 M:0.24 M) for thorium(IV) and uranyl, respectively. The spectra of both acids and their complexes were measured over the range of 200-800 nm using Milli-Q water as the reference. Fig. 5.7. shows that there is an absorption peak at 300 nm for the thorium(IV) glycolate complex, and one at 422 nm for the uranyl-glycolate complex. The absorption spectra of the thorium(IV) and uranyl mandelate complexes are similar to those of glycolate complexes. However, mandelic acid has strong absorption at wavelengths <270 nm. No absorption was observed at wavelengths >500 nm for both the acids and their complexes, which indicated that they would not interfere with the chromatographic detection at 660 nm selected in previous chapter.

5.4.1.2 Preliminary Chromatographic Studies

The retention behaviour of the glycolate complex was initially investigated with a mobile phase consisting of 400 mM glycolate and 10% methanol (pH 4.0). The chromatogram (Fig. 5.8) shown that the elution order of thorium(IV) and uranyl was the same as that with a HIBA eluent. That is, thorium(IV) was eluted before uranyl, even though the thorium(IV) should be present as a neutral *tetra*(glycolate) complex whilst the uranyl as an anionic *tris*(glycolate) species, as calculated using the overall

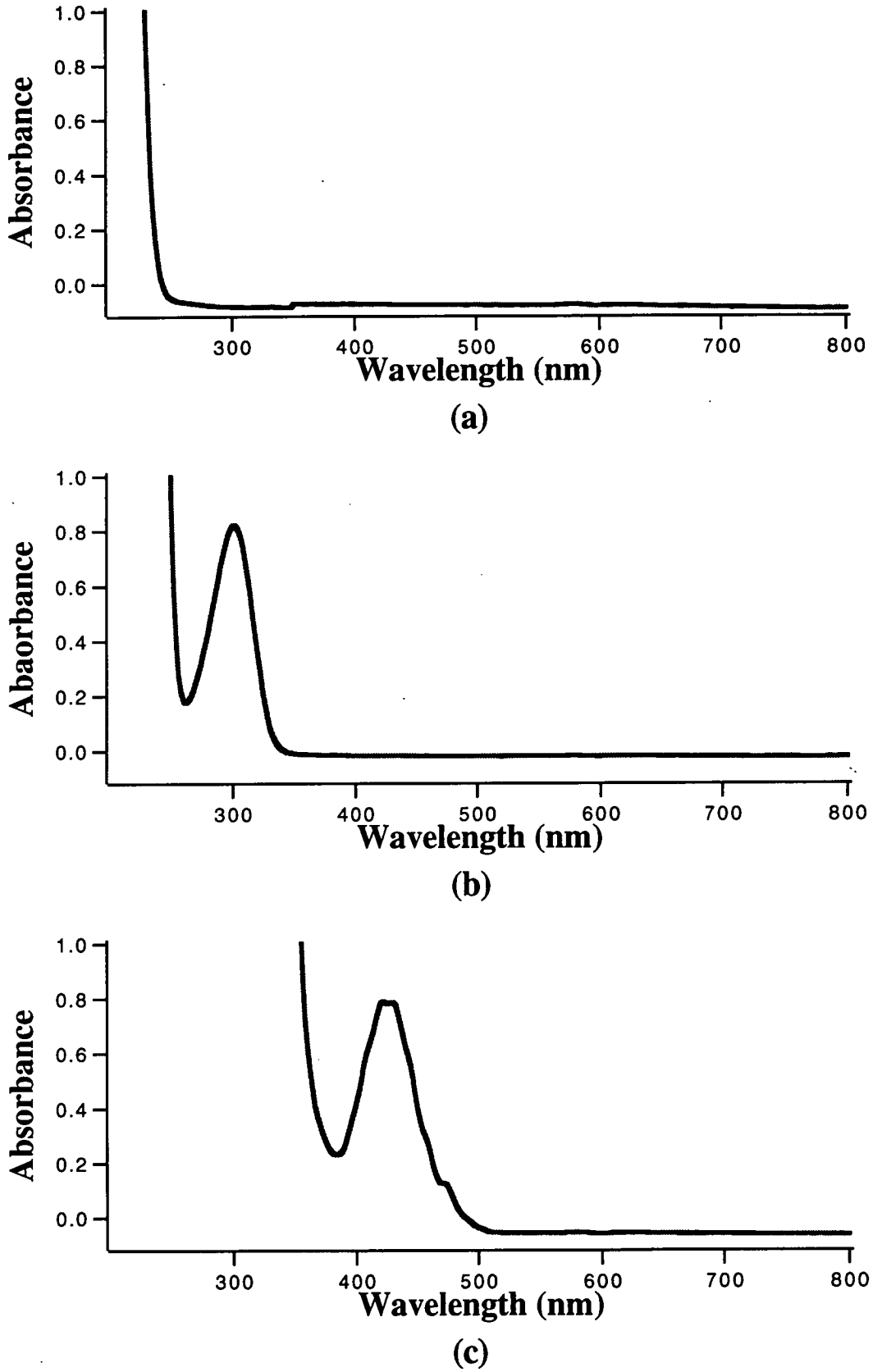

Fig. 5.7 Spectra of glycolic acid and its complexes. (a) 0.240 M glycolic acid, (b) 0.030 M Th(IV)-glycolate and (c) 0.040 M uranyl-glycolate complexes.

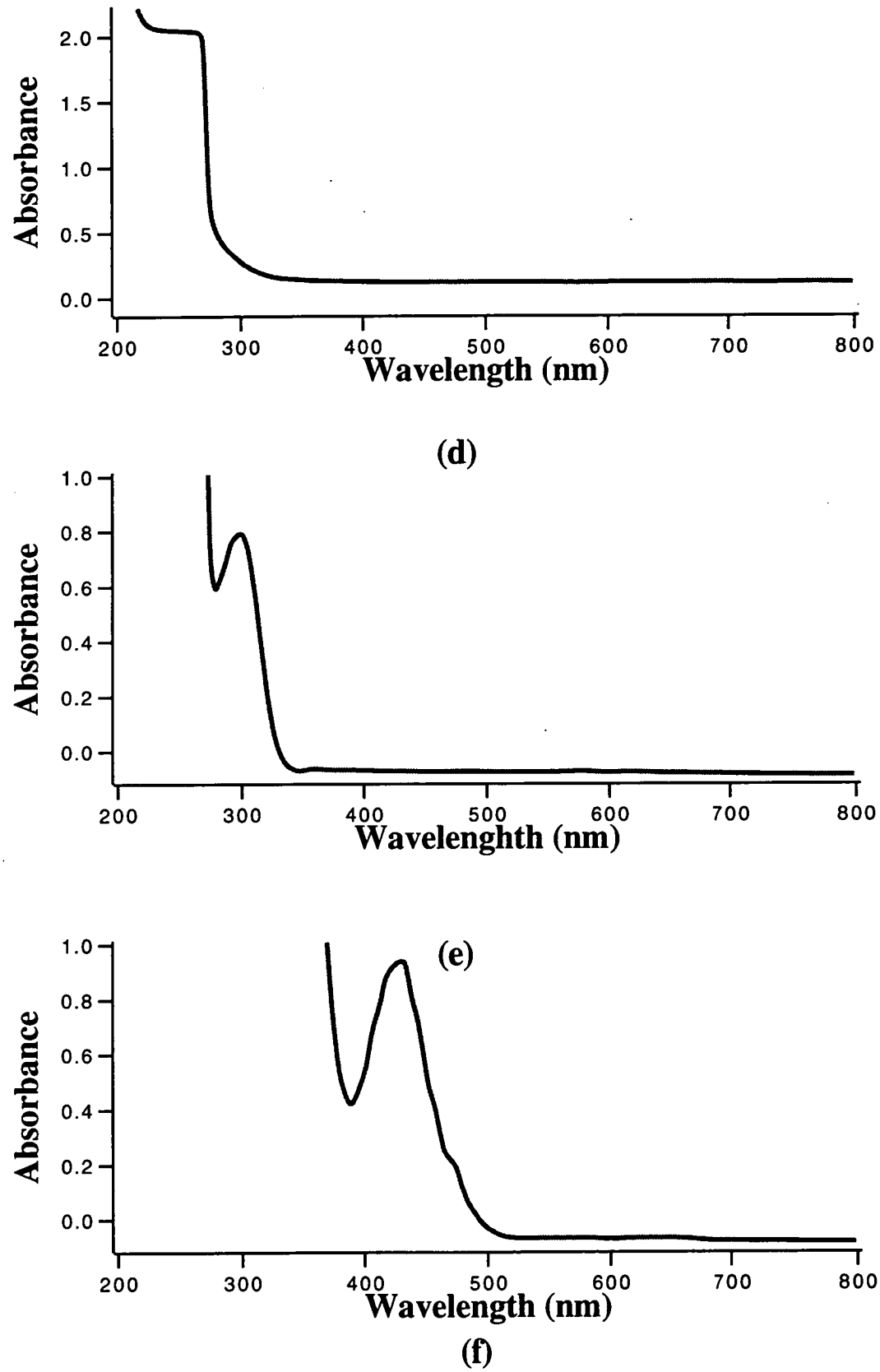

Fig. 5.7 (continued) Spectra of mandelic acid and its complexes. (d) 0.240 M mandelic acid, (e) 0.030 M thorium(IV)-mandelate and (f) 0.040 M uranyl-mandelate complexes.

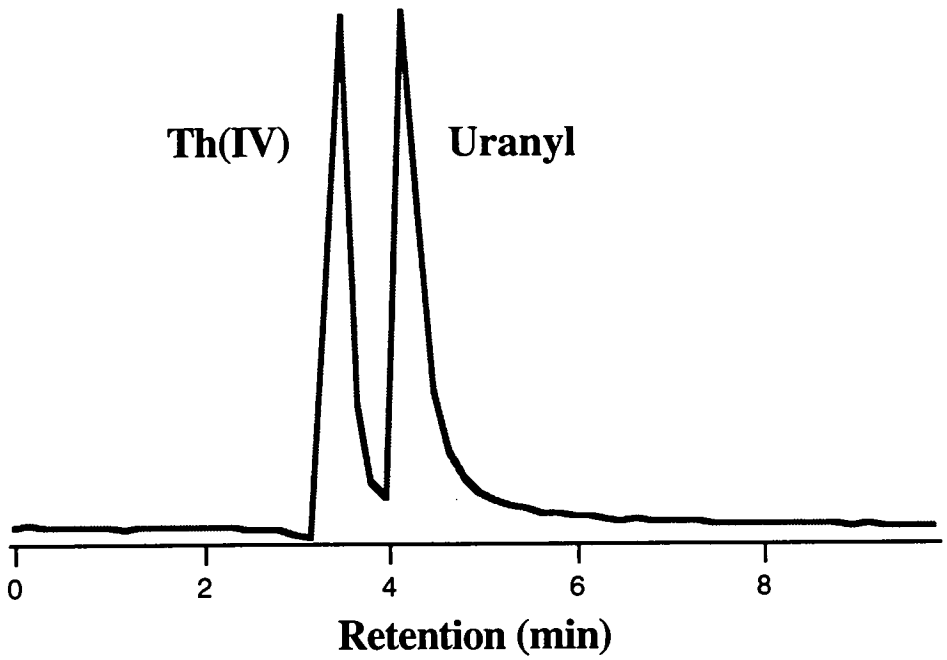

Fig. 5.8 Chromatogram of thorium(IV) and uranyl glycolate complexes. A Waters μ-Bondapak C_{18} column (300 x 3.9 mm I.D.) was used with 400 mM glycolate in 10% methanol at pH 4.0 as the eluent, delivered at 1.0 ml/min. Detection at 658 nm after post-column reaction with Arsenazo III.

formation constants at these conditions. However, comparing with the HIBA eluent, the overall retention times of both thorium(IV) and uranyl glycolate complexes were much shorter, which were in accordance with the theoretical predictions discussed above. Under these conditions the thorium(IV) and uranyl peaks are barely separated. Further experiments showed that the two peaks could be separated completely using a mobile phase comprising 60 mM glycolate and 10% methanol (pH 4.0). Later chromatographic studies of glycolate complexes were all carried out under these conditions, except for the experiment concerning the effect of ligand concentration.

With a 400 mM mandelate mobile phase (pH 4.0), the overall retention times for both thorium(IV) and uranyl were much longer than those obtained using 400 mM HIBA eluent, despite the fact that the mandelate eluent was prepared in 20% methanol (Fig. 5.9). The longer retention can be explained by the phenyl group on the mandelic acid which greatly increased the hydrophobicity of the acid as well as its complexes. Thorium(IV) and uranyl co-eluted in the 400 mM mandelate eluent. Resolution could be achieved when the mandelate concentration reduced to less than 50 mM.

It was interesting to find that the elution order of thorium(IV) and uranyl was reversed in the mandelate eluent. Varying the mandelate concentration or adjusting to different pH could not alter the elution order. This was also observed by other researchers [4]. Two explanations are possible for the retention behaviour. Firstly, the thorium(IV) coordination sphere may be sterically hindered by the phenyl group, so that no hydroxyl takes part in the coordination as suggested in Chapter 4. That is, the thorium(IV) *tetra*(mandelate) is a neutral species under these conditions, so it is eluted after the anionic uranyl *tris*(mandelate) complex. An alternative explanation is that the strong hydrophobicity of the mandelate complexes overshadow the effect of negative charge, so that only the reversed-phase character of the complex is dominant. In this case, the retention order is simply dependent on the ligand number of the complex, thus the uranyl *tris*(mandelate) complex is eluted before the thorium(IV) *tetra*(mandelate) complex.

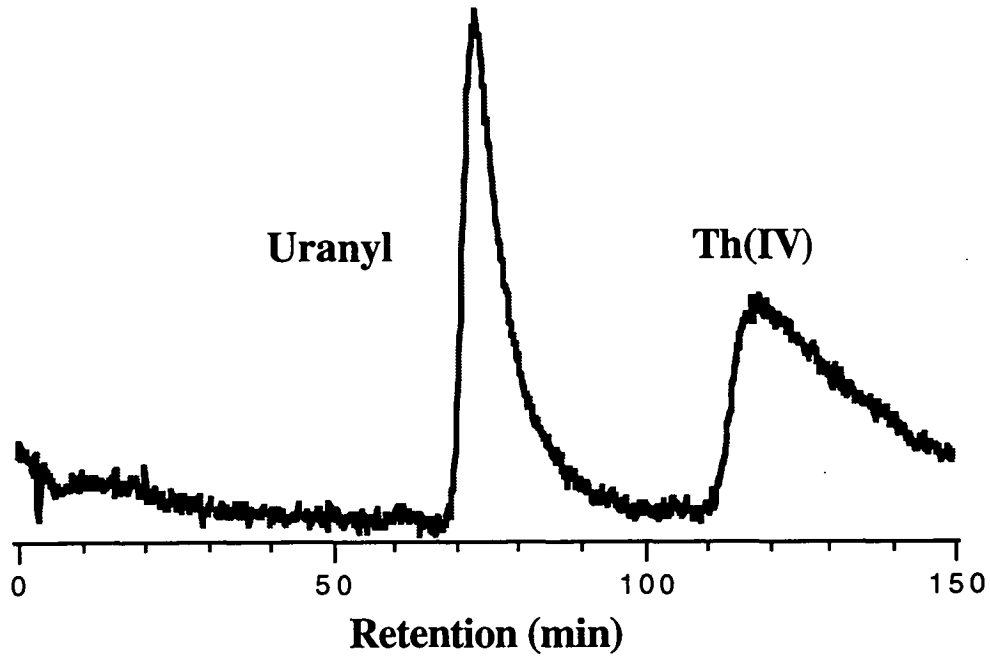

Fig. 5.9 Chromatogram of thorium(IV) and uranyl mandelate complexes. A Waters μ-Bondapak C_{18} column (300 x 3.9 mm I.D.) was used with 50 mM mandelate in 20% methanol at pH 4.0 as the eluent, delivered at 1.0 ml/min. Detection at 658 nm after post-column reaction with Arsenazo III.

5.4.2 FACTORS AFFECTING RETENTION OF GLYCOLATE AND MANDELATE COMPLEXES

5.4.2.1 Organic Modifier in the Mobile Phase

Fig. 5.10 shows the effect of organic modifier on the retention of glycolate and mandelate complexes. Various percentages of methanol were prepared in 60 mM glycolic or 50 mM mandelic acid adjusted to pH 4.0 as the eluent. A decreased retention was observed for thorium(IV) and uranyl as well as phenol, when methanol was increased from 0% to 30% in the glycolate eluent, or from 10% to 50% in the mandelate eluent. Plotting the logarithm of capacity factor against the methanol percentage in the mobile phase gave a linear relationship in all cases:

In the glycolate eluent:

Th(IV):	log k' = 0.5118 - 0.03502 x MeOH%;	R = 0.999
Uranyl:	log k' = 0.9790 - 0.03958 x MeOH%;	R = 0.999
Phenol:	log k' = 0.7796 - 0.02188 x MeOH%;	R = 0.991

In the mandelate eluent:

Th(IV):	log k' = 2.4417 - 0.04237 x MeOH% ;	R = 0.998
Uranyl:	log k' = 2.225 - 0.04231 x MeOH%;	R = 0.998
Phenol:	log k' = 0.7332 - 0.01710 x MeOH%;	R = 1.000

where MeOH% represents the methanol percentage (v/v) in the mobile phase, and R is the correlation coefficient. These results are similar to those obtained using the HIBA eluent, which confirmed that the hydrophobic adsorption mechanism also applied to the thorium(IV) and uranyl complexes with glycolate and mandelate when they are retained on the C_{18} reversed-phase column. At high percentages of methanol,

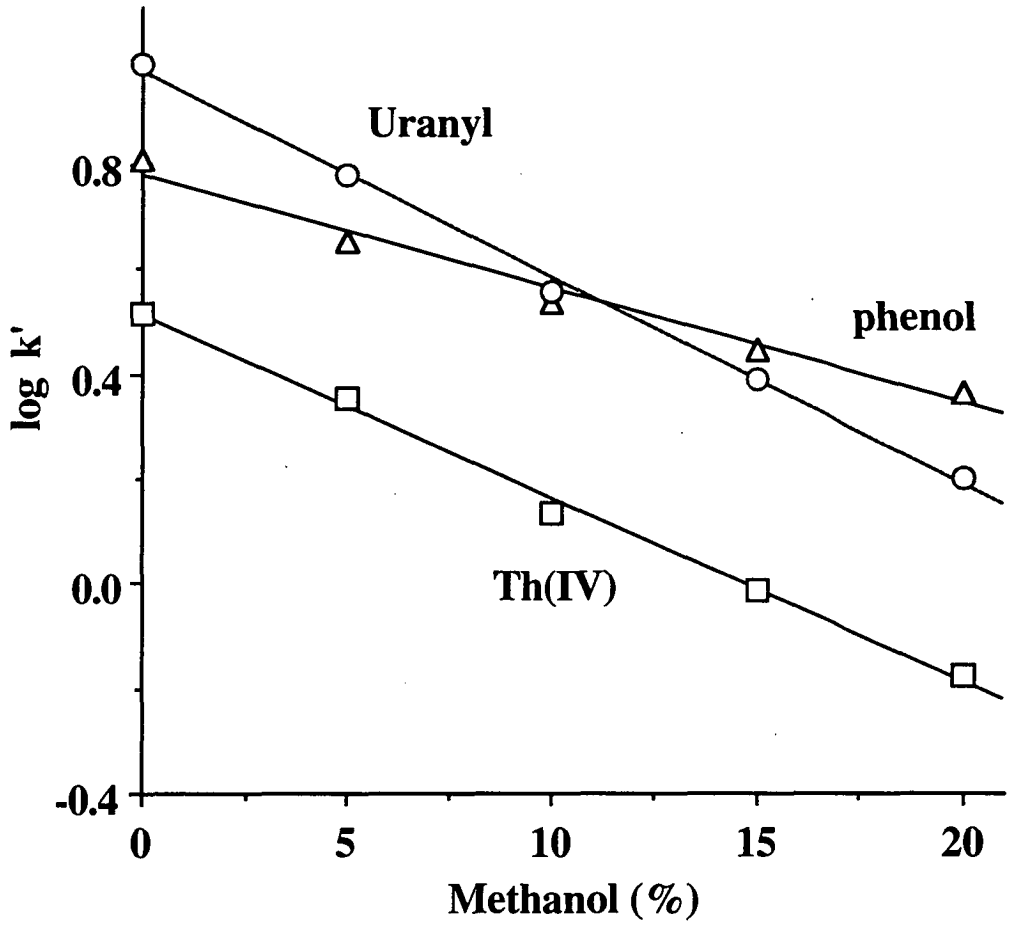

Fig. 5.10a Effect of organic modifier on the retention of phenol and thorium(IV) and uranyl glycolate complexes. The eluent consisted of 60 mM glycolate and various percentages of methanol (pH 4.0). Phenol was monitored directly at 254 nm. Other conditions were the same as in Fig. 5.8.

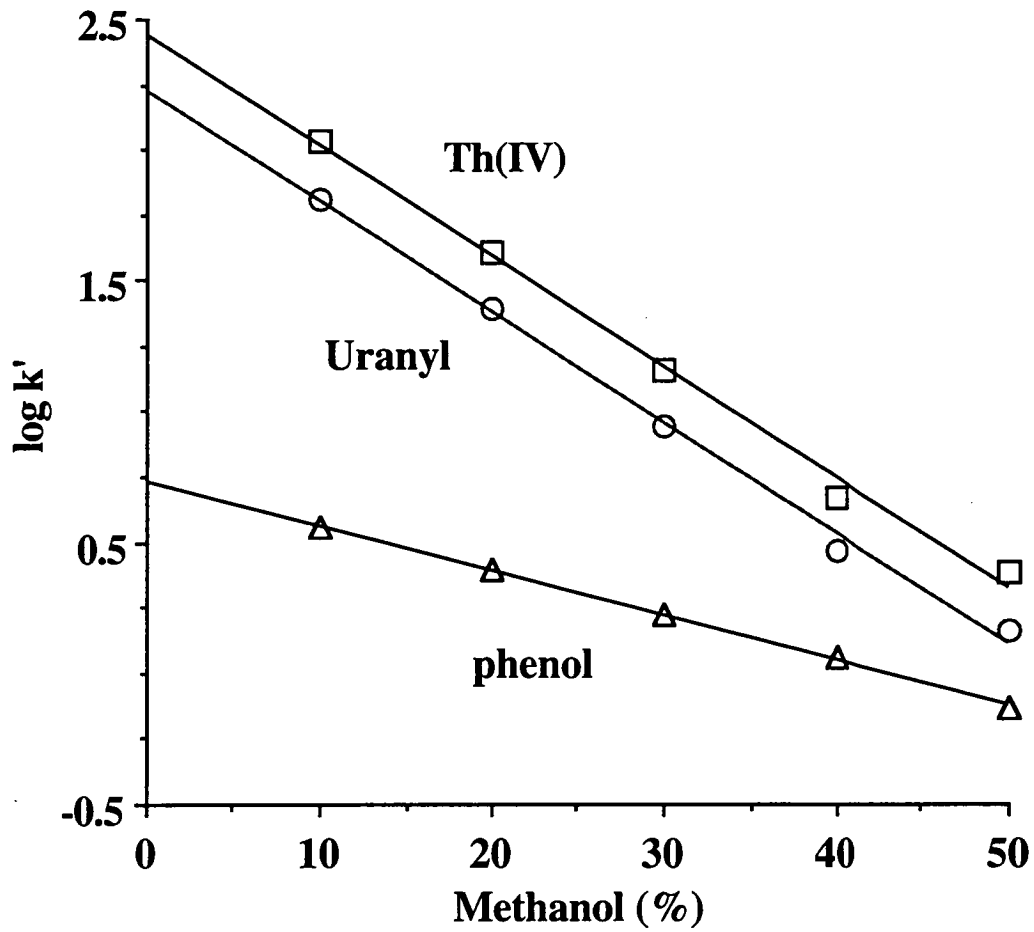

Fig. 5.10b Effect of organic modifier on the retention of phenol and thorium(IV) and uranyl mandelate complexes. The eluent consisted of 50 mM mandelate and various percentages of methanol (pH 4.0). Phenol was monitored directly at 270 nm. Other conditions were the same as in Fig. 5.9.

thorium(IV) and uranyl complexes were co-eluted in both glycolate and mandelate eluents; it is not practicable to undertake routine analysis under these conditions. On the other hand, the mandelate complexes were retained on the reversed-phase stationary phase so strongly that they were eluted out with difficulty when the percentage of methanol was less than 10%. In subsequent experiments with mandelate 20% methanol or more was used in the mobile phase.

5.4.2.2 Column Temperature

When the column temperature was varied, the glycolate and mandelate complexes showed different retention behaviour. Increasing the column temperature from 20 °C to 50 °C using a mandelate eluent caused the retention of thorium(IV), uranyl and phenol to decrease. The behaviour of the thorium(IV) in mandelate mobile phase differs from that observed previously using HIBA eluent, in which the thorium retention increased as the temperature rose.

In contrast, the retention behaviour observed with 60 mM glycolate in 5% methanol (pH 4.0) as the eluent was identical to that noted previously using HIBA mobile phase, namely increased retention at high temperatures for thorium(IV), approximately constant for uranyl, and decreases for phenol. According to reversed-phase retention theory [9], there is an inverse relationship between the capacity factor and the absolute temperature:

$$\ln k' = \Delta H/RT - \Delta S/R + \ln (n_s/n_m) \qquad (5.1)$$

where ΔH and ΔS are the enthalpy and entropy effects for the partition of the solute on the stationary phase, R is the gas constant, T is the absolute temperature, and n_s/n_m is a phase ratio term. In practice this equation is rewritten as below:

$$\ln k' = A/T + B \qquad (5.2)$$

Usually, the coefficient A takes a positive value. Plotting the logarithm of

capacity factor against the inverse of absolute temperature, a linear relationship was obtained for all of the three solutes in both glycolate and mandelate eluents, as listed in Fig. 5.11.

In the glycolate eluent:

Th(IV):	log k' = - 797.9/T + 3.0182	R = 1.000
Uranyl:	log k' = - 8.512/T + 0.7678	R = 0.984
Phenol:	log k' = 310.3/T - 0.4006	R = 0.999

In the mandelate eluent:

Th(IV):	log k' = 269.2/T + 2.568	R = 0.999
Uranyl:	log k' = 384.5/T - 0.9084	R = 0.999
Phenol:	log k' = 332.2/T - 0.9241	R = 0.997

where T is the absolute temperature (K).

The positive coefficients for the three analytes in the mandelate eluent and phenol in the glycolate eluent, indicate that they are retained on the C_{18} column by typical reversed-phase chromatography mechanism. However, the large negative coefficient observed for thorium(IV) in glycolate mobile phase is unusual. The temperature effect on the retention of uranyl glycolate complex is similar, but is much smaller than that observed for thorium(IV) glycolate complexes.

5.4.2.3 Ligand Concentration in the Mobile Phase

Increasing the glycolate concentration over the range of 20-400 mM both thorium(IV) and uranyl retentions were reduced, whilst there was no change in the phenol retention, as shown in Fig. 5.12a. These glycolate eluents were all prepared in 10% methanol and adjusted to pH 4.0. The behaviour of the uranyl glycolate complex

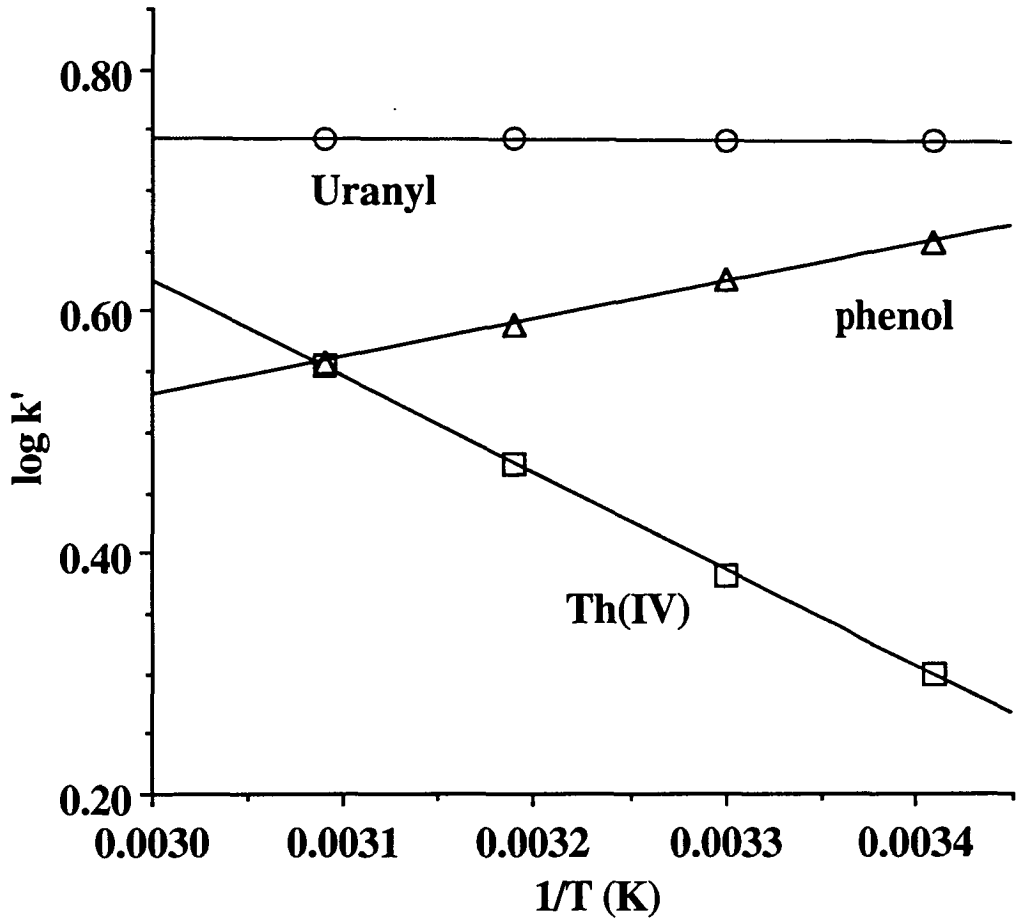

Fig. 5.11a Effect of column temperature on the retention of thorium(IV) and uranyl glycolate complexes, as well as phenol. The eluent comprised 60 mM glycolate and 10% methanol (pH 4.0). Other conditions were the same as in Fig. 5.10a except the column temperature.

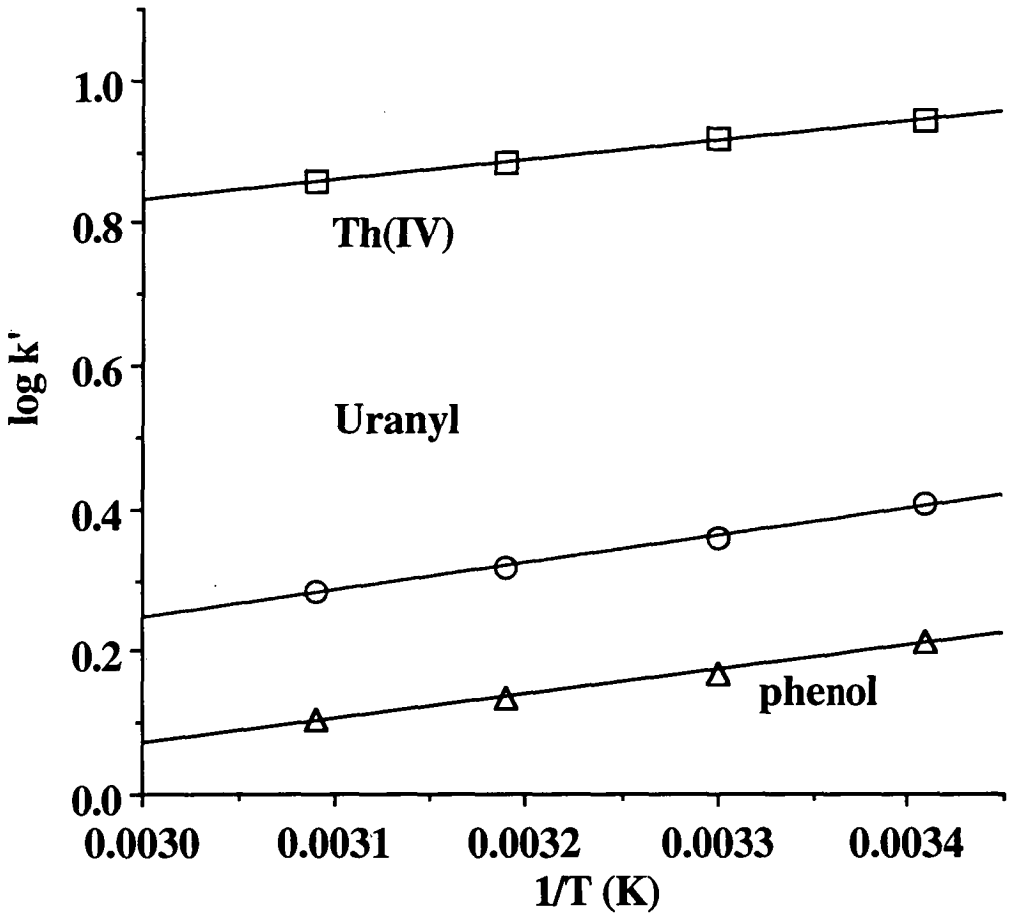

Fig. 5.11b Effect of column temperature on the retention of thorium(IV) and uranyl mandelate complexes, as well as phenol. The eluent was comprised 50 mM mandelate and 20% methanol (pH 4.0). Other conditions were the same as in Fig. 10b except the column temperature.

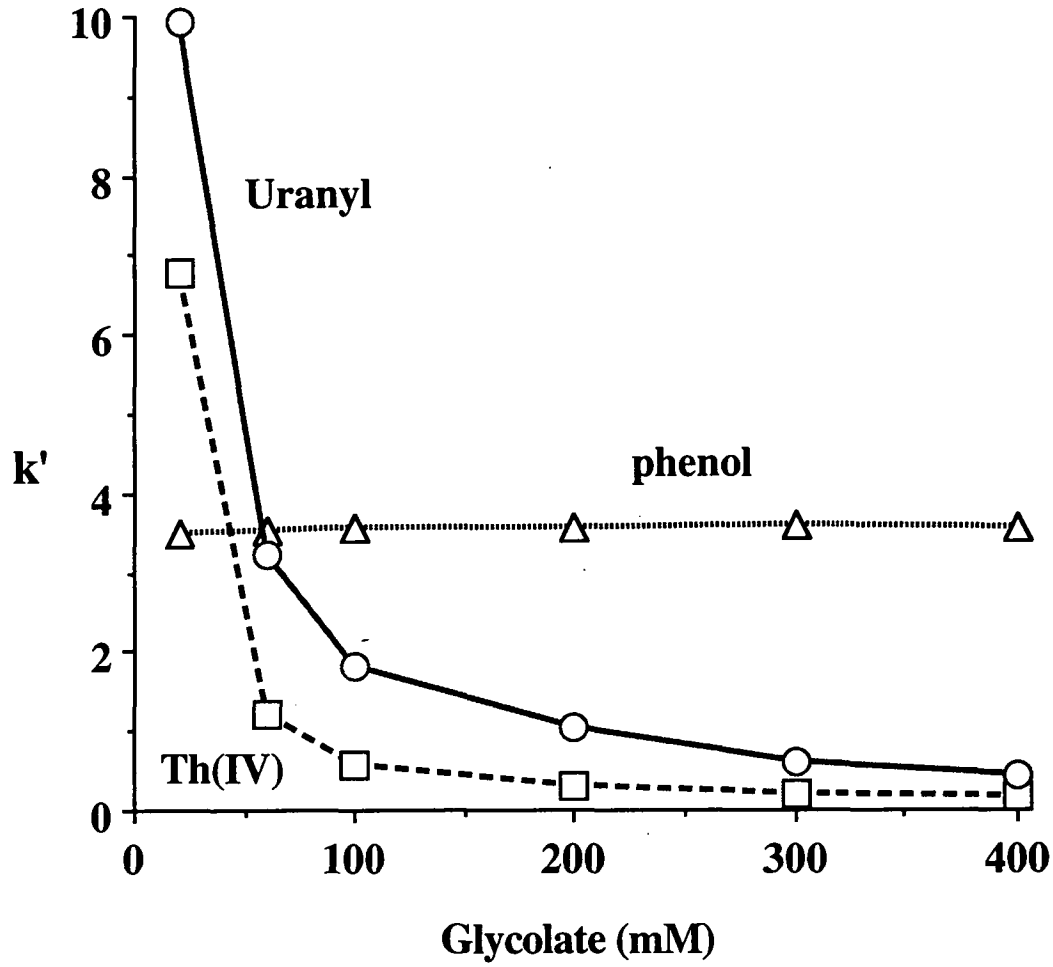

Fig. 5.12a Effect of ligand concentration on the retention of thorium(IV) and uranyl glycolate complexes, as well as phenol. Various concentrations of glycolate prepared in 10% methanol and adjusted to pH 4.0 was used as the eluents. Other conditions were the same as in Fig. 5.10a.

is somewhat different to that observed with the HIBA eluent, in which the uranyl retention increased first and then decreased as the ligand concentration increased, with a maximum retention being observed at about 50 mM HIBA. The thorium(IV) capacity factor quickly dropped to less than one when the glycolate concentration in the mobile phase exceeded 100 mM.

When the mandelate concentration in eluent increased from 20 mM to 500 mM, the thorium(IV) retention was decreased, as shown in Fig. 5.12b. A maximum retention was observed for uranyl at about 50 mM mandelate, which is in accordance with the prediction of the theoretical calculations in section 5.2.2.1 which suggest that the fraction of the neutral uranyl *bis*(mandelate) species reached at maximum at this ligand concentration. The mandelate results are similar to the previous observation with the HIBA eluent, except the elution order of thorium(IV) and uranyl reversed. The phenol retention was decreased slightly over this mandelate concentration range.

5.4.2.4 The Eluent pH

Varying the pH of the glycolate and mandelate eluents over the range 2.5-4.5 caused increasing retention of both thorium(IV) and uranyl, as shown in Fig. 5.13. The likely explanation is that raising the eluent pH benefits thorium(IV) and uranyl complexation. The complexes with high ligand number are more hydrophobicity, so longer retentions are observed.

In this experiment the glycolate concentration selected was 90 mM, because the effective charge on uranyl glycolate complex changed from positive to negative when varying the solution pH from 2.5 to 4.5 at this concentration. Comparing with HIBA, glycolate is a small ligand, so the effective charge on its complex should exert some effect on retention. It is expected that maximum retention would be observed at the point on which the effective charge on uranyl glycolate complex is minimised. The effective charge, δ, on these complexes was calculated as described in Chapter 4:

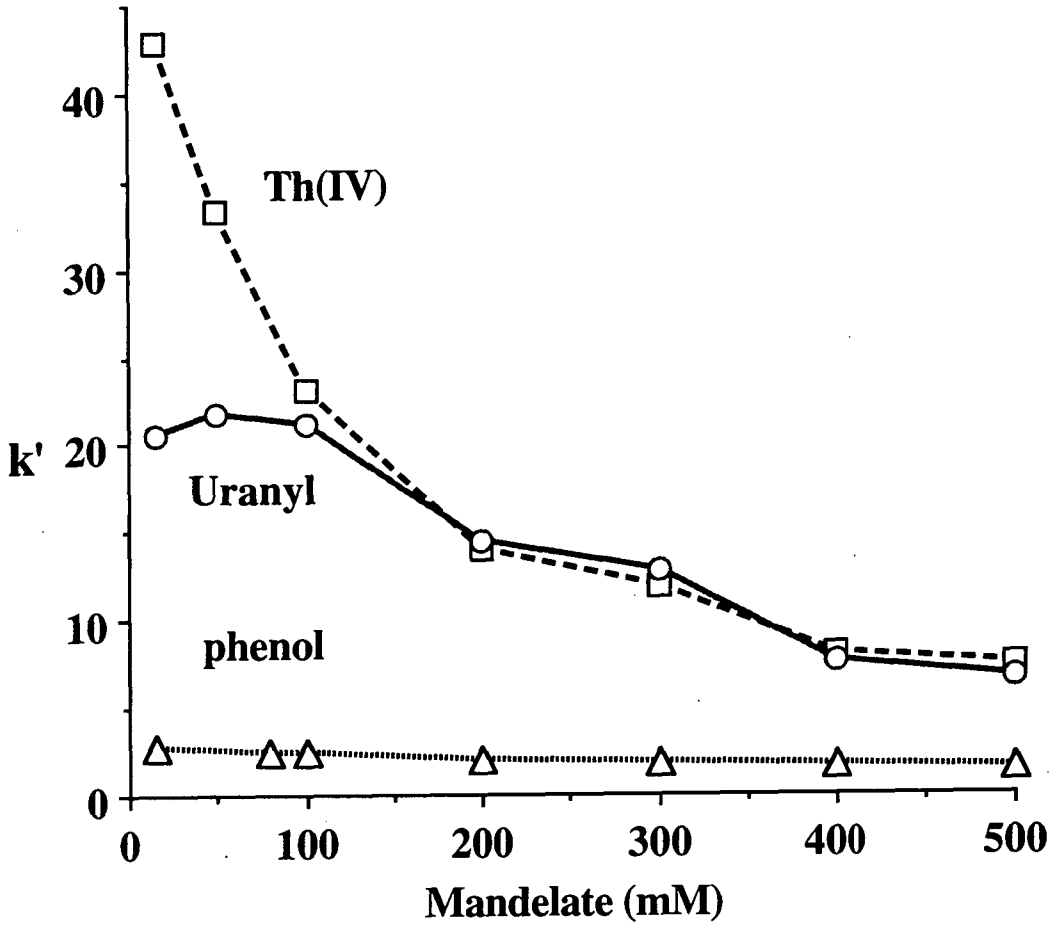

Fig. 5.12b Effect of ligand concentration on the retention of thorium(IV) and uranyl mandelate complexes, as well as phenol. Various concentrations of mandelate were prepared in 20% methanol and adjusted to pH 4.0 were used as the eluents. Other conditions were the same as in Fig. 5.10b.

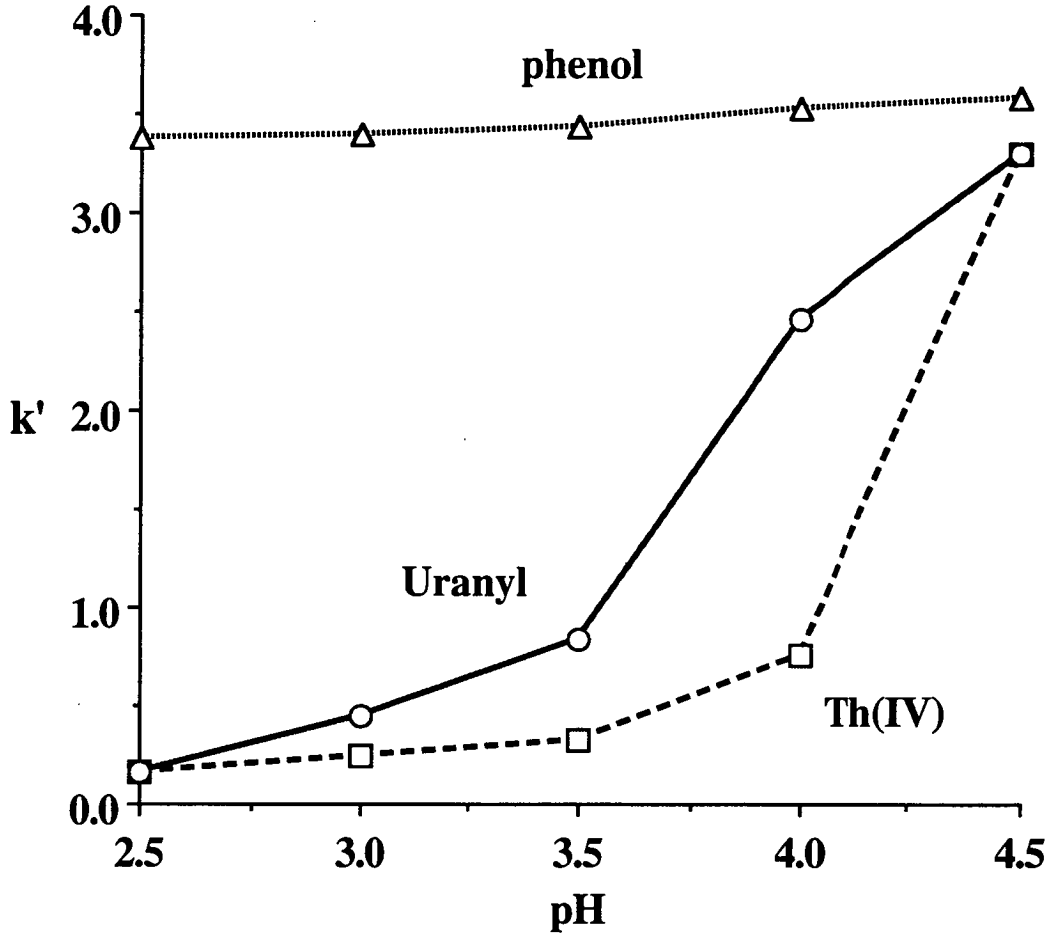

Fig. 5.13a Effect of eluent pH on the retention of thorium(IV) and uranyl glycolate complexes, as well as phenol. A 90 mM glycolate (in 10% methanol) solution adjusted to the indicated pH was used as the mobile phase. Other conditions were the same as in Fig. 10a.

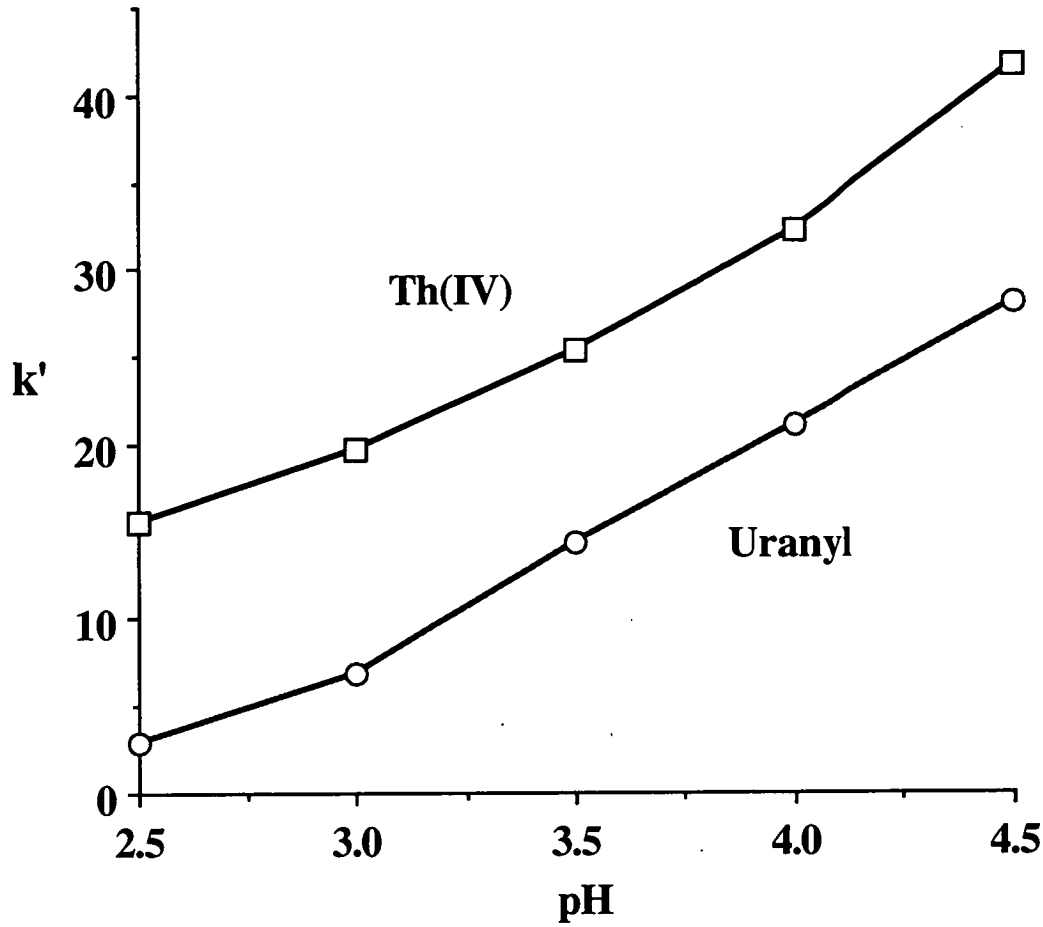

Fig. 5.13b Effect of eluent pH on the retention of thorium(IV) and uranyl mandelate complexes. 50 mM mandelate (in 20% methanol) solution adjusted to the indicated pH was used as the mobile phase. Other conditions were the same as in Fig. 5.10b.

$$\delta_{Uranyl} = 1 \times \alpha_1 + 0 \times \alpha_2 + (-1) \times \alpha_3 \quad (5.3)$$

where α_n represents the fraction of each species complex and the subscript indicates the number of ligands coordinated to the central metal atom. The effective charge on uranyl-glycolate complexes is listed in Table 5.2 which calculated at 90 mM ligand concentration. The results showed that there was no simple relationship between the retention and effective charge for the uranyl-glycolate complex. The effective charge present on the complexes may be overshadowed by the ligand hydrophobicity. It is also observed that thorium(IV) and uranyl can not be separated with a glycolate eluent unless the pH is adjusted to between 3.0 and 4.0.

5.4.3 MECHANISM OF RETENTION

Summarising the above observations and comparing them to the previous HIBA results, it may be help to further understand the retention mechanism of thorium(IV) and uranyl complexes on the reversed-phase column. Perhaps the most common aspect of all the three eluents is that the retention of both thorium(IV) and uranyl decreased as the organic modifier increased, no matter whether these metals were present as anionic or neutral complexes in 400 mM HIBA, 60 mM glycolate or in 50 mM mandelate. The linear relationship between the logarithm of capacity factor and the percentage of organic modifier in the glycolate and mandelate eluents further confirmed that thorium(IV) and uranyl complexes were retained on the reversed-phase column by a hydrophobic adsorption mechanism.

Comparing to the HIBA eluent results, the overall retention of thorium(IV) and uranyl glycolate complexes were much shorter under the same conditions, whilst the mandelate complexes were retained for much longer. The retention difference can be explained by the structures of the three ligands (see Fig. 5.1). In glycolic acid, two hydrogen atoms replace two methyl groups present in HIBA, which reduce the ligand hydrophobicity, so glycolate complexes show weaker retention on the reversed-phase

Table 5.2 DISTRIBUTION OF EACH SPECIES OF URANYL GLYCOLATE COMPLEXES AND EFFECTIVE CHARGE AT VARIOUS pH VALUES

Calculated using the overall formation constants at 0.090 M glycolate.

pH	α_o UO_2^{2+}	α_1 UO_2L^+	α_2 UO_2L_2	α_3 $UO_2L_3^-$	Effective charge
2.0	0.6465	0.327	0.026	0.001	0.326
2.5	0.3425	0.521	0.123	0.013	0.508
3.0	0.1152	0.481	0.311	0.092	0.389
3.5	0.0307	0.286	0.412	0.272	0.014
4.0	0.0110	0.167	0.395	0.426	-0.259
4.5	0.0066	0.125	0.369	0.499	-0.374
5.0	0.0054	0.112	0.358	0.525	-0.414
5.5	0.0050	0.107	0.354	0.534	-0.427
6.0	0.0049	0.106	0.353	0.537	-0.431

Note: L^- represents the glycolate anion.

column. On the other hand, there is a large hydrophobic group, phenyl ($-C_6H_5$), on mandelic acid, which greatly increases the hydrophobicity of the ligand, so a longer retention was observed for the mandelate complexes.

The retention behaviour of uranyl mandelate complex is very similar to that observed previously with the HIBA eluent. Raising the column temperature uranyl as well as phenol showed decreased retention, again confirming the reversed-phase retention mechanism. Varying the ligand concentration in the mobile phase gave a maximum retention for uranyl at 50 mM mandelate. The effect of the ligand in the mobile phase is two-fold. At low concentration increasing the ligand concentration favours the complexation, which results in an increase of the metal complex retention. However, continually raising the ligand concentration results in increase of the non-ionised acid in the mobile phase, which competed with the complex for the adsorption sites on the stationary phase, thus reducing the complex retention. The decreased retention of the neutral reference, phenol, with increasing ligand is further evidence to support this explanation (see Fig. 5.12b). This behaviour is also in accordance with the theoretical calculation, which predicts that the proportion of uranyl present as the neutral *bis*(ligand) species reached a maximum at this ligand concentration. The increased retention observed with raising eluent pH can be simply explained by the increased complexation, and the decreased concentration of neutral ligands resulting in less competition.

However, some anomalous retention behaviour for uranyl was noted using the glycolate eluent. Increasing the glycolate concentration in eluent gave rapidly decreasing retention over the range of 20-100 mM, after which a modest reduction was observed as the glycolate was gradually increased to 400 mM (see Fig. 5.12a). This is in contrast to that observed with HIBA or mandelate eluent, in which there is a maximum uranyl retention at 50 mM ligand concentration. There are two possible explanations for this result. Firstly, the effect of negative charge on the anionic

complex dominates that of hydrophobicity, because the carbon chain of glycolate is short. Another possible explanation is that the uranyl glycolate complex could also be hydrolysed in an aqueous solution, as suggested for the thorium(IV) HIBA complex in Chapter 4. The small sized glycolate can be expected to exhibit less steric resistance to the addition of hydroxyl ligands than HIBA or mandelate. One or more hydroxyls maybe therefore be incorporated into the uranyl coordination sphere. The uranyl glycolate complex retention behaviour therefore becomes very similar to that of the hydrolysed thorium(IV) complex (see Fig. 5.12a).

Another anomalous observation is that the retention of the uranyl glycolate complex remained relatively unchanged when raised the column temperature, whilst the retention of the neutral reference substance, phenol, decreased and the thorium(IV) complex increased (see Fig. 5.11a). Here, the eluent prepared in 60 mM glycolate adjusted to pH 4.0. Calculation based on the overall formation constants indicates that the uranyl should be present mainly as a neutral *bis*(glycolate) species and there is no charged species under these conditions, so the charge effect resulting from the third ligand in the complex can be excluded. The only possible explanation for this observation is that the uranyl-glycolate complex is also hydrolysed, but not as heavily as that of the thorium(IV) complex. Decreasing stability of the mixed ligand uranyl complex at high temperatures caused it to show anomalous retention.

The retention behaviour of the thorium(IV) glycolate complex is much the same as that previously observed with the HIBA eluent, but the thorium(IV) mandelate complex showed somewhat different result to the HIBA and glycolate complexes. With the mandelate eluent, uranyl was eluted before thorium(IV) (see Fig. 5.9), which was in accordance with the theoretical calculation which predicted that thorium(IV) should be present as a neutral complex whilst the uranyl exist as an anionic species. However, the retention behaviour of the thorium(IV) mandelate complex was in contrast to that observed with the HIBA or glycolate eluent, which showed increased retention at high temperatures. In Chapter 4 it was suggested that two or more

hydroxyls are also coordinated into the thorium(IV) HIBA complex, so the multi-charged complex showed weaker retention than the uranyl complex.

A further characteristic of the thorium(IV) mandelate complex was that it showed decreased retention as the column temperature increased, whilst the retention of the glycolate and HIBA complexes increased. A possible explanation for this difference is that the thorium(IV) mandelate complex had not hydrolysed, so it showed typical reversed-phase chromatographic behaviour.

5.5 CONCLUSIONS

The elution characteristics of thorium(IV) and uranyl complexes with α-hydroxy-monocarboxylic acids are dependent chiefly on the ligand hydrophobicity and the chromatographic conditions used. These complexes are retained on a reversed-phase column predominantly by a hydrophobic absorption mechanism, despite the fact that the complexes are anionic under most conditions. Glycolate complexes show a weak retention due to the low hydrophobicity of the ligand, whereas the phenyl group on the mandelic acid renders it very hydrophobic so its complexes have a much longer retention time. In a glycolate eluent, thorium(IV) forms a neutral *tetra*(ligand) complex which is further hydrolysed to produce an anionic species, so that thorium(IV) is eluted before uranyl. On the other hand, in mandelate eluents, this hydrolysis either does not occur due to steric effects, or its influence on retention is overshadowed by the hydrophobicity of the complex. With mandelate, thorium(IV) is eluted after uranyl. The behaviour of thorium(IV) and uranyl in mobile phases containing α-hydroxyl monocarboxylic acids is quite different to that exhibited by lanthanide ions, which are retained by a cation-exchange mechanism even when the same ligands are used. This difference can be explained by the smaller formation constants and lower metal:ligand ratios of these species in comparison to thorium(IV) and uranyl.

5.6 REFERENCES

1 C. H. Knight, R. M. Cassidy, B. M. Recoskie and L. W. Green, *Anal. Chem.*, 56 (1984) 474.

2 D. J. Barkley, M. Blanchette, R. M. Cassidy and S. Elchuk, *Anal. Chem.*, 58 (1986) 2222.

3 R. M. Cassidy, S. Elchuk, N. L. Elliot, L. W. Green, C. H. Knight and B. M. Recoskie, *Anal. Chem.*, 58 (1986) 1181.

4 S. Elchuk, K. I. Burns, R. M. Cassidy and C. A. Lucy, *J. Chromatogr.*, 558 (1991) 197.

5 L. Magon, A. Bismondo, L. Maresca, G. Tomat and R. Portanova. *J. Inorg. Nucl. Chem.*, 35 (1973) 4237.

6 L. Magon, G. Tomat, A. Bismondo, R. Potanova and U. Croatto. *Gazzetta Chimica Italiana*, 104 (1974) 967.

7 R. Larsson, *Acta Chemica Scandinavica*, 19 (1965) 783.

8 A. E. Martell and R. M. Smith, *Critical Stability Constants*, Plenum Press, New York, 1977, Vol. 3.

9 P. J. Schoenmakers, *Optimization of Chromatographic Selectivity*, Elsevier, Amsterdam, 1986, p.67.

Chapter 6

Determination of Thorium(IV) and Uranium in Mineral Sands by Reversed-phase Liquid Chromatography

6.1 INTRODUCTION

Traditionally thorium and uranium are determined using techniques such as radio-chemistry, atomic absorption spectroscopy [1], neutron activation analysis [2], inductively coupled plasma mass spectrometry (ICP-MS) [3], isotope dilution mass spectrometry [4] and X-ray fluorescence (XRF) [5]. However, these techniques are not suited for routine analysis, due to interferences from other metals present in the matrix, cost of operation or poor detection limits [6, 7].

In recent years, ion-chromatography (IC) has been applied widely to the separation of lanthanides and also thorium and uranium [6, 8]. These species are typically separated on a C_{18} reversed-phase column using a mobile phase containing an ion-interaction reagent (IIR), such as n-octanesulfonate, and a complexing reagent (e. g. HIBA) followed by post-column reaction (PCR) with either Arsenazo III {3,6-bis[o-arsenophenyl)azo]-4,5-dihydroxy-2,7-naphthalene disulfonic acid} or PAR [4-(2-pyridylazo) resorcinol] with visible detection. Many publications have reported using the chromatographic approaches to determine thorium and uranium in samples including natural waters [6], uranium ore, irradiated fuel materials [9, 10], artificial UO_2 fuels [11] and geological matrices such as basalt, phosphate rock and river sediments [7, 12].

Results obtained in Chapter 4 and 5 have shown that thorium(IV) and uranium(VI), as the uranyl ion, exhibit somewhat different retention behaviour to the lanthanides in that their HIBA complexes can be retained on a C_{18} column without the

need for an IIR in the mobile phase [13, 14, 15]. Thorium(IV) and uranyl ions can also be retained on the C_{18} column when mandelic acid alone is used in the eluent. In previous chapters this retention behaviour has been studied and it has been found that thorium(IV) and uranyl HIBA, mandelate and glycolate complexes were retained on the reversed-phase column through a mechanism of hydrophobic adsorption rather than dynamic cation-exchange.

In this chapter, trace levels of thorium and uranium in mineral sands has been analysed using the chromatographic method developed in the previous chapters. A number of sample preparation procedures are evaluated. Dissolution procedures investigated included acid leaching and alkali fusion with peroxide, borate, carbonate, hydroxide and pyrosulfate fluxes. Sample clean-up protocols, including solvent extraction, cation-exchange and selective complexation, are then studied in order to overcome the interference effects of the dissolution matrix upon the chromatographic process. The results obtained are compared to those from XRF and ICP-MS for ilmenite, synthetic rutile, zircon and natural rutile mineral sands.

6.1.1 THORIUM AND URANIUM IN MINERAL SANDS

Thorium and uranium are widely distributed in the earth's crust. The average thorium concentration of the outermost layer of the earth's crust is about 12 ppm. It is about three times more abundant than uranium and nearly as abundant as lead. Thorium and uranium are found in many varieties of rocks, such as huttonite ($Th(SiO_4)$ 81.5%), thorite ($Th(SiO_4)$ 81.5%), cheralite ($Th_3(PO_4)_4$, ~ 30%) monazite ($Th_3(PO_4)_4$, ~ 12%), phosphate rocks (U, 0.001%) and some sedimentary marine shales. Usually thorium is hosted in two groups of minerals. The first group minerals are the compounds of uranium, zirconium or cerium, which are isostructural with thorium compounds because the minerals zircon, uraninite, or monazite are capable of accommodating Th^{4+} ion due to the similarity in ionic radius between Th^{4+} and U^{4+}, Zr^{4+} and Ce^{4+}. The second group of host minerals comprises the niobate-tantalates,

where mechanisms also exist for the incorporation of large highly charged cations into the crystal lattice. The mineral sands analysed in this Chapter include natural rutile, synthetic rutile, ilmenite and zircon, and their compositions are listed in Table 6.1. The first three minerals are Ti/Fe matrix based samples , and the zircon sand is mainly comprised of ZrO_2.

6.2 EXPERIMENTAL

6.2.1 INSTRUMENTATION

In this Chapter the direct injection chromatographic system described in Chapter 3 was used. Sample digest solutions were loaded through the cation-exchange pre-treatment cartridges using a Waters Model 501 pump. The rock samples were fused in a muffle furnace (Bamford, Sheffield, England).

6.2.2 REAGENTS

The mobile phase consisted of 400 mM α-hydroxyisobutyric acid (Sigma, St. Louis, MO, USA) and 10% methanol (HPLC grade obtained from Waters) adjusted to pH 4.0 with sodium hydroxide. The analytical mobile phase was delivered at a flow-rate of 1.0 ml/min. The post-column reagent solution contained 0.13 mM Arsenazo III (BDH, Poole, UK), 10.0 mM urea (May & Baker, Dagenham, UK) and 62 mM acetic acid and was delivered at a flow-rate of 1.0 ml/min. All eluents and post column reagents were prepared daily, filtered and degassed. Thorium and uranium standards were prepared from thorium(IV) nitrate and uranyl nitrate (Ajax Chemicals, Sydney, Australia), respectively. Sample pre-treatment was carried out using either Alltech (Deerfield, IL USA) IC H^+ Maxiclean cartridges (sulfonic acid functionalised, capacity: 1 g of 5 mequiv./g resin), Waters Accell CM Sep-Pak cartridge (carboxylic acid functionalised, capacity: 0.4 g of 350 mequiv./g silica) or Waters ion-exclusion Guard-Pak insert cartridges (sulfonic acid functionalised, capacity: 0.2 g of 5 equiv./g resin).

Table 6.1 CONCENTRATION OF THORIUM, URANIUM AND OTHER METALS IN SOME MINERAL SANDS

Samples were analysed using XRF method.

Component	Ilmenite (%)	Synthetic Rutile (%)	Natural Rutile (%)	Zircon (%)
TiO_2	58.5	91.2	95.4	0.16
Fe_2O_3	30.0	4.22	1.15	0.45
FeO	4.2	--	--	--
ZrO_2	0.29	0.12	1.1	66.4
Al_2O_3	1.05	1.14	0.36	0.37
SiO_2	1.13	0.2	0.77	32.5
Mn_3O_4	1.21	1.29	0.01	--
Cr_2O_3	0.25	0.2	0.15	--
V_2O_5	0.17	0.25	0.56	--
Nb_2O_5	0.19	0.25	0.35	--
CaO	0.01	0.01	0.01	--
MgO	0.24	0.35	0.01	--
P_2O_5	0.11	0.02	0.03	0.08
CeO_2	0.11	0.02	0.02	--
SO_3	0.03	1.5	0.01	--
SnO_2	--	--	0.03	--
Th (ppm)	490	430	53	179
U (ppm)	10	15	54	217

Note: Results obtained on solid samples.

6.2.3 SAMPLE DISSOLUTION PROCEDURES

The ilmenite, synthetic rutile, zircon and natural rutile mineral sand samples were initially ground, then treated using a variety of acid leach and fusion procedures, as detailed below:

Acid leach

Samples (0.5 g) were weighed into 250 ml conical flasks, to which 20 ml of concentrated perchloric and nitric acids were added. The solutions were refluxed for 1 hour on a hotplate, and boiled to near dryness. After cooling, 2 g of HIBA were added, dissolved in Milli-Q water. The samples were adjusted to pH 4.0 with sodium hydroxide and made up to 100 ml in a volumetric flask.

Peroxide fusion

Samples (0.5 g) were weighed into a platinum crucible with 4.0 g of sodium peroxide and fused in the muffle furnace at 1100 °C for 15 minutes. The melt was dissolved with 15 ml of 50% sulfuric acid and 15 ml of 30% hydrogen peroxide, then cooled, diluted, filtered and made up to 100 ml in a volumetric flask.

Hydroxide fusion

Samples (0.5 g) were weighed into a zirconium crucible with 4.0 g sodium hydroxide and fused at 1100 °C for 15 min. Concentrated nitric acid (15 ml) was added to the crucible and the slurry heated to near dryness on a hotplate. The solution was cooled, filtered and made up to 100 ml in a volumetric flask.

Carbonate-tetraborate fusion

Samples (0.5 g) were weighed into a platinum crucible with 1.0 g sodium carbonate and 1.0 g sodium tetraborate and fused at 1100 °C for 15 minutes. The melt was poured into a solution of 20 ml concentrated nitric acid, 5.0 ml of 30% hydrogen

peroxide and 25 ml Milli-Q water. The crucible was placed into the above solution and warmed on a hotplate to dissolve the melt. The crucible was then removed and washed with water. After cooling the solution was made up to 100 ml in a volumetric flask.

Tetraborate fusion

Samples (0.5 g) were weighed into a platinum crucible with 2.0 g sodium tetraborate and fused in Muffle furnace at 1100 °C for 15 minutes. The melt was poured into a solution of 5 ml concentrated nitric acid and 50 ml water. The crucible was placed into the above solution and warmed on a hotplate to dissolve the melt. The crucible was then removed, washed with water, the solution cooled, filtered and made up to 100 ml in a volumetric flask.

Pyrosulfate fusion

Samples (0.5 g) were weighed into a Victor quartz 250-ml conic flask with 5 g potassium pyrosulfate and fused over a meaker burner at 800-900 °C to obtain a clear melt. The melt was cooled and 10 ml of concentrated sulfuric acid was added. The solution was warmed to dissolve the melt then 5 ml of concentrated hydrochloric acid and 50 ml water was added. The solution was cooled and made up to 100 ml in a volumetric flask.

Tetraborate-carbonate fusion

Samples (0.5 g) were weighed into a platinum crucible with 2.5 g sodium tetraborate and 1.0 g sodium carbonate and fused at 1100 °C. The melt was poured into a solution of 10 ml concentrated sulfuric acid and 40 ml water. The crucible was placed into the above solution and warmed on a hotplate to dissolve the melt. The crucible was removed and washed with water. After cooling, the solution was made up to 100 ml in a volumetric flask.

6.2.4 CATION-EXCHANGE PRETREATMENT PROCEDURE

The final cation-exchange sample pretreatment procedure used to evaluate the various fusion/digest approaches consisted of firstly conditioning the ion-exclusion cartridge with 5.0 ml 7.5 M nitric acid followed by 5.0 ml of Milli-Q water. The sample digest was then loaded onto the cartridge at 2.0 ml/min with a HPLC pump after diluting the sample to ensure that the acid concentration did not exceed 0.2 M in order to allow quantitative binding of thorium and uranium ions. The cartridge was then washed with 1.0 ml water to remove the interstitial sample and flushed with air to remove the water. Finally, the bound thorium and uranium were eluted from the cartridge with 2.0 ml 2 M HIBA into a pre-rinsed 4.0 ml vial and the cartridge flushed with air to ensure complete collection of the entire 2.0 ml volume.

6.3 RESULTS AND DISCUSSION

6.3.1 PRELIMINARY EXPERIMENTS

In the previous chapters, the retention behaviour of thorium(IV) and uranyl complexes with HIBA, glycolate and mandelate on a C_{18} reversed-phase column was investigated and it was proposed that such complexes were retained by a mechanism of hydrophobic adsorption. Optimal conditions were established for the determination of thorium and uranium which utilised a mobile phase of 400 mM HIBA and 10% methanol at pH 4.0 with a C_{18} column, a post column reagent of Arsenazo III and detection at 658 nm. In this chapter, the reversed-phase chromatographic method is applied to the determination of thorium and uranium in ilmenite, synthetic rutile, zircon and natural rutile mineral sands.

In the previous studies it was noted that thorium(IV) and uranyl exhibited appreciably different retention behaviour to the lanthanides and transition metals, and they were completely resolved from these potentially interfering species using the reversed-phase chromatographic method. Another advantage of this technique was

that it allowed the injection of large sample volumes before significant peak broadening occurred, resulting in detection limits (at 3 x signal-to-noise) of 3.0 and 5.0 ng/ml (using a 1000-µl injection) for thorium and uranium, respectively. The calibration curves were linear (correlation coefficients > 0.9999) from detection limit to approximately 5.0 µg/ml for the same injection volume. Beyond this sample loading, the detector response was over range. As thorium was typically found in mineral sands at higher concentrations than uranium, calibration curves were routinely prepared for the two analytes using different concentrations and injection volumes.

However, despite the excellent linearity and detection limits of the reversed-phase chromatographic method, initial results obtained using the direct injection of samples, prepared using a peroxide fusion (described in the experimental), gave low results (about 10% recovery) when compared to those obtained with XRF, as listed in Table 6.2. The mineral sand samples were then prepared using an alternative dissolution method, a perchloric and nitric acid leach procedure. The results obtained by direct injection of the sample are also shown in Table 6.2. These results indicated one of two possibilities, that either the sample dissolution procedure did not quantitatively release thorium and uranium from the matrix, or that the dissolution matrix was interfering somewhat with subsequent chromatographic analysis. It has been reported previously [16], for the determination of lanthanides by liquid chromatography, that a sulfuric acid level in the injection solution of > 0.09 M reduced the peak heights and retention times of rare earth elements (REEs) when using oxalate as the complexing agent in the mobile phase. The acidity of the sample altered the formation constants of REEs complexes and therefore influenced the degree of complexation of REEs. In the case of thorium(IV) and uranyl HIBA complexes, it appeared that other (complexing) ions in the sample digest solution were competing with HIBA in the coordination sphere of both thorium and uranium. Consequently, these species were chromatographed as other complexed forms, most of which appeared to be eluted at the column void volume.

Table 6.2 THORIUM AND URANIUM CONCENTRATION IN ORIGINAL MINERAL SANDS

Samples fused using sodium peroxide or nitric/perchloric acids leach, then directly injected for chromatographic analysis. A μ-Bondapak C_{18} column (300 x 3.9 mm I.D.) was used with 0.4 M HIBA as the eluent, delivered at 1.0 ml/min. Detected at 658 nm after post-column reaction with Arsenazo III.

Sample	HPLC		XRF[a]	
	Thorium (ppm)	Uranium (ppm)	Thorium (ppm)	Uranium (ppm)
Ilmenite				
Peroxide Fusion	86.4	ND	490	10
Acid leach	426	8.9		
Synthetic rutile				
Peroxide Fusion	69.9	ND	430	15
Acid leach	56.2	ND		
Zircon				
Peroxide Fusion	ND	48.6	179	217
Acid leach	21.1	ND		
Natural rutile				
Peroxide Fusion	8.0	8.0	53	54
Acid leach	29.2	ND		

ND = Not detected.

XRF[a] = Results obtained on solid samples.

The effect of sample acidity on the chromatographic behaviour of thorium was confirmed by preparing 10 µg/ml thorium standard solutions made up in either 1.0 M sulfuric, nitric or hydrochloric acids. The recoveries for the thorium peak were 23%, 71% and 87% in sulfuric, nitric and hydrochloric acids, respectively, when compared to a standard prepared in Milli-Q water. Sulfate, nitrate and chloride all form complexes with thorium [17] and compete effectively with HIBA in the coordination sphere of thorium. In fact, the recovery results reflect the relative degree of stability of these complexes, i.e. sulfate forms more stable anionic complexes with thorium than does either nitrate, or chloride. The overall formation constants of thorium(IV) complexes with sulfate, nitrate and chloride are listed in Table 6.3. Hence the poor recoveries obtained were a result of the other (more polar) complexes of thorium eluting at the column void volume. When the 10 µg/ml thorium standard solution was made up in the 0.1 M sulfuric acid, the recovery for the thorium peak was 100% ; however, such an acid concentration was much too low to effect dissolution of the mineral sand fusion melt. Additionally, when a 10 µg/ml thorium standard solution was made up in 1.0 M sulfuric acid and neutralised with sodium hydroxide before injection, the recovery for the thorium peak was only 8%. This result indicated that either the hydroxyl anion could also compete with HIBA in the coordination sphere of thorium, or that the sulfate complex of thorium was more stable under alkaline conditions. The effect of other anions on the uranium recovery was similar to that for thorium, although not as dramatic, as uranium formed more stable HIBA complexes than thorium. Fig. 6.1 shows the chromatograms of thorium(IV) and uranyl which were prepared in various concentrations of sulfuric acid.

Evidently, some form of further sample treatment prior to the chromatographic determination was necessary in order to determine if the sample fusion/acid dissolution procedures were successfully releasing thorium and uranium from the mineral sand matrix. Options would include a very large dilution of the sample digest; the use of an

Table 6.3 OVERALL FORMATION CONSTANTS OF THORIUM(IV) AND URANYL COMPLEXES

Measured in 2.0 M ionic strength at 25 °C [18].

Metals	Acids	Reaction	log β
	H_2SO_4	$Th^{4+} + SO_4^{2-} \leftrightharpoons ThSO_4^{2+}$	3.22
		$ThSO_4^{2+} + SO_4^{2-} \leftrightharpoons Th(SO_4)_2$	5.53
Th(IV)	HNO_3	$Th^{4+} + NO_3^- \leftrightharpoons ThNO_3^{3+}$	0.67 [a]
	HCl	$Th^{4+} + Cl^- \leftrightharpoons ThCl^{3+}$	0.08
		$ThCl^{3+} + Cl^- \leftrightharpoons ThCl_2^{2+}$	-1.0
	H_2SO_4	$UO_2^{2+} + SO_4^{2-} \leftrightharpoons UO_2SO_4$	1.65 [b]
Uranyl	HNO_3	$UO_2^{2+} + NO_3^- \leftrightharpoons UO_2NO_3^+$	-0.6
	HCl	$UO_2^{2+} + Cl^- \leftrightharpoons UO_2Cl^+$	-0.06

a: Ionic strength 0.5 M, 25 °C.

b: Ionic strength 2.7 M, 25 °C.

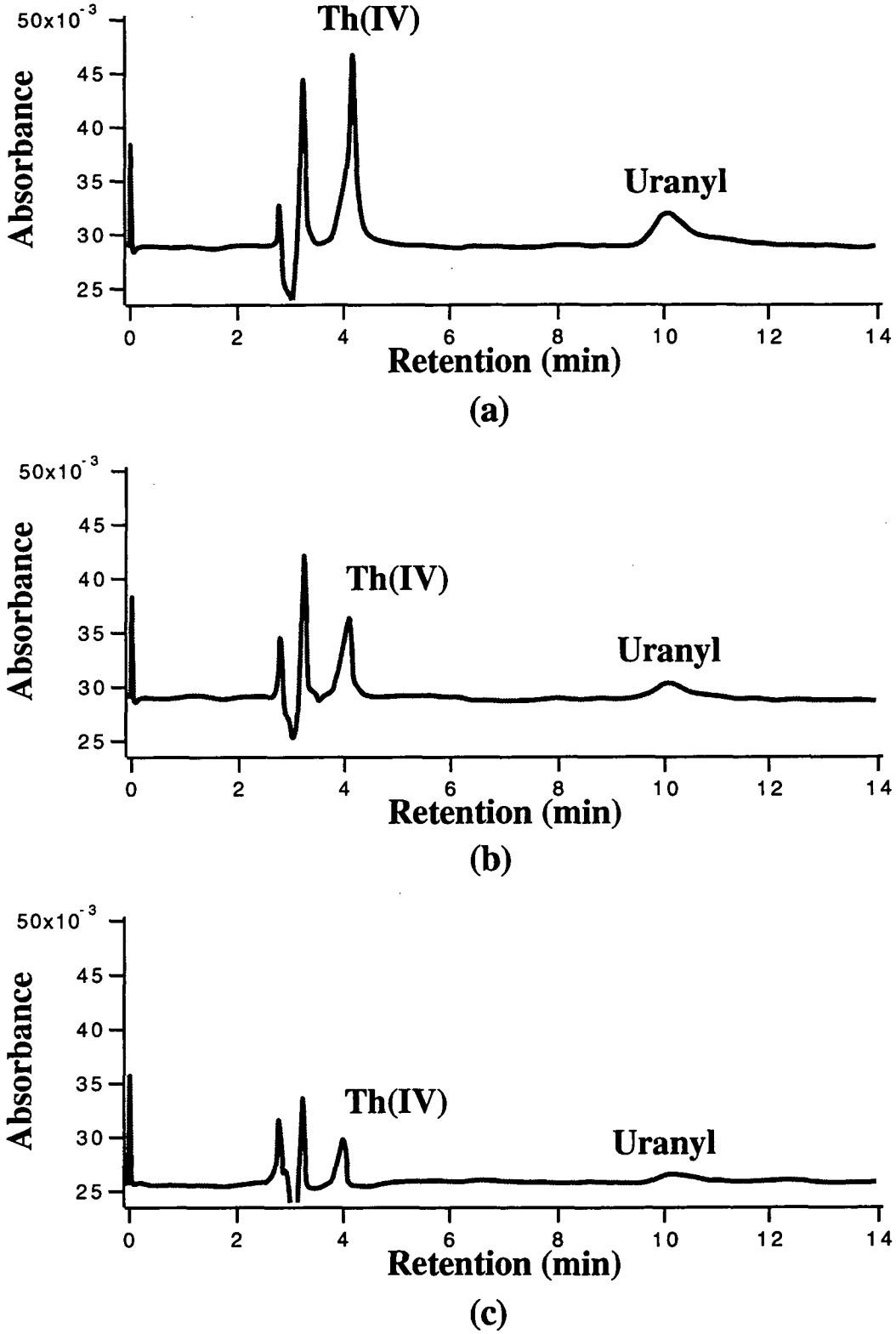

Fig. 6.1 Effect of acids on thorium(IV) and uranyl retention. A μ-Bondapak C_{18} column (300 x 3.9 mm I.D.) was used with 0.4 M HIBA in 10% methanol (pH 4.0) as the eluent (1.0 ml/min). Detection at 658 nm after PCR with Arsenazo III. Injection of 100 μl of 10 ppm Th(IV) and uranyl in (a) 0.1 M, (b) 0.5 M and (c) 1.0 M H_2SO_4.

alternative chromatographic approach where the thorium and uranium responses were not affected by the presence of other ions in solution; or removing thorium and uranium from the dissolution matrix prior to injection. Unfortunately, thorium and uranium are present in the samples at such low concentrations that a large dilution is impractical and other chromatographic approaches, whether using an ion-exchange, reversed-phase or ion-interaction separations, are also likely to be affected by the presence of elevated levels of ions in the sample digest as they all rely on some degree of complexation with the mobile phase to elute the thorium and uranium ions.

6.3.2 SAMPLE PRETREATMENT WITH VARIOUS CATION-EXCHANGER CARTRIDGES

It appeared then that the most appropriate solution to the interference problem was to remove the thorium and uranium from the dissolution matrix prior to the chromatographic step. Two approaches were investigated: solvent extraction and solid-phase (cation-exchange) extraction. It has been long established that thorium and uranium can be extracted from aqueous solutions containing high concentrations of certain metal nitrates using oxygen-containing organic solvents [19]. However, extraction of 10 µg/ml thorium and uranium standard solution (containing 1.0 g/ml aluminium nitrate) with ethyl acetate resulted in recoveries of only 30% and 80% for thorium and uranium, respectively. This approach was abandoned after attempts to extract a fusion/digestion sample with ethyl acetate were unsuccessful due to the formation of stable emulsions.

Cassidy [7] has previously used cation-exchange extraction to concentrate REEs from rock digest matrices prior to chromatographic determination. After digestion with strong acids (nitric and perchloric acids), the sample was prepared in 2.0 ml of 2 M HNO_3 and loaded onto a strong cation-exchanger column. The cartridge was then washed with about 10 ml of 2 M HNO_3 and 0.5 M oxalic acid, followed by 4.0 ml of 6 M HNO_3. Finally the REEs were stripped from the column

with 8 M HNO_3. The REE fraction was evaporated to dryness and dissolved in a small volume (0.5-1 ml) of the HPLC eluent for chromatographic analysis. Alternatively, an iminodiacetate functionalised chelating resin was also shown to allow preconcentration of thorium(IV) and uranyl from rock digests prior to gradient cation-exchange separation [6].

Investigation of the binding affinities of thorium and uranium in nitric acid indicated that both thorium and uranium would bind quantitatively to strong cation-exchange resin, provided that the nitric acid concentration was no greater than 0.1 M [22]. At high nitric acid concentrations, uranium shows a significantly decreased affinity for the cation-exchanger due to formation of anionic nitrate complexes. The recoveries of thorium and uranium on several different cation-exchange cartridges were then evaluated using a cation-exchange pretreatment method based on that of Cassidy [23]. This involved loading an appropriate volume of sample onto a cartridge previously conditioned with 5 ml of 0.1 M nitric acid followed by 1.0 ml of Milli-Q water. The cartridge with the remaining sample was washed with 1.0 ml of Milli-Q water and eluted with varying volumes of 7.5 M nitric acid. The effluent was collected in a 20-ml beaker. This solution was evaporated just to dryness on a hotplate and the sample reconstituted with 2 ml of 400 mM HIBA.

The use of cation-exchange cartridges to quantitatively recover thorium and uranium was initially investigated using a high capacity IC H^+ Maxiclean cartridge and standard solutions. A 10 µg/ml thorium and uranium standard solution was loaded onto the Maxiclean cartridge and the effluent collected. Chromatographic analysis of the effluent indicated that both Th and U were binding quantitatively to the cartridge. Eluting the bound metals with 10 ml of 7.5 M nitric acid resulted in recoveries of only 40% and 55% for thorium and uranium, respectively. This indicated that the sample was binding quantitatively to the cartridge, but 10 ml of 7.5 M nitric acid was insufficient to quantitatively remove the thorium and uranium from the cartridge. The use of a large elution volume (30 ml) of 7.5 M nitric acid resulted in improved

recoveries of 55% and 90% for thorium and uranium, respectively; however it appeared that the cartridge capacity was too high to permit quantitative elution with a reasonable volume of nitric acid.

Two lower-capacity cation-exchangers were then investigated for their ability to be used with the cation-exchange pretreatment procedure; an Accell weak acid functionalised cartridge and an ion-exclusion Guard-Pak strong acid functionalised cartridge. Both of these cartridges gave quantitative (100%) recoveries for a 10 µg/ml thorium and uranium standard solution using an elution volume of only 10 ml of 7.5 M nitric acid. Fig. 6.2 shows the chromatograms of 100 µl injection of a 10 ppm Th(IV) and uranyl standards after pretreatment using these two cartridges.

As the standards appeared to be stripped quantitatively from the lower capacity cation-exchange cartridges, mineral sand samples prepared using a hydroxide fusion were then pretreated using the cation-exchange procedure prior to injection. The fusion/digest solutions were diluted a further ten times to reduce the acid concentration to about 0.1 M in order to ensure quantitative binding of thorium(IV) and uranyl, and 20 ml of this diluted sample was loaded using a HPLC pump. The samples were then eluted with 10 ml of 7.5 M nitric acid, evaporated to dryness and reconstituted in 2.0 ml of 400 mM HIBA. The results obtained for ilmenite, synthetic rutile and zircon mineral sands using both the cation-exchange cartridges are listed in Table 6.4.

The use of the ion-exclusion cartridge pretreatment allowed good results to be obtained for the ilmenite sample, however, lower recoveries were obtained using the Accell cartridge, especially for uranium. While appropriate for standard solutions, it appeared that the weak acid functionalised Accell cartridge did not have sufficient capacity to quantitatively retain dilute acid solutions of thorium and uranium and no further work was carried out using these cartridges. Fig. 6.3a shows a chromatogram of a 100-µl injection of ilmenite prepared by hydroxide fusion directly injected with no pretreatment, while Fig. 6.3b shows a chromatogram of 100-µl of the same sample

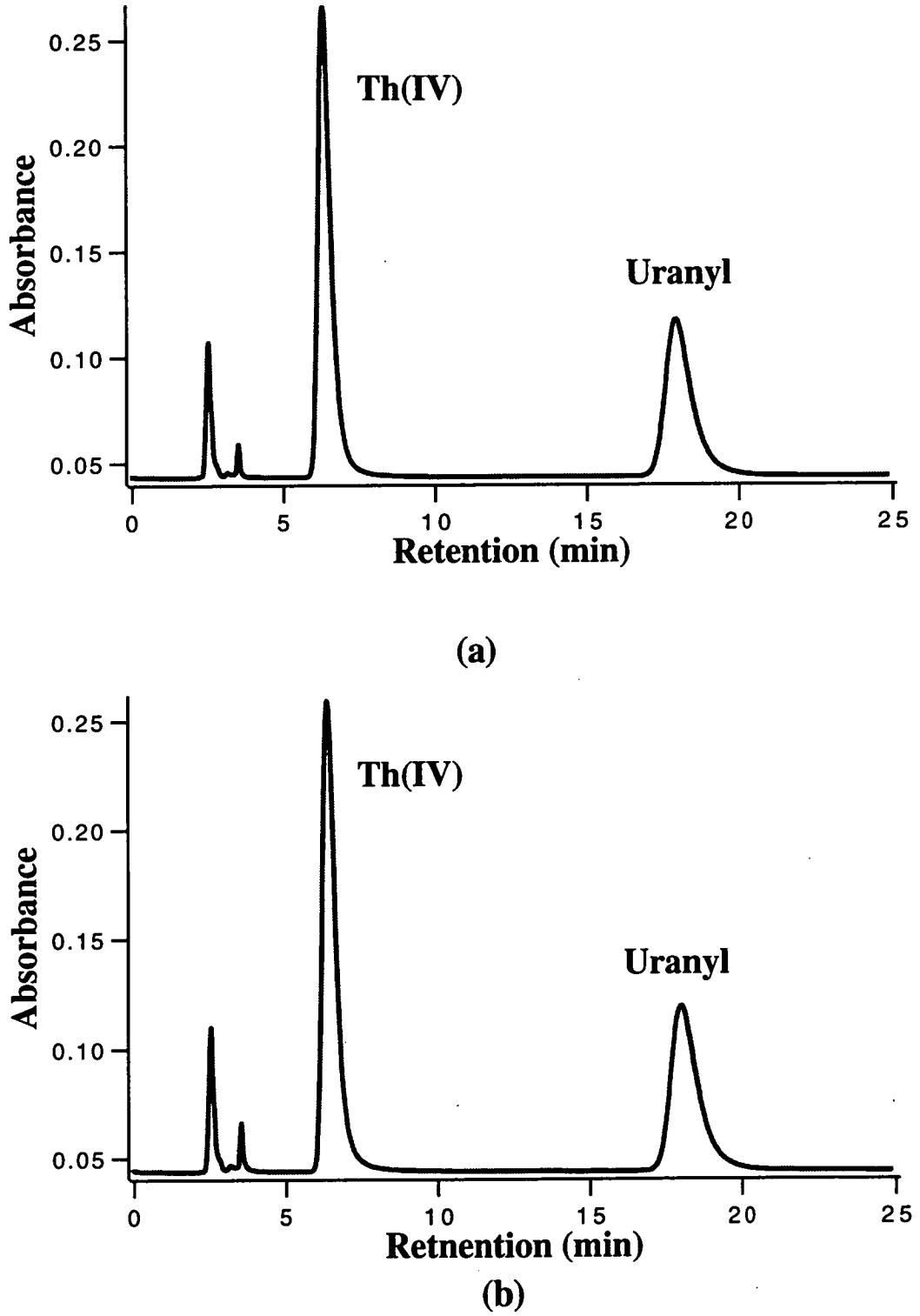

Fig. 6.2 Chromatograms of thorium(IV) and uranyl after pretreatment with (a) CM Sep-Pak cartridge and (b) ion-exclusion Guard-Pak. Injection of 100 µl of 10 ppm thorium(IV) and uranyl pretreated as described in the text. Other chromatographic conditions were the same as in Fig. 6.1.

Table 6.4 THORIUM AND URANIUM CONCENTRATION IN ORIGINAL MINERAL SANDS

Samples fused using hydroxide, then pretreated with cation-exchange before chromatographic analysis. Chromatographic conditions as described in Table 6.2.

Samples	Thorium (ppm)	Uranium (ppm)
Ilmenite		
No pretreatment	195	9.8
Ion-Exclusion cartridge	466	13.4
Accell cartridge	438	3.9
Synthetic rutile		
Ion-exclusion cartridge	332	27.3
Zircon		
Ion-exclusion cartridge	21	ND

ND = Not detected.

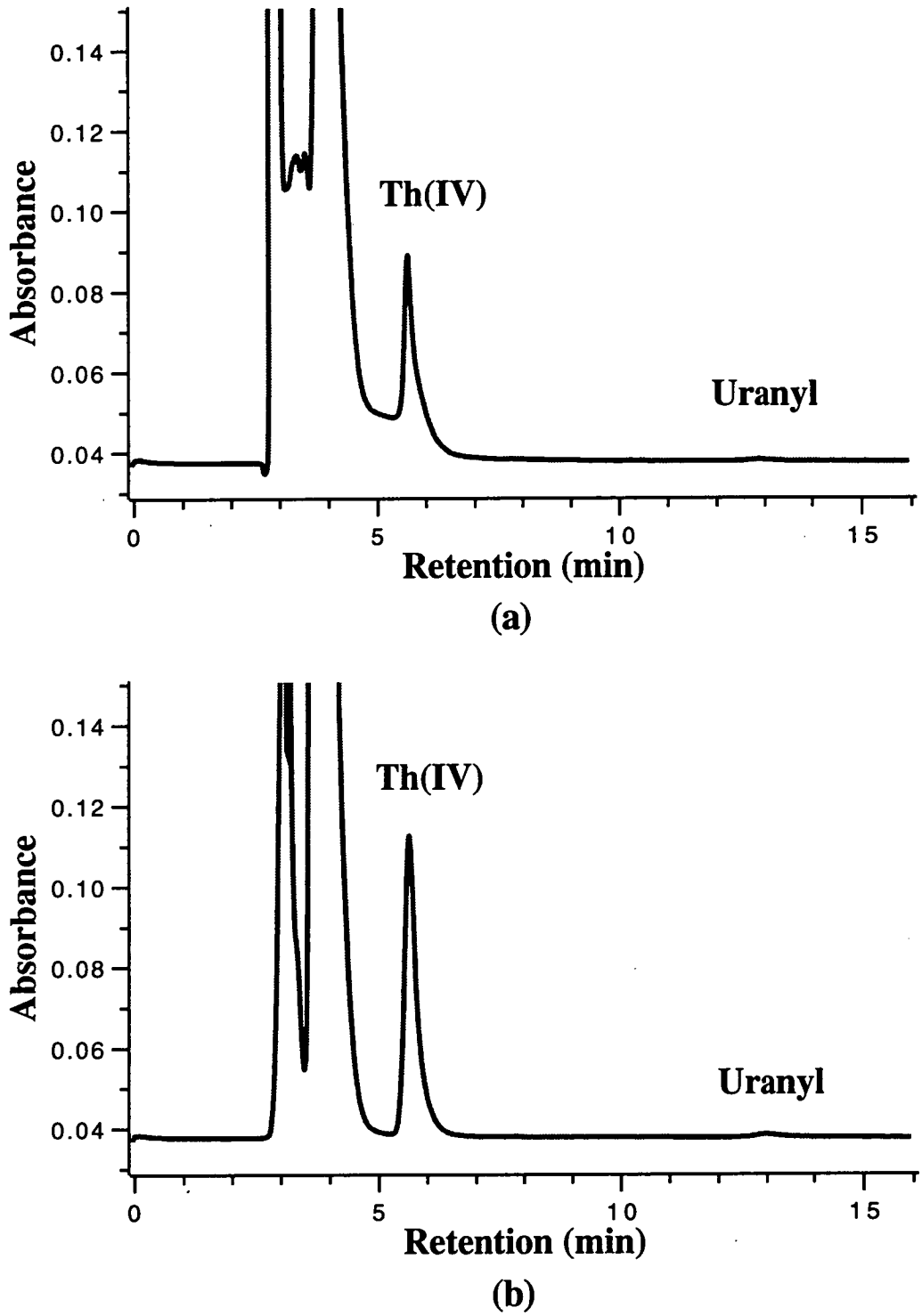

Fig. 6.3 Chromatograms of ilmenite prepared by hydroxide fusion obtained (a) using direct injection and (b) pretreated using Ion-Exclusion Guard-Pak. Other conditions as in Fig. 6.1. Solutes (original concentration): (a) 465.6 ppm thorium and 13.4 ppm uranium, (b) 238.7 ppm thorium and 7.4 ppm uranium.

after cation-exchange pretreatment. The chromatograms show clearly that the recovery and peak shape for thorium were significantly improved using the cation-exchange pretreatment for ilmenite samples. However, the results obtained for synthetic rutile and zircon samples were still poor, perhaps indicating that the hydroxide sample fusion/digestion procedure was inappropriate for this mineral sand type.

6.3.3 COMPARISON OF FUSION/DIGESTION METHODS

Having established the feasibility of using the ion-exclusion Guard-Pak pretreatment to eliminate the dissolution matrix interference problems prior to the chromatographic step, a number of fusion/digest procedures were then evaluated for use in conjunction with the pretreatment procedure. The cation-exchange pretreatment procedure was modified slightly with 2.0 ml of 2.0 M HIBA being used to elute the bound thorium and uranium from the ion-exclusion cartridge, instead of 7.5 M nitric acid. When 1.0 ml of 10 ppm standards was loaded on to the ion-exclusion Guard-Pak, the recoveries were 97.5% and 99.6% for thorium(IV) and uranyl, respectively. This approach avoided the time consuming nitric acid evaporation step and also allowed the possibility for the pretreatment procedure to be automated.

A number of fusion/digestion procedures were evaluated for their applicability for use in conjunction with the cation-exchange clean-up. The final cation-exchange pretreatment procedure used is detailed in the previous experimental. The sample digest solution was further diluted 10 times, and 20 ml loaded onto the ion-exclusion Guard-Pak using a HPLC pump. The results obtained using a variety of fusion/digestion approaches for ilmenite, synthetic rutile and natural rutile samples prior to cation-exchange pretreatment and chromatographic analysis are detailed in Table 6.5.

The results indicated that an hydroxide fusion appeared to be appropriate for ilmenite samples, although it was not appropriate for other sample types. A tetraborate

Table 6.5 THORIUM AND URANIUM CONCENTRATION IN ORIGINAL MINERAL SANDS

Samples fused/digested using various chemicals, then pretreated with cation exchange before chromatographic analysis. Chromatographic conditions were the same as those in Table 6.2.

Sample	Thorium (ppm)	Uranium (ppm)
Ilmenite		
Hydroxide fusion	466	13.4
Tetraborate-carbonate fusion	314	ND
Synthetic rutile		
Tetraborate-carbonate fusion	332	ND
Natural rutile		
Tetraborate-carbonate fusion	56.4	25.3
Tetraborate fusion	62.0	53.1
Pyrosulphate fusion	63.4	11.1
Carbonate-tetraborate fusion	47.7	4.9

ND = Not detected.

procedure appeared to be appropriate for natural rutile, while carbonate-tetraborate, pyrosulfate and tetraborate-carbonate procedures all gave poor recoveries for this sample, particularly for uranium. The most significant difference between the first two procedures (tetraborate/carbonate, tetraborate) and the latter three (pyrosulfate, tetraborate/carbonate, sodium hydroxide) was that TiO_2 was insoluble and was precipitated from acid solution to be filtered off with either of the first two approaches; however, it remained in solution when using other fusion/digestion approaches. It appeared highly probable that Ti(IV) cation in the digest solution was eluting the ion-exclusion cartridge during the sample loading step, resulting in low uranium recoveries. This was confirmed by the fact that ICP-MS analysis of the four natural rutile digests shown in Table 6.5 all yielded similar results for thorium and uranium, indicating that the solutes were being released into the fusion/digestion solutions, but that the chromatographic recoveries obtained after the pretreatment procedure depended upon the dissolution method used.

The tetraborate fusion/nitric acid digestion procedure appeared to be the most appropriate for all the sample types and was further evaluated for use in conjunction with the cation-exchange procedure. All the mineral sand types were prepared using the tetraborate fusion/nitric acid digestion procedure after which the samples were treated using the cation-exchange pretreatment procedure described in the experimental section. The results of the chromatographic analysis, together with the XRF results, are shown in Table 6.6. The ilmenite sample was fused/digested twice and the natural rutile sample was fused/digested five times, hence the multiple entries in the table for these samples. Fig. 6.4 shows the chromatograms obtained of the four mineral sand types prepared using the tetraborate fusion/nitric acid digestion and cation exchange pretreatment. The ilmenite and synthetic rutile chromatograms are shown at an injection volume of 200 µl in order to clearly highlight the uranium peak, although the thorium in these two sample types was typically quantified using a 25-50 µl injection. Considering the difference between the two methods of analysis, the results showed

Table 6.6 THORIUM AND URANIUM CONCENTRATION IN ORIGINAL SAND SAMPLES

Samples fused using tetraborate and dissolved with nitric acid, then pretreated with cation exchange before chromatographic analysis.

Sample	HPLC		XRF[a]	
	Thorium (ppm)	Uranium (ppm)	Thorium (ppm)	Uranium (ppm)
Ilmenite	487	15.0	490	10
	462	12.9		
Synthetic rutile	382	12.8	430	15
Zircon	167	184	179	217
Natural rutile	63.0	47.4	53	54
	59.4	48.9		
	59.1	49.6		
	59.5	49.9		
	62.0	53.1		

XRF[a] = Results obtained on solid samples.

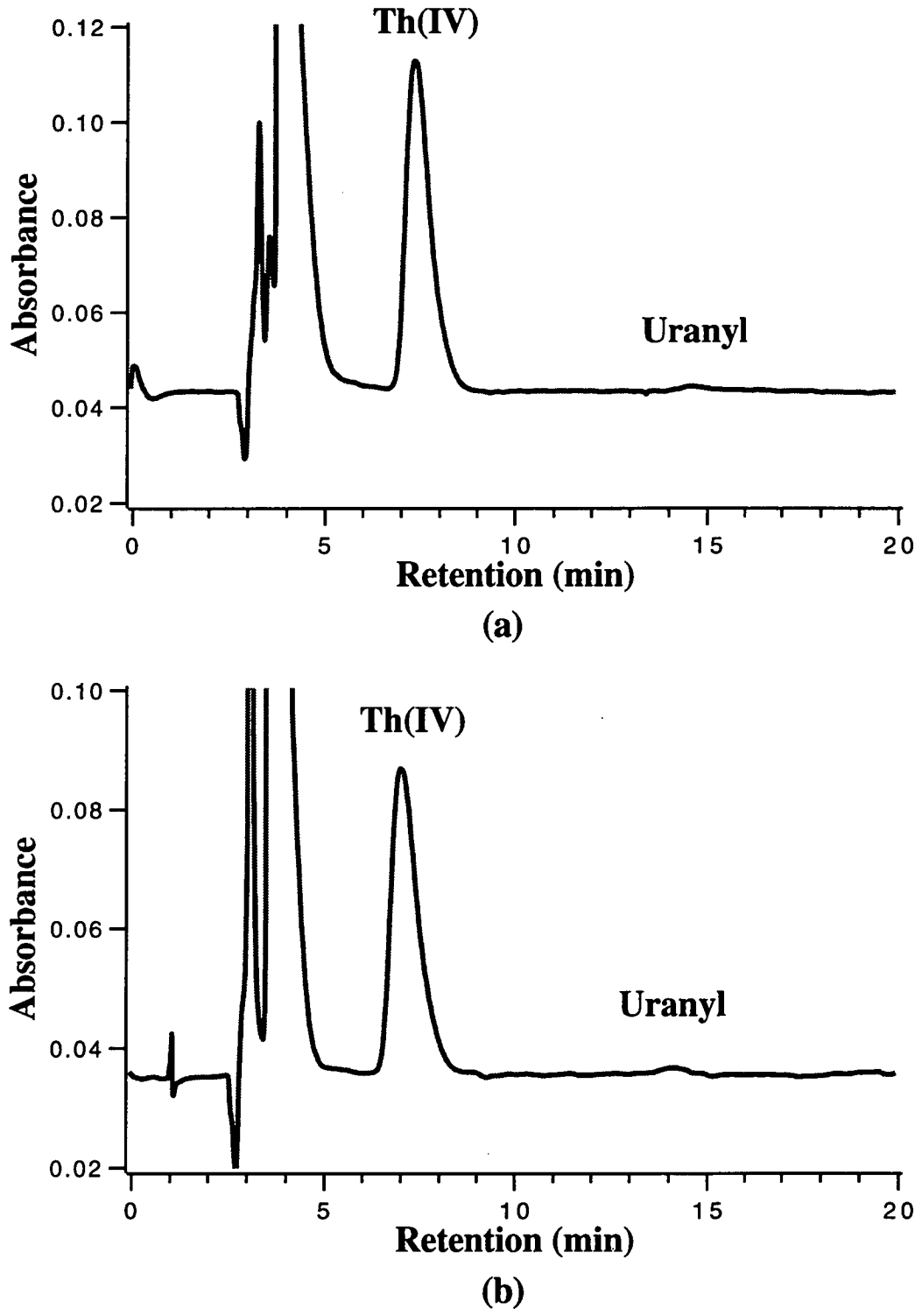

Fig. 6.4 Chromatograms of (a) ilmente and (b) synthetic rutile prepared by tetraborate fusion/nitric acid digestion and cation-exchange pretreatment. The conditions were as described in Fig. 6.1, excpt injection volume: 200 µl. Solutes (original concentration): (a) 462.4 ppm thorium and 12.9 ppm uranium, (b) 381.6 ppm thorium and 12.8 ppm uranium.

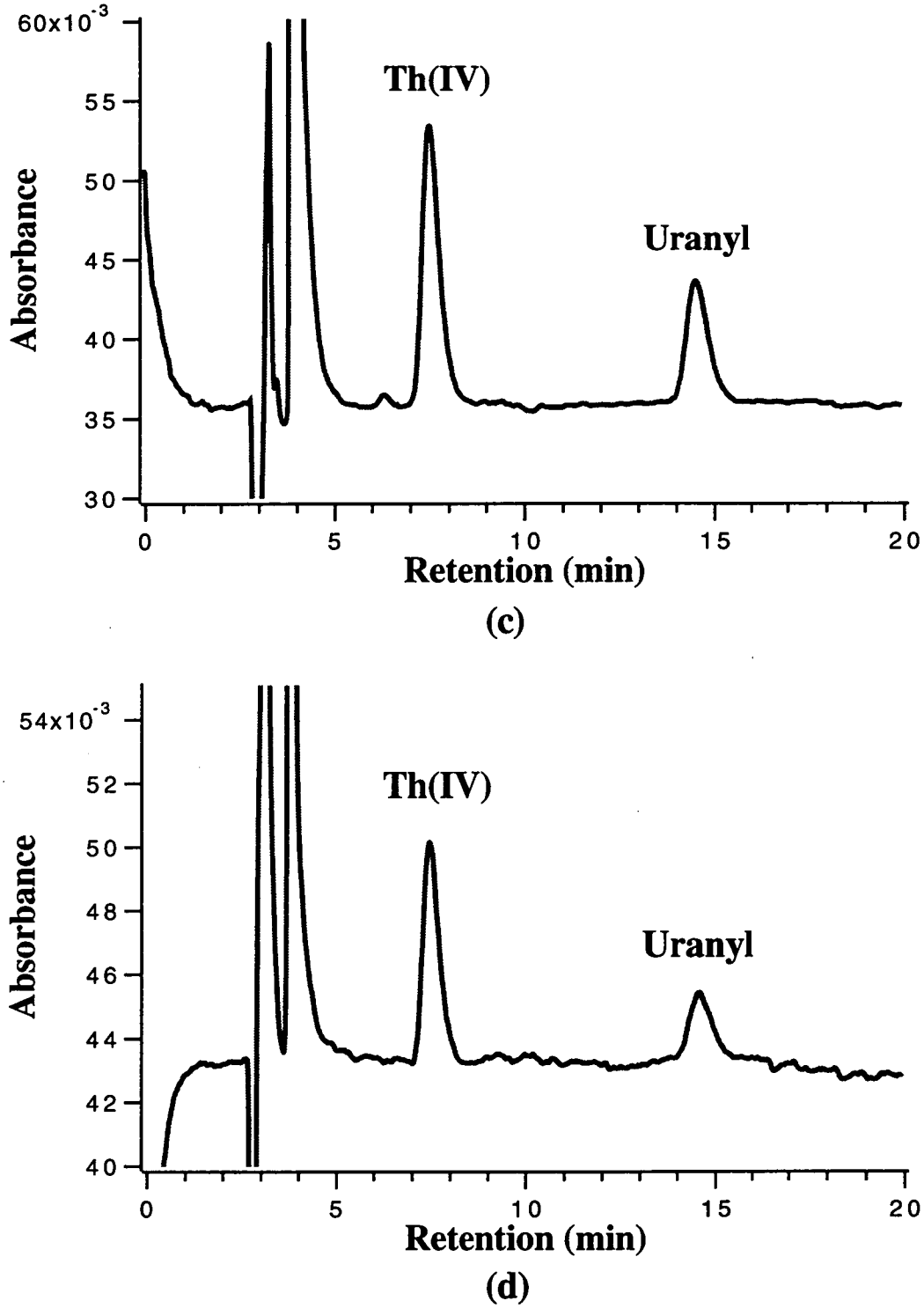

Fig. 6.4 (continued) Chromatograms of (c) zircon and (d) natural rutile prepared by tetraborate fusion/nitric digestion and cation-exchange pretreatment. Injection of 100 µl sample. Solutes (original concentration): (c) 167.2 ppm thorium and 184.2 ppm uranium, (d) 59.4 ppm thorium and 48.9 ppm uranium.

remarkably good agreement. Analysis of the natural rutile digest by ICP-MS gave results for thorium and uranium of 69 and 48 μg/ml, respectively, which compared well to the average results obtained by IC of 60.6 μg/ml thorium (2.9% R.S.D.) and 49.8 μg/ml uranium (4.2% R.S.D.).

6.3.4 DIRECT INJECTION

The cation-exchange pretreatment described above effectively isolated the thorium(IV) and uranyl from the fusion/digest matrix in a HIBA solution before injection into the liquid chromatograph. It is possible to automate this procedure by adding a six-port column switching valve and a HPLC sample loading pump into the system. The use of automated sample clean-up and introduction requires some alternations to the cation-exchange procedure. Firstly the amount of sample loaded onto the cation-exchange cartridge must be significantly less than previously used in order not to overload the analytical column during the chromatographic analysis step. Here 1.0 ml of the 10 times diluted sample was loaded onto the cation-exchange cartridge, instead of 20 ml loaded by manual pretreatment. In this automated sample clean-up procedure, the ion-exclusion Guard-Pak was initially conditioned with 7.5 M nitric acid, then washed with 10 ml Milli-Q water, following which 1.0 ml of 0.5 ppm standards were loaded. However, the recoveries were only 46% and 62% for thorium(IV) and uranyl, respectively, by comparison with the results obtained by direct injection of 50 μl of 10 ppm standards. The thorium(IV) and uranyl peaks were also broadened, which means the 0.4 M HIBA was not strong enough to elute the bound solutes. Increasing the HIBA concentration may be suitable for the stripping step, but it is not practical for the chromatographic separation procedure. A further experiment omitted the nitric acid condition step. Thorium(IV) and uranyl could be quantitatively eluted using the 0.4 M HIBA analytical eluent, but the cation-exchange cartridge showed less affinity for thorium(IV) and uranyl at this condition.

The analysis of samples using a direct injection approach would be preferable to the cation-exchange pretreatment; however, as discussed previously, this would require a very large dilution which was impractical at the thorium and (particularly) uranium concentrations present in the original mineral sands. The success of the cation-exchange pretreatment nevertheless indicated that if thorium and uranium could be fully coordinated with HIBA in the digest solution, then direct injection of the sample would be possible. As the chromatographic detection limits for thorium and uranium were 3.0 and 5.0 ng/ml, respectively, using a 1000-µl injection, it was decided to attempt quantification of the tetraborate fusion/nitric acid digest solutions by direct injection after dilution in HIBA.

The digestion solutions were diluted a further 1:10 and HIBA added to give a final concentration of 400 mM before injection into the liquid chromatograph. Injection volumes of 1000-µl were required for uranium quantification in ilmenite and synthetic rutile, while a 250-µl injection was used to quantify thorium in these samples. Both thorium and uranium could be quantified in zircon and natural rutile samples with a 500-µl injection. Table 6.7 summarises the results and precision obtained by HPLC using the direct injection/HIBA dilution method and Fig. 6.5 shows a typical chromatogram obtained for a zircon sample (compare to Fig. 6.4c obtained using the cation-exchange pretreatment). The results show excellent agreement with those obtained using the cation-exchange pretreatment, although the precision was generally not as high, particularly for the two cations in the natural rutile sample and also uranium in the ilmenite and synthetic rutile, as these solutes were being detected at concentrations approaching the method detection limits. Also, the direct injection approach was not as robust as the cation-exchange procedure as significant increases in the acid concentration of the fusion/digestion solution resulted in low recoveries for both thorium and uranium.

Table 6.7 THORIUM AND URANIUM CONCENTRATIONS IN ORIGINAL MINERAL SANDS

Samples fused using tetraborate and dissolved in nitric acid, then diluted with HIBA and injected directly for chromatographic analysis.

Sample	Thorium (ppm)	Uranium (ppm)
Ilmenite	493 (0.4% R.S.D.)	18.3 (8.1% R.S.D.)
Synthetic rutile	382 (0.5% R.S.D.)	8.4 (10.0% R.S.D.)
Zircon	171 (2.13% R.S.D.)	199 (1.6% R.S.D.)
Natural Rutile	68.6 (7.4% R.S.D.)	46.9 (9.2% R.S.D.)

R.S.D. obtained from five replicate injections.

6.4 CONCLUSIONS

Thorium and uranium can be analysed in mineral sands by IC using a C_{18} reversed-phase column and an eluent of hydroxyisobutyric acid followed by post-column derivatisation with Arsenazo III and visible detection at 658 nm. Sample preparation involved a tetraborate fusion/nitric acid leach followed by either cation-exchange pretreatment or direct injection after dilution in concentrated hydroxyisobutyric acid. The cation-exchange pretreatment resulted in higher precision and could be applied to more acidic sample digests; however, the direct injection approach gave comparable results when using the recommended dissolution procedure and offered significant time savings. The results obtained using the chromatographic method showed excellent agreement with those generated using the significantly more costly techniques of XRF and ICP-MS for ilmenite, synthetic rutile, zircon and rutile mineral sands.

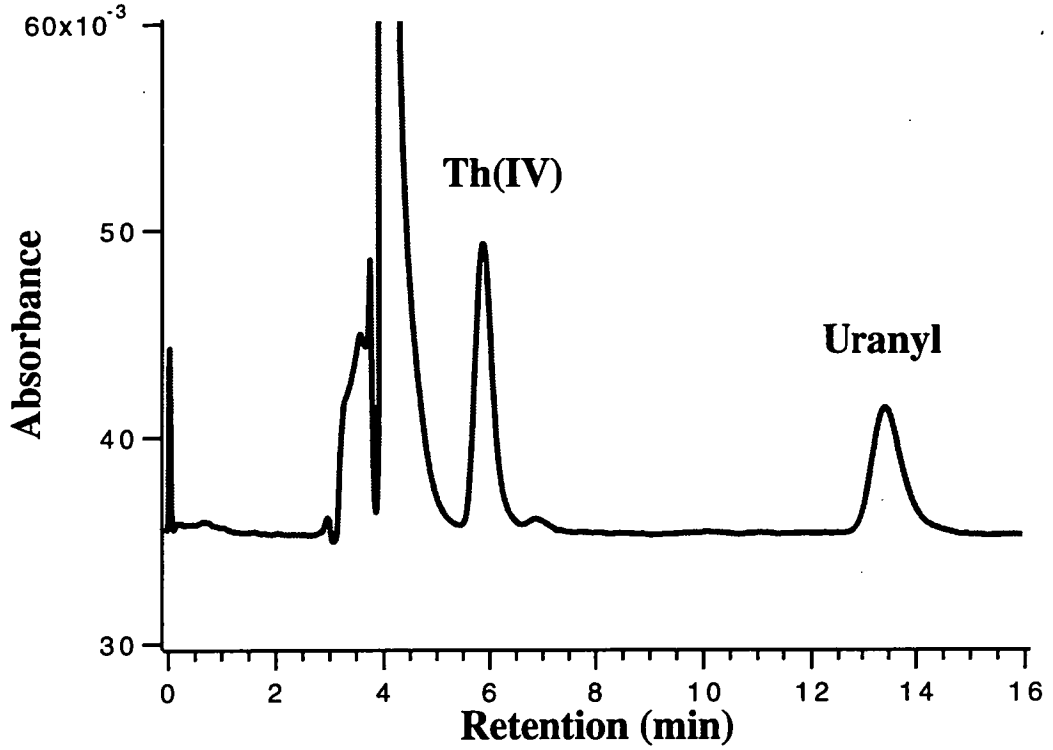

Fig. 6.5 Chromatogram of zircon prepared by tetraborate fusion/nitric acid digestion and direct injection of the HIBA dilution. The chromatographic onditions were as in Fig. 6.1, except injection volume: 500 µl. Solutes (original concentration): 167.2 ppm thorium and 195.8 ppm uranium.

6.5 REFERENCES

1 L. S. Clesceri, A. E. Greenberg and R. R. Trussell, *Standard Methods for the Examination of Water and Wastwater*, American Public Health Association, Washington DC, USA, 17th ed., 1989.

2 T. Honda, T. Oi, T. Ossaka, T. Nozaki and H. Kakihana, *J. Radioanal. Nucl. Chem.*, 139 (1990) 157.

3 Y. Igarashi, C. K. Kim, Y. Takatu, K. Shiraishi, M. Yamamoto and N. Ikeda, *Anal. Sci.*, 6 (1990) 157.

4 A. G. Adriaens, J. D. Fassett, W. R. Kelly, D. S. Simons and F. C. Adams, *Anal. Chem.*, 64 (1992) 2945.

5 P. Robinson, N. C. Higgins and G. A. Jenner, *Chem. Geol.*, 55 (1986) 121.

6 M. P. Harrold, A. Siriraks and J. Riviello, *J. Chromatogr.*, 602 (1992) 119.

7 R. M. Cassidy, *Chem. Geol.*, 67 (1988) 185.

8 A. Mazzucotelli, A. Dadone, R. Frache and F. Baffi, *J. Chromatogr.*, 349 (1985) 137.

9 R. M. Cassidy, S. Elchuk, N. L. Elliot, L. W. Green and B. M. Recoskie, *Anal. Chem.*, 58 (1986) 1181.

10 C. H. Knight, R. M. Cassidy, B. M. Recoskie and L. W. Green, *Anal. Chem.*, 56 (1984) 474.

11 R. M. Cassidy and M. Fraser, *Chromatographia* 18 (1984) 369.

12 Zhang X.-X., Wang M.-S. and Cheng J.-K., *Anal. Chim. Acta*, 237 (1990) 311.

13 A. Kerr, W. Kupferschmidt and M. Attas, *Anal. Chem.*, 60 (1988) 2729.

14 R. Kuroda, M. Adachi, K. Oguma and Y. Sato, *Chromatographia* 30 (1990) 263.

15 R. M. Cassidy, S. Elchuk, L. W. Green, C. H. Knight, F. C. Miller and B. M. Recoskie, *J. Radioanal. Nucl. Chem.*, 139 (1990) 55.

16 E. A. Jones, H. S. Bezuidenhout and J. F. Van Staden, *J. Chromatogr.*, 537 (1991) 227.

17 F. W. E. Strehlow, R. Rethemeyer and C. J. C. Bothma, *Anal. Chem.*, 37 (1965) 107.

18 A. E. Martell and R. M. Smith, Critical Stability Constants, Vol. 3, Plenum Press, New Yeark, 1977.

19 L. Imrie, *Z. Anorg. Chem.*, 164 (1927) 214.

Chapter 7

Determination of Trace Levels of Thorium(IV) and Uranyl by an On-line Preconcentration Technique

7.1 INTRODUCTION

Using ion-chromatographic techniques most inorganic anions and cations can be directly analysed without pretreatment. However, quantitative analysis requires that the solute concentration should be about 1 ppm or higher in order to obtain reliable results. For an analyte below this level, analysis is generally performed either by injecting a large volume of sample or by using a preconcentration technique. The latter method has been widely used for the determination of trace level elements because it is convenient to apply and offers high enrichment factors.

With the on-line preconcentration method a short column, or concentrator, is generally mounted in front of the analytical column. A measured volume of sample solution is pumped through the concentrator, during which time the analytes are trapped on it. Subsequently, the enriched components are transferred onto the analytical column where they are separated and quantified as performed in conventional chromatographic analysis.

The success of the preconcentration process is dependent on the quantitative binding of the analytes on the concentrator column during the sample loading step, and complete transferral of the trapped components onto the analytical column in the following step. There are many parameters which affect preconcentration efficiency, such as the capacity of the concentrator, sample matrix, and the manner in which the sample is loaded. In addition, routine analysis requires that the binding of analytes on

the concentrator and their subsequent stripping should be reproducible, so a re-equilibration step for the concentrator is usually required prior to loading each sample. Another function of the preconcentration procedure is to remove the matrix from the sample. In most cases, the preconcentration system is so selected that the analytes are trapped on the concentrator, whilst the interfering species are washed out during the loading step. Sometimes a separate washing step is also needed after loading the sample.

The on-line preconcentration process can be performed using either a single-valve system or a two-valve system. The former system generally employs a six-port, high-pressure switching valve, which inserts the concentrator column into the flow-path of the analytical eluent or withdraws it. An extra HPLC pump is also needed for sample loading. The single valve system has been used widely due to its advantages of simplicity and ease of operation, which allows to be performed either manually or automatically. Several papers [1, 2, 3] have reported that the on-line preconcentration technique has been used successfully in the determination of trace levels of anions.

In Chapter 6 the reversed-phase chromatographic method was combined with a manual preconcentration procedure to determine trace levels of thorium(IV) and uranyl in mineral sands using a short cation-exchange column as the concentrator. The digested sample solution was prepared in diluted nitric acid and loaded on the concentrator with a HPLC pump. Afterwards, the bound analytes were stripped with a concentrated HIBA solution for chromatographic injection. The chromatographic results showed good agreement with those obtained by using XRF or ICP-MS methods. This manual procedure was then incorporated in an on-line preconcentration system, and performed automatically by the Model 590 programmable pump. However, the results obtained after this on-line preconcentration pretreatment were very low.

In Chapter 4 the retention behaviour of thorium(IV) and uranyl HIBA

complexes on a C_{18} column was studied. It was found that these metal complexes were retained on the reversed-phase column by a conventional hydrophobic absorption mechanism, whilst lanthanides and transition metals were eluted at the solvent front or showed a weak retention. Further study (Chapter 5) found that the thorium(IV) and uranyl mandelate complexes were retained much longer than those of HIBA or glycolate complexes under the same conditions, because the phenyl group on the mandelic acid greatly increased the hydrophobicity of its complexes. From these results it can be expected that thorium(IV) and uranyl preconcentration could be improved if the sample was prepared in a mandelate solution and a reversed-phase column was used as the concentrator.

In this Chapter the on-line preconcentration approach is applied to the determination of ppb levels of thorium(IV) and uranyl. The cation-exchange concentrator (Ion-Exclusion Guard-Pak insert) used in Chapter 6 was replaced with a short C_{18} column and the thorium(IV) and uranyl sample was prepared in a mandelate solution. Different size concentrators and various ligand concentrations have been investigated. The sample loading parameters and the effect of anions and cations in the sample have also been examined. Finally, the on-line preconcentration method was applied to the determination of thorium(IV) and uranyl spiked into sea water.

7.2 EXPERIMENTAL

7.2.1 INSTRUMENTATION

In this Chapter a single-valve preconcentration system was used, which comprised a Millipore-Waters (Milford, MA, U.S.A.) Model 590 programmable pump for loading sample, a Waters six-port Automated Switching Valve and a C_{18} Guard-Pak insert concentrator which housed in a Waters Guard-Pak Pre-column Module, in addition to the direct injection chromatographic system (see Fig. 3.2). A μ-Bondapak C_{18} reversed-phase column (300 x 3.9 mm I.D.) was used as the analytical column. Other instruments were the same as that described in Chapter 3.

7.2.2 REAGENTS

Most of the analytical mobile phases comprised 0.1M HIBA (Sigma, St. Louis, MO, USA) and 10% HPLC grade methanol (Waters), and adjusted to pH 4.0. The post-column reaction (PCR) reagent solution was the same as used in previous chapters (0.13 mM Arsenazo III buffered in an acetic acid-urea solution). Both the mobile phase and PCR solution were filtered through a 0.45 μm filter membrane and degassed in an ultrasonic bath prior to use.

The ppb level thorium(IV) and uranyl standard solutions were freshly prepared each day by diluting the concentrated stock solution (1000 ppm). Most of the low concentration standards were prepared in 30 mM mandelic acid (Koch-light Laboratories Ltd, Colnbrook, Bucks, England) solution and adjusted to pH 4.0 with sodium hydroxide. A 1% methanol was also added into the sample in order to wet the surface of the reversed-phase concentrator. This sample solution was degassed by a vacuum method prior to loading on the concentrator.

Other metal solutions used for the interference studies were directly prepared from their nitrate salts or by dissolving their oxide (analytical grade) in nitric acid. No further purification was applied. The anion solutions were obtained by dilution of the concentrated acids in Milli-Q water and then neutralised with sodium hydroxide.

7.2.3 PRECONCENTRATION SYSTEM AND PROCEDURES

The single-valve preconcentration system was operated using a sequence of four steps, as shown in Fig. 7.1. Firstly, the 0.1 M HIBA mobile phase was pumped through both the concentrator and the analytical columns for equilibration, whilst the sample solution was flushed through the connecting tubes ahead of the valve and thence to the waste (Fig. 7.1a). In the next step, the valve was rotated to insert the concentrator column into the sample flow-path, as shown in Fig. 7.1b, during which the analytes in the sample were trapped on the concentrator. After a measured volume

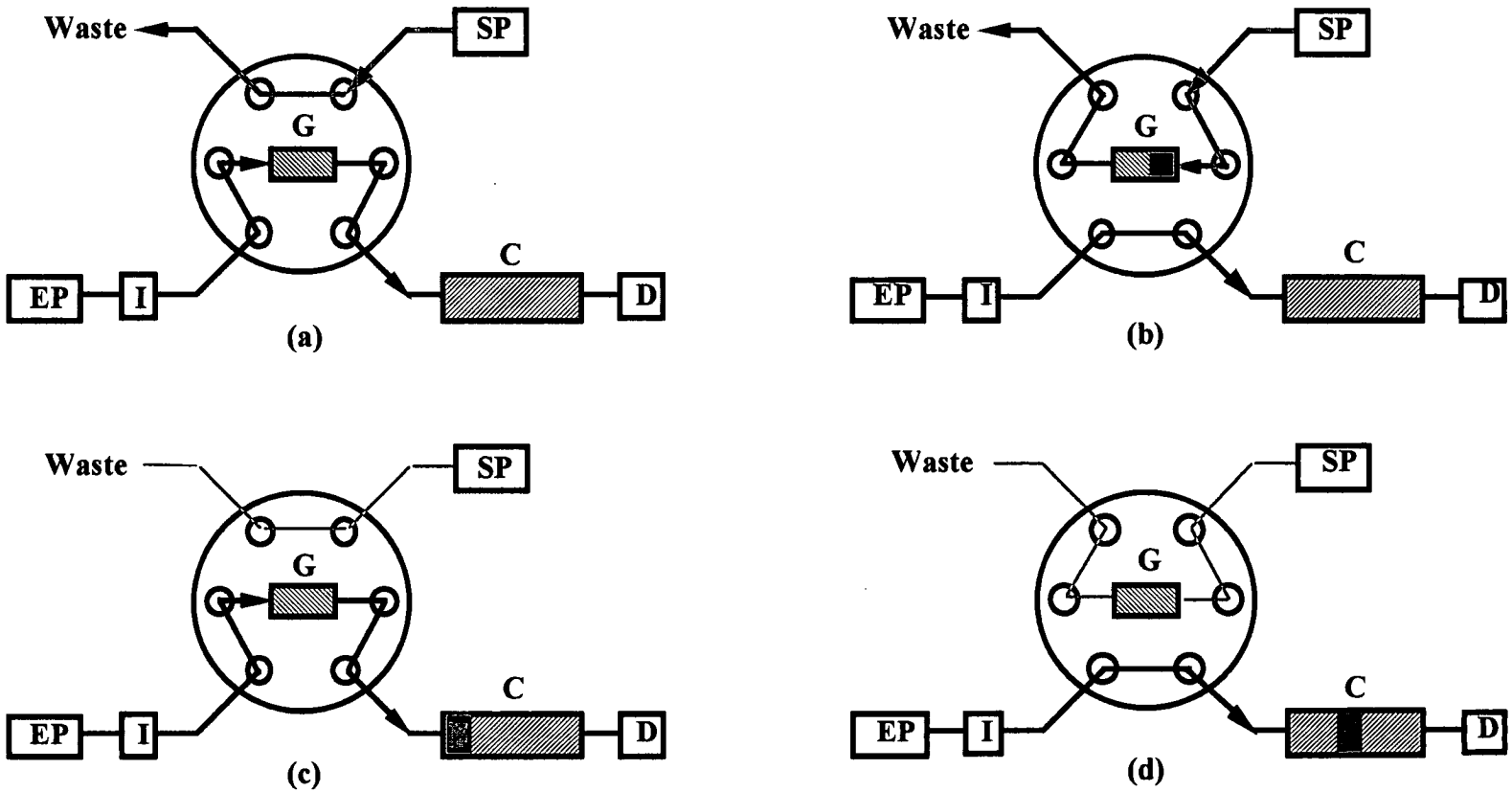

Fig. 7.1 Schematic digramm of on-line preconcentration procedures, (a) concentrator equilibration, (b) loading sample, (c) back -flush, (d) analysis. G: C-18 Guard column concentrator, C: analytical column (300 x 3.9 mm I.D.), SP: sample loading pump, EP: eluent pump, I: U6K injector, D: UV detector.

of sample solution was loaded on the concentrator, the valve was rotated back, and the HIBA analytical eluent used to back-flush the trapped solutes onto the analytical column (Fig. 7.1c). Finally, the concentrator column was withdrawn from the flow-path and the eluent pumped directly into the analytical column where the analytes were separated and quantified in the conventional manner (Fig. 7.1d). The equilibration period, sample loading flow-rate and volume, as well as the analysis procedure were all performed automatically by a program edited in the Model 590 pump, as listed in Table 7.1. A same amount of concentrated thorium(IV) and uranyl standards was injected directly onto the analytical column in order to calculate their recoveries. Thorium(IV), uranyl, lanthanides and transition metals were all detected at 658 nm after PCR reaction with Arsenazo III. Other conditions were the same as that described in Chapter 3. All experiments were carried out at room temperature.

7.3 RESULTS AND DISCUSSION

7.3.1 PRELIMINARY INVESTIGATION

In Chapter 6 a manual procedure was used to pretreat the digested mineral sand sample prior to the chromatographic determination of thorium(IV) and uranyl. A short cation-exchange column (Ion-Exclusion Guard-Pak insert, sulphonic acid functionalised, 0.2 g of 5 mequiv/g resin) was used. The digested mineral sand was prepared in diluted nitric acid, and 20 ml of this solution was loaded onto the short column. The bound analytes were then stripped with 2.0 ml of 2.0 M HIBA and an aliquot was injected directly for chromatographic analysis. The final chromatogram showed that thorium(IV) and uranyl could be separated completely from the matrix, and the analytical results were in good agreement with those obtained using the X-ray fluorescence or inductively coupled plasma mass spectrometry methods. Here, the clean-up step can also be regarded as an off-line preconcentration procedure, for the 20 ml sample loaded at the beginning was stripped with 2.0 ml of eluent, giving an enrichment factor of 10.

Table 7.1 THE MODEL 590 PUMP PROGRAM USED FOR THORIUM(IV) AND URANYL PRECONCENTRATION [4]

Segment No.	Start	Step in Fig. 7.1	Description	Flow ml/min	Event out 12345678	Duration (min)
1	0.00	(a)	Initial sample flush	1.0	FFFFFFFF	0.50
2	0.50	(a)	Sample flush	5.0	FFFFFFFF	2.50
3	3.00	(a)	Reduce flow-rate	1.0	FFFFFFFF	1.00
4	4.00	(b)	Loading sample	1.0	NFFFFFFF	10.00
5	14.00	(c)	Back flush	1.0	FFFFFFFF	4.00
6	18.00	(d)	Analysis and start next performance	1.0	NFFFFNFN	12.00

Event in: 1#, receiving of the trigger signal from the U6K injector or others.

Event out: 1#, to the Valve switch;

6#, to trigger the Chromatography Data Station;

8#, to event in 1# to restart next performance.

At the commencement of this study, an on-line preconcentration system was constructed from the manual procedure simply by adding a six-port column switching valve and a sample loading pump, as shown in Fig. 3.2. The cation-exchange concentrator was conditioned with 7.5 M nitric acid and then washed with 10 ml Milli-Q water. Some alterations were also made to the cation-exchange procedure in order to adapt it for on-line performance. A 1.0 ml of the sample was loaded instead of the 20 ml in the manual procedure, and stripping was performed with the analytical mobile phase which comprised 0.4 M HIBA and 10% methanol (pH 4.0). However, poor recoveries were obtained for 0.5 ppm standards, namely 46% for Th(IV) and 62% for U relative to an equivalent amount injected directly (50 µl of 10 ppm standards). In addition, when the concentrator column was inserted into the analytical eluent flow-path, the trapped cations were eluted as a broad peak and it appeared that the 0.4 M HIBA eluent was not strong enough to elute these cations in a small volume. A stronger eluent (2.0 M HIBA) was then tried, however, this led to excessive band broadening on the analytical column. Alternatively, when the nitric acid concentration used to condition the concentrator column prior to sample loading was reduced, the cations showed less affinity for the exchanger and they could be quantitatively eluted using the 0.4 M HIBA eluent. Unfortunately, these conditions did not allow quantitative binding of the sample digests during the loading step. It seemed that this system was not suitable for on-line preconcentration.

7.3.2 CONCENTRATOR COLUMN

7.3.2.1 Assessment of Different Types of Concentrator

Although there are many parameters which affect the preconcentration efficiency, perhaps the most important of these is the characteristics of the concentrator column. The requirements for quantitative preconcentration are two-fold. Firstly, the capacity of the concentrator should be large enough to bind all the analytes during the loading sample step. For a real sample, not only the analytes become bound on the

concentrator, but some matrix components in the sample are also trapped which required that the capacity of the concentrator should be even larger. On the other hand, the affinity of the concentrator for the analytes should be weak enough to allow the analytes to be removed with the analytical mobile phase in the stripping step, which is governed by the relative strengths of the concentrator and the stripping eluent. In this study the stripping eluent was fixed since the analytical mobile phase was used, so some other types of concentrator were needed.

Previously, Cassidy and Elchuk [5] developed a preconcentration method with a C_{18} Guard-Pak column as the concentrator to determine trace levels of uranium in ground water. The sample was initially prepared in dilute HIBA (0.11 M) solution, then 2 ml of this sample solution were loaded on the concentrator by a HPLC pump. Finally the enriched uranyl was stripped with the analytical mobile phase which comprised HIBA and octanesulfonate (OSA).

The characteristics of C_{18} (μ-Bondapak) and the cation-exchange (Ion-exclusion) Guard-Pak insert concentrators were initially examined by constructing a direct injection system using these concentrators as the analytical column. Fig. 7.2 shows the chromatograms obtained using a mobile phase comprising 0.1 M HIBA and 10% methanol and adjusted to pH 4.0, delivered at 1.0 ml/min. With the C_{18} Guard-Pak column, both thorium(IV) and uranyl were completely eluted within 1.5 min. It can be expected that thorium(IV) and uranyl peaks will be narrow if the C_{18} Guard-Pak column is used as the concentrator for preconcentration. On the other hand, with the Ion-Exclusion Guard-Pak column both thorium(IV) and uranyl were bound so strongly that they were difficult to elute with the 0.1 M HIBA eluent. If the Ion-Exclusion Guard-Pak column is used as the concentrator for the on-line preconcentration, a large volume of eluent would be needed to transfer the bound analytes to the analytical column, which would result in broadening the peaks, as observed in section 7.3.1. Na^+ or Mn^{2+} (nitrate) was added into the 0.1 M HIBA mobile phase to increase its strength, but the chromatogram showed no change. For

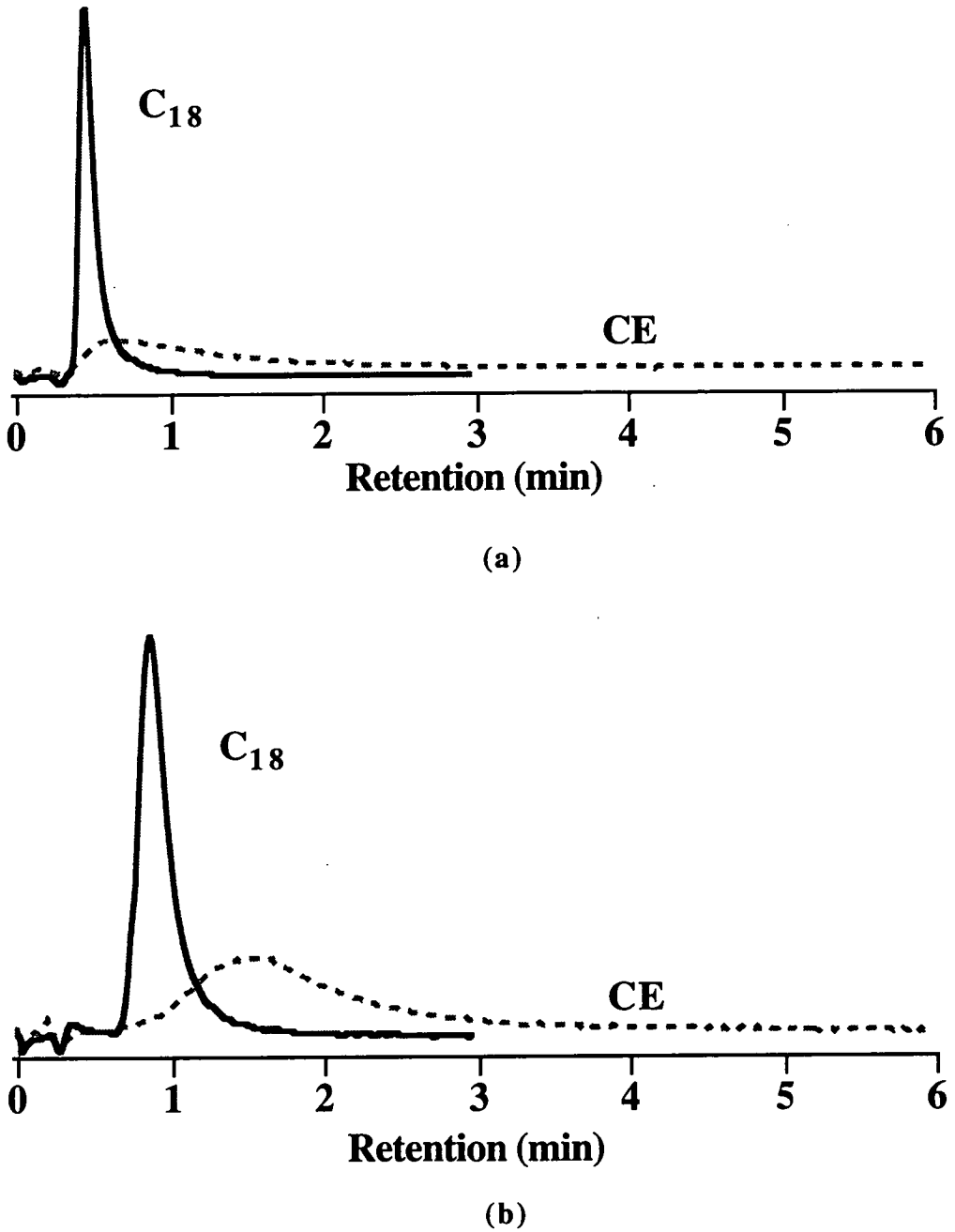

Fig. 7.2 (a) Thorium(IV) and (b) uranyl chromatograms with short columns. A Cation-exchange (CE) and C_{18} Guard-Pak were used as the analytical column, respectively, with 0.1 M HIBA in 10% methanol at pH 4.0 as the eluent. Detection at 658 nm after PCR reaction with Arsenazo III. A 50 µl of 10 ppm Th(IV) and uranyl standards were injected.

all subsequent experiments the C_{18} column was chosen as the concentrator.

7.3.2.2 Breakthrough Volume

There are two useful parameters to evaluate the performance of a preconcentration system. One is by measuring the percentage recovery of the method, which indicates the overall efficiency for an analyte trapped on the concentrator which is then transferred onto the analytical column. Later in this Chapter this parameter is used to examine the thorium and uranyl preconcentration. The second parameter is the breakthrough volume, it measures the total sample volume which can be loaded onto the concentrator without losing the analytes and hence is a useful parameter to examine the concentrator characteristics.

Prior to the on-line preconcentration study the breakthrough volume of the C_{18} Guard-Pak column concentrator was examined in order to determine the maximum sample loading volume. In Chapter 5 it was found that the thorium(IV) and uranyl mandelate complexes were retained on the C_{18} reversed-phase column to a greater extent than certain other ligand complexes. For this reason the thorium(IV) and uranyl samples were prepared in mandelate solution and adjusted to pH 4.0. A 1% methanol was also added into the sample solution in order to wet the stationary phase surface to assist retention of the hydrophobic complexes. The concentrator column was initially conditioned with a mandelate solution which contained the same concentration of mandelate as that in the sample. Thorium(IV) and uranyl samples were pumped through the concentrator by a HPLC pump, and monitored at the outlet at 658 nm after post-column reaction with Arsenazo III.

The early results (Chapter 5) have proved that the thorium(IV) eluted after uranyl on the C_{18} reversed-phase column when mandelate was used as the mobile phase, so in this experiment attention was concentrated mainly on the uranyl breakthrough volume. It can be expected that the thorium(IV) breakthrough volume

would be considerably larger than that of uranyl under the same conditions. The uranyl breakthrough volume was measured by adding various concentrations of mandelate into the sample solution.

Table 7.2 shows that the uranyl breakthrough volume on the C_{18} Guard-Pak column concentrator depends on the mandelate concentration in the sample. When the mandelate concentration was varied over the range of 10-50 mM, a maximum breakthrough volume (60 ml) was observed at 42 mM mandelate. This was in accordance with theoretical calculations which predicted that the distribution of the neutral uranyl *bis*(mandelate) complex reached at maximum at this ligand concentration. The thorium(IV) breakthrough volume decreased as the mandelate concentration increased, but it was still much larger than that of the uranyl complex at the same conditions over the range examined. When the uranyl concentration in the sample was increased from 100 ppb to 400 ppb, only a slight decrease of breakthrough volume was observed (see Fig. 7.3). Comparing with the effect of ligand concentration in sample, the effect of analyte concentration could therefore be neglected.

7.3 3 EFFECT OF LIGAND IN THE SAMPLE SOLUTION

7.3.3.1 Comparison of HIBA, Glycolate and Mandelate in Sample

Having selected a suitable concentrator column, the on-line preconcentration system was constructed using the C_{18} Guard-Pak insert as the concentrator, as shown in Fig. 3.2. In the above section it was found that the breakthrough volume of the C_{18} concentrator mainly depended on the ligand in the sample. Various ligands, such as HIBA, glycolate and mandelate, were added in the sample to compare the performance of the preconcentration system. Fig. 7.4 shows the recoveries obtained with a C_{18} Guard-Pak column concentrator, calculated by comparing the peak area in the preconcentration chromatogram with that obtained by direct injection of the same amount of standards.

Table 7.2 BREAKTHROUGH VOLUME FOR URANYL AND THORIUM(IV) ON A C_{18} GUARD COLUMN

Uranyl and thorium(IV) standards were prepared individually in various mandelate solutions containing 1% methanol at pH 4.0. The samples were directly pumped through a μ-Bondapak C_{18} Guard-Pak cartridge, and monitored at the column outlet at 658 nm after PCR reaction with Arsenazo III.

	Breakthrough volume (ml)			
Mandelate in sample (mM)	100 ppb UO_2^{2+}	200 ppb UO_2^{2+}	400 ppb UO_2^{2+}	200 ppb Th(IV)
10	15.8	12.9	--	--
30	57.5	45.9	48.8	354
42	--	61.5	--	245
50	31.7	29.7	30.0	110

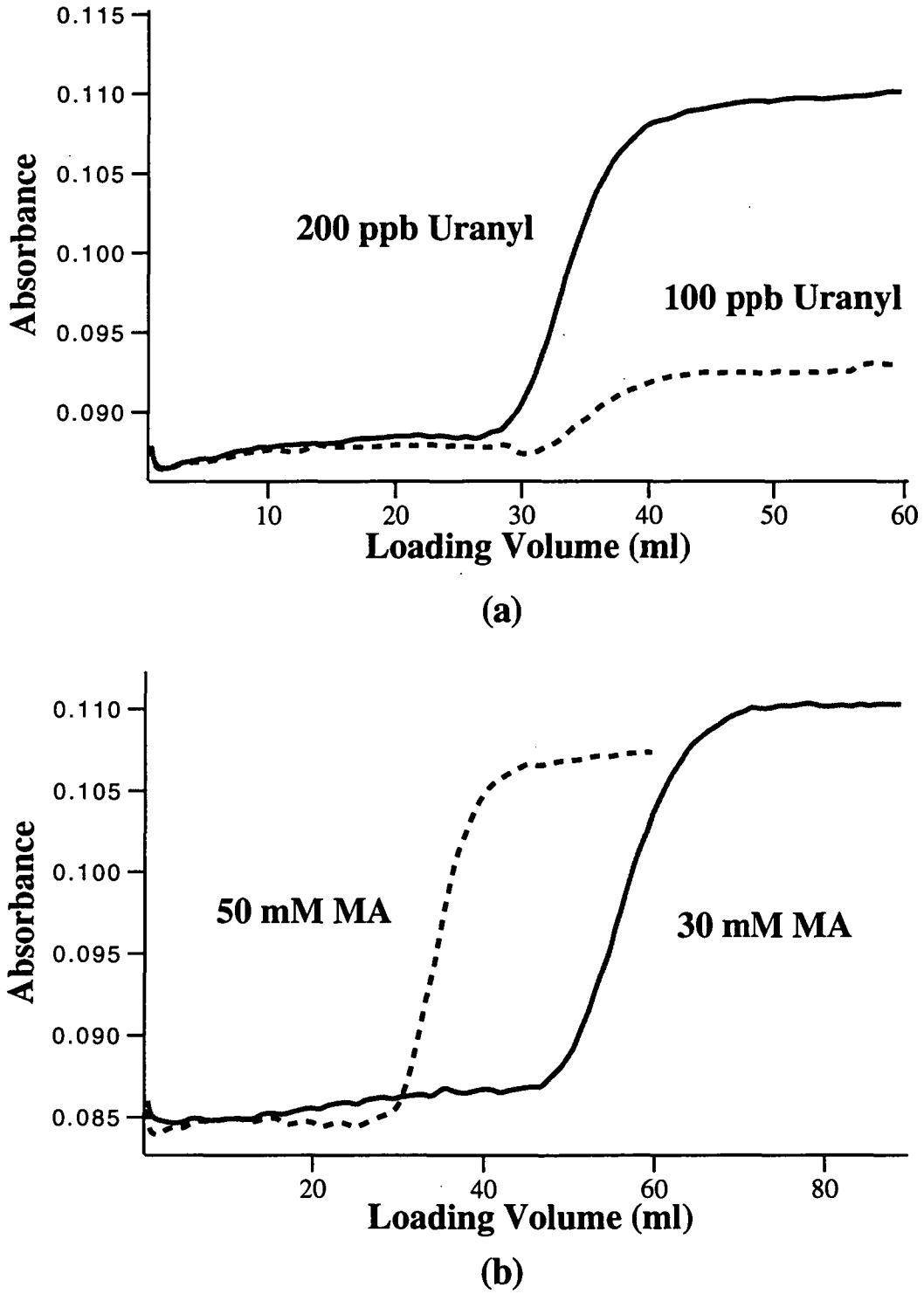

Fig. 7.3 The breakthrough curve of C_{18} Guard-Pak under various conditions. The uranyl sample was continually pumped through the gurad column and monitored at the outlet at 658 nm after PCR with Arsenazo III. Sample: (a) 100 ppb and 200 ppb uranyl in 30 mM mandelate, (b) 400 ppb uranyl prepared in 30 mM and 50 mM mandelate.

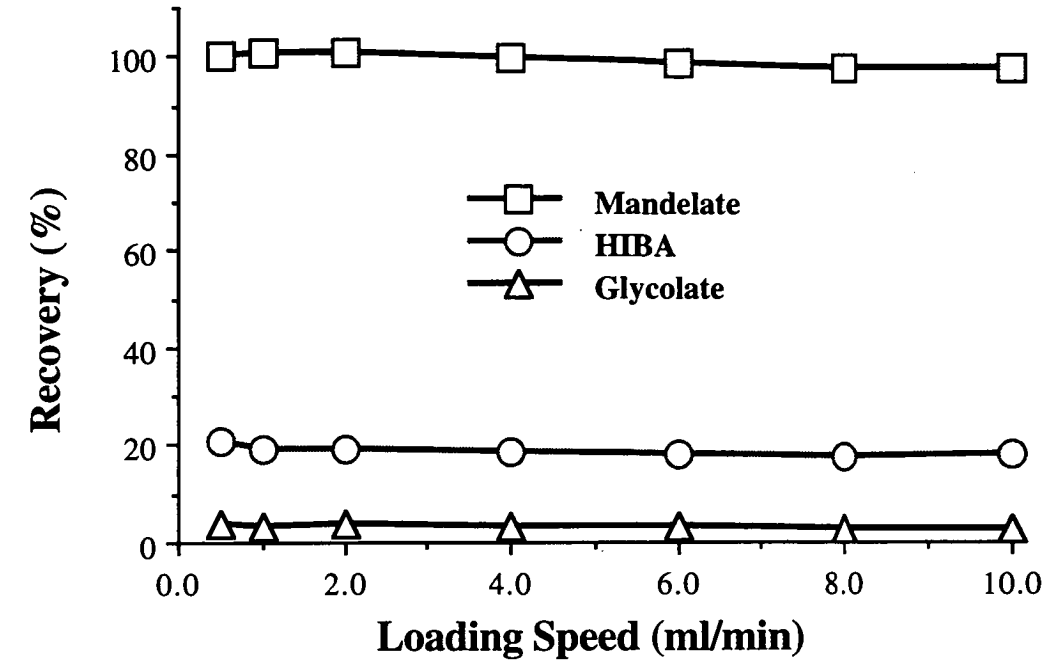

(a)

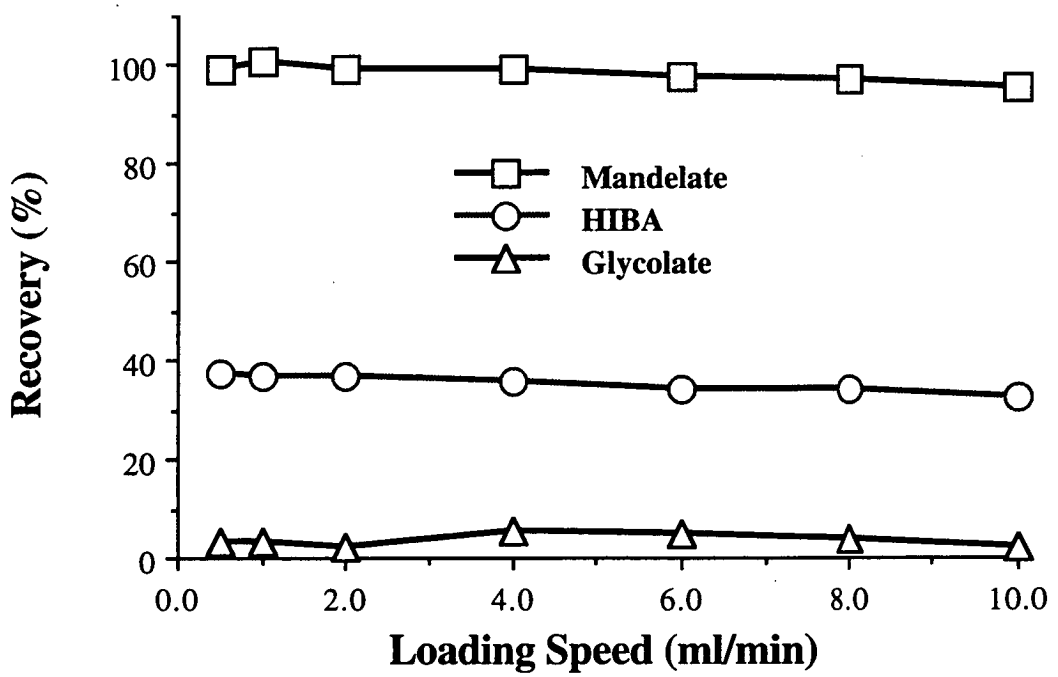

(b)

Fig. 7.4 Effect of different ligands on thorium(IV) and uranyl preconcentration. The sample was prepared in 1% methanol and 30 mM of HIBA, glycolate or mandelate. A 10 ml of 100 ppb (a) Th(IV) and (b) uranyl was loaded on a C_{18} guard column concentrator. A μ-Bondapak C_{18} column (300 x 3.9 mm I.D.) was used as the analytical column with 0.10 M HIBA in 10% methanol as the mobile phase. Detection at 658 nm after PCR with Arsenazo III.

A total of 10 ml of 100 ppb Th(IV) and uranyl mixed standards were concentrated, which prepared in 1% methanol at pH 4.0 with 30 mM mandelate, HIBA and glycolate, respectively. In 30 mM mandelate the recoveries of both thorium(IV) and uranyl were nearly 100%. However, only 20% for Th(IV) and 40% for uranyl were recovered in the HIBA solution, whilst in glycolate both thorium(IV) and uranyl recoveries were less than 10%. Previous theoretical calculations predicted that the distribution of thorium(IV) and uranyl complexes are very similar for the three ligands. The most likely explanation for the observed recoveries is the hydrophobicity differences among the three ligands. For the low hydrophobic ligands (HIBA and glycolate) their complexes could not be quantitatively bound on the C_{18} column during the sample loading step and some of the components directly flow to waste, so the recoveries of these complexes are very low. All samples were subsequently prepared in mandelate for further study of the preconcentration system.

7.3.3.2 Effect of Mandelate Concentration in Sample

Further experiments were undertaken to examine the effect of mandelate concentration in sample on thorium(IV) and uranyl preconcentration. A 100 ppb thorium(IV) and uranyl mixed standards were prepared in various concentrations of mandelate over the range 1-50 mM and 1% methanol at pH 4.0, and the recovery results are plotted in Fig. 7.5. In 1.0 mM mandelate, both thorium(IV) and uranyl recoveries were less than 50%. The recoveries rose as the mandelate concentration increased. In 30 mM mandelate or more, both thorium(IV) and uranyl recoveries reached 100%. According to the theoretical calculation, in 1 mM mandelic acid at pH 4.0 most of the uranyl exists as free metal cation (75%), the neutral uranyl *bis*(mandelate) complex is only 0.72% of the total, whilst the neutral Th(IV) *tetra*(mandelate) complex is 3.2% of the total, so they cannot be quantitatively bound to the hydrophobic surface of the C_{18} column under these conditions. In concentrated mandelate solution, more high ligand number complexes formed. These hydrophobic

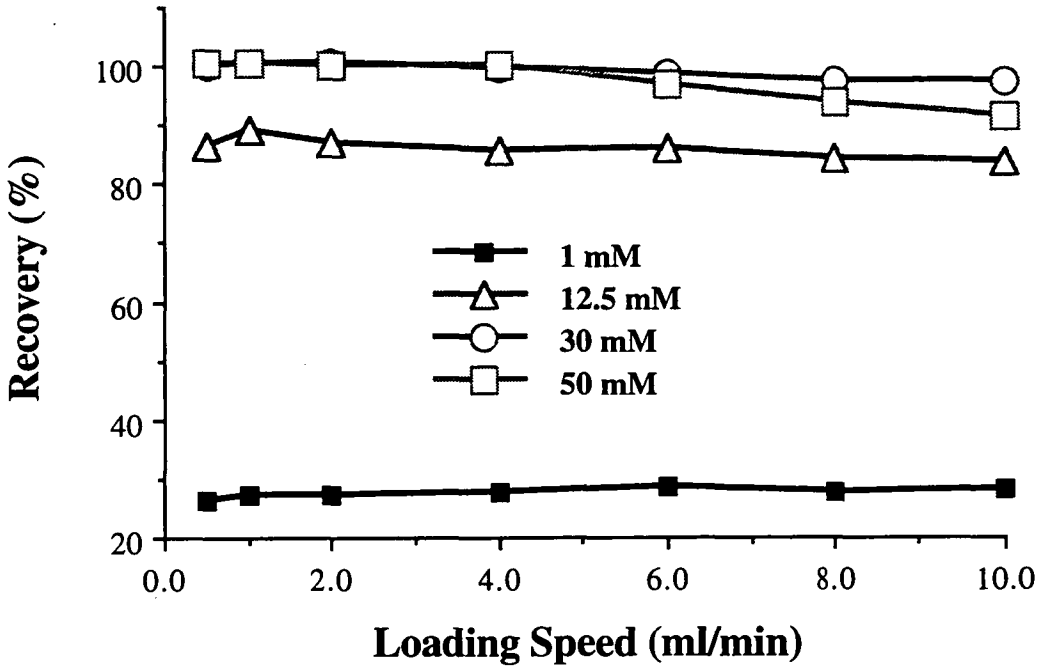

(a)

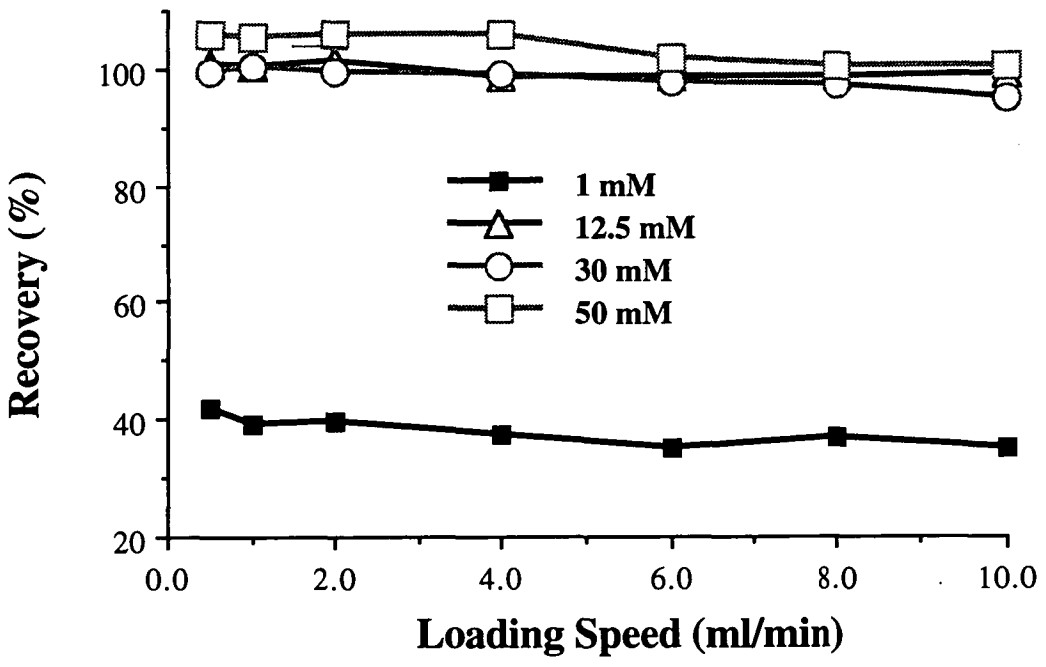

(b)

Fig. 7.5 Effect of mandelate concentration in sample on thorium(IV) and uranyl preconcentration. A C_{18} guard column was used as the concentrator. The sample was prepared in various mandelate concentrations and 1% methanol (pH 4.0). A total of 10 ml of 100 ppb (a) thorium(IV) and (b) uranyl was concentrated.

species are retained on the C_{18} column, leading to high recoveries. These results are in accordance with those observed in the breakthrough volume study.

7.3.4 EFFECT OF SAMPLE LOADING PARAMETERS

7.3.4.1 Effect of Sample Loading Speed

In the ligand effect studies above, the sample loading speed was also investigated. For each of the sample solutions, loading onto the concentrator was conducted at various flow-rates in the range 0.5-10 ml/min, whilst keeping constant of the total loading volume (10 ml). Here, the total volume was far smaller than the breakthrough volume (refer to the concentrator section above), so the concentrator capacity would not be an important factor in the interpretation of the results. With each of the sample solutions, duplicate estimates of the recoveries at various flow-rates were obtained by comparing peak areas from direct injection and the preconcentration runs. The results were also plotted in Fig. 7.4 for different ligands, and Fig. 7.5 for various mandelate concentrations in the sample. These figures show that the sample loading speed had little effect on of thorium(IV) and uranyl preconcentration up to 5.0 ml/min. A slight decrease was observed when the flow-rate was higher than 6.0 ml/min.

7.3.4.2 Calibration Using Loading Volume

A calibration plot using the sample loading volume over the range of 5-120 ml was prepared. A 100 ppb Th(IV) and uranyl mixed standards prepared in 30 mM mandelate and 1% methanol (pH 4.0) were loaded at a flow-rate of 4.0 ml/min. The thorium(IV) and uranyl peak areas were increased as the loading volume rose. A linear relationship between the peak area and loading volume was observed up to 50 ml, as shown in Fig. 7.6 a. However, when more than 50 ml was loaded, both thorium(IV) and uranyl showed decreased response, especially for the uranyl. Similar results were also observed even when the Th(IV) and uranyl concentration were

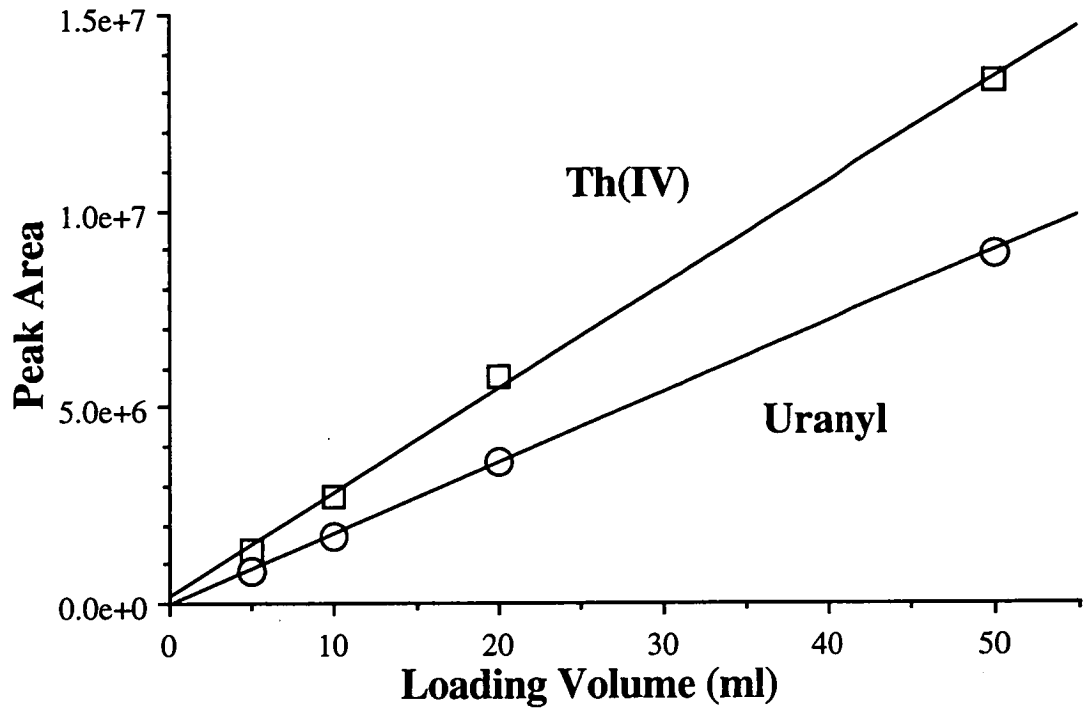

(a)

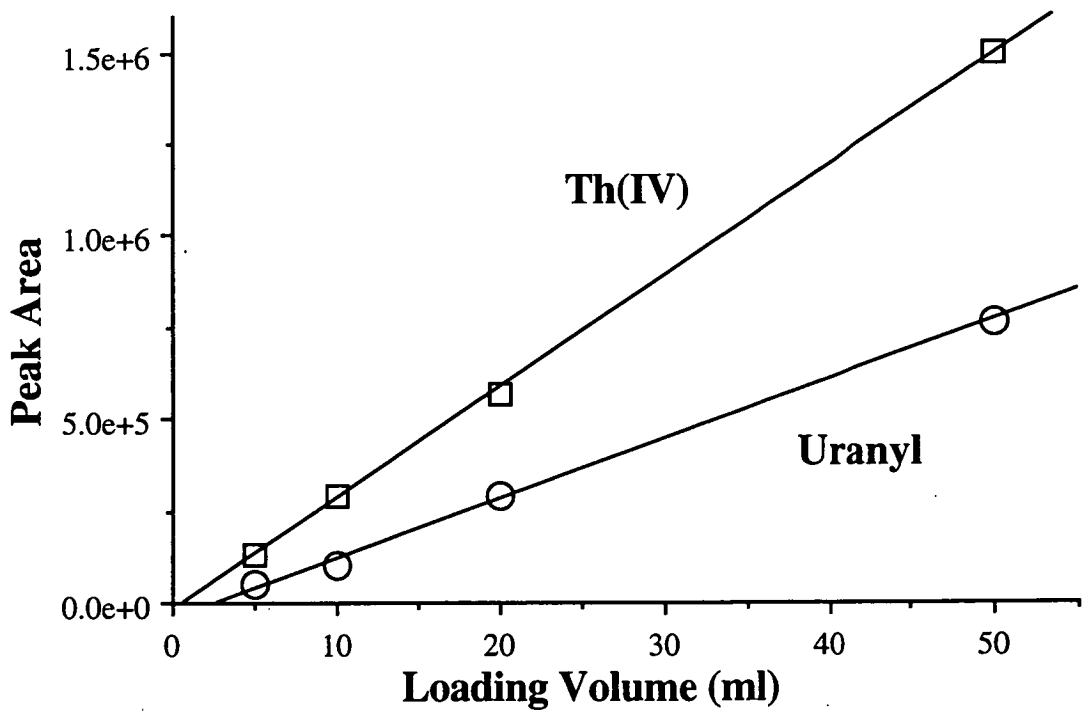

(b)

Fig. 7.6 Calibration using preconcentration volume. (a) 100 ppb and (b) 10 ppb thorium(IV) and uranyl standards prepared in 30 mM mandelate (1% methanol, pH 4.0) and loaded at 5.0 ml/min. Other conditions were the same as in Fig. 7.4.

reduced to 10 ppb at the same ligand concentration (Fig. 7.6b).

Compared to uranyl, the thorium(IV) mandelate complex was strongly retained on the C_{18} Guard-Pak column, so its linear range could be extended up to 100 ml for the 10 ppb sample. These results were in accordance with those observed in the previous breakthrough volume study. When the surface of the stationary phase was fully covered or equilibrated with the complexes, further loading of the sample will cause self-elution. The results above suggested that the critical volume for the C_{18} Guard-Pak column was about 50 ml under these conditions.

7.3.4.3 Calibration Using Sample Concentration

Having determined the highest speed and the total volume which could be loaded on the C_{18} Guard-Pak column concentrator, the effect of sample concentration of thorium(IV) and uranyl was studied. Various concentrations of thorium(IV) and uranyl standards over the range of 1-200 ppb were prepared in 30 mM mandelate and 1% methanol, and adjusted to pH 4.0. A total of 50 ml of these sample solutions was loaded on the C_{18} Guard-Pak column concentrator at a flow-rate of 4.0 ml/min. A linear relationship was observed for both thorium(IV) and uranyl between the peak area and the sample concentration over this range, as shown in Fig. 7.7.

7.3.5 INTERFERENCE EFFECTS

7.3.5.1 Anions in the Sample Solution

Fig. 7.8 shows the effects of common anions added to the sample solution on thorium(IV) and uranyl preconcentration. Various acids, such as nitric, perchloric, hydrochloric, sulphuric and acetic acids were individually added into a 10 ppb Th(IV) and uranyl standard solution (in concentrated mandelate), the solution was then adjusted to pH 4.0 with sodium hydroxide. The final sample solution contained 30 mM mandelate and 1% methanol in addition to the anion. It was observed that the

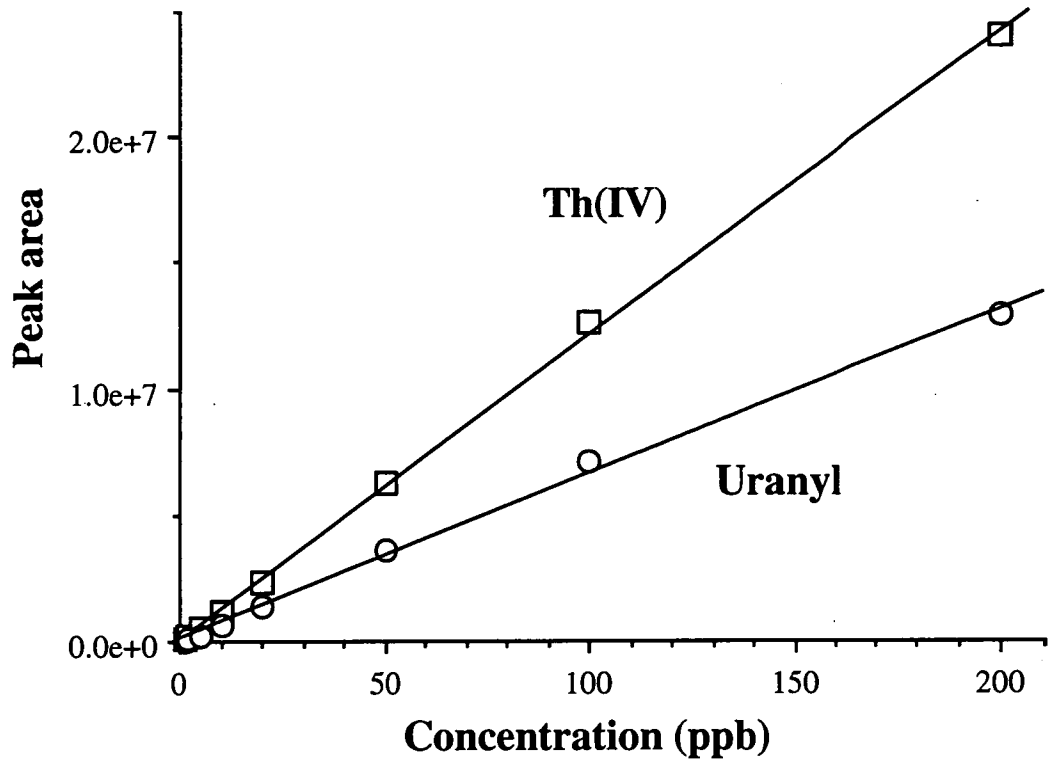

Fig. 7.7 Calibration using sample concentration. Various concentrations of thorium(IV) and uranyl were prepared in 30 mM mandelate (1% methanol pH 4.0). A total of 50 ml of these samples was loaded on a C_{18} guard column concentrator at 5.0 ml/min.

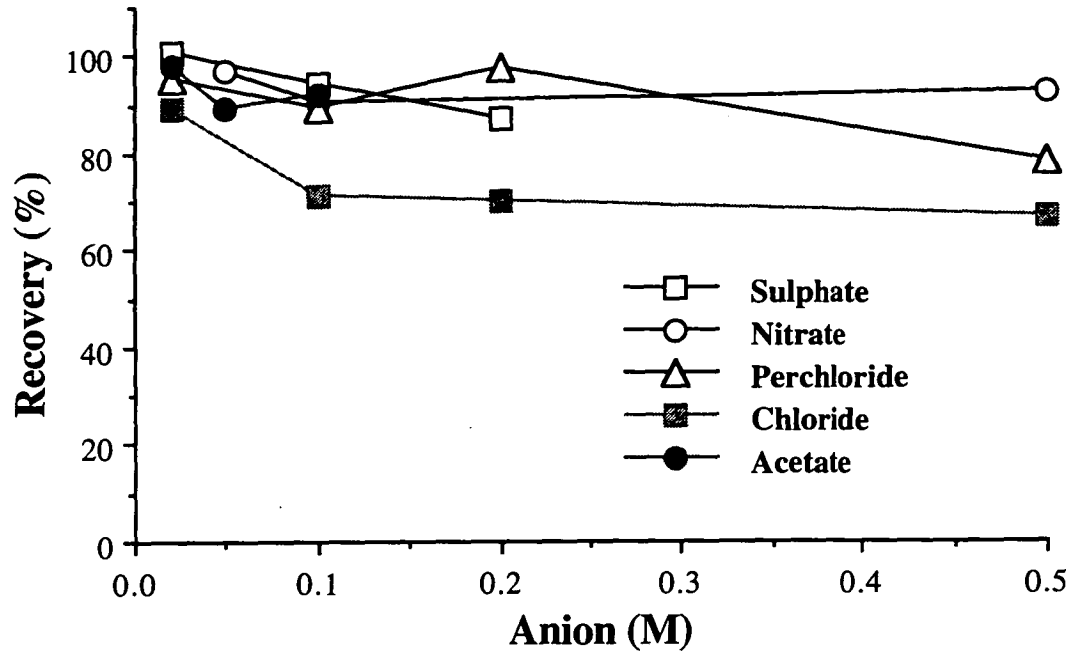

(a)

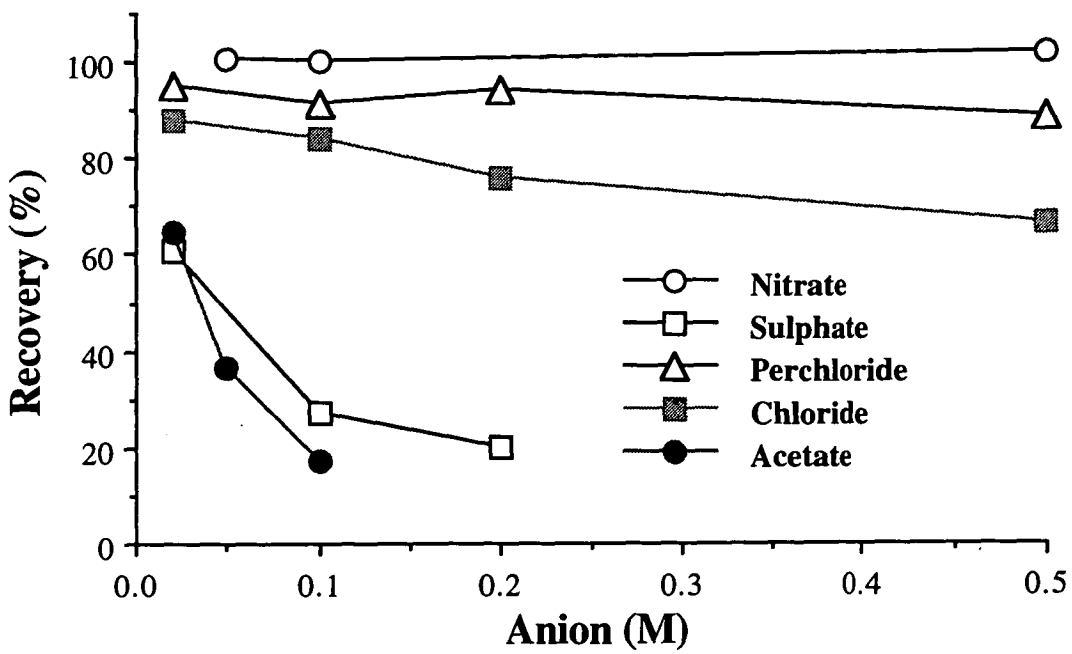

(b)

Fig. 7.8 Effect of anions on (a) thorium(IV) and (b) uranyl preconcentration. Various concentrations of anions were prepared in 10 ppb thorium(IV) and uranyl standards containing 30 mM mandelate and 1% methanol at pH 4.0. A 50 ml of these samples was concentrated.

anions exerted different effects. For the range of 0.025-0.50 M no significant effect on recovery was observed for NO_3^-, whilst a slight decrease of recovery in concentrated ClO_4^- or Cl^- was noted. Sulphate and acetate strongly affected uranium preconcentration, such that in 0.1 M SO_4^{2-} or CH_3COO^- about 70-80% uranyl was lost during the preconcentration procedure; however, there was no interference on thorium. It was likely that the sulphate and acetate ions were incorporated into the uranyl-mandelate coordination sphere, causing uranyl to be self-eluted during the sample loading step. This was also noted that in Chapter 6, where uranyl was eluted at the solvent front when the sample was prepared in sulphuric acid.

7.3.5.2 Cations in the Sample Solution

The effect of cations on thorium(IV) and uranyl preconcentration was examined at different concentration levels. All the tested cations were prepared from their metal nitrate salts, or from their oxides by dissolving in nitric acid. Various concentrations of these metals were added into the 10 ppb Th(IV) and uranyl standard solutions, which previously prepared in 30 mM mandelate and 1% methanol, and adjusted to pH 4.0. A total of 50 ml of these thorium(IV) and uranyl standard solutions were loaded on the C_{18} Guard-Pak column concentrator for preconcentration.

The thorium(IV) and uranyl preconcentration results showed that the cation interferences varied. No significant interference was observed for Na(I), Mn(II), Co(II), Ni(II) and Zn(II), even when they were present in the sample solution at an excess 2500 times over the Th(IV) and uranyl. In fact, the breakthrough volume of the C_{18} concentrator was increased when these metals were present in the thorium(IV) and uranyl standards, perhaps due to a salting-out effect. When the ionic strength of the eluent is raised, this lowers the solubility of the hydrophobic complexes in the eluent. However, when lanthanides and some transition metals, such as Fe(III) and Cu(II), were added to the sample, they also formed complexes with mandelate and

were trapped on the C_{18} concentrator. In the final analysis step, these complexes were eluted as a matrix peak which overlapped the thorium(IV) peak, especially when the interferences were present at higher concentrations than thorium(IV). Fig. 7.9 shows some of the chromatograms obtained with interfering metals in the sample.

7.3.6 PRECISION OF PRECONCENTRATION

The precision of total preconcentration performance was determined at different sample concentration levels. Thorium(IV) and uranyl standards (5, 20 and 100 ppb) were prepared in 30 mM mandelate (and 1% methanol, adjusted to pH 4.0) separately. Repeated loading of this sample on the C_{18} Guard-Pak column concentrator was performed and the precision of the preconcentration performance is listed in Table 7.3.

7.4 DETERMINATION OF TRACE LEVELS OF THORIUM(IV) AND URANYL SPIKED INTO SEA WATER

7.4.1 INITIAL EXPERIMENTS

Having established the on-line preconcentration conditions, the technique was applied to the determination of trace levels of thorium(IV) and uranyl spiked into sea water. The sea water matrix was selected for two reasons. First, it is not uncommon for nuclear waste samples (which were unavailable for this project) to be in the form of brine solutions. Second, sea water represents a challenging matrix in the terms of interferences and an analytical method developed for this matrix is likely to be applicable to a range of less complex sample types. A 10 ppb of thorium(IV) and uranyl were prepared in sea water, to which had previously been added 30 mM mandelate and 1% methanol (pH 4.0). A total of 50 ml of this sample was loaded onto the C_{18} Guard-Pak column concentrator and analysed with the C_{18} reversed-phase column (300 x 3.9 mm I.D.) using 0.1 M HIBA in 10% methanol at pH 4.0 as the mobile phase. The initial chromatogram showed that thorium(IV) and uranyl could be concentrated under these conditions (see Fig. 7.10). However, a large matrix peak

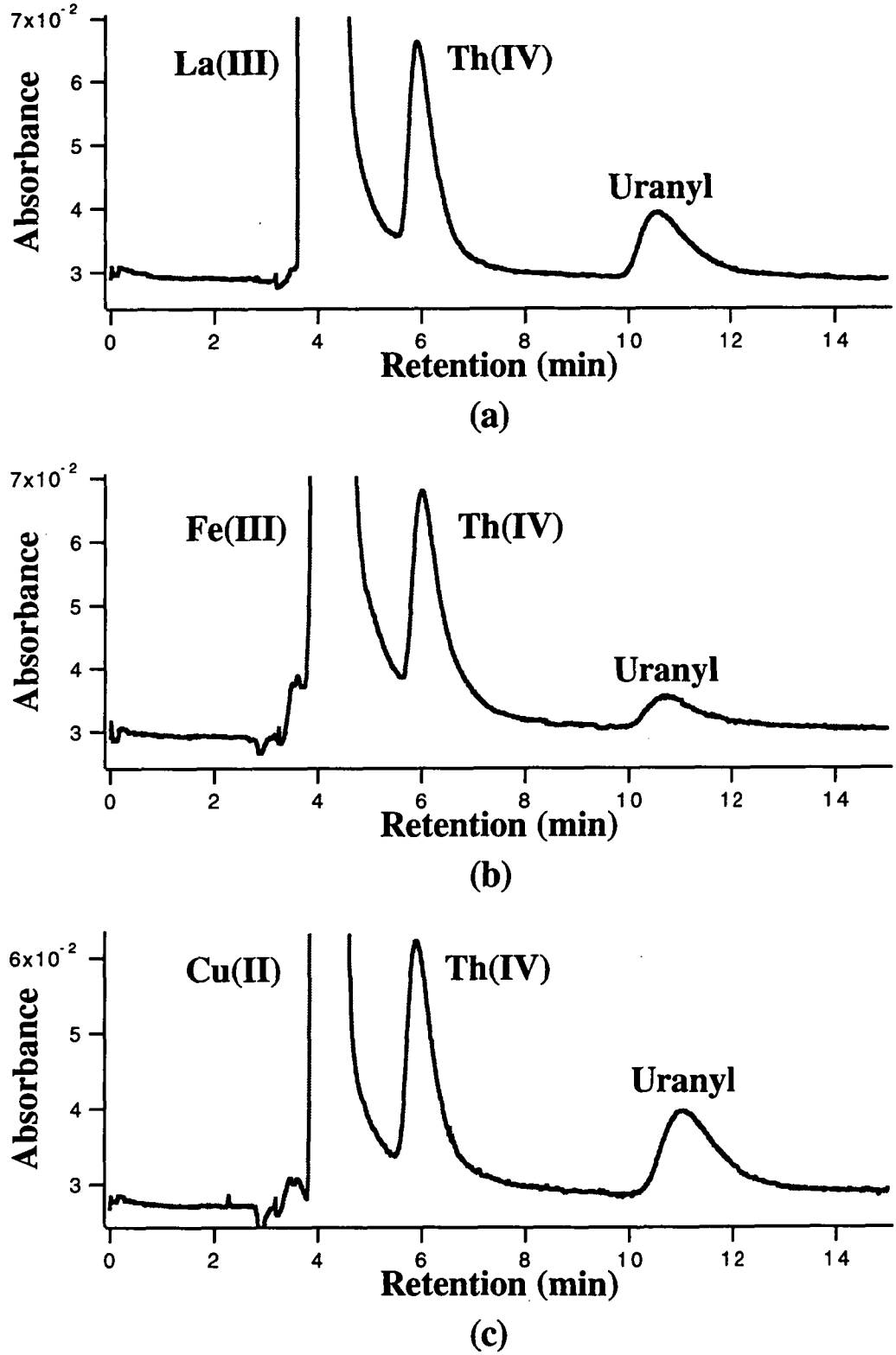

Fig. 7.9 Preconcentration chromatograms of thorium(IV) and uranyl obtained by preparing the sample in various metal cation solutions. 10 ppb Th(VI) and uranyl prepared in 30 mM mandelate and 10 ppm (a) La(III), (b) Fe(III) and (c) Cu(II). Preconcentration volume: 10.0 ml. Other conditions as in Fig. 7.4.

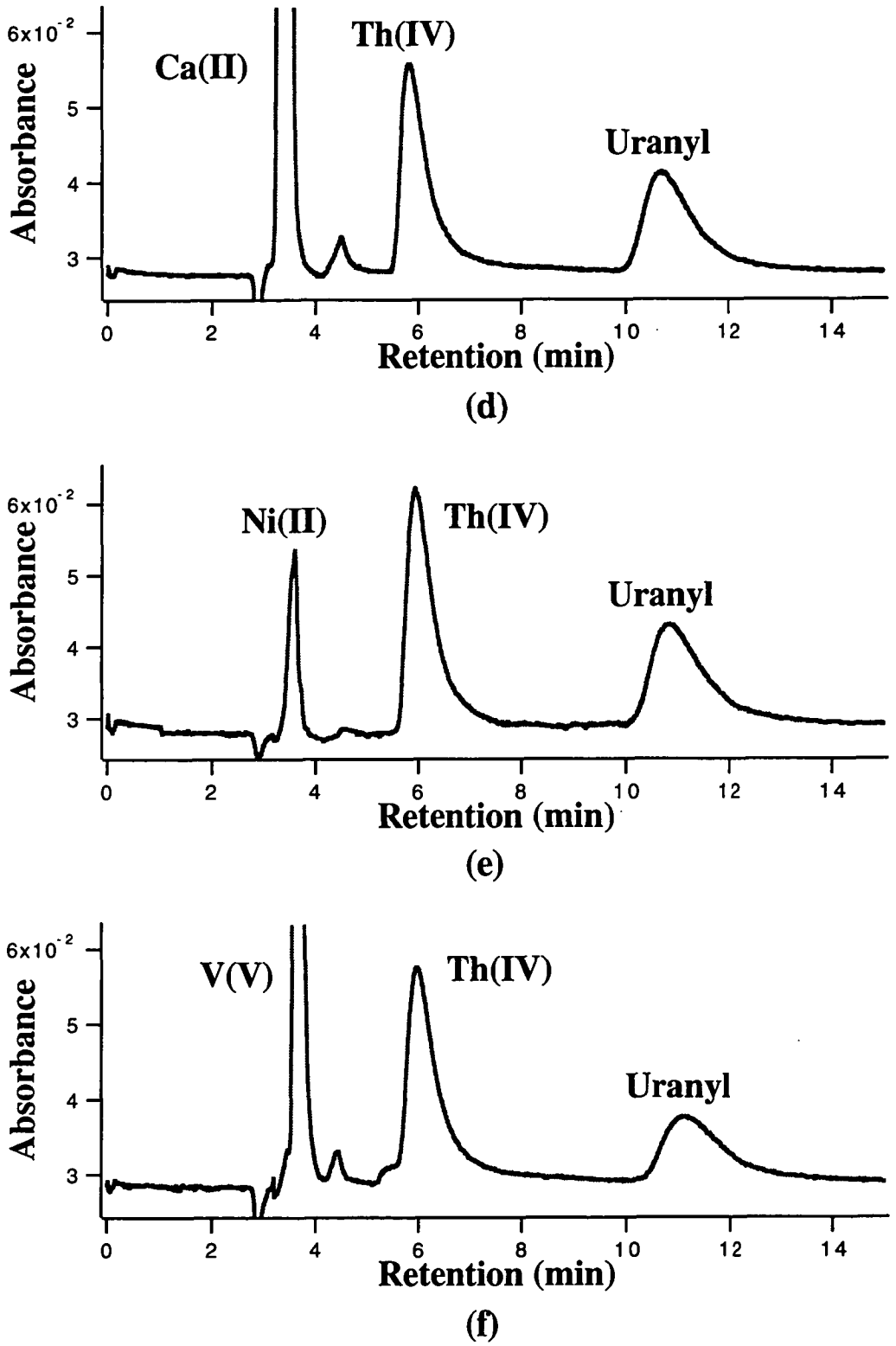

Fig. 7.9 (continued) Preconcentration chromatograms of thorium(IV) and uranyl obtained by preparing the sample in various metal cation solutions. 10 ppb Th(VI) and uranyl prepared in 30 mM mandelate and 10 ppm (d) Ca(II), (e) Ni(II) and (f) V(V). Preconcentration volume: 10.0 ml. Other conditions as in Fig. 7.4.

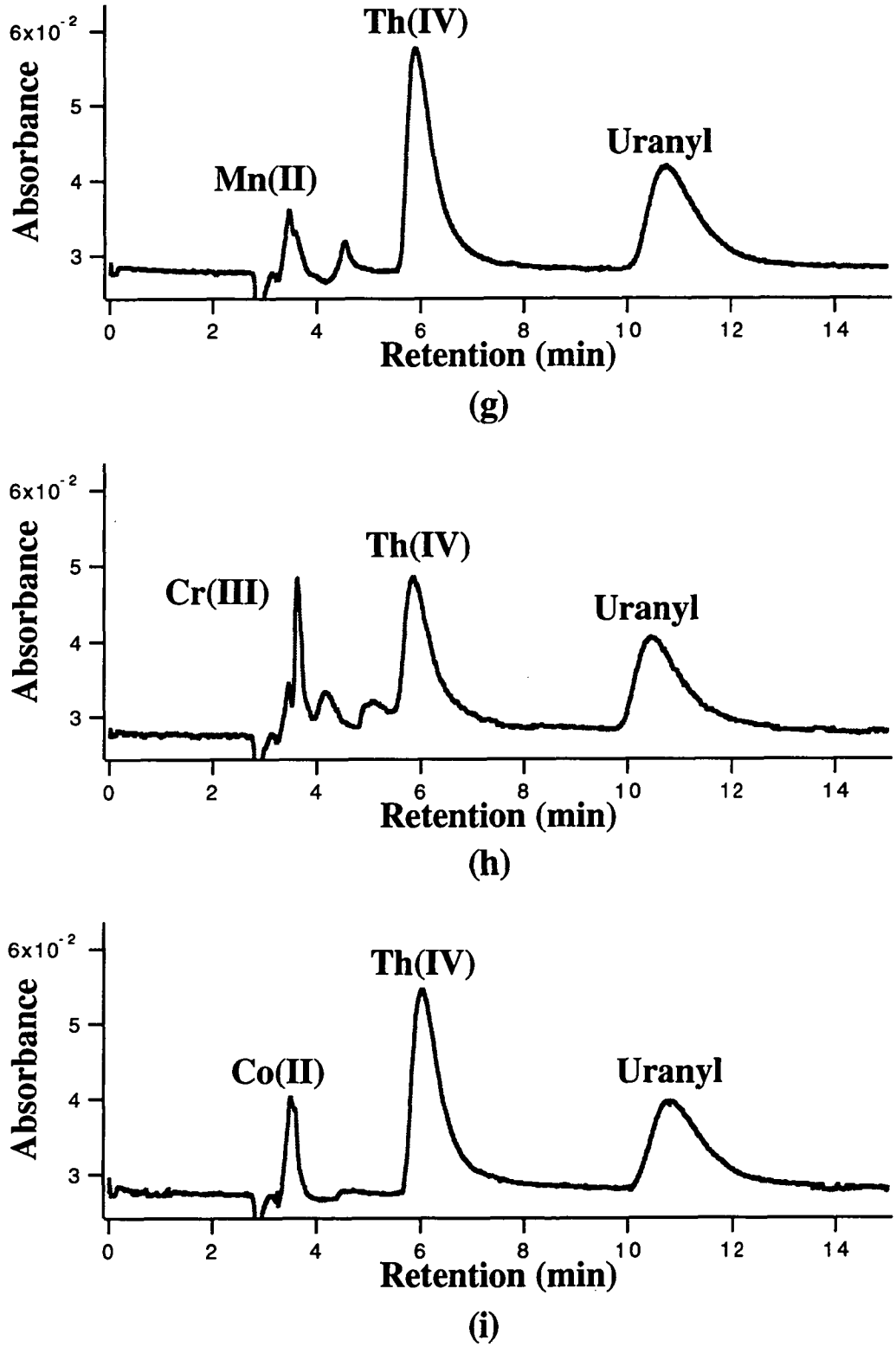

Fig. 7.9 (continued) Preconcentration chromatograms of thorium(IV) and uranyl obtained by preparing the sample in various metal cation solutions. 10 ppb Th(VI) and uranyl prepared in 30 mM mandelate and 10 ppm (g) Mn(II), (h) Cr(II) and (i) Co(II). Preconcentration volume: 10.0 ml. Other conditions as in Fig. 7.4.

Table 7.3 PRECISION OF THORIUM AND URANIUM PRECONCENTRATION

Various concentrations of thorium(IV) and uranyl standards were prepared in 30 mM mandelic acid (1% methanol, pH 4.0). A total of 50 ml of these samples was loaded onto a C_{18} guard column concentrator. A C_{18} μ-Bondapak column (300 x 3.9 mm I.D.) was used as the analytical column with 100 mM HIBA and 10% methanol at pH 4.0 as the analytical mobile phase. Detection at 658 nm after post-column reaction with Arsenazo III.

	5 ppb Th	5 ppb U	20 ppb Th	20 ppb U	100 ppb Th	100 ppb U
Peak area	1120463	588770	2438080	1221352	11009598	6472679
	1119022	587577	2281227	1218086	11117485	6454631
	1141758	589612	2206266	1199085	11210205	6472050
	1108737	589354	2190346	1201723	11298141	6474804
	1131315	587548	2254723	1228356	11328760	6462422
	1122282	582513	2252193	1204320	11412079	6464982
Average	1123930	587562	2270473	1212154	11229378	6466928
RSD (%)	1.01	0.45	3.91	0.99	1.32	0.12

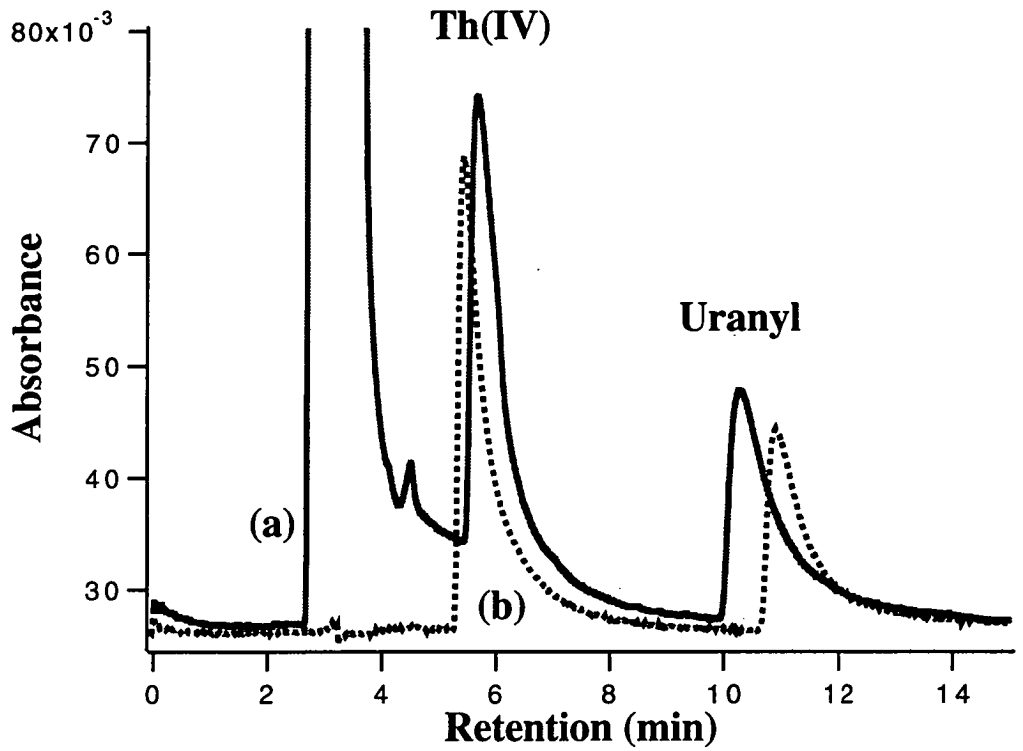

Fig. 7.10 Chromatogram of thorium(IV) and uranyl spiked into sea water. (a) 50 mlof 10 ppb Th(IV) and uranyl in sea water (42 mM mandelate and 1% methanol at pH 4.0) was concentrated on a μ-Bondapak C_{18} concentrator, (b) 50 μl of 10 ppm Th(IV) and uranyl were directly injected for comparision. Other conditions were as in Fig. 7.4.

was also observed which partially overlapped the front part of the thorium(IV) peak. The matrix peak was produced by other metals in the sea water which also formed hydrophobic complexes with mandelate and were trapped on the concentrator. This indicated that the on-line preconcentration system needed some modification for the sea water analysis, despite the evidence of high recovery and linear calibration for standards.

7.4.2 MODIFICATION OF THE ELUENT COMPOSITION

Sea water in the open ocean contains about 3.5% total salts, mainly as sodium chloride. The major ionic components of the sea water are listed in Table 7.4. Despite the transition metals being present at low concentrations, a significant amount of these species were accumulated on the concentrator when 10 ml of sea water was concentrated. Here, the preconcentration performance has two functions. The first is concentrating the analytes, and the second is to remove interfering components in the sample; that is, to eliminate the matrix. In previous chapters it was noted that thorium(IV) and uranyl were retained on the C_{18} reversed-phase column based on a hydrophobic absorption mechanism, when HIBA, glycolic or mandelic acid were used as the mobile phase. This retention mechanism is different to that of lanthanides and transition metals. In order to remove the interfering metals from the concentrated thorium(IV) and uranyl, the analytical mobile phase was slightly modified by increasing the HIBA concentration and decreasing the organic modifier (methanol), without changing the hardware of the chromatographic system. Fig. 7.11 shows the chromatograms obtained using various analytical eluents. When the HIBA concentration increased from 0.1 M to 0.2 M and other conditions were kept constant, the thorium(IV) peak moved toward the solvent peak which made the separation even worse. The retention of thorium(IV) could be delayed by decreasing the methanol percentage in the mobile phase. However, only a small improvement was observed for the separation of thorium(IV) from the matrix peak.

Table. 7.4 THE MAJOR IONS OF SEA WATER IN THE OPEN OCEAN [6]

Measured at the total salinity of 3.5%.

Ion	**g/kg**
Cl^-	**19.35**
SO_4^{2-}	2.712
Br^-	0.0673
F^-	0.0013
B	0.0045
Na^+	**10.77**
Mg^{2+}	1.290
Ca^{2+}	0.4121
K^+	0.399
Sr^{2+}	0.0079

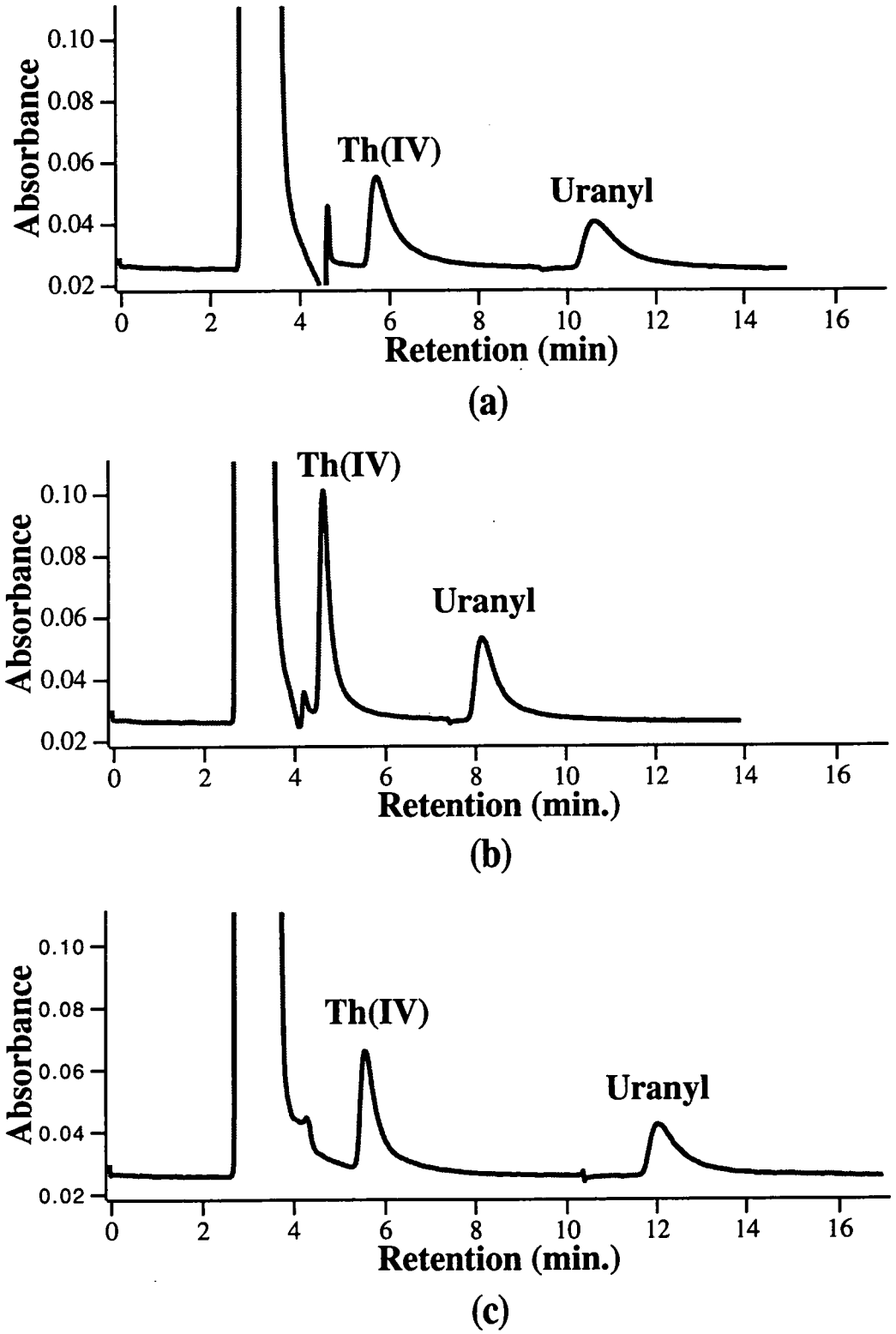

Fig. 7.11 Thorium(IV) and uranyl preconcentration chromatograms obtained using various eluents: (a) 100 mM HIBA and 10% methanol, (b) 200 mM HIBA and 10% methanol, (c) 200 mM HIBA and 5% methanol, all buffered at pH 4.0. Other conditions were as in Fig. 7.4, except the sample: 50 ppb Th(IV) and uranyl spiked into sea water (containing 42 mM mandelate and 1% methanol pH 4.0).

7.4.3 SELECTION OF A SUITABLE CONCENTRATOR COLUMN

It appeared that the most likely solution for the separation problems was to change to a longer concentrator column, instead of the Guard-Pak insert. Various sizes of C_{18} reversed-phase column concentrators were examined. It was expected that thorium(IV) and uranyl would be quantitatively bound on a longer concentrator, and would be separated from the interfering metals during the sample loading step due to differences in hydrophobicity. The use of a longer concentrator would cause an increase in the total time for the final analysis step. However, this drawback could be compensated by reducing the analytical column length (e. g. by using a Nova-Pak C_{18}, 150 x 3.9 mm I.D.).

Fig. 7.12 shows the chromatograms obtained by using different size concentrator columns. With a 5 cm or 10 cm concentrator, thorium(IV) could be completely separated from the matrix peak, and both thorium(IV) and uranyl recoveries reached 100%. However, the use of 10 cm concentrator was not practical because the back pressure was too high when it was switched into the analytical eluent flow-path, and the total chromatographic time was too long. All the sea water analyses were therefore carried out with the Nova-Pak C_{18} (50 x 3.9 mm I.D.) column as concentrator. For comparison, a Nova-Pak C_{18} guard column was also examined under the same conditions, the chromatogram (Fig. 7.12a) showed that the separation of thorium(IV) and the matrix peak was even worse than that using the μ-Bondapak guard column.

In order to determine the maximum loading volume for the 5 cm concentrator column, its breakthrough volume was evaluated under different conditions. 200 ppb uranyl standard solution containing 42 mM mandelate and 1% methanol (pH 4.0) was continually pumped through the column, and monitored at the outlet of the column after post-column reaction with Arsenazo III. Fig. 7.13a shows the breakthrough curve of the Nova-Pak C_{18} column concentrator (50 x 3.9 mm I.D.), which indicates

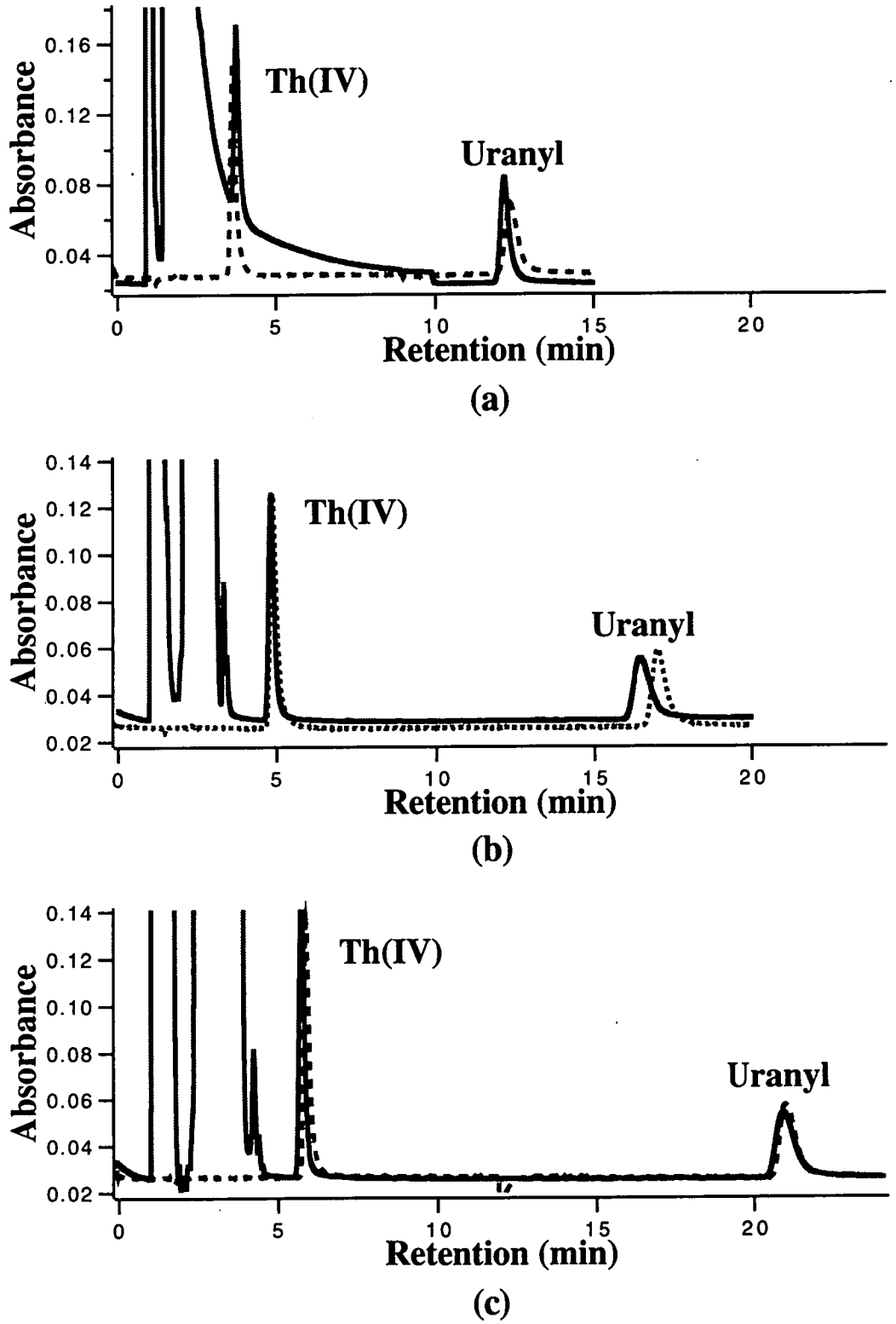

Fig. 7.12 Chromatograms of thorium(IV) and uranyl obtained by using various concentrators: (a) Guard-Pak, (b) 50 x 3.9 mm and (c) 100 x 3.9 mm. A Nova-Pak C_{18} column (100 x 3.9 mm I.D.) was used as the analytical column with 0.20 M HIBA in 5% methanol at pH 4.0 as the eluent. Other conditions as in Fig. 7.10. The dashed lines show direct injections of Th(IV) and uranyl standards.

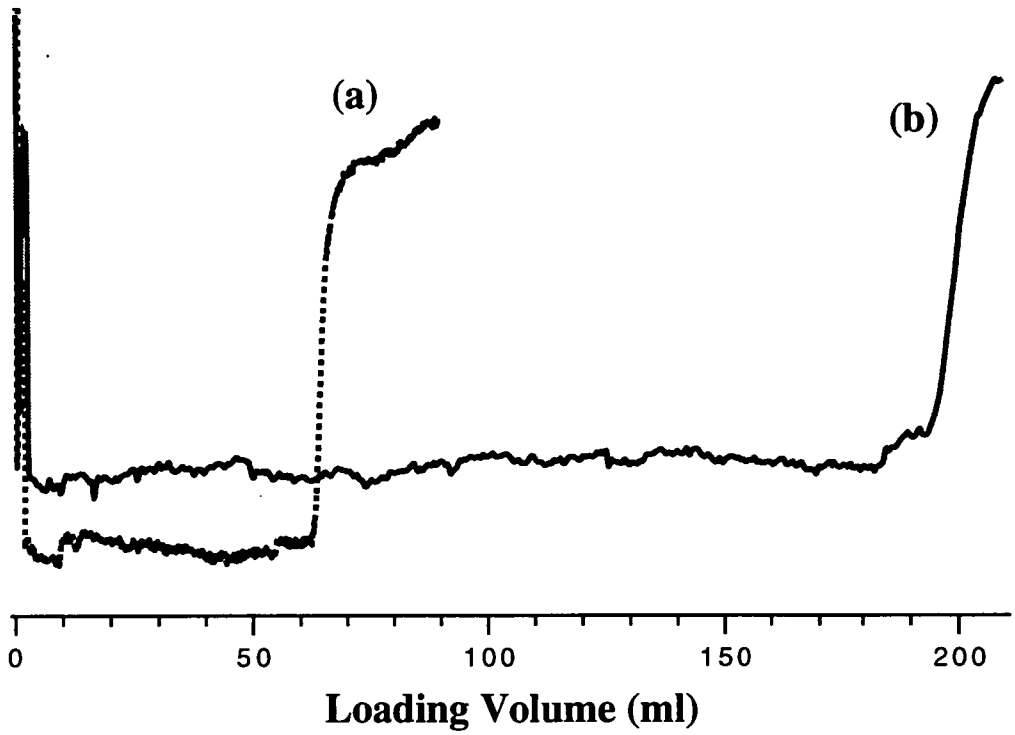

Fig. 7.13 Effect of salt in sample on breakthorough volume. (a) 200 ppb uranyl prepared in 42 mM mandelate and 1% methanol, adjusted to pH 4.0, (b) 3% NaCl was added into above sample solution. Sample was pumped through a Nova-Pak C_{18} column (50 x 3.9 mmI.D.) and detected at the outlet after PCR with Arsenazo III.

that the maximum loading volume is only 60 ml under these conditions. However, the breakthrough volume was greatly increased when 3.5% NaCl was added into the uranyl standard solution, as shown in Fig. 7.13b. This behaviour may again be explained by the salting-out effect.

7.4.4 CALIBRATION PLOTS

Having optimised the on-line preconcentration system for sea water analysis, calibration curves were prepared using the 5 cm concentrator. The enriched thorium(IV) and uranyl were back-flushed onto the analytical column with an eluent which comprised 0.2 M HIBA and 5% methanol at pH 4.0. A Nova-Pak C_{18} (150 x 3.9 mm I.D.) was used as the analytical column. Fig. 7.14a shows the relationship between the peak area and the sample loading volume, using a sample containing 50 ppb thorium(IV) and uranyl standards spiked into sea water which had been previously prepared in 42 mM mandelate and 1% methanol and adjusted to pH 4.0. The sample was loaded at 4.0 ml/min. The linear range extended up to 90 ml for uranyl, and even more for thorium(IV). Fig. 7.14b shows the calibration curves which were obtained by loading 90 ml of various concentrations of thorium(IV) and uranyl spiked into sea water.

7.4.5 SINGLE COLUMN PRECONCENTRATION AND ANALYSIS

As a final possibility the use of a single column for both preconcentration and analysis was examined. The configuration of the new chromatographic system was similar to that of the preconcentration system used above, except without the analytical column. In the last analysis step, the analytical mobile phase was pumped through the column in the opposite direction to that of the sample introduced. Fig. 7.15 shows the single column preconcentration chromatograms obtained by using various size columns. The advantage of using a short column was that the analysis time was minimised. With a 5 cm column, the total analysis could be completed within 4 min. However, the thorium(IV) peak could not be separated completely from the matrix

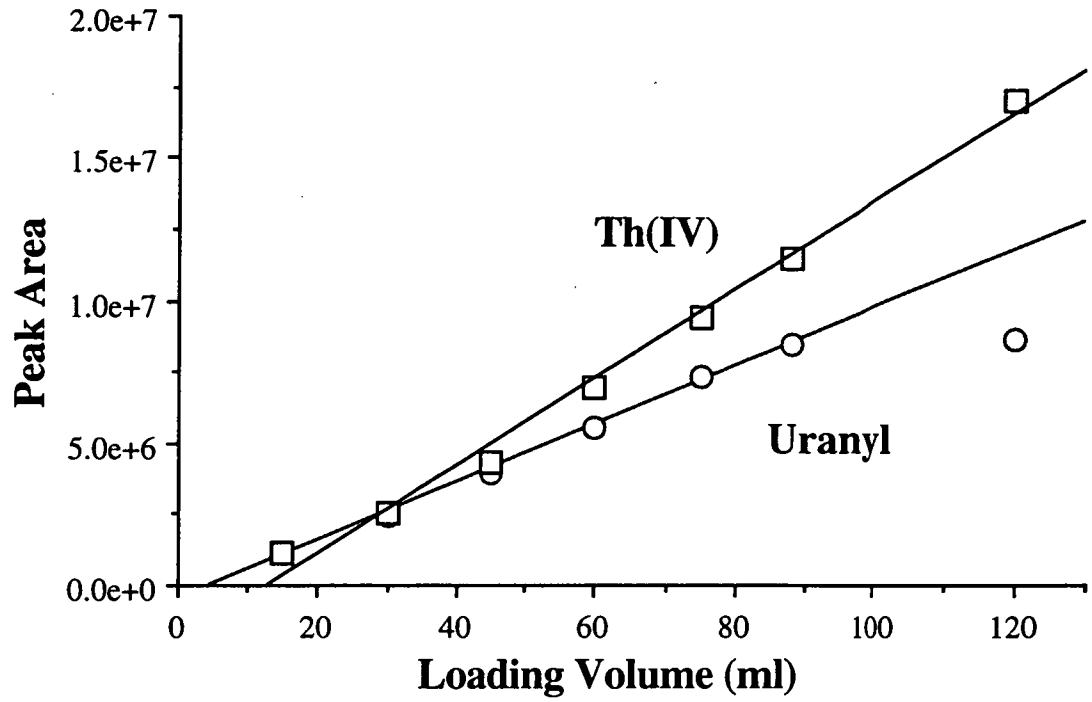

(a)

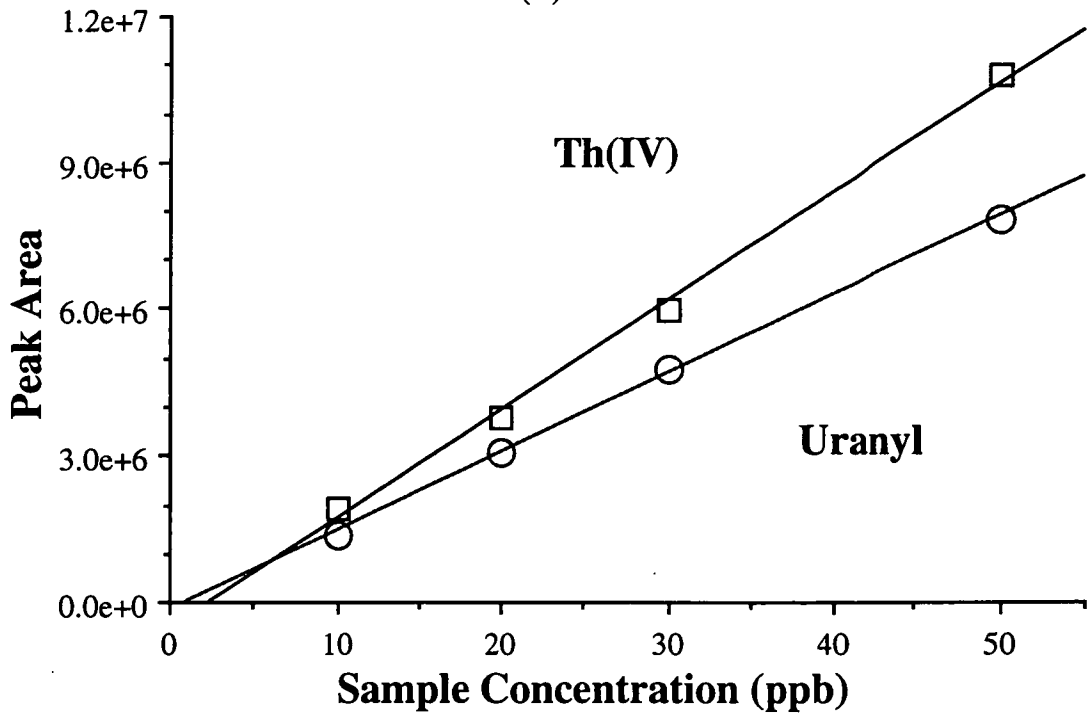

(b)

Fig. 7.14 Calibration plots of thorium(IV) and uranyl spiked into sea water. (a) various volumes of 50 ppb Th(IV) and uranyl, and (b) 90 ml of various concentrations of Th(IV) and uranyl were concentrated. Other conditions as in Fig. 7.10, except the concentrator: Nova-Pak cartridge (50 x 3.9 mm I.D.).

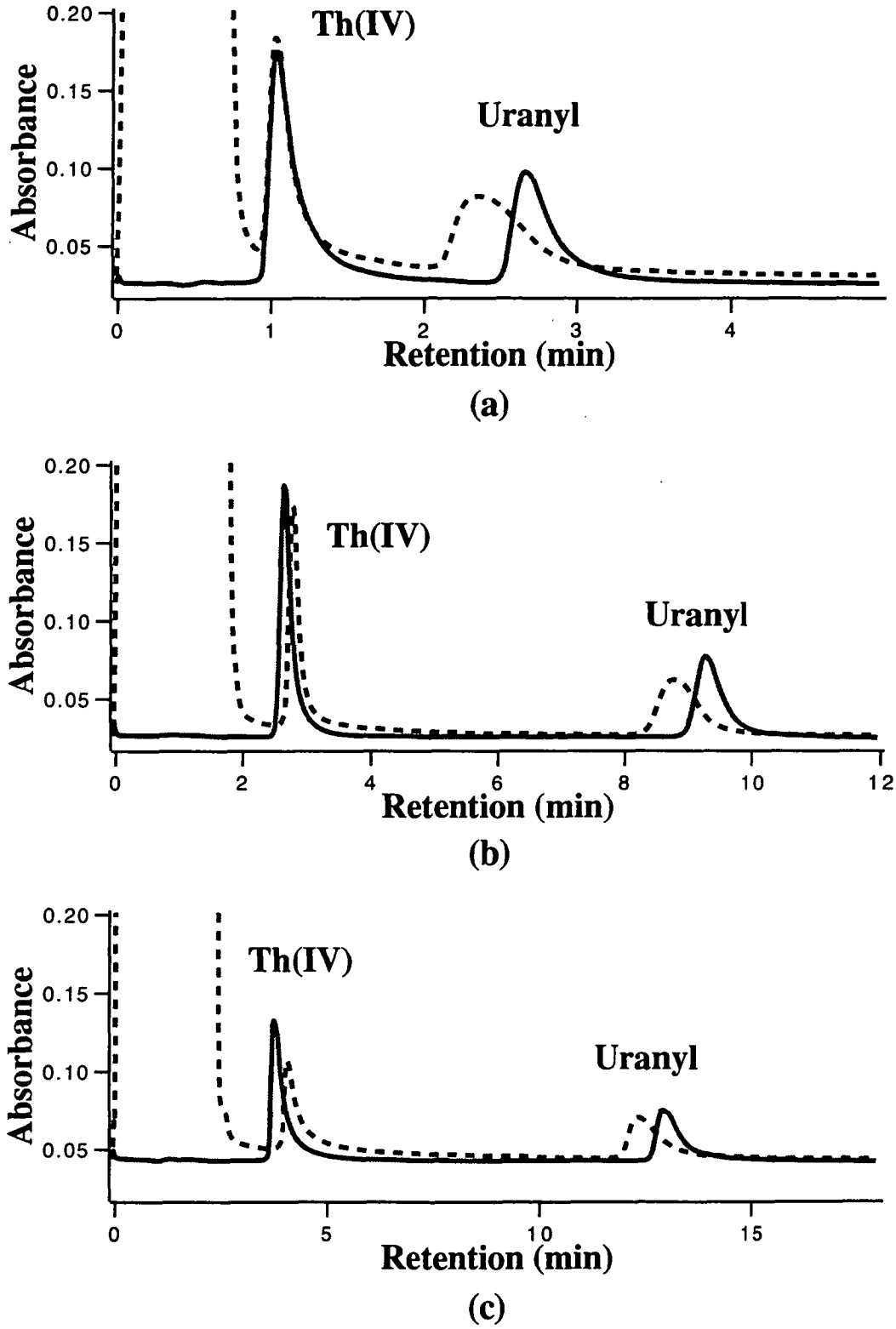

Fig. 7.15 Single column preconcentration chromatograms. A Nova-Pak column (a) 50 x 3.9 mm, (b) 100 x 3.9 mm and (c) 150 x 3.9 mm were used with 0.2 M HIBA in 5% methanol at pH 4.0 as the eluent. 15 ml of 50 ppb Th(IV) and uranyl spiked into sea water was loaded (dashed line), and 75 µl of10 ppm Th(IV) and uranyl was injected directly for comparision (solid line) under the same conditions.

peak under these conditions (Fig. 7.15 a). This problem can be solved by using a longer column, as shown in Fig 7.15b and Fig. 7.15c. These figures show that the 10 cm column is the best one of the three, which gives good separation and a relatively short analysis time.

An equivalent amount of thorium(IV) and uranyl was injected directly in each case for comparison. Uranyl gave about 100% recovery with each column, but the thorium(IV) recovery was only 80% at best. It is possible that some of the thorium(IV) was flushed to waste during the sample loading step because the column had been conditioned with the HIBA eluent. In a further experiment, an equilibration step with mandelate was added prior to each preconcentration, which improved the thorium(IV) recovery to 87%. Fig. 7.16 shows the calibration curves obtained by preconcentration of thorium(IV) and uranyl on a single column.

7.5 CONCLUSIONS

In the preconcentration of thorium and uranium using a short C_{18} column as the concentrator, the most important factor is the nature and concentration of the ligand used to prepare the sample solution. The more hydrophobic mandelic acid gave better results than HIBA or glycolic acid, and in 30 mM (or more) mandelic acid both thorium and uranium recoveries reached 100%. The sample loading speed onto the concentrator gave no effect on the recovery within the range of 0.5-5.0 ml/min. There was a linear relationship between the peak area and loading volume up to 50 ml, but the bound solutes self-eluted when the loading volume was excess 50 ml. Most of the common mineral acids had no effect on thorium(IV) and uranyl enrichment, except sulphuric and acetic acids for their incorporation into the uranyl-mandelate coordination sphere causing the complex to self-elute. The cation interferences were varied. No significant interference was observed for Na(I), Mn(II), Co(II), Ni(II) and Zn(II), even when these cations were present in the sample solution at an excess 2500 times over the thorium(IV) and uranyl. It was found that the breakthrough volume of

the C_{18} column concentrator was increased when these metals were present in the thorium(IV) and uranyl standard solutions due to salting-out effects. However, lanthanides, and some transition metals, such as Fe(II) and Cu(II), also formed complexes with mandelate and were trapped on the C_{18} concentrator. In the final analysis step, these complexes were eluted as a matrix peak which overlapped the thorium(IV) peak. This on-line preconcentration technique has been successfully applied to the analysis of trace levels of thorium(IV) and uranyl in a saline sample (spiked sea water) after little modification to the system.

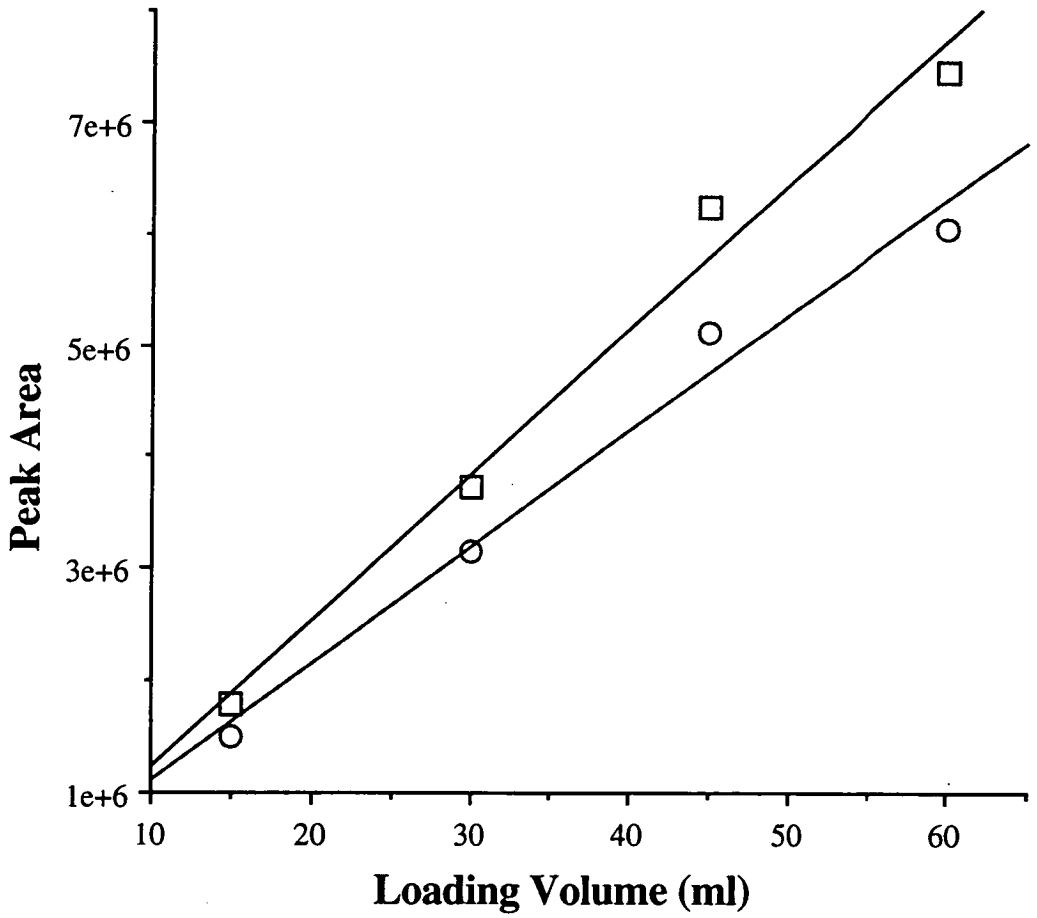

Fig. 7.16 Calibration plot obtained using a single column as the concentrator and the analytical column. A Nova-Pak column (100 x 3.9 mm I.D.) was used with 0.2 M HIBA in 5% methanol at pH 4.0 as the eluent. 50 ppb thorium(IV) and uranyl spiked into sea water containing 42 mM mandelate and 1% methanol (pH 4.0) was used as the sample. Detection at 658 nm after PCR with Arsenazo III.

7.6 REFERENCES

1 A. L. Heckenberg and P. R. Haddad, *J. Chromatogr.*, 299 (1984) 95.

2 P. R. Haddad and A. L. Heckenberg, *J. Chromatogr.*, 318 (1985) 279.

3 P. R. Haddad and P. E. Jackson, *J. Chromatogr.*, 367 (1986) 301.

4 Waters, *Model 590 Programmable Solvent Delivery Module Operator's Manual*, September, 1988.

5 R. M. Cassidy and S. Elchuk, *Inter. J. Environ. Anal. Chem.*, 10 (1981) 287.

6 J. P. Riley and G. Skirrow, *Chemical Oceanography*, Academic Press, London, 1975, 2nd. ed. Vol. 1 p.366.

Chapter 8

Chromatographic Determination of Thorium and Uranium in Digested Phosphate Rock Solution Combined with On-line Matrix Elimination

8.1 INTRODUCTION

Thorium and uranium are present at trace level concentrations in phosphate rocks. Digestion of these rocks with concentrated nitric acid in fertiliser production processes leads to dissolve these metals into the resulting nitrophosphate solution. The nitrophosphate solution also contains about 3% calcium, 5 g/l lanthanides and 10 g/l of transition metals, in addition to concentrated phosphoric and nitric acids [1]. A typical solution is listed in Table 8.1. It is difficult to directly analyse the trace levels of thorium and uranium in this complicated matrix, for both the cations and anions in the sample interfere with the analysis.

Recently, Al-Shawi and Dahl [2] used a cation-exchange chromatographic method to determine thorium(IV) and uranyl in phosphate rock samples. A strong acid cation-exchange column was used with a strongly acidic solution as the eluent, such as 2 M hydrochloric or 2 M nitric acids, followed by detection at 658 nm after post-column reaction (PCR) with Arsenazo III. The nitrophosphate solution was directly analysed without pretreatment. The resulting chromatograms showed that thorium(IV) and uranyl could be separated from the sample matrix. However, a large peak due to the lanthanides was also observed, located adjacent to the thorium(IV) peak. This created difficulties in the quantification of the trace levels of thorium(IV).

An alternative approach could be the measurement of thorium and uranium after their on-line separation from the complete matrix [3]. Such on-line matrix

Table 8.1 COMPOSITION OF A TYPICAL NITROPHOSPHATE LEACH SOLUTION [1]

Ions	Concentration (%)	Concentration (mg/l)
P	9.27-10.17	
F	0.28-0.31	
N (NO_3^-)	6.13-6.34	
N (NH_4^+)	5.03-5.06	
Ca	3.09-3.26	
Na		1600-2105
Mg		430-510
Sr		5100-5133
Ba		130-151
Al		3400-3668
Ti		580-840
V		79-83
Mn		190-191
Fe		2000-2175
Cu		37-38
Zn		26-28
Y		212-240
La		1200-1238
Ce		2350-2375
Pr		220-230
Nd		950-965
Sm		121-125
Eu		35-36
Gd		90-94
Tb		9-11
Dy		45-60
Ho		8-9
Er		16-24
Tm		2-2.3
Yb		8-11
Lu		1-1.3
Th		11-12
U		4-4.2

elimination is usually carried out with a pre-column. In Chapter 6, a manual procedure was described for pretreating a digested mineral sand sample with a cation-exchange cartridge (Ion-exclusion Guard-Pak Insert). The final chromatograms showed that the trace levels of thorium(IV) and uranyl could be completely separated from the matrix and the results were in good agreement with those obtained by using X-ray fluorescence (XRF) or inductively coupled plasma mass spectrometry (ICP-MS) methods. This manual procedure was then developed as an on-line preconcentration technique using a short C_{18} column as the concentrator (Chapter 7). When prepared in 42 mM mandelate solution, A 50 ml of 10 ppb thorium(IV) and uranyl sample solution could be concentrated without loss. The on-line preconcentration can also be regard as matrix elimination technique, for 3.5% salts in the sea water was removed during the procedure.

In this chapter, an on-line matrix elimination procedure was employed to pretreat the nitrophosphate solution sample, prior to thorium and uranium analysis with a reversed-phase chromatographic method. Two nitrophosphate solutions, Kola Mother Liquor (KML) and BouCraa Mother Liquor (BML), were obtained from the processing line of a fertiliser factory. These samples were initially tried with direct injection and preconcentration techniques. Finally, an on-line matrix elimination system was constructed, which could be automatically performed by a programmable pump.

8.2 EXPERIMENTAL

8.2.1 INSTRUMENTATION

The chromatographic system used in this chapter was rather more complicated than that employed in previous chapters. A Model 590 programmable pump was used to deliver the washing eluents as well as to control the on-line matrix elimination procedure. Two high-pressure valves and one low-pressure solvent selection valve were used to construct the on-line matrix elimination system, as shown in Fig. 8.1.

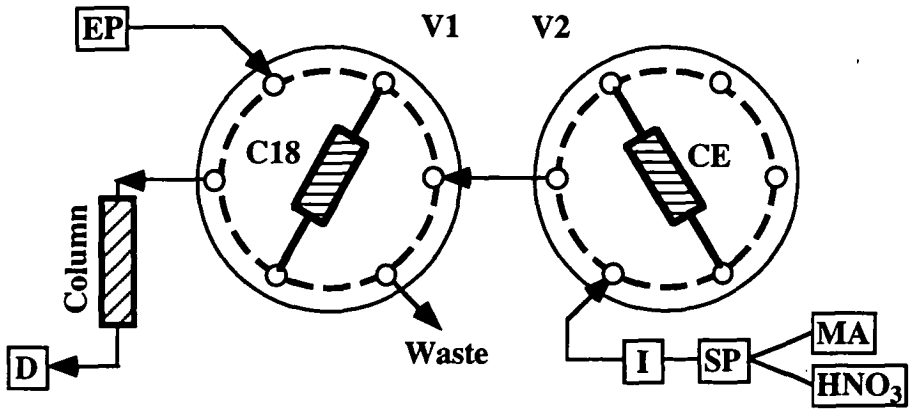

Fig. 8.1 Schematic diagram of the instrumentation used for on-line matrix elimination.

EP: analytical eluent pump; SP: sample washing pump;

CE: cation-exchange guard column; C18: short C_{18} column (50 x 3.9 mm);

I: Injector; D: UV detector; V1: valve1; V2: valve2;

MA: 0.4 M mandelate solution; HNO_3: 0.08 M nitric acid.

Other apparatus was the same as that described in Chapter 3, except the analytical column was replaced with a Waters Nova-Pak C_{18} column (150 x 3.9 mm I.D.). A cation-exchange (CE) guard cartridge (Waters Ion-Exclusion Guard-Pak Insert, sulphonic acid functionalised, 0.2 g of 5 mequiv./g resin) and a Waters short Nova-Pak C_{18} column (50 x 3.9 mm I.D.) were used for the matrix elimination. All the experiments were carried out at room temperature.

8.2.2 REAGENTS

The chromatographic eluent consisted of 200 mM HIBA and 5% methanol, adjusted to pH 4.0 with sodium hydroxide. A 0.08 M nitric acid (Ajax Chemicals, Sydney, N.S.W.) solution was used as the washing eluent for the cation-exchange pretreatment, and 0.4 M mandelic acid (Koch-light Laboratories Ltd, Colnbrook, Bucks, England) in 1% methanol adjusted to pH 4.0 was used for the C_{18} precolumn.

The thorium(IV) and uranyl standards, PCR solution and other chemicals were the same as described in Chapter 3.

8.2.3 PROCEDURE FOR ON-LINE MATRIX ELIMINATION

The final on-line matrix elimination procedure was performed in a sequence of eight steps, as illustrated in Fig. 8.2:

(1) Nitric acid flush. Since the sample pump was used to load sample as well as for delivery of the washing eluents, it was necessary to flush the pump itself and the interconnecting tubing prior to insertion of the precolumn into the flow-path or when changing the eluents. The sample pump and the tubing were initially flushed with the 0.08 M nitric acid solution, whilst the C_{18} precolumn and the analytical column were equilibrated with the chromatographic HIBA eluent (Fig. 8.2a).

(2) Cation-exchanger equilibration. The cation-exchange (CE) precolumn was inserted into the nitric acid eluent flow-path for equilibration by rotating valve 2.

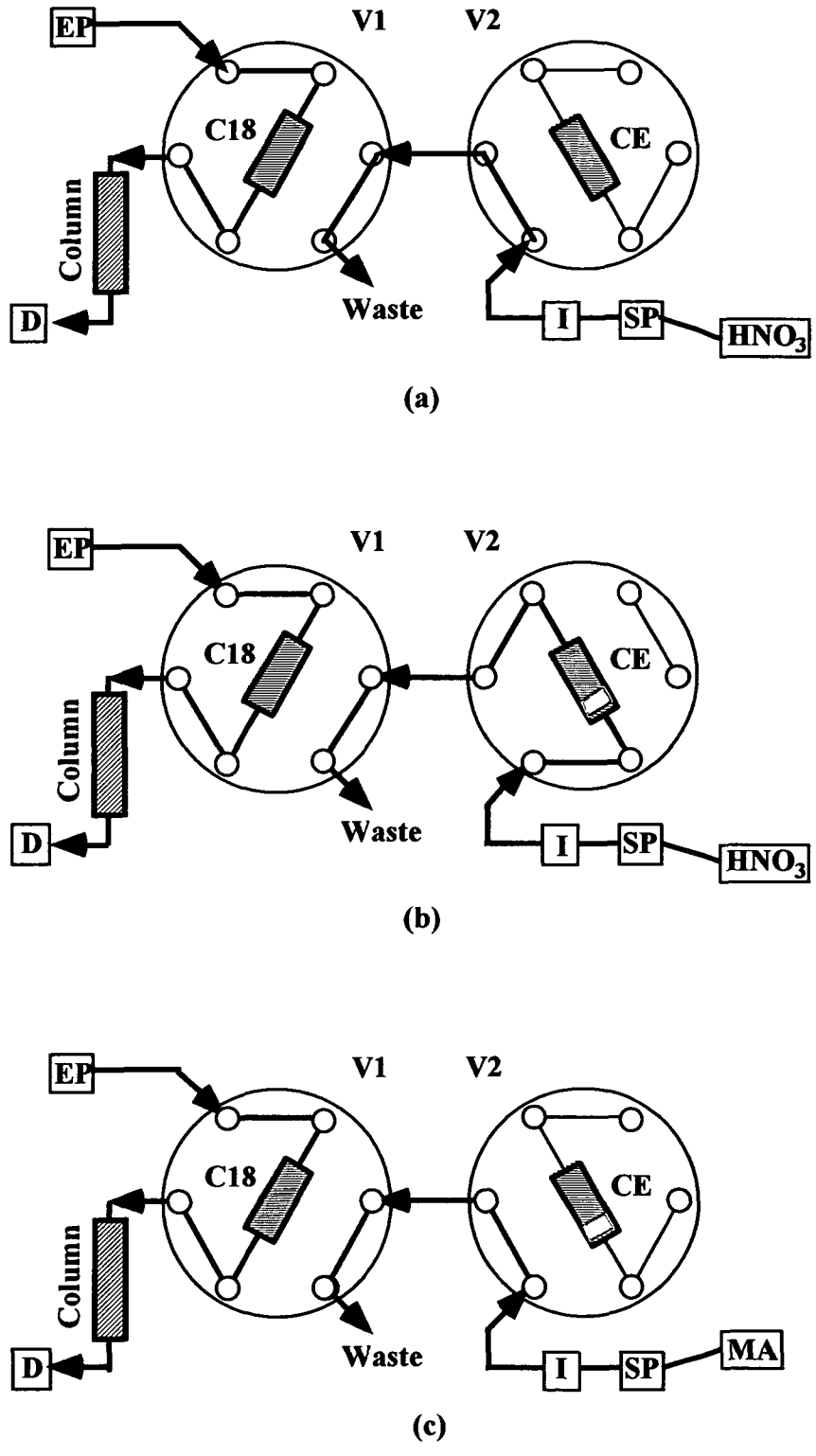

Fig. 8.2 Configuration diagram of the on-line matrix elimination procedure. (a) nitric acid flush, (b) nitric acid washing and (c) mandelate washing. Other notes refer to Fig. 8.1.

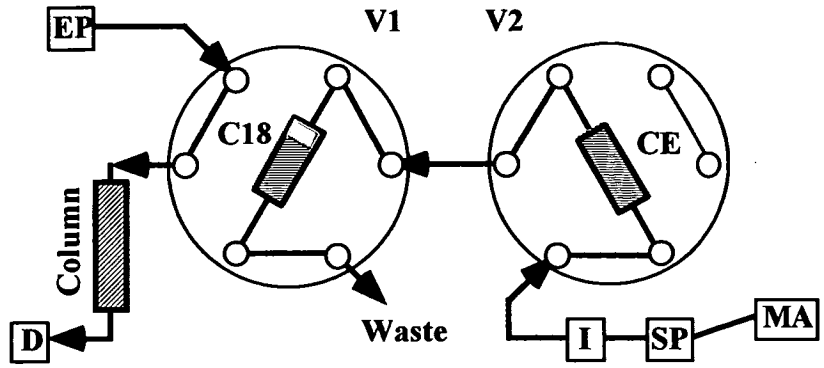

(d)

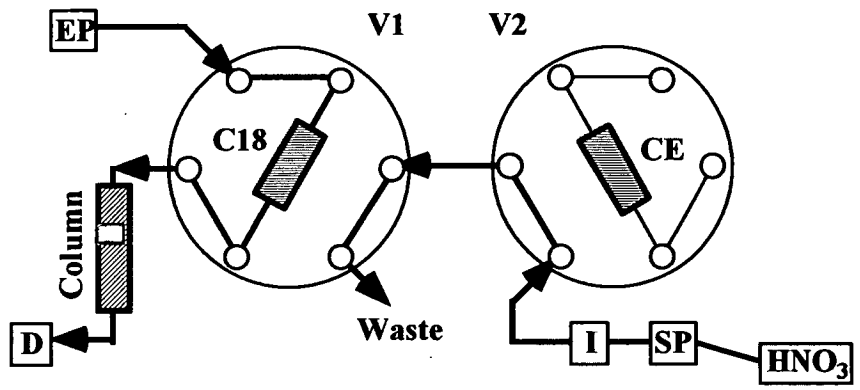

(e)

Fig. 8.2 (Continued) Configuration of the on-line matrix elimination procedure. (d) mandelate washing, (e) analysis. Other notes refer to Fig. 8.1.

(3) Loading sample. After diluting 10 times, an aliquot of nitrophosphate solution was directly loaded on the CE precolumn by means of an injector. The injector also triggered the chromatography data system and the M 590 pump program.

(4) Cation-exchange washing. The CE-precolumn was washed with the nitric acid eluent to remove phosphate and other anions, during which thorium(IV) and uranyl as well as other metal cations remained trapped on the precolumn. From step 2 to 4, the instrumental configuration remained no change, as shown in Fig. 8.2b.

(5) Mandelate flush. Valve 2 was rotated back, the sample pump and the interconnecting tubing were flushed with the mandelate eluent (Fig. 8.2c).

(6) C_{18} precolumn washing. In this step both the precolumns were switched into the sample flow-path to transfer the trapped cations from the CE cartridge onto the C_{18} precolumn with the mandelate eluent (Fig. 8.2d). Under these conditions thorium(IV) and uranyl were retained selectively on the C_{18} precolumn, whilst the lanthanides and transition metals were directly flushed to waste due to their weaker retention.

(7) Sample stripping. The C_{18} precolumn was switched into the chromatographic eluent flow-path and thorium(IV) and uranyl were transferred onto the analytical column (Fig. 8.2e).

(8) Analysis. Finally, thorium(IV) and uranyl were separated on the C_{18} reversed-phase column with the HIBA eluent and detected after post-column reaction with Arsenazo III.

8.3 RESULTS AND DISCUSSION

8.3.1 PRELIMINARY INVESTIGATION

At the commence of this study the nitrophosphate sample was tried by directly injecting 50 µl of original solution into the reversed-phase chromatographic system. A

large solvent peak was observed for both of the KML and BML samples, which swamped the entire chromatogram, as shown in Fig. 8.3. Thorium(IV) and uranyl were either flushed out at the solvent front or overshadowed by the matrix peak. After a 50 times dilution in the chromatographic mobile phase and injected again, the matrix peak became smaller, but still no for thorium(IV) or uranyl peak was observed. Thorium(IV) and uranyl concentrations in the diluted sample were too low to be detected. Clearly, the trace level thorium and uranium in the nitrophosphate solution could not be directly analysed without pretreatment.

In Chapter 7 an on-line preconcentration method was used for the determination of thorium(IV) and uranyl spiked into sea water using a short C_{18} reversed-phase column as the concentrator. The sea water sample was prepared in a mandelate solution and concentrated on. It was found that thorium(IV) and uranyl could be selectively trapped on the concentrator because they formed hydrophobic complexes with mandelate, whilst the transition metals were flushed directly to waste due to their weaker retention. The on-line preconcentration procedure offered two functions: enriching the analytes and removing the sample matrix. With this method a large volume (50 ml) of sample solution could be concentrated without loss of thorium(IV) and uranyl. The final chromatogram showed that the sea water matrix (3.5% salt) could be almost completely eliminated.

Followed the procedure described in Chapter 7, the nitrophosphate sample was further tried with the preconcentration technique using a short C_{18} column (50 x 3.9 mm I.D.) concentrator. It was expected that thorium(IV) and uranyl would be enriched on the C_{18} concentrator, whilst the matrix was removed from the sample during the preconcentration procedure. After a 50 times dilution in 42 mM mandelate and 1% methanol (pH 4.0), a 10 ml of the nitrophosphate solution was loaded, then inserted the C_{18} concentrator into the chromatographic eluent flow-path for analysis. Again, a large matrix peak was observed which swamped the entire chromatogram (Fig. 8.4a). It was clear that other metal cations in the nitrophosphate solution were

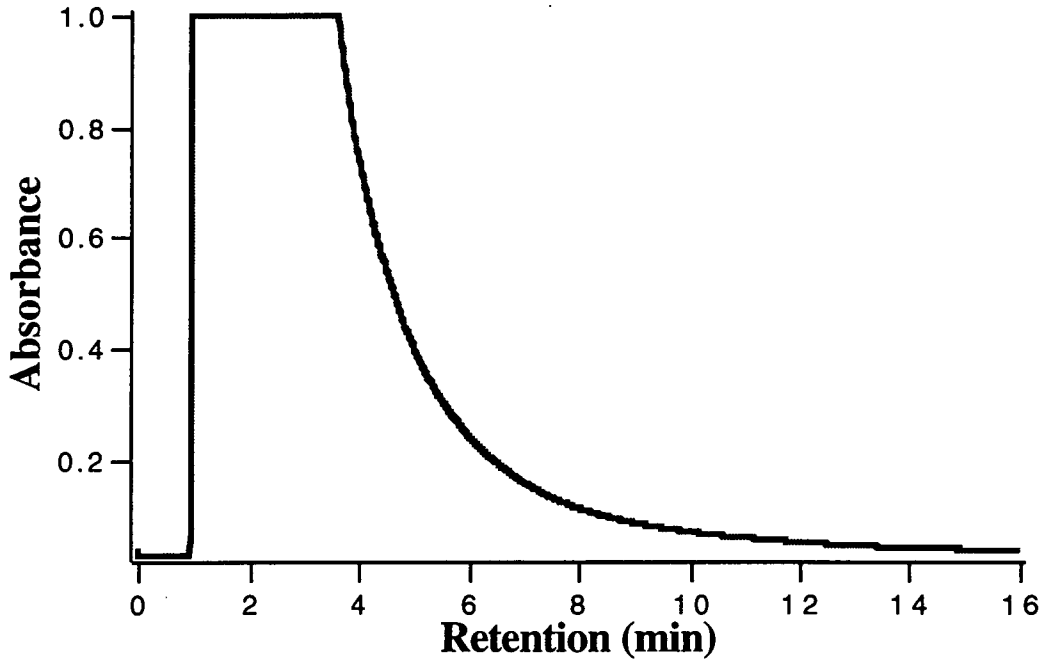

(a)

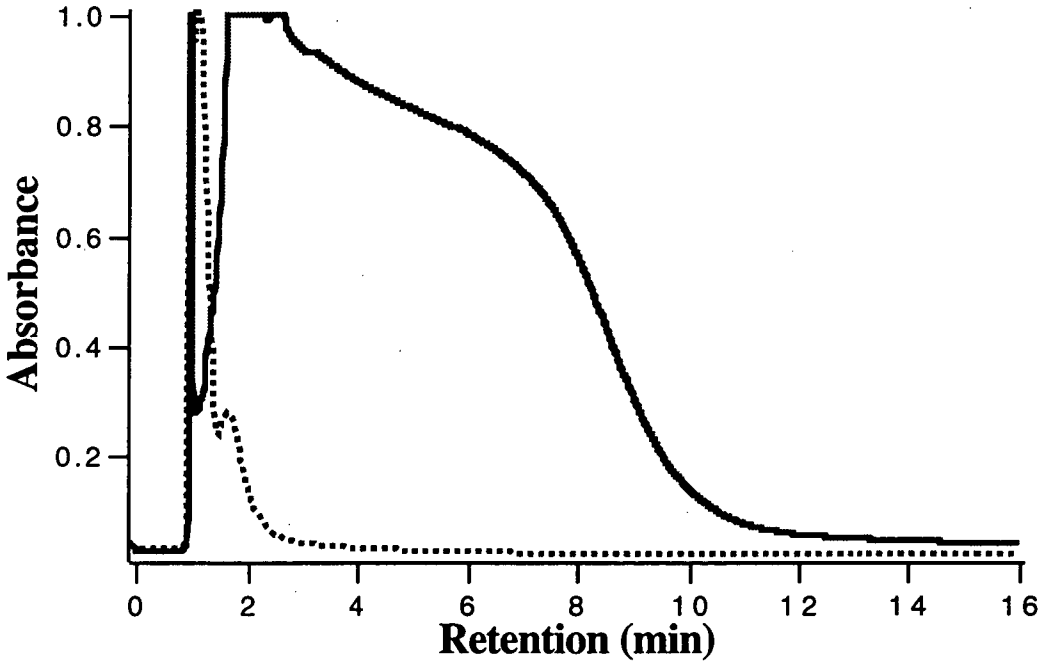

(b)

Fig. 8.3 Chromatograms of nitrophosphate obtained by direction injection. A C_{18} column (150 x 3.9 mm I.D.) was used with 0.2 M HIBA in 5% methanol (pH 4.0) as the eluent. A 50 µl of (a) KML and (b) BML (diluted 50 times for the dashed line) was injected, and detected at 658 nm after post-column reaction with Arsenazo III.

also trapped on the concentrator during the preconcentration procedure. Reducing the sample size to 2.0 ml caused the matrix peak to become smaller, but still neither a thorium(IV) nor uranyl peak appeared (Fig. 8.4b).

It has been reported [1] that the nitrophosphate solution contained an excess of about 500 times of the lanthanides and 1000 times of transition metals compared to thorium, in addition to 3% calcium. These metals, mainly the lanthanides, also formed complexes with mandelate and were retained on the reversed-phase concentrator column, resulting in the large matrix peak. These interfering metals must be therefore removed from the sample prior to thorium(IV) and uranyl chromatographic analyses.

8.3.2 LANTHANIDE SEPARATION

Elchuk *et al.*[4] have reported that thorium(IV), uranyl and lanthanides could be separated on a C_{18} reversed-phase column using a mandelate mobile phase. When mandelate alone was used in the eluent, the lanthanides were eluted before uranyl and thorium(IV). In Chapters 4 and 5 the retention behaviour of thorium(IV) and uranyl was examined on the C_{18} reversed-phase column using HIBA, glycolate or mandelate eluent. It was found that these complexes were retained on the C_{18} column through a hydrophobic absorption mechanism, which was different to that of the lanthanides. It can therefore be expected that thorium(IV) and uranyl should be separated from the lanthanides on a reversed-phase column with a mandelate eluent and an appropriate concentration of organic modifier.

Table 8.2 lists the retention parameters of lanthanum(III),thorium(IV) and uranyl on a short C_{18} cartridge (50 x 3.9 mm I D) with 0.4 M mandelate in various percentages of methanol at pH 4.0 as the eluents; 10 ppm La(III), 5 ppm Th(IV) and 5 ppm uranyl standards were injected individually. When the organic modifier decreased over the range 20%-1%, an increased retention was observed for all the three metals. However, thorium(IV) and uranyl retention rose much more rapidly,

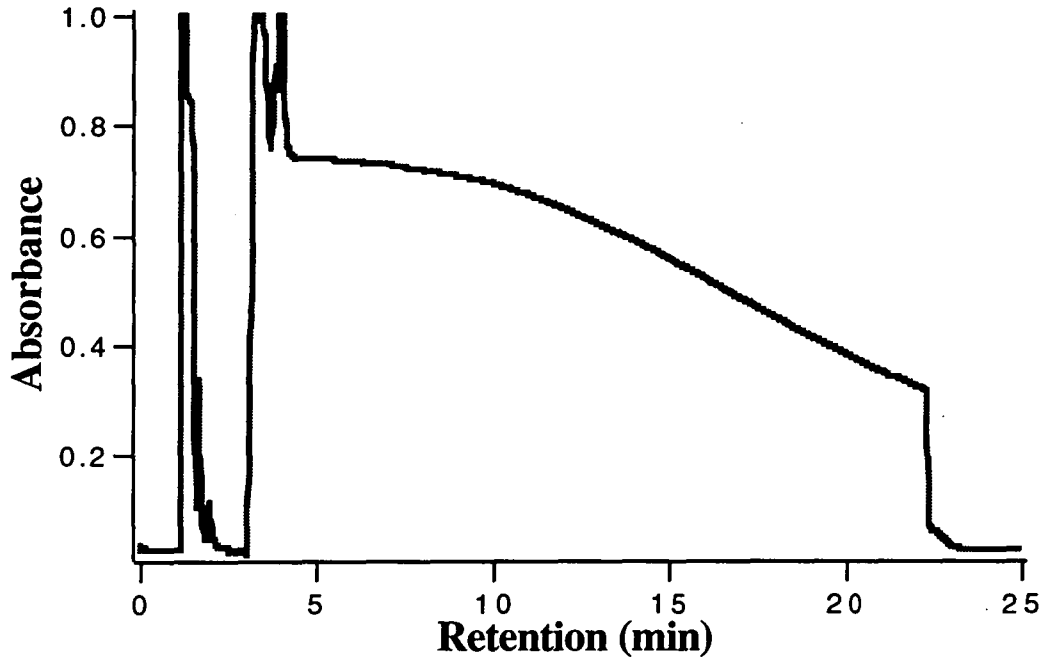

(a)

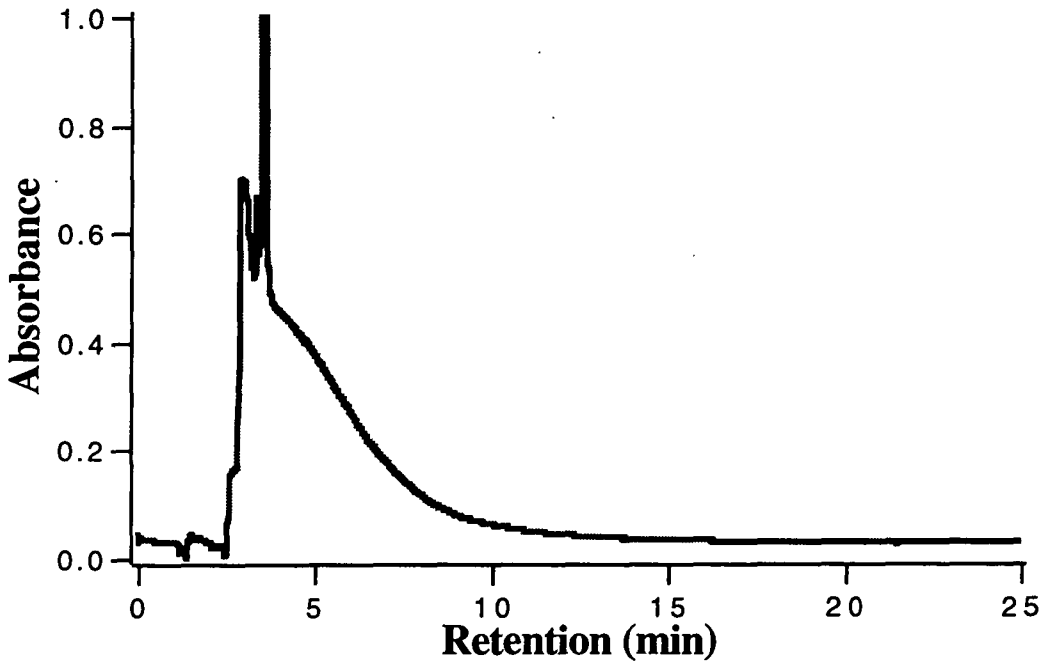

(b)

Fig. 8.4 Chromatograms of nitrophosphate obtained by preconcentration. After diluted 50 times in 42 mM mandelate, (a) 10 ml and (b) 2.0 ml of sample solution were loaded on a C18 concentrator column (50 x 3.9 mm I.D.) then transferred onto the analytical column for analysis. Other conditions were the same as in Fig. 8.3.

Table 8.2 RETENTION OF LANTHANUM(III), URANYL AND THORIUM(IV) ON A REVERSED-PHASE COLUMN USING A MANDELATE ELUENT

A Nova-Pak C_{18} column (50 x 3.9 mm I.D., Waters) was used with 0.4 M mandelate in various percentages of methanol at pH 4.0 as the eluent, delivered at 2.0 ml/min. A 50 µl of 10 ppm and 500 ppm La(III), 5 ppm Th(IV) and 5 ppm uranyl standards were injected individually. Detection at 658 nm after PCR reaction with Arsenazo III.

Methanol		Peak start (min)	t_r (min)	Peak end (min)	k'	$\frac{k'}{k'_{La}}$
1%	La(III)	4.975	6.642	8.292	29.2	--
	La(III) (500 ppm)	4.908	N/A	8.208	N/A	--
	Uranyl	27.733	29.200	32.767	131.7	4.5
	Th(IV)	40.167	43.008	48.708	194.5	6.7
5%	La(III)	3.550	4.2	5.292	18.1	--
	La(III) (500 ppm)	3.417	N/A	5.858	N/A	--
	Uranyl	14.000	15.242	17.875	68.3	3.8
	Th(IV)	20.225	21.742	25.367	97.8	5.4
20%	La(III)	1.883	2.267	2.983	9.3	--
	La(III) (500 ppm)	1.783	N/A	3.925	N/A	--
	Uranyl	3.983	4.467	5.383	19.3	2.1
	Th(IV)	6.850	7.508	9.783	33.1	3.6

to = 2.2 (min).

N/A: There was no retention time (tr) available when 50 µl of 500 ppm La(III) was injected, as its signal was over scale on the UV detector.

so the separation of Th(IV)-La(III) and uranyl-La(III) were both improved in a lower organic modifier eluent, as shown in the far left column in Table 8.2. In practice a suitable eluent should give both a proper separation and short retention time. For the purpose of matrix elimination, it was expected that the lanthanides could be separated from uranyl and thorium(IV) and quickly eluted out from the concentrator column. Under each eluent condition, 500 ppm La(III) standard was also injected in order to examine the separation of uranyl from a more concentrated lanthanide sample, since the nitrophosphate solution contained a high ratio of lanthanides. Fig. 8.5 shows a chromatogram obtained by injecting 50 µl of 500 ppm La(III), 5 ppm Th(IV) and 5 ppm uranyl standards with 0.4 M mandelate eluent in 20% methanol at pH 4.0. Under these conditions thorium(IV) and uranyl can be completely separated from the lanthanides within a relatively short time (8 minutes at a flow-rate of 2.0 ml/min).

Some other size columns were also examined for the separation of lanthanum(III) from thorium(IV) and uranyl, such as Nova-Pak C_{18} column (100 x 3.9 mm I.D.) and Nova-Pak C_{18} Guard-Pak Insert. Although the longer column gave a better separation under the same conditions, the system back pressure was greatly increased when it was inserted into the chromatographic eluent flow-path. It was not considered to be practical for routine analysis. The C_{18} guard column was too short to offer sufficient capacity for the separation of thorium(IV) and uranyl from the concentrated lanthanum(III).

Based on the above experiments, a single valve on-line matrix elimination system was constructed, the configuration was the same as that shown in Fig. 3.2. A short C_{18} cartridge (50 x 3.9 mm ID) served as the precolumn, which was switched in or out of the chromatographic eluent flow-path by a high-pressure valve, and a HPLC pump was used for delivering the washing eluent. The C_{18} precolumn was equilibrated with the 0.4 M mandelate eluent (in 20% methanol, pH 4.0) prior to each injection. After a 5 times dilution, a 100 µl of the nitrophosphate sample was loaded onto the C_{18} precolumn, and washed with the mandelate eluent for 8.0 min at a flow-

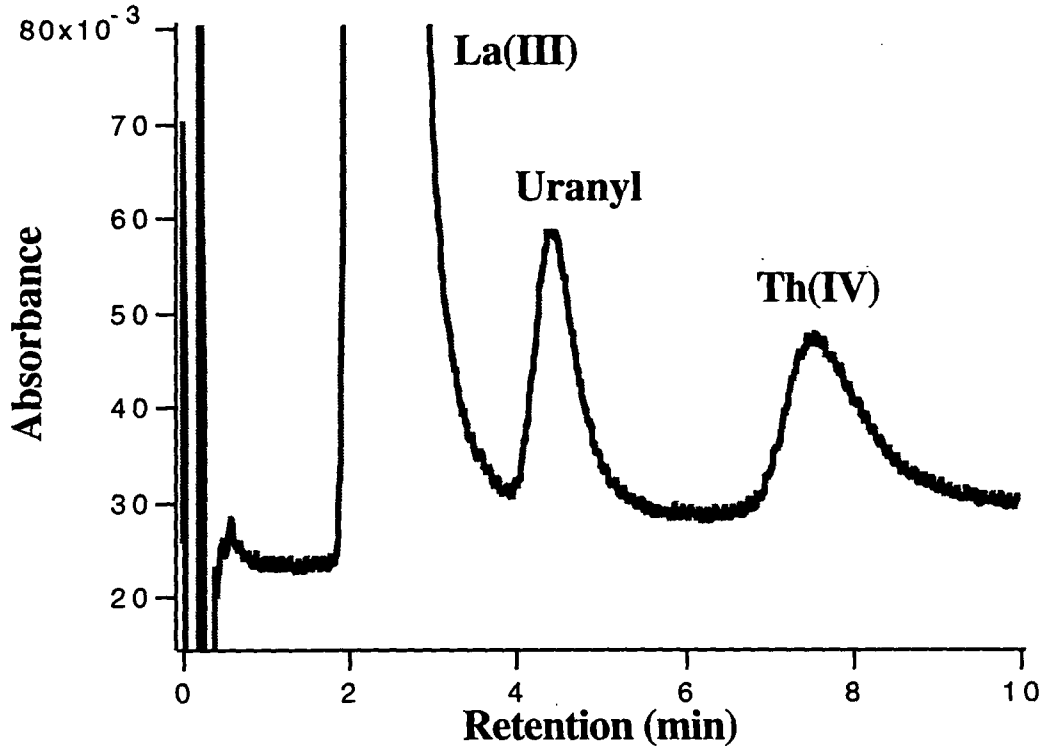

Fig. 8.5 Separation of lanthanum(III), uranyl and thorium(IV). A Nova-Pak C_{18} column (50 x 3.9 mm I.D.) was used with 0.4 M mandelate in 20% methanol (pH 4.0) as eluent, delivered at 2.0 ml/min. A 50 µl of 500 ppm La(III), 5 ppm Th(IV) and 5ppm uranyl mixed standards were injected. Other conditions were as in text.

rate of 2.0 ml/min to remove the interfering metals. The C_{18} precolumn was then inserted into the chromatographic eluent flow-path to quantify thorium(IV) and uranyl.

Fig. 8.6a shows the chromatogram of the KML sample obtained by using the on-line matrix elimination described above. The lanthanides and transition metals were completely removed from the sample after washing with 16.0 ml (8.0 min x 2.0 ml/min) of the mandelate eluent. Unfortunately, neither thorium(IV) nor uranyl peak was observed for the BML sample when it was analysed under the same conditions. The chromatogram of the BML sample was improved by reducing the washing volume to 7.0 ml, as shown in Fig 8.6b. However, reducing the washing volume decreased the efficiency of matrix elimination. A large lanthanide peak emerged which masked the adjacent thorium(IV) peak. These working conditions therefore still do not appear optimal. A further serious problem was that the nitrophosphate formed a precipitate when it mixed with the mandelate washing eluent, which should be avoided in any HPLC analysis.

8.3.3 PHOSPHATE INTERFERENCE

It has been noted previously [2] that some low solubility products were formed when the nitrophosphate solution was neutralised. This precipitation resulted from the reaction of the sample components when the pH was raised. A test conducted by dropping diluted sodium hydroxide into 20 ml of 0.2 M mandelate mixed with 0.5 ml of the nitrophosphate solution showed that a precipitate started to form when the pH exceeded 2.

Uranyl and phosphate form two types of precipitates [5]:

$$3\ UO_2^{2+} + 2\ PO_4^{3-} \leftrightharpoons (UO_2)_3(PO_4)_2 \downarrow$$

$$UO_2^{2+} + HPO_4^{2-} \leftrightharpoons UO_2HPO_4 \downarrow$$

The K_{sp} values for these reactions are listed in Table 8.3.

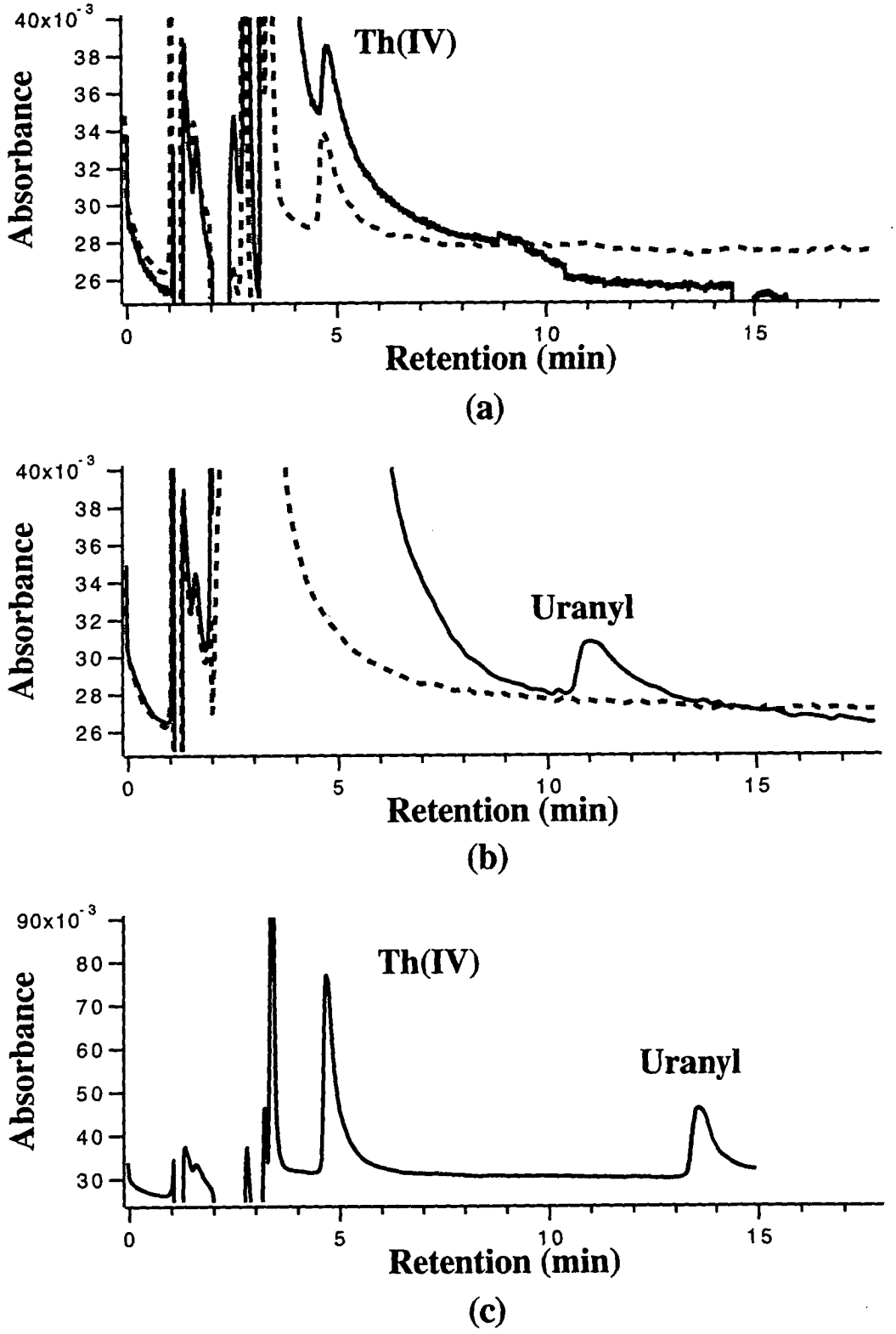

Fig. 8.6 Chromatograms of nitrophosphate obtained by on-line matrix elimination. 100 µl of sample solution was loaded onto a C_{18} precolumn (50 x 3.9 mm I.D.) and washed with 0.4 M mandelate for 16.0 ml (solid line) or 7.0 ml (dash line). Analysed as in Fig. 8.4. (a) KML; (b) BML; (c) 5 ppm Th(IV) and 5 ppm uranyl.

Table 8.3 EQUILIBRIUM CONSTANTS OF PHOSPHATE REACTIONS

Measured in 0.5 M phosphate at 25 °C.

Metal	Complex or Precipitate	log K
Th(IV) [6]	$ThH_2PO_4^{3+}$	3.96
	$Th(H_2PO_4)_2^{2+}$	7.5
UO_2^{2+}[5]	$(UO_2)_3(PO_4)_2$ (s) ↓	-49.7
	UO_2HPO_4 (s) ↓	-12.17
La^{3+}[7]	$LaH_2PO_4^{2+}$	1.61
	$LaPO_4$ (s) ↓	-22.43
Gd^{3+} [7]	$GdPO_4$ (s) ↓	-22.26
Fe^{3+} [8]	$FeHPO_4^{+}$	9.3
	$FeH_2PO_4^{2+}$	3.47
Mg^{2+} [8]	$(Mg)_3(HPO_4)_2(H_2O)_8$ (s) ↓	-25.2
	$MgHPO_4(H_2O)_3$ (s) ↓	-5.82
Ca^{2+} [8]	$CaHPO_4(H_2O)_2$ (s) ↓	-6.58

The nitrophosphate solution contains about 3 M phosphate [1]. Assuming that the sample was diluted 10 times for pretreatment, there would still be about 0.3 M phosphate present in it. Calculation using the K_{sp} values given in Table 8.3 at this phosphate concentration, the maximum concentration of free uranyl existing at various pH values is listed in Table 8.4. Uranium is present at ppm level concentration in the nitrophosphate solution (see Table 8.1), so the nitrophosphate sample should be adjusted to pH 3.0 or lower in order to keep all the uranyl as free anions in the sample solution.

In addition, lanthanum(III), gadolinium(III) and some other metals in the nitrophosphate solution also form precipitates with phosphate or hydrogen phosphate, such as $LaPO_4$, $GdPO_4$ [7], $(Mg)_3(HPO_4)_2(H_2O)_8$, $MgHPO_4(H_2O)_3$ and $CaHPO_4(H_2O)_2$ [8]. The K_{sp} values for these precipitates are also listed in Table 8.3. These reactions further restrict the nitrophosphate solution in a low pH value range in order to prevent forming precipitates, for these metals are much more concentrated than uranyl in the sample solution.

On the other hand, phosphate affects thorium(IV) somewhat differently. Dihydrogen phosphate forms two step complexes with thorium(IV) [6]:

$$Th^{4+} + H_2PO_4^- \leftrightharpoons ThH_2PO_4^{3+}$$

$$ThH_2PO_4^{3+} + H_2PO_4^- \leftrightharpoons Th(H_2PO_4)_2^{2+}$$

These ionic complexes will reduce thorium(IV) retention on the reversed-phase column. When mandelate is mixed into nitrophosphate solution, it competes with dihydrogen phosphate for thorium(IV) forming its complexes. The equilibrium concentrations of these complexes depend upon both the ligands concentrations and the solution pH value. The distribution of each thorium(IV) complex at various mandelate concentrations is plotted in Fig. 8.7a, which calculated using the formation constants at pH 4.0 and 0.3 M phosphate. Some species, such as $ThH_2PO_4^{3+}$,

Table 8.4 FREE URANYL CONCENTRATION AT VARIOUS pH VALUES

Calculated using the K_{sp} values at 0.30 M phosphate.

	$3UO_2^{2+} + 2PO_4^{3-} \leftrightharpoons (UO_2)_3(PO_4)_2 \downarrow$		$UO_2^{2+} + HPO_4^{2-} \leftrightharpoons UO_2HPO_4 \downarrow$	
pH	$[UO_2^{2+}]$ (M) = $\sqrt[3]{Ksp / [PO_4^{3-}]^2}$	U (ppm)	$[UO_2^{2+}]$ (M) = $K_{sp} / [HPO_4^{2-}]$	U (ppm)
0.0	0.03	7.1×10^{6}	4.9×10^{-3}	1.2×10^{6}
0.5	0.003	7.1×10^{5}	5.0×10^{-4}	1.2×10^{5}
1.0	3.1×10^{-4}	7.4×10^{4}	5.2×10^{-5}	1.2×10^{4}
1.5	3.4×10^{-5}	8.1×10^{3}	6.0×10^{-6}	1.4×10^{3}
2.0	4.3×10^{-6}	1.0×10^{3}	8.5×10^{-7}	200
2.5	6.6×10^{-7}	160	1.6×10^{-7}	39
3.0	1.2×10^{-7}	29	4.1×10^{-8}	9.8
3.5	2.5×10^{-8}	6.0	1.2×10^{-8}	2.9
4.0	5.3×10^{-9}	1.3	3.7×10^{-9}	0.88
4.5	1.1×10^{-9}	0.27	1.2×10^{-9}	0.28
5.0	2.4×10^{-10}	0.058	3.7×10^{-10}	0.087
5.5	5.3×10^{-11}	0.013	1.2×10^{-10}	0.028
6.0	1.2×10^{-11}	0.003	3.9×10^{-11}	0.009

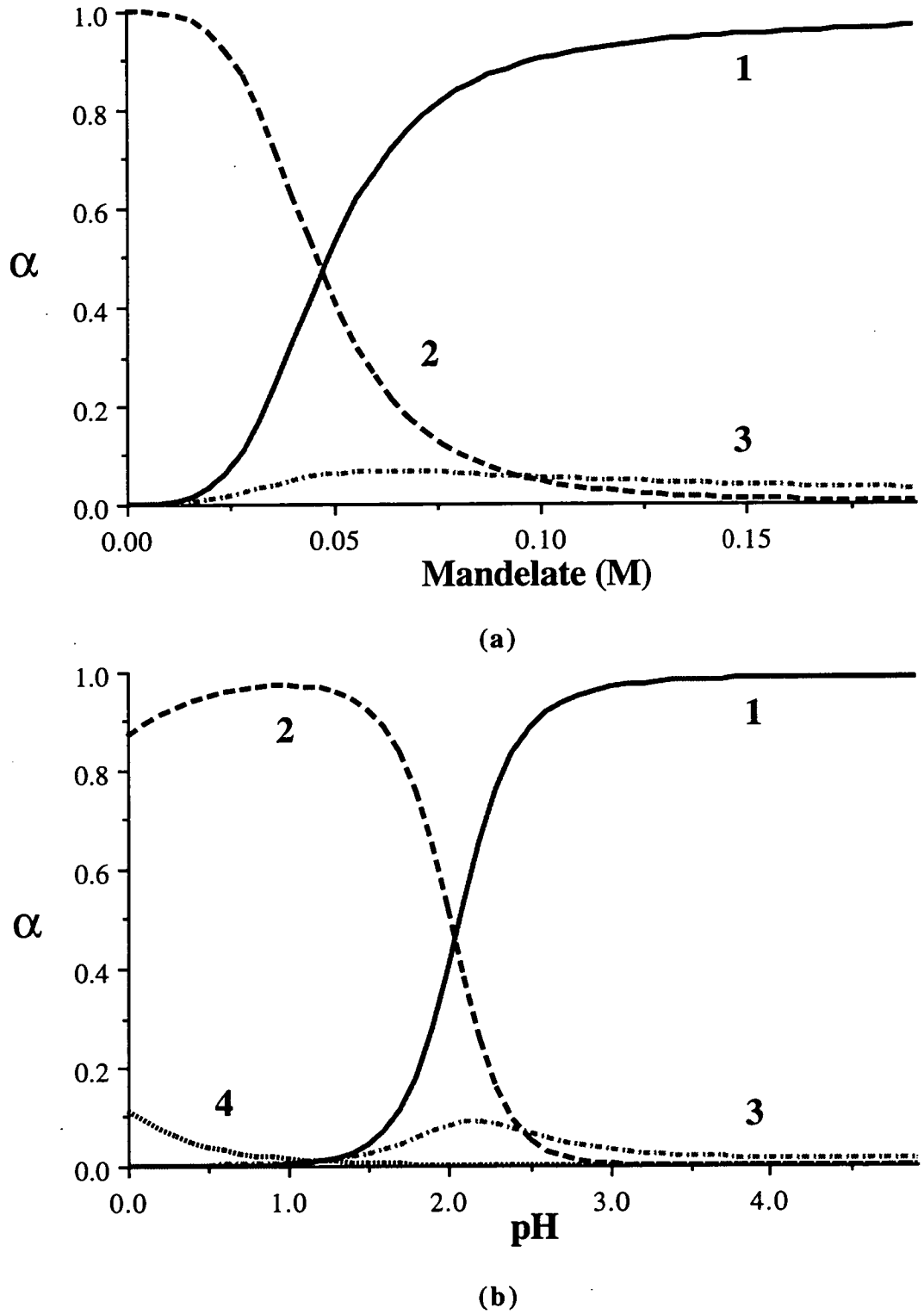

Fig. 8.7 Distribution of thorium(IV) complexes (a) at various mandelate (MA) concentrations, calculated using the formation constants at pH 4.0 and 0.30 M phosphate; (b) at various pH values, calculated at 0.40 mandelate and 0.30 M phosphate. (1) $Th(MA)_4$; (2) $Th(H_2PO_4)_2^{2+}$; (3) $Th(MA)_3^{+}$; (4) $ThH_2PO_4^{3+}$.

$Th(MA)^{3+}$ and $Th(MA)_2^{2+}$, are not included in this figure, for they present as negligible fractions at any mandelate concentration. At low mandelate concentration, most of the thorium(IV) is present as $Th(H_2PO_4)_2^{2+}$. As the mandelate concentration increased the phosphate complexes are gradually dissociated and converted into the mandelate complexes. However, the neutral species of thorium(IV) *tetra*(mandelate) does not dominate (>95%) until the mandelate concentration reaches 150 mM. In order to completely convert the thorium(IV) phosphate species into the mandelate complex, the mandelate in the sample should therefore be more than 200 mM.

Assuming the nitrophosphate solution is diluted 10 times in 400 mM mandelate solution, it still contains about 0.3 M phosphate. Fig. 8.7b shows the distribution of thorium(IV) complexes at various pH values calculated at this phosphate concentration. At low pH value most thorium(IV) presents as the *bis*(dihydrogen phosphate) complex, but its fraction is quickly decreased as the solution pH raises. When the solution pH exceeds 3, the thorium(IV) *tetra*(mandelate) complex becomes the dominant species (95%). In order to quantitatively analyse thorium(IV) in the nitrophosphate solution, the mandelate eluent pH should therefore be adjusted to 3.0 or higher. This contrasts with the uranyl requirement described above. The phosphate reactions also influence the validity of the lanthanides separation conditions established in section 8.3.2. It is impossible to eliminate the interference of both the lanthanides and phosphate in one step using a C_{18} precolumn and a mandelate washing eluent. The phosphate should therefore be removed from the sample prior to the separation of thorium(IV) and uranyl from the lanthanides.

8.3.4 ON-LINE MATRIX ELIMINATION

In Chapter 6 a manual cation-exchange procedure was used to remove the matrix from the digested mineral sand sample. It was found that thorium(IV) and uranyl could be quantitatively bound on the cation-exchange cartridge, providing the nitric acid in the sample did not exceed 0.1 M. The Ion-exclusion Guard-Pak (Waters)

was the optimal cartridge, for it provides sufficient capacity to host thorium(IV) and uranyl, and also allows the analytes to be stripped from the cartridge with a HIBA solution.

Following the experiment described in Chapter 6, the nitrophosphate solution was pretreated on a cation-exchange (CE) cartridge (Ion-exclusion Guard-Pak Insert, Waters) with a dilute nitric acid eluent. The requirements for the washing eluent are twofold. Firstly, the nitric acid concentration should not exceed 0.1 M (pH > 1), in order to ensure quantitative bounding metal cations on the CE cartridge [9]. Secondly, the washing eluent pH should not exceed 2, otherwise the nitrophosphate sample forms precipitates as mentioned in section 8.3.3. For this reason 0.08 M nitric acid was chosen as the washing eluent. It was expected that phosphate and other anions in the sample could be removed by this pretreatment, whilst thorium(IV), uranyl and other cations would be trapped on the CE cartridge. Concentrated (500 ppm) thorium(IV), uranyl and lanthanum(III) standards were investigated, with the effluent being directly introduced to the detector through the PCR reactor. It was observed that both thorium(IV) and uranyl started to elute out after 3.0 minutes when washed at 0.5 ml/min, as listed in Table 8.5. Increasing the eluent flow-rate or using a concentrated acid eluent caused all the cations to be eluted out in a shorter time, making it more likely that some loss of the analytes could occur.

Having established the cation-exchange washing pretreatment, it was combined with the lanthanides separation forming an on-line matrix elimination procedure together with the reversed-phase chromatographic analysis. The procedure was performed automatically by the programmable pump as described in the experimental section. Table 8.6 lists the time sequence of the control program entered into the Model 590 programmable pump. In order to ensure thorium(IV) and uranyl could be quantitatively bound on the CE cartridge, the nitrophosphate solution was diluted 10 times in Milli-Q water to reduce the acid concentration. Fig. 8.8 shows the chromatograms of the nitrophosphate solutions obtained by using the on-line matrix

Table 8.5 RETENTION OF LANTHANUM(III), URANYL AND THORIUM(IV) ON A CATION-EXCHANGE CARTRIDGE USING NITRIC ACID ELUENTS

An Ion-Exclusion Guard-Pak Insert was used with diluted nitric acid as the eluent, delivered at various speeds. A 50 µl of 500 ppm La(III), uranyl and Th(IV) standards were injected individually and monitored at the outlet of the cartridge after PCR reaction with Arsenazo III.

Eluent and flow-rate	Metal	Peak start (min)	t_r (min)
0.15 M HNO_3, 2.0 ml/min	La(III)	1.80	3.29
	UO_2^{2+}	1.76	2.97
	Th(IV)	1.85	3.20
0.08 M HNO_3, 1.0 ml/min	La(III)	1.98	3.16
0.08M HNO_3, 0.5 ml/min	La(III)	4.88	6.76
	UO_2^{2+}	4.13	5.99
	Th(IV)	4.74	7.06

Table 8.6 OPERATIONAL SEQUENCE OF THE MODEL 590 PUMP WHEN USED FOR ON-LINE MATRIX ELIMINATION

Segment	Time (min)	Flow-rate (ml/min)	Event out	Function
1	Event in 1#	0.5	NNFNFFFF	Nitric acid washing.
2	3.0	2.0	NFFFNFFF	MA flushing (low speed)
3	4.0	5.0	NFFFNFFF	MA flushing (high speed)
4	7.5	2.0	NFFFNFFF	MA flushing (reduced speed)
5	8.0	2.0	FNFFNFFF	MA washing
6	18.0	2.0	NFFNFPFF	Start analysis HNO_3 (low speed)
7	18.5	5.0	NFFNFFFF	HNO_3 (high speed)
8	22.0	0.5	NNFNFFFF	Equilibrate Ion-Exclusion column

Note: Event in: 1#, to receive signal from the U6K injector.

Event out: 1#, to Switch Valve 1;

2#, to Switch Valve 2;

4#, to the low pressure valve 4 (HNO_3 washing eluent);

5#, to the low pressure valve 5 (mandelate washing eluent);

6#, to trigger the Chromatographic Data Station;

8#, to Event in 1# for cycling the program.

elimination technique. Under the same conditions 100 µl of 500 ppm La(III) was injected as a blank and no peak was observed, showing that this species had been removed during the matrix elimination step. The recovery was 101.0% and 145.6% for thorium(IV) and uranyl, respectively. The cause of high recovery for uranyl remains unknown. Calibration plots for thorium(IV) and uranyl after on-line matrix elimination pretreatment are shown in Fig. 8.9. The precision (% R.S.D. for 5 repeat injections) was 5.47 and 4.08 for thorium(IV) and uranyl, respectively. The nitrophosphate results obtained using the on-line matrix elimination for analysis of the nitrophosphate solution are listed in Table 8.7 below. These are actual values and do not take account of the high recovery shown above for uranyl.

Table 8.7 THORIUM AND URANIUM IN NITROPHOSPHATE SOLUTION Analysed after on-line matrix elimination as described in the text.

	Thorium (ppm)	Uranium (ppm)
Kola Mother Liquor	18.3	1.9
BouCraa Mother Liquor	1.5	57.2

8.4 CONCLUSIONS

The nitrophosphate solution contains about 3 M phosphate and a total of 5 g/l lanthanides in addition to concentrated nitric acid. Phosphate forms stable complexes with thorium(IV), and precipitates with uranyl, whereas the lanthanides produce a large peak which overlaps those of the thorium(IV) and uranyl. Both phosphate and the lanthanides interfered with the thorium(IV) and uranyl analysis when the nitrophosphate solution was injected directly. These interferences can be overcome by pretreating the sample with an on-line matrix elimination protocol. Phosphate and

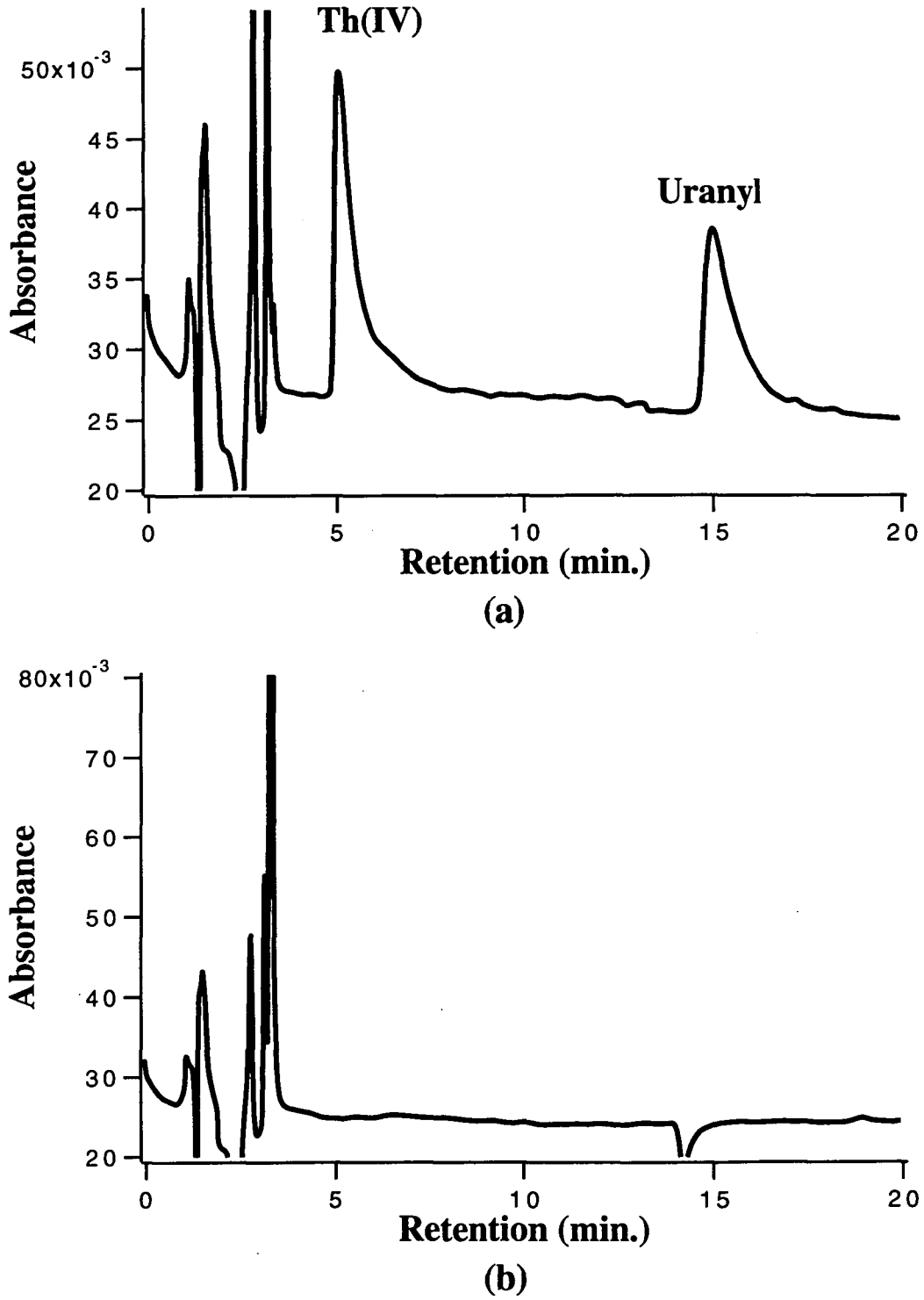

Fig. 8.8 Thorium and uranium chromatogram after on-line matrix elimination. Samples were pretreated on a cation-exchange Guard column with 0.1 N HNO_3 for 3 minutes, then on a C_{18} short column (50 x 3.9 mm) with 0.40 M mandelate for 10 minutes. Other conditions as in Fig. 8.4. (a) 100 µl of 5.0 ppm Th(IV) and uranyl mixed standards; (b) 100 µl of 500 ppm lanthanum(III).

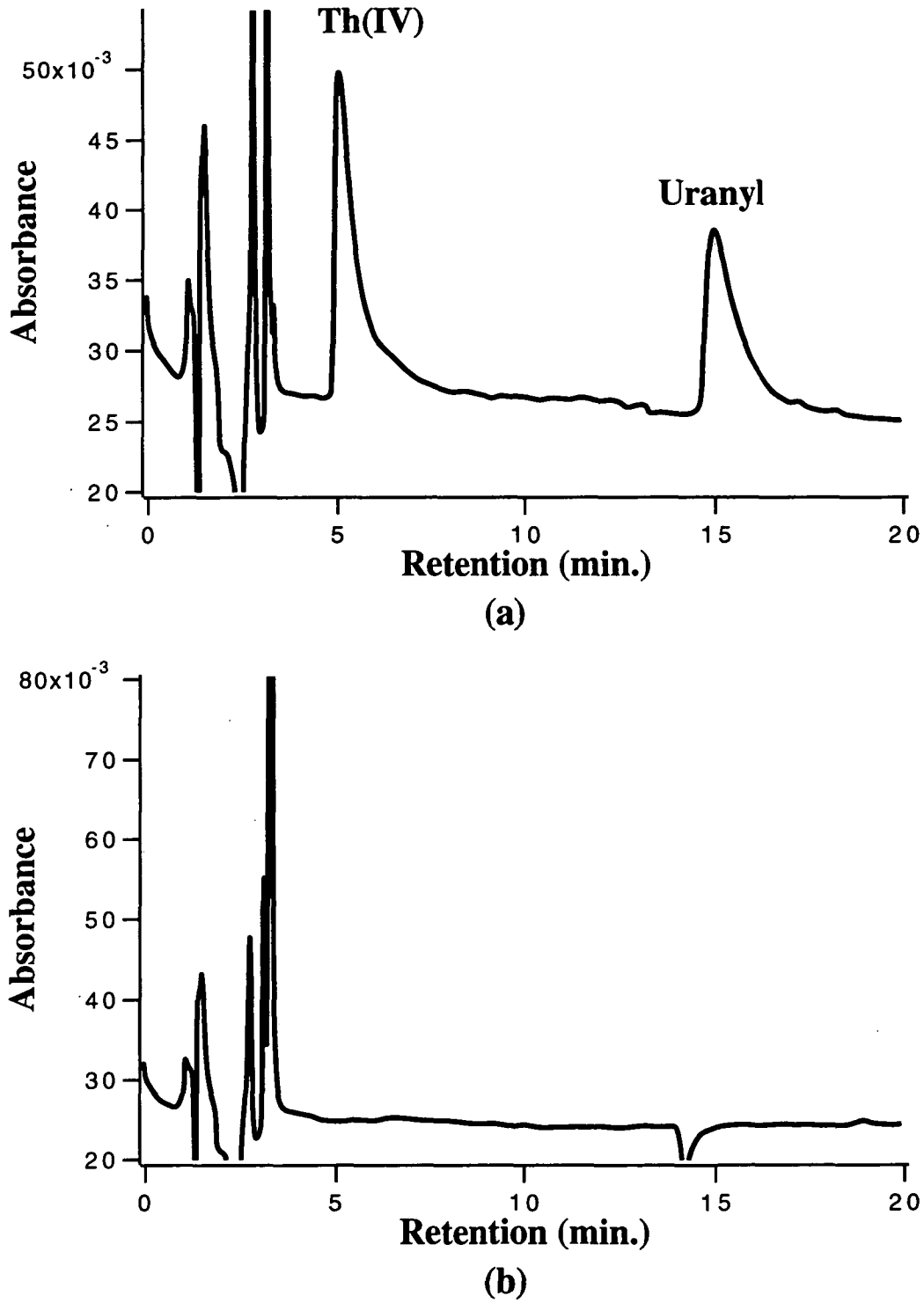

Fig. 8.8 Thorium and uranium chromatogram after on-line matrix elimination. Samples were pretreated on a cation-exchange Guard column with 0.1 N HNO_3 for 3 minutes, then on a C_{18} short column (50 x 3.9 mm) with 0.40 M mandelate for 10 minutes. Other conditions as in Fig. 8.4. (a) 100 µl of 5.0 ppm Th(IV) and uranyl mixed standards; (b) 100 µl of 500 ppm lanthanum(III).

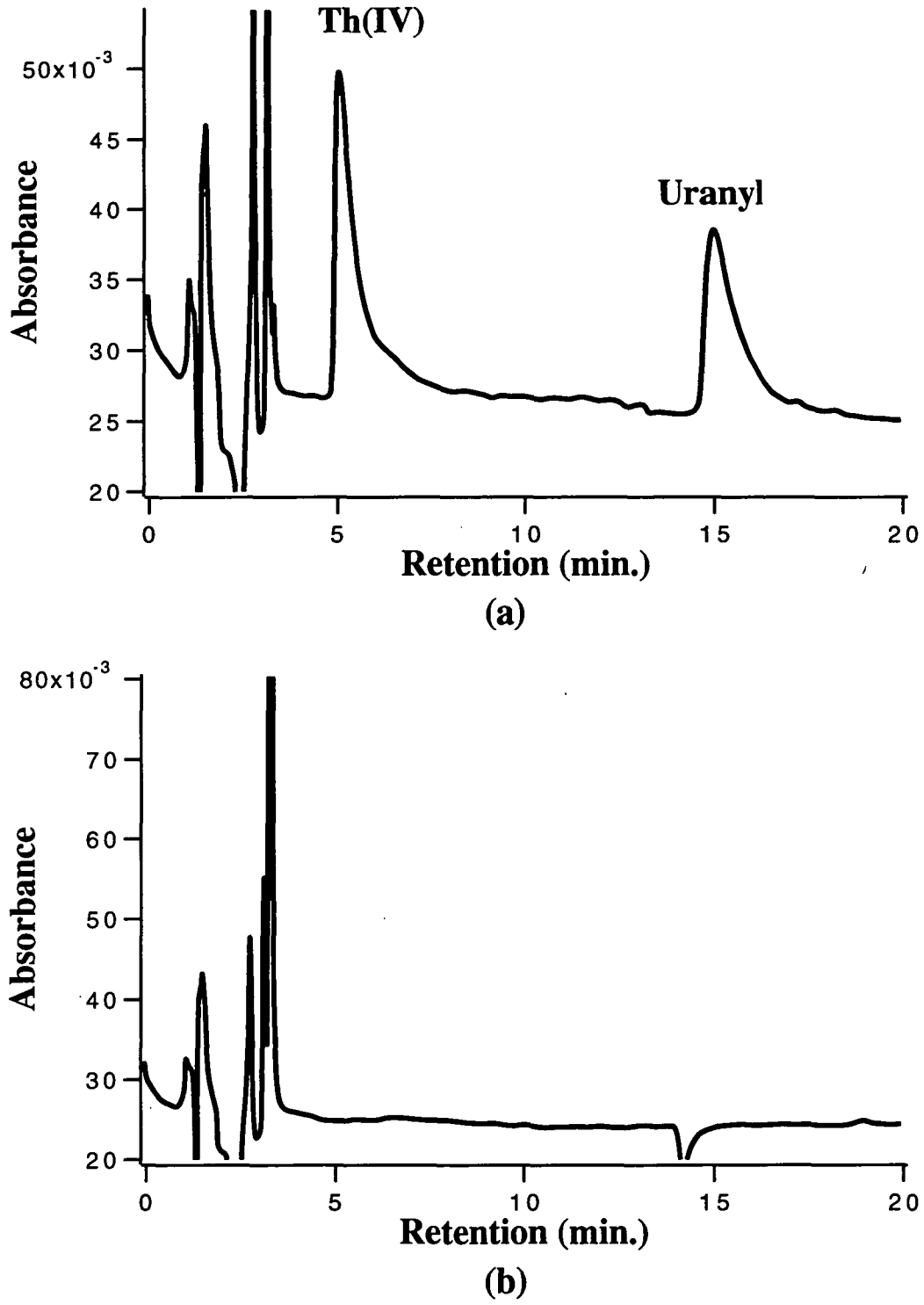

Fig. 8.8 Thorium and uranium chromatogram after on-line matrix elimination. Samples were pretreated on a cation-exchange Guard column with 0.1 N HNO_3 for 3 minutes, then on a C_{18} short column (50 x 3.9 mm) with 0.40 M mandelate for 10 minutes. Other conditions as in Fig. 8.4. (a) 100 µl of 5.0 ppm Th(IV) and uranyl mixed standards; (b) 100 µl of 500 ppm lanthanum(III).

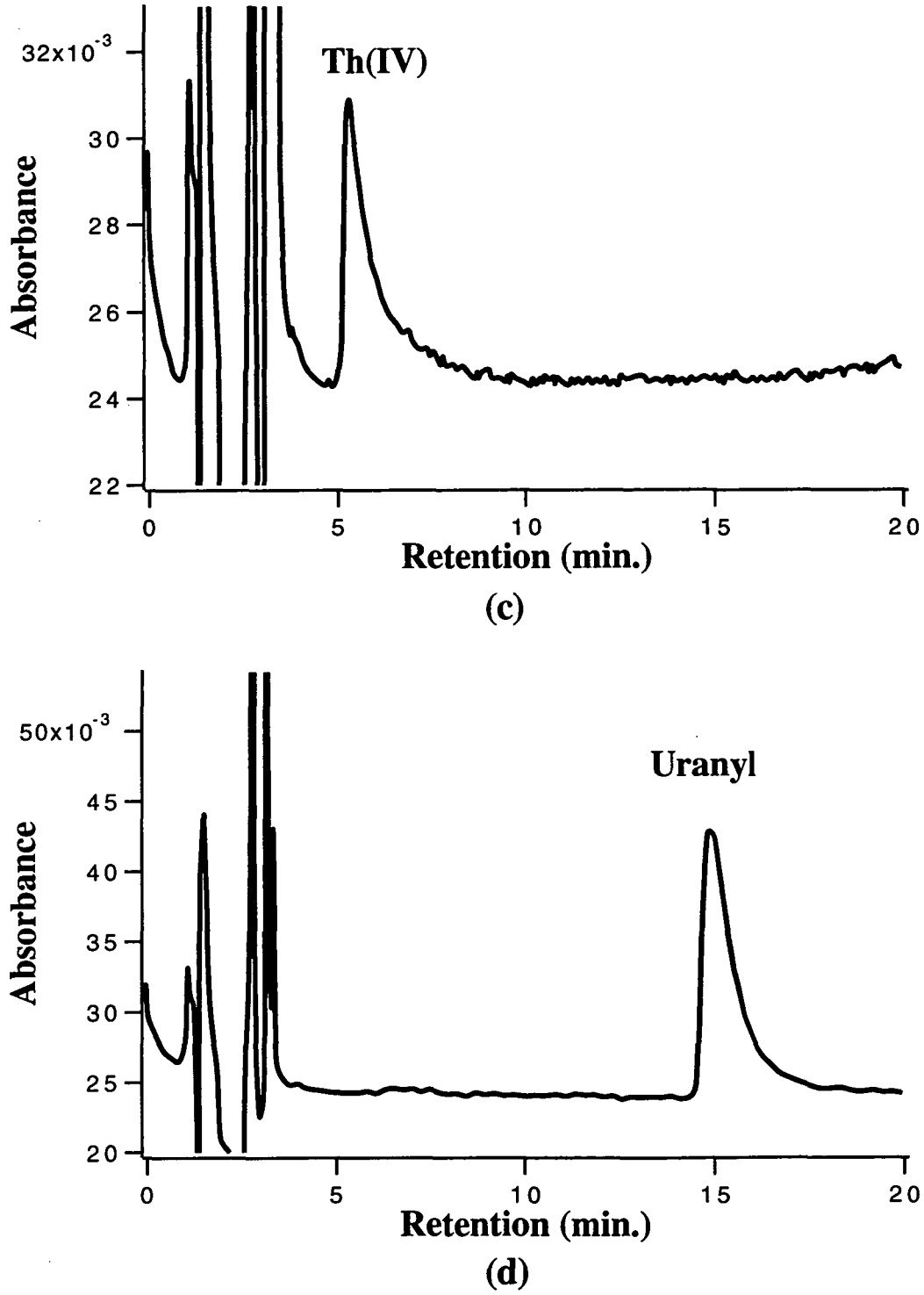

Fig. 8.8 (continued) Chromatograms of nitrophosphate obtained by on-line matrix elimination. After diluting 10 times in Milli-Q water, 100 µl of the sample was injected. (c) Kola mother liquor; (d) BouCraa mother liquor.

other anions are firstly removed after retention of thorium(IV), uranyl and other cations on a cation-exchange column using 0.08 M nitric acid solution, then the lanthanides and transition metals are removed from the sample on a short C_{18} cartridge with 0.4 M mandelate eluent. Finally thorium(IV) and uranyl were separated and quantified on an analytical C_{18} column, and detected at 658 nm after PCR with Arsenazo III.

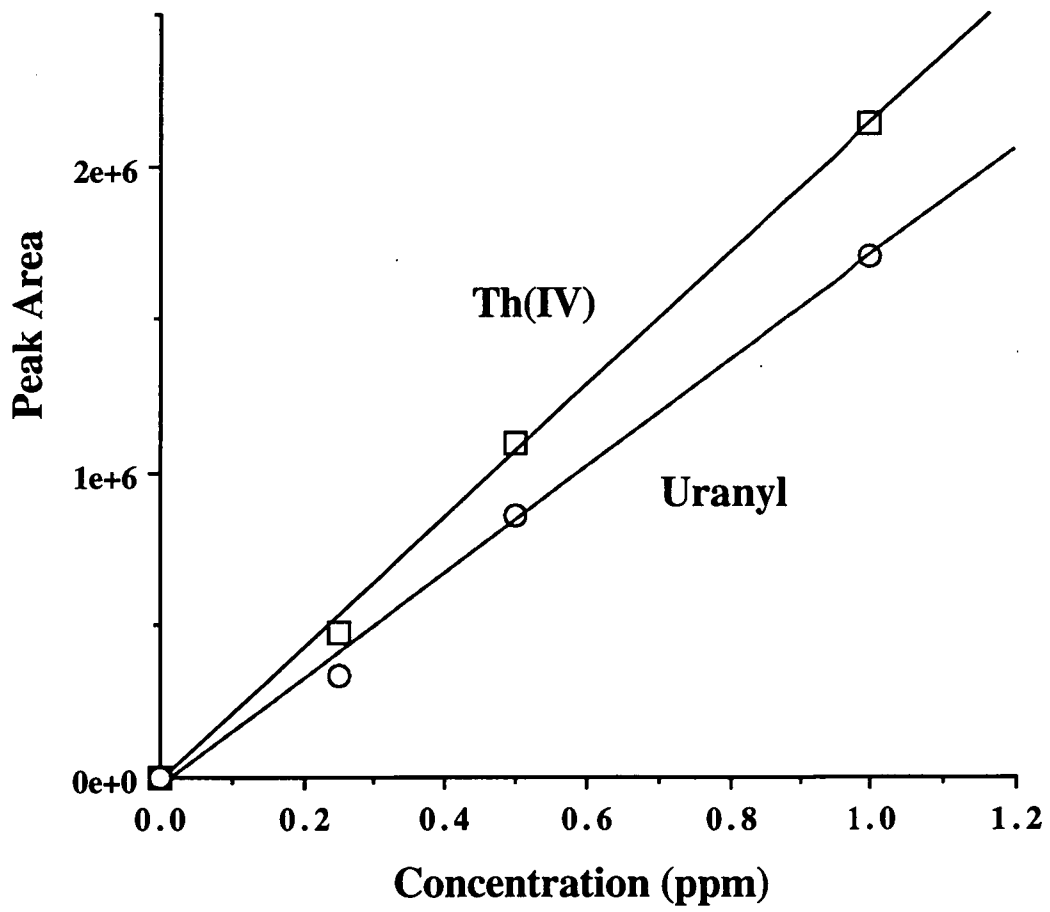

Fig. 8.9 Calibration plots for thorium(IV) and uranyl after on-line matrix elimination. Washed with 0.08 M HNO_3 on a cation-exchanger (Guard-Pak), then with 0.40 M mandelate on a C_{18} column (50 x 3.9 mm I.D.). Other conditions are the same as in Fig. 8.8.

8.5 REFERENCES

1 Abdulla W. Al-Shawi and R. Dahl, *J. Chromatogr.*, 671 (1994) 173.

2 Abdulla W. Al-Shawi and R. Dahl, *International Ion-Chromatography Symposium '94*, September 1994, Turin, Italy.

3 P. R. Haddad and P. E. Jackson, *Ion-chromatography: Principle and Applications*, Elsevier, Amsterdam, 1990, p.454.

4 S. Elchuk, K. I. Burns, R. M. Cassidy and C. A. Lucy, *J. Chromatogr.*, 558 (1991) 197.

5 V. Vesely, V. Pekarek and M. Abbrent, *J. Inorg. Nucl. Chem.*, 17 (1965) 1159.

6 E. L. Zebroski, H. W. Alter and F. K. Heumann, *J. Amer. Chem. Soc.*, 73 (1951) 5646.

7 I. V. Tananaev and V. P. Vasileva, *Russ. J. Inorg. Chem.*, 8 (1963) 555.

8 A. E. Martell and R. M. Smith, *Critical Stability Constants*, Plenum Press, New York, 1966, Vol. 4, p.56.

9 F. W. E. Strehlow, R. Rethemeyer and C. J. C. Bothma, *Anal. Chem.*, 37 (1965) 107.

Chapter 9

Conclusions

The retention behaviour of thorium(IV) and uranyl complexes on a reversed-phase column has been examined using a mobile phase comprising hydrophobic complexing ligands without the presence of ion-interaction reagents. Three different ligands and various parameters which affect the complexation and retention were investigated in detail, such as the organic modifier, column temperature, ligand concentration and the eluent pH. Optional chromatographic conditions were selected based on these results.

The elution characteristics of thorium(IV) and uranyl complexes with α-hydroxyisobutyric acid (HIBA) are dependent on the particular metal complexes existing in solution under the chromatographic conditions used. With a 400 mM HIBA (pH 4.0) eluent both thorium(IV) and uranyl are retained on the reversed-phase column by hydrophobic adsorption, despite theoretical calculations which predict that the anionic uranyl *tris*(HIBA) complex is the dominant species at these conditions, whilst thorium(IV) is predicted to be present as a neutral *tetra*(HIBA) complex. The thorium(IV) complex is however eluted prior to the uranyl complex, and shows an opposite behaviour to that normally encountered in reversed-phase chromatography. This is likely to be due to the propensity for thorium(IV) hydrolysis to produce an anionic complex probably containing two or more coordinated hydroxyl ions. The retention behaviour of thorium(IV) and uranyl in HIBA mobile phases is quite different to that exhibited by the lanthanides, which are retained by a cation-exchange mechanism.

The hydrophobicity of the complexing ligand has a great effect on the retention of thorium(IV) and uranyl. Although glycolic and mandelic acids have similar characteristics to that of HIBA when they form complexes with thorium(IV) and

uranyl, compared to HIBA complexes the retention of glycolate complexes is greatly reduced due to the less hydrophobic nature of this ligand. Mandelate complexes, however, are more strongly retained due to the strongly hydrophobic phenyl group attached to the ligand. In the glycolate eluent the retention of thorium(IV) and uranyl complexes shows some unusual behaviour as the column temperature is raised, probably due to both thorium(IV) and uranyl complexes being hydrolysed. However, in mandelate eluent this hydrolysis either does not occur due to steric effects, or its influence on retention is overshadowed by the hydrophobicity of the complex, therefore the elution order of thorium(IV) and uranyl is reversed to that observed in HIBA and glycolate eluents. The experimental results observed with glycolate and mandelate eluents further confirm that thorium(IV) and uranyl complexes are retained on the reversed-phase column through a hydrophobic absorption mechanism.

The above reversed-phase chromatographic method has been successfully applied to the determination of thorium and uranium in mineral sands using a HIBA eluent, with detection at 658 nm after post-column reaction with Arsenazo III. A number of sample digestion methods were investigated together with a range of sample pretreatment techniques. The optimal process involves a tetraborate fusion/nitric acid leach followed by either cation-exchange pretreatment or direct injection after dilution in concentrated hydroxyisobutyric acid. The cation-exchange pretreatment resulted in higher precision and can be applied to more acidic sample digests. The direct injection approach gives comparable results when using the recommended dissolution procedure and offered significant time savings. The results obtained using the chromatographic method show excellent agreement with those generated using the significantly more costly techniques of XRF and ICP-MS for ilmenite, synthetic rutile, zircon and rutile mineral sands.

Trace levels of thorium(IV) and uranyl were analysed by an on-line preconcentration technique using a short C_{18} cartridge as the concentrator column after preparing the sample in a mandelate solution. The ligand hydrophobicity and

concentration in the sample are the two most important factors which affect the preconcentration efficiency. The recoveries of thorium(IV) and uranyl in mandelate solutions are much greater than those obtained using HIBA or glycolate. The maximum breakthrough volume for the C_{18} guard column concentrator was observed using 42 mM mandelate. The flow-rate of sample loading on the concentrator has little effect on the recoveries of thorium(IV) and uranyl within the range of 0.5-5.0 ml/min. There is a linear relationship between the peak area and the loading volume up to 50 ml. Most of the common anions also have no affect on thorium(IV) and uranyl enrichment, except sulfate and acetate which incorporate into the uranyl-mandelate coordination sphere and cause the complex to self-elute. Cation interferences are varied. The breakthrough volume of the C_{18} column concentrator increased when NaCl was present in the thorium(IV) and uranyl standard solutions due to a salting-out effect. The lanthanides and some transition metals also form complexes with mandelate and are trapped on the C_{18} concentrator. They are eluted as a matrix peak that partially overlaps the thorium(IV) peak in the final analysis step. This on-line preconcentration technique was successfully applied to the analysis of trace levels of thorium(IV) and uranyl spiked into sea water.

Thorium and uranium in phosphate rock samples can be analysed by a combination of the reversed-phase chromatographic method with an on-line matrix elimination protocol. The digested phosphate rock solution contains about 3 M phosphate and 5 g/l lanthanides, as well as large amounts of interfering anions and cations. Phosphate is incorporated into the thorium(IV)-mandelate coordination sphere and forms precipitates with uranyl. Phosphate and other anions are removed after retention of thorium(IV), uranyl and other cations on a cation-exchange column from a 0.08 M nitric acid solution. Then the lanthanides and transition metals are removed from the sample onto a short C_{18} cartridge with a 0.4 M mandelate eluent. Finally thorium(IV) and uranyl are transferred onto a C_{18} analytical column for quantification.